OESOPHAGEAL PREMOTOR MECHANISMS IN THE RAT

CENTRE FOR NEWFOUNDLAND STUDIES

TOTAL OF 10 PAGES ONLY
MAY BE XEROXED

(Without Author's Permission)

WEI-YANG LU

OESOPHAGEAL PREMOTOR MECHANISMS IN THE RAT

By

© Wei-Yang Lu, M.D., M. Sc.

A thesis submitted to the School of Graduate Studies

in partial fulfilment of the requirements for

the degree of Doctor of Philosophy

Faculty of Medicine

Memorial University of Newfoundland

July 1996

St. John's Newfoundland

National Library of Canada
Acquisitions and Bibliographic Services Branch
395 Wellington Street
Ottawa, Ontario
K1A 0N4

Bibliothèque nationale du Canada
Direction des acquisitions et des services bibliographiques
395, rue Wellington
Ottawa (Ontario)
K1A 0N4

Your file Votre référence

Our file Notre référence

The author has granted an irrevocable non-exclusive licence allowing the National Library of Canada to reproduce, loan, distribute or sell copies of his/her thesis by any means and in any form or format, making this thesis available to interested persons.

L'auteur a accordé une licence irrévocable et non exclusive permettant à la Bibliothèque nationale du Canada de reproduire, prêter, distribuer ou vendre des copies de sa thèse de quelque manière et sous quelque forme que ce soit pour mettre des exemplaires de cette thèse à la disposition des personnes intéressées.

The author retains ownership of the copyright in his/her thesis. Neither the thesis nor substantial extracts from it may be printed or otherwise reproduced without his/her permission.

L'auteur conserve la propriété du droit d'auteur qui protège sa thèse. Ni la thèse ni des extraits substantiels de celle-ci ne doivent être imprimés ou autrement reproduits sans son autorisation.

ISBN 0-612-17615-0

Canada

ABSTRACT

The functional organization and neurotransmitter mechanisms of oesophageal premotor neurons in the subnucleus centralis of the nucleus tractus solitarii (NTS_c) were investigated *in vivo* in the anaesthetized rat and *in vitro* in a rat brainstem slice preparation.

Results from neurophysiological and pharmacological investigations indicate that the striated muscle of the oesophagus shows segmentally organized reflex responses to local distension, i.e. the proximal portion produces monophasic peristalsis, whereas the distal portion generates rhythmic peristaltic motility. The afferent limbs of these loops synapse in the NTS_c. Organotopically organized projections from the NTS_c to the compact formation of the nucleus ambiguus (AMB_c) represent the chief internuncial pathway connecting oesophageal reflex interneurons (or premotor neurons) with motoneurons of the efferent limb.

Neurons in the NTS_c receive both excitatory amino acid (EAA)ergic and cholinergic inputs. However, vagal afferents from the oesophagus employ an EAA rather than acetylcholine to convey excitatory input to ipsilateral NTS_c premotor neurons. Cholinergic input to the NTS_c arises from propriobulbar sources and serves to facilitate oesophageal stage coupling, to promote aboral propagation of peristalsis and to generate slow esophagomotor rhythms.

Results from *in vitro* experiments reveal that activation of muscarinic cholinoceptors (mAChRs) in the NTS_c region evokes rhythmic synaptic activity in single oesophageal motoneurons in the AMB_c, demonstrating that the interneuronal network in the NTS_c can generate rhythmic esophagomotor activity in the absence of phasic sensory input.

When stimulated via N-methyl-D-aspartate (NMDA) receptors and/or mAChRs in the presence of tetrodotoxin (TTX), single neurons of the NTS_c region generate two distinct rhythmic oscillations that mirror two types of *in vivo* peristaltic rhythm. These observations support the idea that the oesophageal premotor neurons possess conditional oscillator properties.

In summary, the present investigations provide strong evidence that the premotor neuronal circuits in the NTS_c function as esophagomotor pattern generators. Subject to regulation by EAAergic and cholinergic inputs, these premotor circuits generate segmentally and/or coordinatively organized esophagomotor patterns.

ACKNOWLEDGMENTS

I am deeply indebted to my supervisor, Dr. Detlef Bieger, for his guidance and advice during the progress of this work; for his continuous support and encouragement in matters both academic and non-academic and especially for his patience in trying to improve my English.

I am very grateful to Dr. Richard S. Neuman for his input during the electrophysiological experiments, and enlightening discussion throughout the graduate program as co-supervisor. I am also indebted to him for his consistent support in affairs both academic and non-academic and for his helpful criticism during the writing of this thesis.

I would like to extend my gratitude to:

Dr. Jim Reynolds for his academic counsel when he was a member of my supervisory committee.

Dr. Penny Moody-Corbett for her academic counsel as a member of my supervisory committee and for her recommendation of financial support when she was Acting Assistant Dean of Graduate Studies and Research, Faculty of Medicine.

Dr. Verna Skanes, Assistant Dean of Graduate Studies and Research, Faculty of Medicine, for financial and moral support.

Dr. Yutian Wang for his helpful scientific advice during the first half year of my

graduate program.

Ms. Janet Robinson for her expert technical assistance throughout my research project and for her consistent encouragement and moral support in many non-academic affairs.

Mrs. Mette Bieger and Mrs. Judy Neuman for their support and encouragement.

Mrs. Betty Granter and Ms. Shirley Atkins for their assistance in secretarial and administrative work.

Ms. Pauline Cole for her ready assistance in all administrative matters pertaining to my graduate work.

The School of Graduate Studies and the Faculty of Medicine for providing financial support.

All my friends and colleagues in Medicine and especially to the members of Neuroscience group.

This work would not have been possible without the love and support of my wife and my family to whom I remain forever indebted.

TABLE OF CONTENTS

ABSTRACT.....(ii)

ACKNOWLEDGMENTS.....(iv)

TABLE OF CONTENTS.....(vi)

LIST OF FIGURES & TABLE.....(x)

LIST OF ABBREVIATIONS.....(xvi)

Chapter 1 INTRODUCTION..... 1

1.1 Oesophagomotor Substrates.....2
1.1.1 Oesophageal Musculature.....2
1.1.2 Oesophageal Innervation.....5

1.2 Oesophagomotor Patterns.....12
1.2.1 Primary Peristalsis.....13
1.2.2 Secondary Peristalsis.....13
1.2.3 Tertiary Peristalsis.....14

1.3 Neurophysiological Correlates.....15
1.3.1 Mechanisms of Central Control.....15
1.3.2 Basic Mechanisms of Central Pattern Generation.....18
1.3.3 Organization of "Swallowing Center".....23
1.3.4 Oesophagomotor Pattern Generator.....25

1.4 Putative Transmitters in the Brainstem Oesophagomotor Network.....28
1.4.1 Excitatory Transmitters in the NTS_{c}.....29
1.4.2 Excitatory Transmitters in the NTS_{im}.....32
1.4.3 Inhibitory Transmitters at NTS Premotor Deglutitive Loci.....34
1.4.4 Transmitters in the AMB_{c}.....35

1.5 Research Plan.....36
1.5.1 Rationale.....36
1.5.2 Hypotheses.....39
1.5.3 Objectives.....39

Chapter 2 OESOPHAGEAL REFLEXES: PREMOTOR CHOLINERGIC AND GLUTAMATERGIC CONTROL.....41

2.1 Methods and Materials.....42

2.2 Results.....50
2.2.1 Characterization of Reflex Responses.....50
2.2.2 Effects of Vagotomy and Curarization.....59
2.2.3 Cholinergic Effects.....63
2.2.4 Effects of NMDA Receptor Antagonists.....72

2.3 Discussion.....76
2.3.1 Organization of Reflex Responses.....76
2.3.2 Central Cholinergic Modulation.....80
2.3.3 Excitatory Amino-acidergic Transmission.....81

Chapter 3 OESOPHAGEAL REFLEXES: BRAINSTEM NEURONAL CORRELATES AND VAGAL AFFERENT TRANSMITTER.....84

3.1 Methods and Materials.....85

3.2 Results.....92
3.2.1 Distension-Evoked Medullary Multiunit Discharges *In Vivo*.....92
i. Localization of medullary oesophageal neurons.....92
ii. Segmental differences.....94
iii. Effect of vagotomy.....98
iv. Effect of curarization.....98
v. Effects of activation and blockade of mAChRs in ipsilateral NTS.....103
vi. Effects of activation and blockade of mAChRs in contralateral NTS.....110
vii. Effects of EAA antagonists.....110
3.2.2 Evoked Synaptic Responses in the NTS_c In Vitro.....113
i. EPSPs and miniature spikes.....113
ii. Effects of mAChR stimulation or blockade.....116
ii. Effect of EAA antagonists.....116
3.3 Discussion.....119
3.3.1 Functional Anatomical Considerations.....119
3.3.2 Premotor Connectivity.....121
3.3.3 Role of Reafferent Input.....123

3.3.4 Oesophageal Reflex Afferent Neurotransmission.....125

Chapter 4 CHOLINERGIC INPUT AND PATTERN GENERATION.....129

4.1 Methods and Materials.....131

4.2 Results.....135
4.2.1 Facilitatory Effects on Oesophageal Peristalsis of Muscarinic Stimulation.....135
4.2.2 Effects of Activation and Blockade of NTS_c mAChRs on Rhythmic Oesophageal, Cardiovascular and Respiratory Activity.....143
4.2.3 Responses of Oesophageal Motoneurons to Activation and Blockade of mAChRs in the NTS.....148
4.2.4 Effect of Curarization on Rhythmic Oesophagomotoneuronal Activity....153
4.2.5 Rhythmic AMB_c Neuronal Activity Induced by Activation of NTS_c mAChRs in a Brainstem Slice Preparation.....153
4.2.6 Effects of Stimulation and Inhibition of the ZIRP Region *In Vivo*.....164
4.2.7 Effects of Muscarinic Activation or ZIRP Stimulation on NTS_c Neuronal Response in Brainstem Slices.....164

4.3 Discussion.....169
4.3.1 Contributions of Cholinergic Mechanisms toEsophagomotorPatternGeneration.....169
4.3.2 Generation of Oesophagomotor Rhythm without Re-afferent Sensory Inputs.....174
4.3.3 Involvement of Propriobulbar Cholinergic Neurons.....179

Chapter 5 CHOLINERGIC AND GLUTAMATERGIC INTERACTION IN OESOPHAGOMOTOR RHYTHMOGENESIS.....181

5.1 Methods and Materials.....181

5.2 Results.....184
5.2.1 *In Vivo* Multi-Unit Discharges.....184
5.2.2 General Properties of Single NTS_c neurons *In Vitro*.....187
i. Spontaneous activity.....187
ii. Responses to intracellular current- or voltage-pulses.....198
5.2.3 Agonist-Driven Oscillations in Single Neurons.....203
i. NMDAR-driven oscillations.....205
ii. MAChR-driven oscillations.....214

5.3 Discussion....227
5.3.1 Oesophageal Premotor Rhythmic Activity....227
5.3.2 Identification of NTS_e Neurons in Brainstem Slices....229
5.3.3 Spontaneous Activity....230
5.3.4 NMDAR-Driven Burst Oscillations (0.5-0.9 Hz)....232
5.3.5 MAChR-Driven Slow Burst Oscillations....236
5.3.6 Physiological Implications....240

Chapter 6 SUMMARY AND SYNTHESIS....243

6.1 Summary....243

6.2 Synthesis....246

6.3 Further Directions....249

REFERENCES....252

FIGURES & TABLE

Figure 1.1 Schematic diagram showing oesophageal innervation.....3

Figure 2.1 Pressure-volume and diameter-volume relationship of the inflation balloon.....43

Figure 2.2 Segmental oesophageal responses to balloon inflation.....51

Figure 2.3 Propulsive nature of local oesophageal reflex elicited by inflation.....54

Figure 2.4 Coordinated oesophageal reflex response.....55

Figure 2.5 Coordinated response to distal oesophageal inflation.....57

Figure 2.6 Descending inhibition of rhythmic reflex response by proximal peristalsis.....58

Figure 2.7 Effect of acute unilateral vagotomy on the reflex oesophageal response...60

Figure 2.8 Inhibition of reflex oesophageal responses by curarization 61

Figure 2.9 Inhibition of the coordinated oesophageal reflex response by blockade of central muscarinic cholinoceptors.....64

Figure 2.10 Inhibition of reflex oesophageal responses by CNS-permeant, but not-impermeant mAChR antagonist.....65

Figure 2.11 Inhibition of type II response by mAChR antagonists applied to NTS surface.....68

Figure 2.12 Effects on reflex oesophageal response of intravenous acetylcholinesterase (AChE)-inhibitors.....70

Figure 2.13 Facilitation of reflex response by AChE-inhibitors applied to NTS surface.....73

Figure 2.14 Blockade of oesophageal reflex responses by NMDA receptor antagonists.....74

Figure 3.1 Distribution of medullary loci where unit-discharges are evoked by oesophageal distension.....90

Figure 3.2 Neural discharge patterns in brainstem recorded during distension-evoked reflex response of oesophagus.....93

Figure 3.3 Analysis of reflex-evoked rhythmic esophagomotor discharge pattern....95

Figure 3.4 Phase-relationship between type II esophagomotor burst discharges and oesophageal pressure wave activity 96

Figure 3.5 Effects of contra- and ipsilateral vagotomy on oesophageal distension-evoked neural discharges in medulla oblongata.....99

Figure 3.6 Effects of curarization on oesophageal distension-evoked activity at premotor and motoneuronal levels.....101

Figure 3.7 Effects of ipsilateral activation of NTS mAChRs on premotor and motoneuronal activity evoked by oesophageal inflation.....104

Figure 3.8 Effects of ipsilateral NTS muscarinic cholinoceptors blockade on premotor and motoneuronal activity evoked by oesophageal inflation....106

Figure 3.9 Effect of contralateral activation and blockade of NTS mAChRs on motoneuronal activity evoked by oesophageal inflation.....108

Figure 3.10 Effect of glutamate receptor blockade in the NTS_c on oesophageal inflation-evoked neural activity in the subnucleus centralis and nucleus ambiguus.....111

Figure 3.11 Excitatory postsynaptic potentials (EPSPs) evoked by solitary tract stimulation in the subnucleus centralis region.....114

Figure 3.12 Muscarinic effects on synaptic responses in the NTS_c.....115

Figure 3.13 Blocking effects of glutamate receptor antagonists on NTS_c synaptic response elicited by stimulation of solitary tract.....117

Figure 3.14 Elimination of evoked miniature spikes by blockade of glutamate but not muscarinic receptors.....118

Figure 4.1 Diagram illustrating procedure used to make oblique sagittal brainstem slice.....133

Figure 4.2 Demonstration of a central esophagomotor coupling mechanisms in rats.....136

Figure 4.3 Swallowing responses evoked by glutamate pulse-applied in swallowing loci of caudal portion of the intermediate NTS.....138

Figure 4.4 Facilitation of peristaltic esophagomotor propagation by inhibition of cholinesterase in the NTS.....140

Figure 4.5 Selective inhibition of oesophageal stage of swallowing by mAChR blockade in the NTS.....141

Figure 4.6 Rhythmic activity patterns in the oesophagus evoked by muscarinic activation.....144

Figure 4.7 Cardiovascular, respiratory and oesophageal responses to muscarinic cholinoceptor stimulation in the NTS.....146

Figure 4.8 *In vivo* esophagomotoneuronal activity in the compact formation of the nucleus ambiguus (AMB_c).....149

Figure 4.9 Effect of curarization on rhythmic esophagomotoneuronal activity....151

Figure 4.10 Esophagomotor rhythm generation in a medullary slice preparation...154

Figure 4.11 Effects on esophagomotor rhythm generation of mAChR activation or blockade in medullary slice preparation.....157

Figure 4.12 Difference in response pattern of oesophageal motoneurons evoked by stimulation of muscarinic and NMDA receptors in the NTS_c.....159

Figure 4.13 Effect of $GABA_A$ receptor stimulation in the ZIRP region on fictive peristalsis evoked by indirect and direct stimulation of mAChRs in the NTS.....162

Figure 4.14 Cholinergic facilitation of glutamate response in NTS_c cells.....165

Figure 4.15 Failure of glutamatergic chemostimulation in the ZIRP region to facilitate NTS_c excitatory response in oblique brainstem slice.....167

Figure 5.1 Unit discharge pattern in the NTS_c and motor response of the upper alimentary tract evoked by application of muscarine and NMDA to the ipsilateral solitarius complex.....185

Figure 5.2 Neurobiotin-labeled neurons in the NTS_c region.....188

Figure 5.3 Different types of spontaneous spiking activity of neurons in the NTS_c region.....190

Figure 5.4 Elimination of spontaneous firing of neurons in the NTS_c region by blockade of NMDARs.....192

Figure 5.5 Two examples of spontaneous burst-oscillations in the NTS_c region.....194

Figure 5.6 Effects of mAChR activation on membrane excitability.....196

Figure 5.7 Hyperpolarization-produced anomalous rectification followed by postinhibitory rebound (PIR).....200

Figure 5.8 Effect of muscarinic activation on PIR in the presence of tetrodotoxin.....201

Figure 5.9 Examples of voltage-dependent NMDAR-driven membrane oscillations of neurons in NTS_c region.....207

Figure 5.10 Loss of NMDAR-driven current oscillations in Mg^{2+}-free ACSF.....209

Figure 5.11 Disappearance of NMDAR-driven oscillations in Ca^{2+}-free medium...211

Figure 5.12 Dose-dependence of NMDA Oscillations.....212

Figure 5.13 Enhancement of NMDAR-driven oscillations by ACh.....213

Figure 5.14 Examples of ACh-driven slow burst-oscillations in neurons of the NTS_c region.....215

Figure 5.15 Restoration of TTX-sensitive mAChR-driven oscillations in two representative neurons by concurrent stimulation of NMDARs.....218

Figure 5.16 Suppression of mAChR-driven oscillations in neurons of the NTS_c region by NMDAR blockade.....220

Figure 5.17 NMDAR-mediated fast oscillations in TTX-sensitive mAChR-driven oscillator of the NTS_c region.....222

Figure 5.18 Modulation of NMDAR-mediated fast oscillations by muscarinic cholinoceptor stimulation.....223

Figure 5.19 Persistence of TTX-insensitive mAChR-driven oscillations in neurons in NTS_c region during NMDAR blockade.....224

Figure 5.20 Absence of oscillations during NMDAR stimulation in TTX-insensitive mAChR-driven oscillator.....225

Figure 6.1 Schematic diagram of postulated model of brainstem oesophagomotor network.....247

Table 5.1 Agonist-driven oscillations in the NTS_c.....204

ABBREVIATIONS

5-HT	5-hydroxytryptamine (serotonin)
ACh	acetylcholine
AChE	acetylcholinesterase
ACSF	artificial cerebrospinal fluid
ADP	afterdepolarization
AHP	afterhyperpolarization
AMB	nucleus ambiguus
AMB_c	compact formation of AMB
AMPA	alpha-amino-3-hydroxy-5-methyl-4-isoxazolepropionic acid
AP	area postrema
AP-5	D,L-2-amino-5-phosphonovaleric acid
AP-7	D,L-2-amino-7-phosphonoheptanoic acid
Bicu.	bicuculline
BP	blood pressure
BW284c51 (BW)	1,5-bis(4-allyldimethylammoniumphenyl)pentane-3-onedibromide
CD	cis-2-methyl-dimethylaminomethyl-1,3-dioxolane methiodide
CE	cervical oesophagus
ChAT	choline acetyltransferase
CGRP	calcitonin gene-related peptide
CPG	central pattern generator

CPP	3-((RS)-2-carboxypiperazin-4-yl)-propyl-1-phosphoric acid
CNQX	6-cyano-7-nitroquinoxaline-2,3-dione
DAB	3,3'-diaminobenzidine tetrachloride
D-β-E	dihydro-β-erythroidine
DE	distal oesophagus
DGG	γ-D-glutamylglycine
DMV	dorsal motor nucleus of the vagus
dTc	d-tubocurarine
EAA	excitatory amino acid
ENK	enkephalin
EPSP	excitatory postsynaptic potential
E.S.	electrical stimulation
GABA	gamma-aminobutyric acid
$GABA_AR$	$GABA_A$ receptor
Glu (G)	glutamate
I⁻	negative current
I⁺	positive current
I_A	transient potassium current
I_h (I_Q, I_{AR}, I_f)	hyperpolarization-activated inward K^+ and Na^+ current
$I_{K(Ca)}$ (I_{AHP})	calcium-activated potassium current responsible for afterhyperpolarization (AHP)

I_M	muscarinic receptor-suppressed potassium current
iGluR	ionotropic glutamate receptor
IPSP	inhibitory postsynaptic potential
IV	fourth ventricle
KA	kainate
Kyn.	kynurenate (kynurenic acid)
LES	lower oesophageal sphincter
mAChR	muscarinic cholinoceptor
mGluR	metabotropic glutamate receptor
mRNA	messenger ribonucleic acid
MK-801	(+)-5-methyl-10,11-dihydro-5H-dibenzo[a,d]-cyclohepten-5,10-imine
MSCP	scopolamine methylbromide
Mus.	muscarine
nAChR	nicotinic cholinoceptor
NADPH	nicotinamide adenine dinucleotide phosphate
NANC	non-adrenergic non-cholinergic
NE	noradrenaline
NG	nodose ganglion
NMDA	N-methyl-D-aspartate
NPY	neuropeptide Y

NO	nitric oxide
NOS	nitric oxide synthase
NTS	nucleus tractus solitarii
NTS_c	subnucleus centralis of NTS
NTS_{int}	subnucleus intermedialis of NTS
NTS_v	subnucleus ventralis of NTS
pl	picoliter
P	pharynx
P_i	intra-balloon pressure
PBS	phosphate-buffered saline
PIR	postinhibitory rebound
PTX	pertussis toxin
R	respiration
s	seconds
Scop.	scopolamine hydrobromide
SLN	superior laryngeal nerve
SP	substance P
SST	somatostatin
TMM	tunica muscularis mucosae
TMP	tunica muscularis propria
ST (ts)	solitary tract

TTX	tetrodotoxin
UES	upper oesophageal sphincter
VII_m	facial nucleus
V_T	threshold volume
W_T	weight
XII	hypoglossal nucleus
ZIRP	zona intermedialis reticularis parvicellularis of medulla oblongata

Chapter 1

INTRODUCTION

Swallowing serves such vital functions as the intake of nutrients and the protection of the upper airway. Based on its temporal sequence, swallowing has been described as having three phases, viz. the buccal (linguo-palatal), pharyngeal and oesophageal phase. In fact, the buccal and pharyngeal phases are often considered as one stage. Thus swallowing can be divided into the buccopharyngeal stage and the oesophageal stage (Doty,1968; Jean,1990). Though coupled during normal deglutition, the two stages may operate independently of each other, e.g. when oesophageal peristalsis is initiated by distension of the oesophagus. Therefore, oesophageal motility can be presumed to be controlled by a distinct neural network. Within the last fifteen years, substantial progress has been made in elucidating the brainstem networks controlling swallowing and oesophageal motility. These advances have been reviewed in depth (Bieger, 1991, 1993; Carpenter,1989; Christensen, 1984, 1987; Cunningham & Sawchenko,1990; Diamant and El-Sharkawy,1977; Diamant, 1989a,b; Gidda, 1985; Goyal & Cobb, 1981; Goyal and Crist, 1989; Hendrix, 1980; Jean,1984, 1990; Miller,1982, 1986, 1987; Miller et al., 1996; Roman,1982, 1986; Roman & Gonella, 1981, 1987). The mammalian oesophagus can be functionally divided into three portions comprising the upper oesophageal sphincter (UES), oesophageal body and lower oesophageal sphincter (LES) (Diamant, 1989a,b; Christensen,1987). In keeping with the main thrust of this dissertation, however, the following overview will address neural systems controlling peristaltic

motility in the oesophageal body.

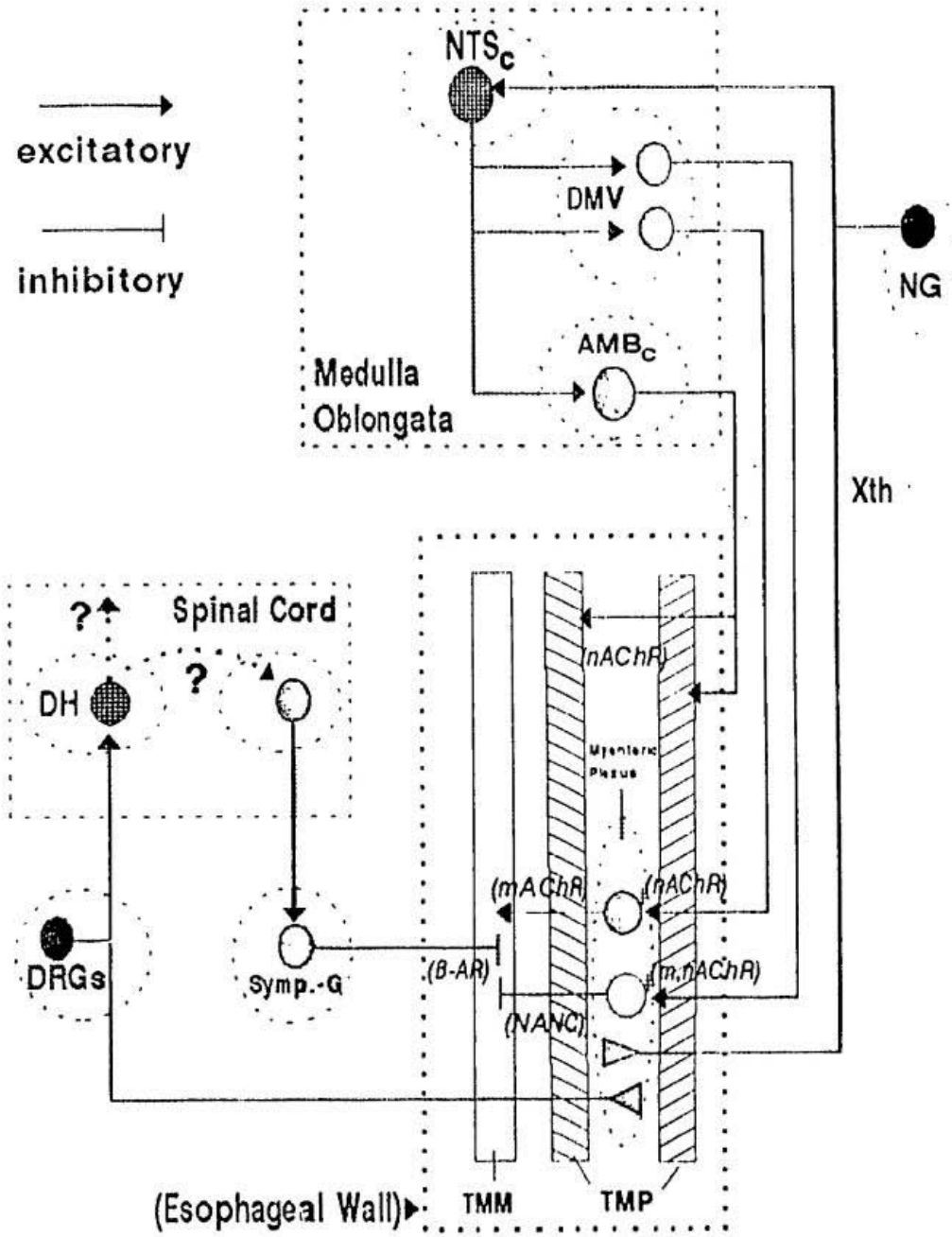
1.1 Esophagomotor Substrates

1.1.1 Oesophageal Musculature

The mammalian oesophageal body begins at the inferior border of the cricopharyngeus muscle and possesses two main muscle layers: the tunica muscularis propria (TMP) and the tunica muscularis mucosae (TMM). The TMP consists of two layers. Muscle fibres of the outer layer are arranged predominantly in the longitudinal axis, whereas those of the inner layer mainly have a circular orientation (Kauffmann et al.,1968). The arrangement in the rat is different from that of the human in that the muscle fibres of both TMP layers have a spiral orientation, with the outer layer running clockwise and the inner layer counterclockwise (Gruber,1978; Marsh & Bieger,1986). The TMP contains both striated and smooth muscle. The proportion of these two muscle types varies markedly among species. In the dog, sheep and rat, nearly the entire TMP is made up of striated muscle (Bieger,1993; Diamant,1989a,b; Miller,1982; Roman, 1982).In the human, cat and opossum, only the proximal segment of the oesophagus consists of striated muscle, whereas the distal segment gives way to smooth muscle at different levels (Diamant,1989a,b; Miller,1982; Roman,1982). During primary peristalsis, a ring of contraction moves in an uninterrupted sequence from the striated to the smooth muscle portion of the TMP. Lying between the TMP and the mucosa, the TMM of the rat oesophagus consists of bundles of obliquely oriented smooth muscle fibres throughout the length of the oesophagus. The rat TMM is thus capable of

Fig. 1.1 Schematic diagram showing oesophageal innervation. The shaded areas enclosed by dotted lines represent neural structures, including the medulla oblongata, spinal cord, peripheral extrinsic ganglia. Oesophageal musculature and myenteric plexus are shown in the open box (bottom-right). Abbreviations: AMB_c, compact formation of the nucleus ambiguus; DH, dorsal horn of spinal cord; DMV, dorsal motor nucleus of the vagus; DRGs, dorsal root ganglia; β-AR, β-adrenoceptor; mAChRs, muscarinic cholinoceptors; nAChRs, nicotinic cholinoceptors; NANC, non-adrenergic non-cholinergic fibers; NG, nodose ganglion; NTS_c, subnucleus centralis of the nucleus tractus solitarii; Symp.G, sympathetic ganglion; TMM, tunica muscularis mucosae; TMP, tunica muscularis propria; Xth, vagus nerve. (After: Bieger, 1993; Cunningham & Sawchenko, 1990; Christensen, 1987; Diamant, 1989a).

Oesophageal Innervation



producing longitudinal and transverse tension (Bieger & Triggle,1985). However, the contribution of the oesophageal TMM to bolus transport remains unclear (Bieger,1991).

1.1.2 Oesophageal Innervation

As shown in Fig. 1.1, the oesophagus is innervated by an *intrinsic plexus* and by *extrinsic vagal and sympathetic nerves*. Beside processing and conducting sensory information, the oesophageal innervation provides the peripheral mechanisms for excitation and/or inhibition of the TMP and TMM that underlie peristalsis.

1.1.2.1 *Intrinsic Innervation*

Lying between the two layers of the TMP, the myenteric nerve plexus is found in both the striated and smooth muscle regions of the oesophagus. The submucosal plexus surrounds the smooth muscle of the TMM (Christensen,1978).

In the striated muscle of the oesophagus, the myenteric plexus is believed to serve mainly a sensory role (Christensen,1987; Diamant,1989a,b). Interestingly, a nitrergic innervation of motor endplates from the myenteric neurons has been reported in the rat oesophagus (Neuhuber et al.,1994; Wörl et al.,1994). Thus, peripheral mechanisms controlling peristalsis in the striated muscle of the oesophagus may be more complex than hitherto assumed.

In the smooth muscle of the oesophagus, the intramural plexus contains at least two types of effector neurons: one capable of mediating cholinergic excitation of the smooth muscle predominantly through mAChRs, and the other mediating nonadrenergic,

noncholinergic (NANC) inhibition of the smooth muscle (Diamant,1989a; Miller et al., 1996). The transmitter released by the latter type of neurons is uncertain. Nitric oxide synthase (NOS) (Anand & Paterson,1994; Christinck et al.,1991; Murray et al.,1991) has been found in neurons in the myenteric plexus. Evidence accumulated in recent years suggests that intramural nitrergic neurons may be involved in the NANC inhibitory transmission in the oesophageal body and sphincter (Allescher et al.,1992; Bayguinov & Sanders,1993; Paterson & Indrakrishnan,1995; Tøttrup et al.,1991).

1.1.2.2 *Extrinsic Innervation*

i. *Vagal innervation*

a. Afferents. Vagal afferent fibres of the oesophagus arise from primary sensory neurons located in the nodose ganglion (Altschuler et al.,1989; Neuhuber,1987). Travelling in the cervical vagal trunk and superior laryngeal nerve (SLN), they project mainly to the myenteric ganglionic plexus of the striated and smooth muscle segments of the oesophagus (Christensen,1978; Neuhuber,1987). These abundant peripheral axonal terminals, perhaps associated with ganglion cells and other structures in the myenteric plexus, are considered to function as mechanoceptors responsive to oesophageal distension and contraction (Neuhuber,1987; Christensen,1984). The properties of these tension receptors have been described in electrophysiological studies (Falempin et al.,1978; Falempin & Rousseau,1984; Mei,1970; Mei et al.,1974). Tonic activity is recorded from some oesophageal vagal afferent fibres at rest (Andrew,1956; Mei,1970; Falempin et al.,1978), suggesting a role for tonic information flow from the periphery

in esophagomotor regulation. Based on the characteristics of the response to oesophageal distension, two types of oesophageal vagal afferent fibres have been identified in the opossum (Sengupta et al.,1989). Available data from studies on the sheep suggests that information coding the response to distension of the oesophageal wall and oesophageal contraction are conveyed by two different fibres (Falempin & Rousseau,1984; Sengupta et al.,1989). These vagal afferents play important roles in the regulation of esophagomotor function. Afferent fibres arising, at least in part, from muscle spindles have also been described in striated muscle of the dog oesophagus (Asaad et al.,1983). However, whether afferent fibres from muscle spindles exist in the oesophagus of other species and how such afferents participate in esophagomotor regulation remains unknown.

*b. **Brainstem pathways.*** In the last ten years, brainstem esophagomotor pathways have been delineated in finer detail, particularly in the rat. The central axons of oesophageal primary sensory neurons in the nodose ganglion project to a circumscribed region in the medulla oblongata, known as the **NTS_c** (Altschuler et al., 1989). It should be noted that some investigators (Ruggiero et al., 1990) have imputed other functions to the NTS_c, as part of the medial NTS, specifically in relation to baroreceptor and respiratory reflex regulation. The oesophageal afferents within the NTS_c have a crude organotopic distribution, in that fibres arising from more proximal levels of the oesophagus terminate at more rostral levels of the subnucleus (Altschuler et al., 1989). Preliminary anterograde tracing studies suggest that the central projection from the nodose ganglion to the NTS_c is uncrossed (Bieger, unpublished observation). As yet, the

vagal afferents to the NTS_c have not been characterized immunohistochemically. Therefore, clues as to the transmitter(s) utilized by these fibres are still tentative (Bieger, 1993).

Except for afferent inputs from the oesophagus, a paucity of inputs from other brain regions to the NTS_c has been noted in anatomical studies (Cunningham & Sawchenko, 1990). However, the dendro-architecture of NTS_c neurons is not sufficiently known. For instance, unpublished work in this laboratory has revealed that nicotinamide adenine dinucleotide phosphate (NADPH) diaphorase-positive NTS_c neurons send their dendritic processes dorso-laterally into adjacent solitary subnuclei, such as the intermediate subnucleus (NTS_{int}) which is thought to contain interneurons controlling the buccopharyngeal stage of swallowing.

Knowledge about the projection of NTS_c interneurons is only available from studies performed on the rat. The efferent projections of NTS_c neurons form loose bundles traversing the parvicellular reticular formation, to make monosynaptic contact with the rostral subdivision of the nucleus ambiguus (or ventral vagal complex), representing the AMB_c (Cunningham & Swachenko, 1989, Cunningham et al., 1991; Hashim, 1989). The majority of NTS_c efferent fibres converge onto the caudal pole of the AMB_c, then branch out into a dense neuropil that caudorostrally outlines the compact formation (Bieger, 1993). The AMB_c consists of vagal motoneurons that innervate oesophageal striated muscle (Bieger & Hopkins, 1987; Barrett et al., 1994). By virtue of their connectivity, the cells of the NTS_c thus fit the description of oesophageal second-order sensory neurons or oesophageal premotor neurons.

Output to the AMB_c from each NTS_c appears to be exclusively ipsilateral (Cunningham & Sawchenko, 1989), although cells in a medial subdivision of the NTS_c project to the contralateral NTS_c region (Hashim, 1989). In unilaterally vagotomized animals, activation of the NTS_c contra- but not ipsilaterally produces oesophageal peristalsis (Wang, 1992), suggesting the presence of two neuroanatomically defined medullary oesophagomotor pathways, one in each half of the brainstem.

There is no clear evidence that rat NTS_c interneurons send efferent processes to other medullary structures (Hashim 1989; Cunningham & Sawchenko 1989). However, preliminary studies with NADPH-diaphorase staining (unpublished observations) reveal that some dendrites of preganglionic neurons in the dorsal motor nucleus of the vagus (or dorsal vagal complex, DMV) intrude into the NTS_c and vice versa. Conceivably the DMV preganglionic neurons receive afferent inputs from the NTS_c or directly from oesophageal primary afferent fibres.

Anatomical studies related specifically to brainstem connectivity between dorsal (NTS) oesophageal interneurons and ventral (AMB) oesophageal motoneurons are lacking in non-rodent species. Interneurons and motoneurons involved in swallowing function in both sides of the brainstem are presently viewed by some investigators as a "swallowing center" (Diamant, 1989a, b; Jean, 1990; Roman, 1982). In this model of the "center", a dorsal coordinating structure in the NTS initiates and organizes the entire swallowing sequence, and the ventral coordinating structure in the reticular formation serves to "switch" the swallowing commands to the various swallowing motoneurons. However, in the rat, efferents from functionally identified deglutitive NTS loci can be traced to

virtually all motor nuclei known to contain motoneurons active in swallowing (Hashim, 1989). The direct pathway between NTS_c oesophageal interneurons and AMB_c oesophageal motoneurons is remarkable for its massiveness and the density of its terminal axons, and more to the point, it is not evident that NTS_c efferents project to the ventral medullary reticular formation (Cunningham & Sawchenko, 1989). Therefore, at least in the rat, the existence of "switching" interneurons within the ventral reticular formation remains uncertain.

*c. **Efferents.*** The vagal motor innervation differs according to the type of muscle supplied. In the striated muscle of the oesophagus, efferent fibres originate from motoneurons in the AMB_c. The projection of these motoneurons shows a crude rostrocaudal organotopy (Bieger & Hopkins, 1987). Axons of AMB_c neurons exit through the vagal trunk and two of its major branches, the SLN and the recurrent nerve (Bieger & Hopkins, 1987). Their terminals end on striated muscle cells, forming nicotinic cholinergic synapses analogous to the endplates of skeletal muscle fibres (Diamant, 1989a; Miller, 1982; Roman, 1982; Marsh & Bieger, 1986). Smooth muscle of the oesophagus, like that elsewhere in the digestive tract, is innervated by a vago-parasympathetic visceromotor pathway. Most likely the preganglionic cell bodies lie within the DMV (Collman et al., 1993). The axons of these DMV preganglionic neurons, travelling also in the vagal trunk, are relayed by parasympathetic postganglionic neurons located in intramural plexus (Diamant, 1989a). As discussed above, the muscarinic cholinergic and NANC neurons in the intramural plexus in turn send their postganglionic fibres to the oesophageal smooth muscle. By virtue of its innervation by intrinsic and extrinsic nerves,

the oesophageal smooth muscle is subject to integrated central and peripheral control.

ii. *Spinal innervation*

a. ***Afferents.*** Some neurons in the lower cervical and upper thoracic dorsal root ganglia send their peripheral axons to the oesophagus (Hazarika et al. 1964; Hudson & Cummings 1985). Centrally, these oesophageal afferents project to the dorsal horn. Oesophageal distension evokes unit discharges in the paravertebral sympathetic chain afferents of the opossum (Sengupta et al.,1990) and neuronal activity in the dorsal horn of rat spinal cord (Euchner-Wamser et al.,1993). The fibres of spinal afferents to the oesophagus contain substance P (SP) and calcitonin gene-related peptide (CGRP) and freely terminate in the submucosal and muscular layers of the oesophagus (Uddman et al.,1995). There is no physiological evidence to suggest that the spinal afferents are capable of independently mediating oesophageal motility. According to the consensus view, this non-vagal afferent pathway is involved in nociception of the oesophagus (Sengupta et al.,1990; Euchner-Wamser et al.,1993).

b. ***Efferents.*** Spinal efferent fibers to the oesophagus are derived from postganglionic noradrenergic neurons in the cervical and thoracic paravertebral sympathetic ganglia, which are innervated by sympathetic preganglionic neurons in the thoracic spinal cord (Hudson and Cummings,1985; Neil et al.,1980; Neuhuber et al.,1986). These noradrenergic fibres also contain neuropeptide Y (NPY) (Uddman et al., 1995) and innervate blood vessels, myenteric ganglia and muscular layers of the oesophagus at all segments. Under physiological conditions, noradrenaline (NE) appears to inhibit contractions of smooth muscle of the oesophagus, most probably via β-

receptors (Lyrenäs & Abrahamsson,1986).

1.2 Esophagomotor Patterns

The motor functions of the oesophagus are better understood than those of any other part of the mammalian alimentary tract because this region is more accessible to *in vivo* study (Christensen, 1987). Major aspects of the motility patterns of the oesophagus have been studied in humans (Andreollo et al.,1987; Baylis et al.,1955; Creamer & Schlegel,1957; Dodds et al.,1981; Fleshler et al., 1959; Hollis & Castell,1976; Paterson et al.,1991; Ren et al.,1993, 1995) and largely confirmed in experimental animals, such as the baboon (Roman & Tieffenbach,1972), rhesus monkey (Janssens, 1978), dog (Camp,1935; Harris et al.,1960; Janssens et al.,1974; Longhi & Jordan,1971; Meltzer,1907; Sellers & Titchen,1959; Valdez & SalapateK,1993), sheep (Falempin & Rousseau,1984; Jean, 1972a,b), cat (Blank et al.,1989; Greenwood et al.,1992; Mayrand et al., 1994; Miller,1972a; Mittal et al.,1990; Reynolds et al.,1985;), opossum (Christensen, 1970; Christensen & Lund,1969; Dodds et al.,1978; Gidda et al.,1981; Gidda & Buyniski,1986; Gilbert and Dodds,1986; Lund & Christensen,1969; Paterson et al.,1988, 1991), rabbit (cited from Meltzer,1907; Sumi,1964) and rat (Bieger, 1984; Hashim & Bieger,1989; Wang and Bieger,1991; Wang et al.,1991a,b,c). In anaesthetized animals, rhythmic or tonic contractions have not been recorded under resting conditions (Christensen 1987; Diamant 1989a), although spontaneous contractions reportedly occur in the distal oesophagus of patients with brain injury (Sinclair & Suter, 1987). The basic pattern of oesophageal movement is characterized by an orderly

propulsive contraction that passes from the upper oesophageal sphincter through the entire oesophageal body (Diamant & El-Sharkawy,1977). The pattern is generally described as ***peristalsis***. Oesophageal peristalsis has three principal modes of initiation.

1.2.1 Primary Peristalsis

When preceded by a voluntary or reflex swallow, the ensuing oesophageal contraction is called primary peristalsis (Meltzer, 1907). During repetitive swallowing, primary peristalsis does not necessarily follow buccopharyngeal deglutition in a one to one ratio. When repetitive swallowing is elicited in quick succession and a previous primary peristaltic wave progresses through the striated muscle oesophagus, a second swallow causes rapid and complete inhibition of the ongoing peristalsis that progresses no further (Hellemans et al.,1974). This phenomenon is known as "deglutitive inhibition of the oesophagus", resulting from cessation of excitatory discharges from the central program (Diamant & El-Sharkawy, 1977). Once the previous peristalsis has reached the smooth muscle oesophagus, it can proceed distally for at least 3 seconds after a second swallow, its amplitude diminishing progressively until it disappears. The disappearance of the contraction in the smooth muscle portion of the oesophagus may result from an absence of excitatory vagal efferent activity and activation of NANC inhibitory neurons (Diamant & El-Sharkawy, 1977).

1.2.2 Secondary Peristalsis

The presence of a bolus within the oesophageal lumen can also evoke propulsive

activity in the oesophageal body that closely resembles that initiated by swallowing. Meltzer (1907) termed bolus-evoked oesophageal activity *secondary peristalsis*. Under physiological conditions, secondary (reflex) peristalsis occurs when gastric contents reflux into the oesophagus, or a bolus of food remains in the oesophagus after primary peristalsis. If the contents are not completely propelled into the stomach by a single reflex peristaltic oesophageal contraction, rhythmic peristalsis is generated. Experimentally, an inflated freely-moving balloon can be propelled distally through the striated and smooth muscle segments of the oesophagus (Meltzer,1907; Roman,1982; Sellers & Titchen, 1959). When the balloon remains stationary in a portion of the oesophagus, distension evokes rhythmic peristaltic contractions in humans (Baylis et al., 1955), dogs (Sellers & Titchen, 1959) and sheep (Falempin & Rousseau,1984). Upon deflation of the stationary balloon, the oesophagus produces a propagated contraction below the point of stretch (Blank et al., 1989; Creamer & Schlegel, 1957; Christensen,1970; Fleshler et al., 1959; Paterson, 1991). This so-called "*off-response*" has been commonly referred to as secondary peristalsis by some investigators (Blank et al.,1989, Paterson, 1991), although its function has not been fully elucidated.

1.2.3 Tertiary Peristalsis

The smooth muscle portion of the opossum (Christensen & Lund,1969; Paterson & Indrakrishnan, 1995) and cat (Diamant,1974) oesophagus can generate a propulsive contraction *in vitro* in response to simply pinching the muscle, inflating the oesophagus with a balloon or electrical field stimulation of the intramural plexus. This type of

oesophageal motion is called ***"tertiary (autonomous) peristalsis"*** (Roman & Tieffenbach, 1972). When distension remains localized to a smooth muscle portion of the opossum oesophagus, three types of responses are generally recorded: The *"on"* response, a brief contraction above the point of distension, occurs following inflation of the distending balloon. The *"off"* response, consisting of either a simultaneous or propagated contraction of the oesophagus below the point of stretch, occurs after deflation of the balloon. The low-amplitude *"duration"* response, recorded at the lower segment, is sustained for the duration of the distension (Christensen and Lund,1969, Christensen, 1970). These three types of response have also been observed in the cat (Roman & Tieffenbach, 1972). The on- and off-responses involve circular muscle whereas the duration-response involves the longitudinal muscle and the muscularis mucosae (Roman, 1982). The on-response depends on vagal pathways and mACh transmission (Diamant & El-Sharkawy, 1977; Paterson, 1991). The off-response mechanism has been explained as a rebound response (Diamant & El-Sharkawy, 1977) that follows a hyperpolarization of the smooth muscle through activation of intramural nitric oxidergic inhibitory neurons (Anand & Paterson, 1994; Christinck et al., 1991; Murray et al.,1991; Tøttrup et al.,1991; Yamato et al.,1992). These complex motor responses presuppose the existence of integrated control mechanisms involving both extrinsic and intrinsic neural systems.

1.3 Neurophysiological Correlates

1.3.1 Mechanisms of Central Control

In the striated muscle oesophagus, both primary and secondary peristalsis are fully

dependent on brainstem mechanisms as both are abolished by bilateral vagotomy (Cannon, 1907; Higgs & Ellis,1965; Hwang et al.,1947; Roman,1966; Ueda et al.,1972) or reversible cooling of the vagal trunks (Reynolds et al.,1985). However, the question of control mechanisms directing and modulating peristalsis in the smooth muscle segment of the oesophagus has generated considerable debate (Diamant,1989a,b). On the one hand, output from the central program causes different efferent motor fibres to fire sequentially during both primary and secondary peristalsis in the smooth as well as the striated muscle oesophagus (Roman & Tieffenbach, 1972). On the other hand, the smooth muscle oesophagus can generate propulsive response *in vitro* to balloon inflation or electrical field stimulation (see section 1.2.3). Regarding the control of peristalsis in the smooth muscle, two hypotheses have been proposed (Diamant, 1989a,b). The first holds that a central mechanism programmes peristalsis and an intramural mechanism modulates the activity (Diamant, 1989a,b). The second hypothesis proposes that the central mechanism triggers the intramural mechanism, which then is primarily responsible for coordinating the peristalsis (Christensen, 1987). Studies to date have not established which hypothesis explains control of peristalsis in the smooth muscle oesophagus, but strong arguments can be made for a primary involvement of the central level in controlling smooth muscle peristalsis. For instance, the off-response is observed in both striated and smooth muscle portions of the cat oesophagus (Blank et al., 1989). In both baboon and opossum, vagal efferent fibres discharge with a timing that corresponds to the peristaltic contractions in both striated and smooth muscle segments (Roman & Tieffenbach, 1972). In the cat, neither primary nor secondary peristalsis occurs in the

smooth muscle oesophagus when the vagi are temporarily blocked in the neck (Reynolds et al., 1985). Since oesophageal peristalsis is a coordinated motor sequence throughout the oesophagus in normal swallowing, some investigators support the first hypothesis giving primacy to central control (Diamant, 1989a,b; Jean, 1990; Roman, 1982).

Likewise, two contrary hypotheses have been proposed to account for how the central nervous system controls the complete motor sequence of the pharyngeal and oesophageal phases of swallowing. Debate arose over the question of how much sensory input is needed for each successive stage of swallowing. Pioneered by Mosso (1876), the "*centralist*" view held that, once initiated, a swallow would progress through all its stages without the need of new afferent stimuli. Later, Meltzer (1899, 1907) postulated that swallowing-induced (primary) peristalsis is "practically a single reflex" but that bolus-initiated (secondary) peristalsis employs a mechanism that consists of a *"chain of reflexes"*, each movement stimulates peripheral receptors whose afferent impulses trigger the next movement. This hypothesis emphasizes the idea that sequential peripheral sensory input triggers and maintains patterned esophagomotor output. The debate between these hypotheses remains alive in contemporary research (Miller et al.,1996). Doty (1967, 1968, 1976) revived the concept of the swallowing center as a group of specific neurons whose coordinated action produces a stereotyped swallowing response. Roman (1982) called the central organizing system which programs deglutition a "*central chain of neurons*". In the contemporary literature (Miller,1982), the swallowing center has been referred to as a *"central pattern generator (CPG)"*.

1.3.2 Basic Mechanisms of Central Pattern Generation

A motor program is defined as " a set of muscle commands which are structured before a movement begins and which can be sent to the muscle with the correct timing so that the entire sequence is carried out in the absence of peripheral feedback" (Pearson, 1993). The neuronal network in which a motor program originates is termed "central pattern generator (CPG)". In recent years, the most extensive analysis of the organization of CPGs has been carried out in rhythmic motor systems (Pearson,1993). The operation of a CPG depends on the cellular, synaptic and network properties that constitute the building blocks of the CPG (Getting,1989). The mechanisms for pattern generation are diverse. CPGs can be formed from multiple functional neuronal circuits, i.e. a CPG can be divided into several small functional units. For instance, the isolated spinal cord can be divided into several smaller parts down to around three segments ["segmental circuitry" (Grillner et al.,1991)], each of which can produce fictive locomotor activity with intersegmental propulsion (Grillner et al.,1988). According to this concept, a pattern generating network is flexibly organized such that it can generate multiple motor patterns in the same set of muscle groups to allow functioning in different motor tasks (Getting, 1989; Pearson, 1993).

Although a motor program can be generated in an isolated CPG network without afferent input, no instance has been found in which the movement and the associated motor patterns are identical to those normally observed (Pearson,1993), indicating the importance of afferent input for pattern modulation. As reviewed by Pearson (1993), a CPG is believed to receive three different sources of input, including: (a) high level

commands; (b) peripheral sensory inputs; and (c) neuromodulatory input. The signal from the **high level command system** initiates the motor activity, but does not provide detailed information on the movement. **Peripheral sensory feedforward and feedback inputs** also trigger the CPG network and regulate the ongoing motor pattern by (1) establishing details of the temporal order, (2) controlling transitions from one phase of a movement to another in rhythmic activity and (3) reinforcing the motor output. **Neuromodulatory systems** (Harris-Warrick,1991) modify the output from the CPG in two ways: (1) modulating the intrinsic properties of voltage-gated ionic conductances in certain component neurons, thus facilitating/depressing ongoing motor acts, or initiating patterned motor activity; (2) presynaptically regulating transmitter release or postsynaptically modulating receptor-gated ion channel complexes to change the efficacy of synaptic activity in the circuit, so as to re-organize or switch the functional connectivity of the CPG from one mode to another. Thus, neuromodulators play a key role in motor pattern generation by establishing the configuration of a neuronal circuit for a specific behavioral pattern.

Certain neurons in a CPG network may play a key role in the motor pattern generation. For example, some neurons can generate rhythmic bursts of action potentials in the absence of phasic synaptic input. These oscillatory properties are determined by a combination of membrane ionic conductances. Oscillatory neurons often display bistable properties, or "plateau potentials". These neurons have two fairly stable potentials: a depolarized plateau state with tonic spikes and a hyperpolarized state with little or no activity (Llinás,1988). Many bursting neurons respond to hyperpolarization

with a rebound excitation that can trigger action potentials. This process, called postinhibitory rebound (PIR), has been invoked as an important mechanism in the generation of rhythmic motor patterns. PIR may result from activation of a low threshold Ca^{2+} conductance (Jahnsen & Llinás, 1984a,b) or activation of a hyperpolarization-activated inward cation current (Johnson & Getting, 1991) variously known as I_h, I_Q, I_{IR} or I_f (Hille,1992). I_h and I_h-mediated PIR are modulated by intracellular second messenger systems (Hille,1992). The PIR is also influenced by the transient K^+ current, I_A, which can delay or "merge" the PIR (Dekin, 1993). Terminating a burst, the Ca^{2+}-activated K^+ current ($I_{K(Ca)}$ or I_{AHP}), which generates a slow afterhyperpolarizing potential (AHP), plays an important role in regulating bursting-rhythms. The firing pattern of a cell can be profoundly affected by the slow AHPs. Inhibition of the slow AHP results in prolonged bursting (Hille,1992). Many bursting neurons are "conditional oscillators", i.e., they only burst in the presence of neuromodulatory substance. In such cases, modulatory neurons and related modulatory substances have pronounced influence on the properties of the ionic conductances in these neurons (Harris-Warrick,1991).

Central cholinergic transmission plays modulatory effects in many functional control systems. Most reported central cholinergic effects are mediated by mAChRs (Caulfield,1993). Muscarinic actions are frequently described as "slow" in comparison with nicotinic ones, because they result from modulation of ion fluxes via guanine nucleotide binding proteins (G-proteins) and the formation of second messengers (Caulfield, 1993). By pre- or postsynaptically up- or down-regulating voltage-gated K^+

or Ca^{2+} channels (Caulfield, 1993) or receptor-gated ion channels (Markram & Segal, 1990a, 1990b), hence modulating cellular or synaptic properties, mAChRs mediate diverse functional responses in the central nervous systems (CNS) (Caulfield, 1993a, b). For example, mAChR activation suppresses many K^+-conductances including the I_M (Halliwell & Adams, 1982), $I_{K(leak)}$ (Madison et al.,1987), $I_{K(Ca)}$ (Benardo & Prince, 1982; Cole & Nicoll, 1984) and selectively enhances NMDA receptor-mediated synaptic responses (Markram & Segal, 1990a) in hippocampal neurons. Inhibitory muscarinic effects are also observed in the CNS (Egan & North, 1986; McCormick & Prince, 1986). It appears that these are due to activation of a K^+ conductance (McCormick & Prince, 1986).

The apparent multiplicity of muscarinic effect in the CNS is not surprising in view of the diversity of mAChR subtypes. So far, five subtypes of mAChRs have been identified. There is general agreement that excitatory muscarinic actions are mediated by the M_1, M_3 and M_5 receptor subtypes coupled via a pertussis toxin (PTX) insensitive G-protein to activation of phospholipase C (Hulme et al.,1990; Caulfield, 1993). By contrast, hyperpolarizing responses in single neurons are mediated by M_2 and M_4 receptors via inhibiting adenylyl cyclase and opening of K^+ channels (Hulme et al.,1990; Caulfield, 1993). It should be appreciated, however, that the hyperpolarization may switch a neuron from one functional state to another. For instance, a mAChR-mediated hyperpolarization in thalamic reticular neurons has been proposed to de-inactivate a low-threshold Ca^{2+}-conductance which results in bursting discharge of the neuron (McCormick and Prince, 1986).

EAAs, mainly glutamate, are thought to mediate synaptic transmission at most fast excitatory synapses in the CNS (Cotman & Iversen,1987; Headley et al.,1987; Headley & Grillner,1990; Jahr & Stevens,1987; Larson-Prior et al.,1990;) via activation of different subtypes of ionotropic glutamate receptors (iGluRs), including AMPA/kainate and NMDA subtypes. Glutamate also activates receptors associated with G-protein, the metabotropic glutamate receptors (mGluRs). Glutamate neurotransmission in different synapses is mediated through distinct receptors. The AMPA/kainate receptors evoke fast, voltage-independent synaptic responses and in turn promote the activation of voltage-dependent NMDA receptors. The mGluR subtypes exert long-lasting actions through the activation and inhibition of intracellular signals (Nakanishi,1992).

By virtue of its voltage-dependence (Konnerth et al.,1990; MacDonald et al., 1982; MacDonald & Nowak,1990; Mayer et al.,1984), the NMDA receptor-channel complex mediates rhythmic plateau potentials in many mammalian CNS neurons, including interneurons and motor neurons in the spinal cord (Hochman et al.,1994a, 1994b), trigeminal motoneurons (Kim & Chandler,1995), nucleus basalis neurons (Khateb et al.,1995), supraoptic nucleus neurons (Hu & Bourque,1992) and neurons in the intermediate and ventral NTS (Tell & Jean, 1991a,b, 1993). These conditional pacemaker oscillations depend importantly on the voltage-dependence and the high permeability to Ca^{2+} of the NMDAR. The properties of the NMDA receptor-channel complex have been well studied (Ascher & Nowak, 1987; D'Angelo et al.,1990; Forsythe & Westbrook, 1988; Fox et al.,1990; Greengard et al.,1991; Jahr and Stevens, 1990; Johnson & Ascher, 1987; Kessler et al.,1989; Lerma,1992; Lerma et al.,1990;

Mayer et al.,1984; Mayer & Westbrook,1987; McLarnon & Curry,1990; Sah et al.,1989; Stone & Burton,1988; Thomson et al., 1989, 1990a,b). When the NMDAR-gated channel is opened by agonist-binding to the receptor, depolarization resulting from any mechanism relieves the Mg^{2+} blockade thereby further increasing the entry of Na^{+} and Ca^{2+}. Ca^{2+} influx through the NMDAR-gated channels and voltage-gated Ca^{2+} channels activates $I_{K(Ca)}$ that repolarizes the membrane and restores blockade of the channel by Mg^{2+}. If the NMDA receptor-channel complex remains activated, the membrane will again depolarize, thereby repeating the cycle of pacemaker-like oscillation (Grillner & Wallén, 1985b). The properties of the NMDA receptor-channel complex can be modulated by second-messenger systems (Wroblewski & Danysz, 1989).

1.3.3 Organization of "Swallowing Center"

It has long been realized that swallowing involves central control mechanisms (Mosso, 1876, Meltzer, 1907). Studies employing brain transections and lesions (Doty et al.,1967) showed that structures responsible for generating the basic motor activity of swallowing lie within the rhombencephalon, especially within the medulla oblongata. Based on the results from lesion experiments on the dog and cat, Doty et al. (1967) localized the "swallowing center" to a region of the pontine and medullary reticular formation extending from the rostral pole of the inferior olive to the posterior pole of the facial motor nucleus.

Studies employing extracellular recording in sheep and rats have provided more information about the medullary structures related to deglutition (Jean, 1972a; Jean, Car

& Roman, 1975; Kessler & Jean, 1985). These electrophysiological studies implicate the NTS as the principal neural substrate involved in the organization of swallowing. Electrical stimulation of the NTS and the adjacent ventrally situated reticular region evokes swallowing (Miller, 1972a,b; Kessler & Jean, 1985), whereas lesions of the medial part of the NTS selectively impair the oesophageal stage of swallowing evoked by electrical stimulation of the SLN (Jean, 1972a,b). Electrical stimulation of the SLN evokes single unit discharges in the NTS (Jean, 1972b; Kessler & Jean, 1985; Sessle & Henry, 1989). Sumi (1964) showed that neurons in the rostral NTS of the anaesthetized rabbit discharge to light touch of the pharyngolaryngeal mucosa or to pressure on a tooth. Furthermore, Jean (1972b) has recorded swallowing-related single neuronal discharges from the medulla oblongata in anaesthetized sheep by stimulation of the SLN and divided these neurons into a dorsal and a ventral group. The former lies in the NTS and adjacent reticular formation, whereas the latter resides in the reticular formation near the AMB. According to the time course of discharges prior to or subsequent to the onset of evoked pharyngeal activity, these neurons were classified into "early", "late" and "very late" - discharging neurons, implying that these neurons are related to functional control of different stages of swallowing (Jean, 1972b). This scheme has been corroborated in the rat (Kessler and Jean, 1985). Based on these experimental results, Jean (1990) proposed that the dorsal group of swallowing neurons executes overall deglutitive programming, whereas the ventral group performs a "switching" function by receiving input from the dorsal group and distributing output to individual motor nuclei. Roughly consistent with the anatomical findings, these neurophysiological studies have functionally given a

general view of the distribution of swallowing-related neurons in the medulla oblongata. However, it should be noted that SLN stimulation-evoked swallowing-related neuronal activity may be involved as well in the coordination of the swallowing synergy with other brainstem functions, because SLN stimulation elicits a complex response related to respiration, the cardiovascular system and swallowing (Sumi, 1963; Weerasuriya et al., 1980). Similarly, swallowing-loci determined by electrical stimulation or extracellular recording may not represent the medullary region where the cell bodies of swallowing neurons are located, because fibres of passage related to swallowing may well be stimulated or activity recorded from them. Nevertheless, repetitive swallowing is induced by microinjection of glutamate and glutamate agonists into the intermediate NTS (NTS_{int}) (Bieger, 1984; Hashim & Bieger, 1989; Hashim et al. 1989; Kessler et al., 1990; Wang 1992, Wang & Bieger 1991). Furthermore, NMDA receptor-mediated rhythmic bursting activity has been recorded in single neurons in the NTS_{int} region *in vitro*, suggesting a CPG mechanisms.

1.3.4 Esophagomotor Pattern Generator

Two functionally distinct CPGs have been postulated to control the pharyngeal and oesophageal phases of swallowing (Miller, 1982). However, evidence accumulated in recent years favours the CPG hypothesis mainly for the buccopharyngeal phase. The issue as to whether the coupled activity of the oesophageal stage is governed by a distinct CPG remains under debate.

The original studies by Mosso (1876) showed that oesophageal transection in dogs

did not completely prevent the progress of the primary peristaltic contraction. This has been substantiated by studies on the dog and rhesus monkey oesophagus by Janssens et al. (1976, 1978). They showed that neither oesophageal transection nor deviation of a bolus completely eliminated the peristaltic activity below the section. However, Longhi and Jordan (1971), demonstrated in the dog that the presence of a bolus in the oesophagus is necessary for maintenance of primary peristalsis. Deviation of the bolus abolished all peristaltic movement below the level of the bolus deviation. By suturing the central end of the proximally severed vagus to the accessory nerve, Roman (1966) demonstrated that motor activity could be sequentially recorded from the reinnervated sternomastoid muscle during evoked primary oesophageal peristalsis. However, given that the contralateral vagus still carries sensory input from the oesophagus to the medulla oblongata, this model fails to provide irrefutable evidence for the existence of an oesophageal CPG.

Swallowing-related "late" or "very late" discharges of NTS interneurons, which are also sensitive to oesophageal distension (Jean, 1972b), persist and the latency of onset remains unchanged after elimination of sensory feedback from striated muscle by motor paralysis (Jean, 1972b, Kessler & Jean, 1985). In this study, however, swallowing-related neuronal activity was elicited by electrical stimulation of the SLN. The same nerve probably contains sensory fibres supplying the upper oesophagus. Nevertheless, in baboons, evoked primary peristalsis in the smooth muscle oesophagus persists after the striated muscle of the cervical oesophagus is paralysed with curare (Roman & Tieffenbach, 1972). More to the point, in patients with poliomyelitis, in whom the

pharyngeal components were virtually absent, the oesophageal phase remained active during attempted swallows (Sanchez et al., 1953). These observations generally suggest that primary peristalsis is a centrally programmed motor event that once initiated may run its full sequence. Roman (1982) has claimed that the interneurons and motoneurons involved in both primary and secondary peristalsis are the same. During primary peristalsis the central chain of the deglutitive interneurons is excited from the start, whereas during secondary peristalsis the excitation starts at an internal link in the chain.

As discussed above, since the component stages of swallowing are known to function independently, the internuncial neuron pool or neuronal network for swallowing must either be capable of organising itself into different subcircuit configurations, or comprise anatomically distinct regions whose synaptic interconnections allow them to operate as independent substage synergies (Bieger, 1984; 1991). The available anatomical evidence in the rat (Altschuler et al., 1989; Bieger & Hopkins, 1987; Barrett et al., 1994) seems to favour the second viewpoint, in that the oesophagus striated muscle appears to be controlled by distinct medullary neural substrates, specifically the NTS_c-AMB_c pathway. To date neurophysiological aspects related to this esophagomotor pathway have not been reported in the literature, though neurotransmission mechanisms in the pathway have been well studied by neuropharmacological approaches (Bieger, 1984; Hashim & Bieger, 1989, Hashim et al. 1989; Wang & Bieger, 1991; Wang et al., 1991a,b,c; Wang 1992; Zhang et al., 1993).

Peripheral feedback is thought to be important to "finely tune" the coordinated esophagomotor pattern, although a medullary CPG network is able to program the motor

sequence in the absence of the peripheral inputs (Miller,1982). For example, the number of peristaltic contractions progressing through the oesophagus decreases with deflection of the bolus (Tieffenbach & Roman,1972; Janssens,1978), suggesting that continuous sensory feedback modifies the duration and intensity of motor output and may even maintain the excitability of the "center" or CPG (Miller,1982). Roman (1982) has proposed that excitation of the *central neuronal chain* is weaker during secondary than during primary peristalsis. If central excitation is not continuously reinforced by afferent feedback during secondary peristalsis, it will not proceed to the end of the chain.

Whereas many investigators agree that oesophageal peristalsis, at least in the striated muscle, is centrally programmed, the requirement for peripheral input from the oesophagus remains an issue under active investigation. Since neither the oesophageal sensory portion of the NTS nor the oesophageal motor portion of the AMB appears to receive particularly prominent input from other swallowing-related parts of the medulla, some authors have postulated that both primary and secondary peristalsis occur in response to oesophageal distension, with primary peristalsis being the result of passive opening of the UES and consequent exposure of the oesophageal lumen to atmospheric pressure (Cunningham and Sawchenko,1990). This viewpoint is incompatible with the CPG hypothesis since it postulates that peripheral sensory input to the brainstem is a prerequisite for both the initiation and maintenance of patterned esophagomotor activity.

1.4 Putative Transmitters in the Brainstem Esophagomotor Network

To avoid electrical stimulation of fibres of passage, chemo-microstimulation, i.e.

focal ejection of receptor agonists or antagonists in a confined deglutitive region, has been used for the selective activation of neurons in such loci. Bieger (1984) pioneered this pharmacological approach to map deglutitive response loci and to study the neurotransmitter mechanisms operating in the swallowing network in the rat brainstem. Progressively refined microinjection techniques applied in these studies not only enabled the deglutitive loci in the medulla to be mapped with increased precision, but also allowed the exploration of putative neurotransmitters utilized at synapses in these loci (Hashim & Bieger, 1989; Hashim et al., 1989). Since medullary esophagomotor circuitry can now be studied *in vitro* (Wang et al., 1991a,b; Wang et al., 1993; Zhang et al., 1993), it has been possible to apply specific pharmacological information obtained *in vivo* to study synaptic mechanisms at the single cell level.

1.4.1 Excitatory Transmitters in the NTS_c

i. *Acetylcholine*

Bieger (1984) demonstrated the importance of central mAChR-mediated processes in the control of oesophageal peristalsis in the rat. Thus, surface application of mAChR agonists to the NTS or micro-ejection of the agonists at intrasolitary loci overlapping with the NTS_c give rise to rhythmic peristaltic contractions of the oesophagus unaccompanied by phase-locked buccopharyngeal activity. This implies that activation of mAChRs in the NTS_c leads to patterned oesophagomotor activity. Moreover, the oesophageal component of reflex swallowing is readily suppressed following the intravenous adminstration of muscarinic antagonists such as scopolamine, which is capable of crossing the blood-brain

barrier. However, the quaternary compound, methscopolamine, is effective only at a ten-fold higher dosage (Bieger, 1984). A dense terminal field of choline-acetyltransferase (ChAT)-immunoreactive fibres is located in the NTS_c (Ruggiero et al., 1990). These findings strongly suggest that ACh is a neurotransmitter in the rat NTS_c and that the cholinergic innervation of the NTS_c makes a key contribution to oesophagomotor control.

It is relevant to note that in other species, including cat (Blank et al. 1989) and human (Paterson et al., 1991), oesophageal activity is also suppressed by systemic administration of mAChR antagonists. This effect has been attributed solely to a peripheral blockade of oesophageal smooth muscle (Blank et al., 1989; Diamant & El-Sharkawy, 1977; Paterson et al., 1991). However, a reduction in oesophageal striated muscle activity is also noted in the cat following intravenous application of atropine (Blank et al., 1989), a compound that is able to penetrate into the CNS. Therefore, it seems warranted to re-examine the interpretation of anticholinergic effects on esophagomotor function, since the effect of central mAChR blockade may have been overlooked in these studies.

The source of the cholinergic innervation of the NTS_c remains unknown. Moderate numbers of ChAT-positive cell bodies have been reported in two principal locations at the junction of the rostral and intermediate third of the NTS (Ruggiero et al., 1990): (i) the NTS_{int}, a region containing buccopharyngeal interneurons, and adjacent portions of the medial subnucleus (the dorsal portion of the NTS_c) and (ii) the ventral NTS (NTS_v); suggesting that significant numbers of cells are able to synthesize ACh in the NTS. A group of ChAT-positive neurons in the zona intermedialis reticularis

parvicellularis (ZIRP) have been retrogradely labeled by depositing tracer at functionally defined oesophageal loci in the NTS_c (Vyas et al., 1990; Wang, 1992). Therefore, the ZIRP is another possible propriobulbar source of the cholinergic innervation of the NTS_c. Given the paucity of the identified propriobulbar cholinergic inputs to the NTS_c and the presence of ChAT-immunoreactivity in a subset of neuronal perikarya in the nodose ganglion of rats (Palouzier et al., 1987), rabbits, cats, dogs and sheep (Falempin et al., 1989; Ternaux et al., 1989), the possibility that vagal afferents from the oesophagus are cholinergic warrants study.

Given the poor selectivity of mAChR antagonists, at present, the subtypes of mAChRs that mediate cholinergic responses in the NTS_c remain unknown.

ii. ***Excitatory amino acid***

In addition to ACh, studies by Bieger (1984) and Hashim and Bieger (1989) suggest that an EAA-like substance (glutamate or aspartate) is involved in oesophageal premotor control at the level of the NTS_c. The source of the EAA innervation is yet to be determined. Given that 1) glutamate has been identified as the main transmitter utilized by several types of vagal visceral sensory fibres terminating in the NTS (Andresen & Yang, 1990; Dietrich et al., 1982; Drewe et al., 1990; Perrone, 1981; Wang & Bradley, 1995), and 2) that the NTS_c receives afferents mainly from the periphery (Cunningham & Sawchenko, 1989, 1990), the possibility that the oesophageal vagal afferents are glutamatergic appears plausible.

NMDA is more potent in eliciting an oesophageal response than kainate and/or quisqualate when directly ejected at oesophageal loci in the NTS_c (Hashim & Bieger,

1989). Moreover, the selective NMDA receptor antagonists 2-amino-5-phosphonovaleric acid (AP-5) and 2-amino-7-phosphonoheptanoic acid (AP-7) consistently and reversibly block esophagomotor responses evoked by glutamate pressure-ejected in the NTS_c. A recent study employing *in situ* hybridization reveals that NTS_c oesophageal premotoneurons express NMDAR1 mRNA (Broussard et al., 1994). Taken together, these results suggest a preferential association of the NMDA receptor (NMDAR) with oesophageal premotoneurons.

iii. ***Nitric oxide***

Nitric oxide has been defined as a neurotransmitter in various central and peripheral neurotransmission processes (Fazeli, 1992; Garthwaite, 1991; Rand, 1992; Snyder, 1992). Studies with NADPH-diaphorase histochemistry have revealed dense nitric oxide synthase (NOS)-positive neurons and neuropil field in the NTS_c region (Ohta et al., 1993). Since NADPH diaphorase-positive neurons are present in the nodose ganglion (Lü et al., 1994), some investigators have postulated that the NOS-positive neuropil in the NTS_c are partially axonal terminals from peripheral afferents (Lü et al., 1994). An involvement of NO in oesophageal function in the premotor level remains to be determined.

1.4.2 Excitatory Transmitters in the NTS_{int}

i. ***Excitatory amino acid***

The NTS_{int} is coextensive with regions where early (buccopharnygeal) swallowing-related unit discharges are evoked by SLN stimulation (Kessler and Jean, 1985). In

addition, pharmacological study indicates that chemostimulation of the NTS_{int} with glutamate results in pharyngeal deglutition or complete swallowing (Bieger, 1984; Hashim and Bieger, 1989; Kessler et al.,1990; Kessler & Jean, 1991). This suggests that EAAs are transmitters in this region. In contrast to the effect in the NTS_{c}, kainate is most potent at pharyngeal loci in the NTS_{int} (Hashim & Bieger,1989). Applied to the surface of the NTS, kainate produces repetitive pharyngeal contractions (Hashim and Bieger, 1989; Wang and Bieger,1991). In addition, when applied to the NTS, small doses of NMDA evoke repetitive complete swallows, whereas larger doses of NMDA produce only repetitive pharyngomotor activity, not swallows (Bieger, personal communication). Ejection of NMDA near the NTS_{int} region produces rhythmic pharyngomotor activity (Kessler et al.,1990). NMDA-evoked rhythmic burst discharges have been recorded extracellularly by Tell and Jean (1990a) in neurons of the NTS_{int} *in vitro*. These authors speculate that these rhythmically bursting neurons belong to the swallowing CPG. In further studies (Tell & Jean, 1991b, 1993), they have observed membrane oscillations in a subset of NTS_{int} neurons in the presence of TTX, indicating conditional pacemaker oscillatory properties of these neurons.

ii. ***Other excitatory transmitters***

When applied to the surface of the NTS, several neurochemicals, such as serotonin (5-HT) (Bieger, 1981; Bieger et al.,1972; Bieger & Neuman, 1991; Hashim & Bieger, 1987), noradrenaline (NE) (Bieger, 1991), dopamine (Bieger,1974; Bieger et al., 1977), thyrotropin-releasing hormone (TRH) (Bieger, 1991) and vasopressin (Bieger, 1991) produce repetitive swallowing, suggesting that they are putative neuro-

mediators/modulators in NTS structures concerned with swallowing. It has been reported that TRH produces slow rhythmic membrane oscillations in NTS_c neurons in the presence of TTX (Dekin et al., 1985). The role of these substances in the NTS in deglutitive control remains unclear.

1.4.3 Inhibitory Transmitters at NTS Premotor Deglutitive Loci.

i. *γ-aminobutyric acid (GABA)*

Rhythmic oesophageal peristalsis can be induced by blockade of $GABA_A$ receptors with bicuculline ejected in the NTS_c (Wang & Bieger, 1991). When either applied to the NTS surface or pressure-ejected into the NTS_{int}, bicuculline evokes repetitive complete swallowing (Wang & Bieger,1991). These results suggest that: (1) GABA is an inhibitory transmitter utilized in the NTS premotor deglutitive loci; (2) there exist pharyngeal and oesophageal CPGs that are tonically inhibited by GABAergic innervation.

ii. *Other inhibitory transmitters*

In contrast to the effect of small doses of 5-HT and NE, large doses inhibit reflex swallowing when topically applied to the NTS surface or directly injected into the NTS (Kessler & Jean, 1986a, 1986b), suggesting involvement of additional receptor subtypes mediating these deglutitive responses. In addition, an enkephalin-like substance may function as an inhibitory transmitter in the NTS involved in the control of swallowing (Bieger,1991). In morphine-treated animals, application of naloxone, an antagonist at opioid receptors, produces repetitive swallowing (Bieger, Loomis & Young, 1991).

1.4.4 Transmitters in the AMB_C

i. *EAA*

Bieger (1984) demonstrated that glutamate, when ejected to the AMB_C, evokes a short latency oesophageal contraction. Subsequent neurophysiological studies have implicated an EAA as the primary transmitter in the solitary-ambigual esophagomotor pathway which acts at NMDA and AMPA receptor subtypes (Wang et al., 1991b). Thus, EPSPs in AMB_C neurons elicited by electrical stimulation of the solitary-ambigual pathway are completely eliminated by a combined blockade of EAA receptor subtypes (Wang et al., 1991b). *In situ* hybridization reveals that the NMDA receptor in the AMB_C is of NMDAR1 subtype (Broussard et al., 1994).

ii. *NO*

By combining trans-synaptic retrograde tracing with pseudorabies virus injected into the oesophagus and NADPH-diaphorase histochemistry treatment of brain sections, Wiedner et al. (1995) and Gai et al. (1995) demonstrated that most oesophageal premotoneurons in the NTS_C contain NOS and send their NOS positive terminals to the AMB_C surrounding oesophageal motoneurons. Thus NO could also be involved in transmission between oesophageal premotoneurons and motoneurons.

iii. *ACh*

When ejected into the AMB_C, ACh evokes short-latency oesophageal contractions (Bieger, 1984; Wang et al., 1991a). Both nicotinic acetylcholine receptors (nAChRs) and mAChRs have been demonstrated within the AMB_C (Arneric et al., 1990; Swanson et al., 1987; Wada et al., 1988, 1989). However, the response induced by ACh in the AMB_C

both *in vivo* (Bieger, 1984) and *in vitro* (Wang et al., 1991a; Zhang et al., 1993), unlike that evoked from the NTS_c, is not rhythmic and is scopolamine-resistant (Wang et al., 1991a; Zhang et al., 1993). Since ChAT-positive cell bodies are absent in the vast majority of NTS_c cells (Ruggiero et al., 1990), ACh does not appear to be a primary transmitter from NTS_c neurons projecting to the AMB_c, but instead is likely to arise from another source. Retrograde neuronal tracing combined with ChAT-immunocytochemistry reveals that the AMB_c receives a projection from a subpopulation of cholinergic neurons in the ZIRP. Electrical stimulation of this region in slices evokes fast EPSPs in AMB_c neurons that are inhibited by nAChR antagonists (Zhang et al., 1993). The physiological significance of this cholinergic innervation of oesophageal motoneurons remains unclear.

iv. ***Somatostatin (SST) and Enkephalin (ENK)***

Two peptides, SST and ENK, have been identified in two subpopulations of NTS_c neurons projecting to the AMB_c (Cunningham & Sawchenko, 1989; Cunningham et al., 1991). It is not known whether these peptides are associated with the main EAA transmitter in this pathway. SST inhibits cholinergic, while facilitating glutamatergic responses at the AMB_c oesophageal motoneurons (Wang et al., 1991c, 1993).

1.5 Research Plan

1.5.1 Rationale

Over the past ten years, knowledge of brainstem mechanisms controlling oesophageal peristalsis has advanced significantly, owing largely to studies in the rat.

Like other rodents, the rat employs mainly striated muscle for oesophageal bolus propulsion and thus seems ideally suited for the study of brainstem esophagomotor mechanisms, because the complexities inherent in intramural neural mechanisms regulating oesophageal smooth musculature are circumvented. Neurons in the rat NTS_c receive the majority, if not all, of the vagal afferents from the oesophagus and directly project to oesophageal motoneurons of the AMB_c, functioning as second order sensory and premotor neurons. Therefore, an esophagomotor pattern generator network is proposed to reside, at least partially, within the NTS_c.

ACh and EAA have been defined as major transmitter candidates in this interneuronal pool of the medullary circuit. At NTS_c interneurons, mAChRs, interacting with EAA receptors, are likely to play a key role in oesophagomotor pattern control. However, various aspects concerning the mode of operation of the NTS cholinergic mechanisms are as yet unclear, specifically as these relate to the following points:

First, blockade of mAChRs in the rat NTS_c eliminates primary oesophageal peristalsis, while activation of these receptors results in oesophageal peristalsis without pharyngomotor output, resembling secondary peristalsis in appearance. To date, however, secondary (reflex) oesophageal peristalsis in the rat has not been characterized, specifically with regard to the role of NTS mAChRs.

Second, while the NTS_c contains a dense ChAT-immunoreactive terminal field, the transmitter of oesophageal afferents to the NTS_c remains unknown. Given the paucity of identified propriobulbar inputs to the NTS_c (Cunningham & Sawchenko, 1990) and the demonstration of ChAT-immunoreactivity in nodose ganglionic perikarya in rats

(Palouzier et al., 1987) and rabbits (Ternaux et al.,1989), the visceral afferents from the oesophagus could be cholinergic. On the other hand, ChAT-positive neurons have been found in the NTS (Ruggiero et al.,1990) and another possible propriobulbar source of cholinergic input to the NTS has also been noted (Wang, 1992).

Third, the oesophageal peristalsis evoked by activation of subnucleus centralis mAChRs is characterized by its rhythmicity. As the hypothesized oesophageal CPG lacks unequivocal support, and in fact is questioned by some authors (Cunningham & Sawchenko, 1990), the issue of whether esophagomotor rhythmic activity is centrally generated or requires phasic peripheral afferent feedback needs to be resolved.

Fourth, nothing is known about the mechanisms by which cholinergic and non-cholinergic transmitter systems in the NTS_c interact in esophagomotor pattern generation.

These considerations prompt the following questions:

1. Is the cholinergic link in the NTS_c involved in secondary (reflex) oesophageal peristalsis and if so, how?

2. Does the cholinergic link represent vagal afferent or propriobulbar input?

3. Does the cholinergic link enable rhythmic esophagomotor output to be generated without peripheral sensory feedback?

4. Do cholinergic and EAA inputs interact in the NTS_c in esophagomotor rhythmogenesis and if so, how?

1.5.2 Hypotheses

Based on anatomical and pharmacological data obtained in the rat, the following working hypotheses are proposed:

i. By facilitating the excitability of the second order sensory neurons, the cholinergic link in the NTS_c is involved in, but may not be absolutely required for, the generation of secondary (reflex) peristalsis.

ii. As a corollary to hypothese (i), vagal afferent input from the oesophagus to the NTS_c employs an EAA, but not ACh, as transmitter.

iii. Commands from the deglutitive premotor neurons trigger the oesophageal premotor neurons through a central link to initiate primary oesophageal peristalsis. The cholinergic input to the NTS_c represents a component of this link which operates to (a) strengthen pharyngo-oesophageal stage-coupling and (b) enable oesophageal premotor neurons to generate rhythmic oesophageal peristalsis without peripheral sensory input.

iv. Mediating inputs from reflex afferents, iGluRs on NTS_c neurons, specifically those of the NMDA subtype, interact with mAChRs in the process of esophagomotor control and rhythmogenesis.

1.5.3 Objectives

To provide experimental support for the above hypotheses, four specific objectives will be pursued in the present study:

i. To characterize the reflex responses to balloon distension of the rat oesophagus with a view to determining the roles of cholinergic and EAAergic inputs to the NTS in the control of secondary peristalsis (Chapter 1).

ii. To investigate the putative transmitters utilized by oesophageal afferent fibres by determining the effects of iGluR and mAChR antagonists on evoked NTS_c neuronal activity (Chapter 2).

iii. To investigate *in vivo* and *in vitro* whether the patterned oesophagomotor activity can be generated without reafferent input and whether it depends on cholinergic input to the NTS_c (Chapter 3).

iv. To study *in vitro* how cholinergic modulatory inputs interact with EAAergic inputs in generating oesophageal premotor rhythm(s) on NTS_c interneurons (Chapter 4).

Chapter 2

OESOPHAGEAL REFLEXES: CHOLINERGIC AND GLUTAMATERGIC CONTROL

Secondary or distension-evoked reflex peristalsis serves to clear residue or refluxed gastric contents from the oesophagus into the stomach. Despite extensive studies in humans (Baylis et al.,1955; Creamer & Schlegel, 1957; Ren et al.,1995) and other species, including the dog (Meltzer, 1907; Sellers & Titchen, 1959), sheep (Falempin & Rousseau, 1984), cat (Blank et al.,1989) and opossum (Christensen, 1970; Paterson, 1991), knowledge of the underlying central control mechanism is still incomplete.

According to the prevailing hypothesis, oesophageal peristalsis is governed by a brainstem interneuronal network, most likely located in the NTS (Bieger, 1993; Jean, 1990; Roman,1982). The most detailed information about the connectivity of the brainstem esophagomotor reflex pathway has come from neuroanatomical studies in the rat (Altschuler et al.,1989; Barrett et al.,1994; Bieger & Hopkins,1987; Cunningham & Sawchenko,1989; Gai et al.,1995). In this species, neurons in the NTS_c function dually as second-order sensory element and major internuncial link between afferent and efferent fibers subserving oesophageal reflex peristalsis (Bieger,1993). To date, however, neither physiological nor pharmacological aspects of reflex oesophageal peristalsis have been investigated in the rat. Furthermore, both mAChRs (Wamsley et al.,1981) and NMDARs (Broussard et al.,1994) are present in the NTS_c and have been shown to mediate discrete esophagomotor responses (Bieger,1984; Hashim & Bieger,1989; Wang et al.,1991b).

Accordingly, mAChRs and NMDARs in the NTS_c appear to contribute to rat esophagomotor control.

The present work sought (1) to characterize esophagomotor responses to luminal distension and (2) to examine the involvement of cholinergic and EAA-ergic mechanisms operating at the level of oesophageal premotor neurons in the NTS region.

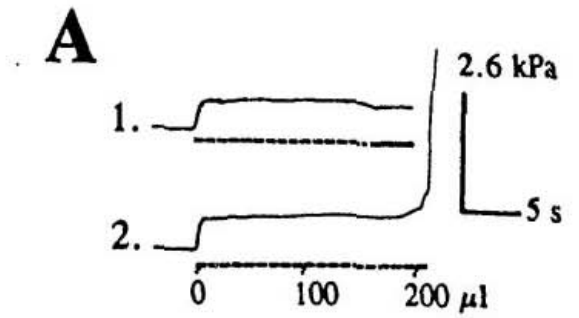
2.1 Methods and Materials

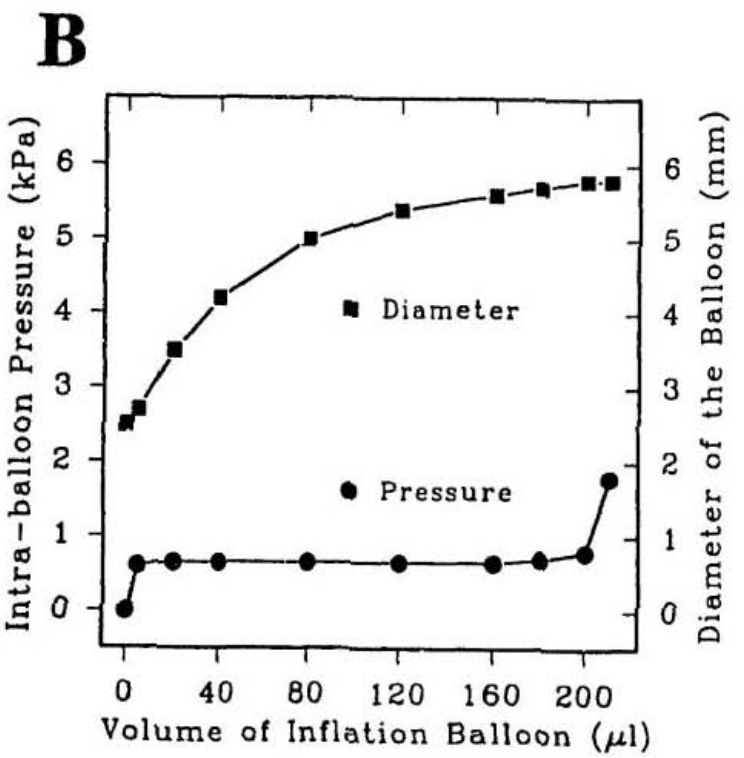
Experiments were performed in 72 adult male Sprague-Dawley rats weighing between 350 g and 450 g. After anaesthesia with intraperitoneal urethane (1.0-1.2 g/kg body wt), a tracheal tube was inserted and the right external jugular vein cannulated for intravenous infusion of saline and drugs. In some animals, the cervical vagi were isolated and looped with silk thread for subsequent vagotomy. Rats were maintained at a rectal temperature between 37.5-38°C by means of radiant heat and spontaneous respiratory activity derived from tidal pressure fluctuations was continuously recorded. D-tubocurarine (0.075 - 0.15 μmol/kg) was given by intravenous bolus while animals were artificially ventilated with oxygen-enriched air by means of a respirator (Harvard). Ventilation was maintained at a rate of 100 cycles.min^{-1} and a tidal volume of 2.5-3 ml.

2.1.1 Manometry and Distension Procedures

Miniature balloon-tipped catheters constructed from PE 90 polyethylene tubing were filled with water and connected by means of a three-way stopcock to pressure transducers. Pressure signals from each transducer were filtered (to reduce

Fig. 2.1. Pressure-volume and diameter-volume relationships of the inflation balloon as determined outside the animal. The maximal diameter of the fully inflated balloon is about 6 mm; the maximal unstressed volume about 210 μl. The balloon is filled with water by a syringe-pump at a fixed rate of 9 $\mu l.s^{-1}$. Broken portion of line beneath pressure traces (**A-1**, **2**) indicates the infusion period; during the solid portion (**A-1**) the infusion is stopped. At the start of infusion, a step increase in pressure is evident (**A-1** and **B**). This represents the pressure required to overcome the resistance to flow through the catheter into the balloon. Between 5 and 210 μl of injection, the transverse maximal diameter at the center of the balloon expands from 2.5 mm to 6.0 mm, with a negligible change in internal pressure (**A-2** and **B**), indicating the high compliance of the balloon. When the infusion volume exceeds 210 μl, a small increase in infusion volume causes an abrupt and large increase in intra-balloon pressure (**A-2** and **B**).


A
1.
2.
2.6 kPa
5 s
0
100
200 μl


B
Intra-balloon Pressure (kPa)
Diameter of the Balloon (mm)
Diameter
Pressure
0
1
2
3
4
5
6
0
40
80
120
160
200
Volume of Inflation Balloon (μl)

interference from cardiac and respiratory movements) at a frequency of 0.5-3 Hz and displayed on a polygraph (Grass, Model 7D). Balloons used for recording intraluminal pressure had an outer-diameter of $\leq$ 4 mm; balloons used for oesophageal distension had a diameter of 6 mm and a volume of 200-215 μl when fully inflated. The balloon for distension was filled with water (n = 68 / 72) or room air (n = 4 / 72) and connected in parallel to a 500 μl microsyringe. Oesophageal distension was accomplished manually or controlled by a variable speed syringe-pump (Sage Instruments, Model 355). The pressure-volume relationship and the diameter-volume relationship of the inflation balloon were determined before insertion into the oesophagus. As shown in Fig. 2.1, a small step increase in pressure during the first 5 μl injection represented the force required to keep water flowing into the balloon. Between 5 and 200 μl of filling volume, the diameter of the balloon expanded from 2.7 mm to 5.8 mm without further change in pressure, indicating a high compliance of the balloon. The length of the catheter from the centre of the balloon was marked in centimetres. Prior to insertion, the balloons were deflated and thickly coated with 2% xylocaine jelly. When positioned in the upper alimentary tract, the recording balloons were filled with 20-25 μl water and briefly equilibrated with atmospheric pressure.

2.1.2 Experimental Procedure I: Characterization of Reflex Responses

Segmental responses. Since under physiological conditions the strongest reflex contraction should occur just proximal to the food bolus, we first characterized the local motor response to inflation. The inflation balloon was designed to mimic bolus

stimulation. The inflation balloon was positioned in different segments of the cervical (CE) thoracic (TE) and distal (DE) oesophagus (Fig. 2.2). To reduce sensory adaptation, the inflation balloon was reduced in diameter to less than 3 mm during the interdistension interval. For distension of the oesophagus, the balloon was filled by means of the syringe-pump at a predetermined rate of 4.5 $\mu l.s^{-1}$ or 9.0 $\mu l.s^{-1}$. When an esophagomotor response was elicited, the pump was stopped and inflation maintained for 20 -50 seconds before the balloon was manually deflated and the pump reset. At each oesophageal level, at least four consistent distension trials were performed.

The smallest inflation-volume (μl) that elicited a reproducible oesophageal response was defined as the threshold volume (V_T). The V_T values were determined by recording both syringe plunger displacement and duration of the pump on-cycle. To examine whether the distension-produced oesophageal contraction was propulsive, the inflation balloon was left free to move during the distension. In addition, to record any aboral movement of the inflated balloon, the balloon catheter was tethered to a tension transducer (Fig. 2.3) in some experiments.

Multi-segmental responses. To examine responses of the entire oesophageal body to local inflation, the placement of manometric catheters was arranged in two ways. For observation of *proximal and distal responses to distension of the thoracic oesophagus*, the inflation balloon was positioned in the thoracic segment (9 cm from upper incisors). Two additional recording balloons were placed 1-2 cm distal and proximal to the inflation balloon. For investigating *proximal responses to distension of the distal oesophagus*, the inflation balloon was positioned in the distal oesophagus (1 l

cm from upper incisors) and two proximal recording balloons were located in the cervical and thoracic oesophagus, respectively. In most of the experiments, a recording balloon was positioned in the pharynx (P) to monitor pharyngeal response, if any, during the oesophageal distension. Correct positioning of the balloons was not only based on measuring the intraluminal length of the manometric catheters but also ascertained by intra-tracheal tactile stimulation-induced reflex swallowing which resulted in a propulsive oesophageal contraction. In most of these experiments, V_T was first determined by a ramp inflation and subsequent oesophageal distensions were manually performed with one-step injection. To examine the inflation volume-response relationship, serial oesophageal distensions were performed with volumes being increased by 5 or 10 μl steps.

Vagotomy. Effects of uni- and bilateral vagotomy were examined in animals breathing spontaneously. The cervical vagal trunk was gently dissected free and severed with micro-scissors. Post-vagotomy reflex oesophageal responses were tested up to 40 minutes.

Post-mortem studies At the termination of the experiment, the position of the balloons was visually identified in 23 animals and the intraluminal length of the manometric catheters was re-checked after an intravenous overdose of urethane and a thoracotomy. For male rats weighing 400 grams, the total length of oesophagus was about 9 cm. The length from the upper incisors to the pharyngo-oesophageal junction, first rib, diaphragm and cardia were about 4 cm, 7 cm, 11 cm and 13 cm, respectively. With the centre of the inflation balloon being taken to indicate the segment distended,

the CE, TE and DE were located 4-7 cm, 7-10 cm and 10-13 cm from the upper incisors. Considering the movement of the diaphragm with respiratory cycles, the segment 10 to 12 cm from the upper incisor was defined as the intraeural portion of the oesophagus.

2.1.3 Experimental Procedures II: Pharmacological Studies

Drug application. To investigate the role of cholinergic and EAA-ergic mechanisms in oesophageal premotor reflex control, mAChR and NMDAR antagonists were either given by intravenous bolus injection or topically applied to the medulla oblongata.

For topical applications, the animals were mounted in a stereotaxic frame after manometric catheters were secured in their appropriate positions. The caudal roof of the fourth ventricle and surrounding structures of the dorsal medulla were surgically exposed under a dissection microscope. Cerebrospinal fluid was drained continuously with a wick. Drug solutions were applied by means of a microliter-syringe to the extraventricular surface of the NTS region, including an area 0 -100 μm rostral to the cranial edge of the area postrema and between 500 - 700 μm lateral to the midline. For control, drugs were applied to adjacent sites on the dorsal surface of the medulla oblongata as follows: i) the midline at the cranial edge of the area postrema (AP); ii) 1150 to 1250 μm lateral to the midline at the cranial margin of the AP; iii) 500 μm rostral to the cranial margin of the AP and 800 to 900 μm lateral to the midline. The volume applied was kept within 0.05 µl in order to minimize drug spread beyond the targeted region.

In some animals, drugs were pneumophoretically applied in the NTS_c or the AMB_c by means of a three-barrel glass micro-pipette. Each barrel of the micropipete was filled with a different drug solution. Drugs were pressure-ejected by means of a nitrogen-pressured Picrospritzer pump (General Valve Corp). The volume ejected with each pressure pulse was estimated by measuring the diameter of the ejected droplet under a microscope equipped with a calibration eyepiece and was kept in the range of 20 -100 pl. The doses stated in the results are estimates based on detective limit of 10 pl. As described previously (Bieger 1984; Hashim & Bieger 1989; Hashim et al. 1989; Wang et al. 1991b), this protocol permitted accurate location of swallowing substrates associated with both the NTS and AMB. At these loci, a glutamate pulse invariably evoked a short-latency (< 1 s) pharyngeal or oesophageal pressure wave. Extensive characterization of the swallowing response to stimulation loci within the NTS has previously been carried out in this laboratory and has established that the buccopharyngeal and oesophageal sites are coextensive with the NTS_{int} and NTS_c, respectively.

Drugs used. Physostigmine, 1,5-bis(4-allyldimethylammoniumphenyl)pentan-3-one dibromide (BW284c51), DL-muscarine, scopolamine, methscopolamine, glutamate, (±)-2-amino-5-phosphonopentanoic acid (AP-5), γ-D-glutamyl-glycine (γ-DGG) and D-tubocurarine were obtained from Sigma Chemical Company; 6-cyano-7-nitroquinoxaline-2,3-dione (CNQX) from Research Biochemical International (RBI); ketamine hydrochloride from Rogar/STB Inc (London, Ont.) and dihydro-β-erythroidine (D-β-E) was a gift from Merck Sharp & Dohme Res. Lab..

2.1.4 Data Analysis

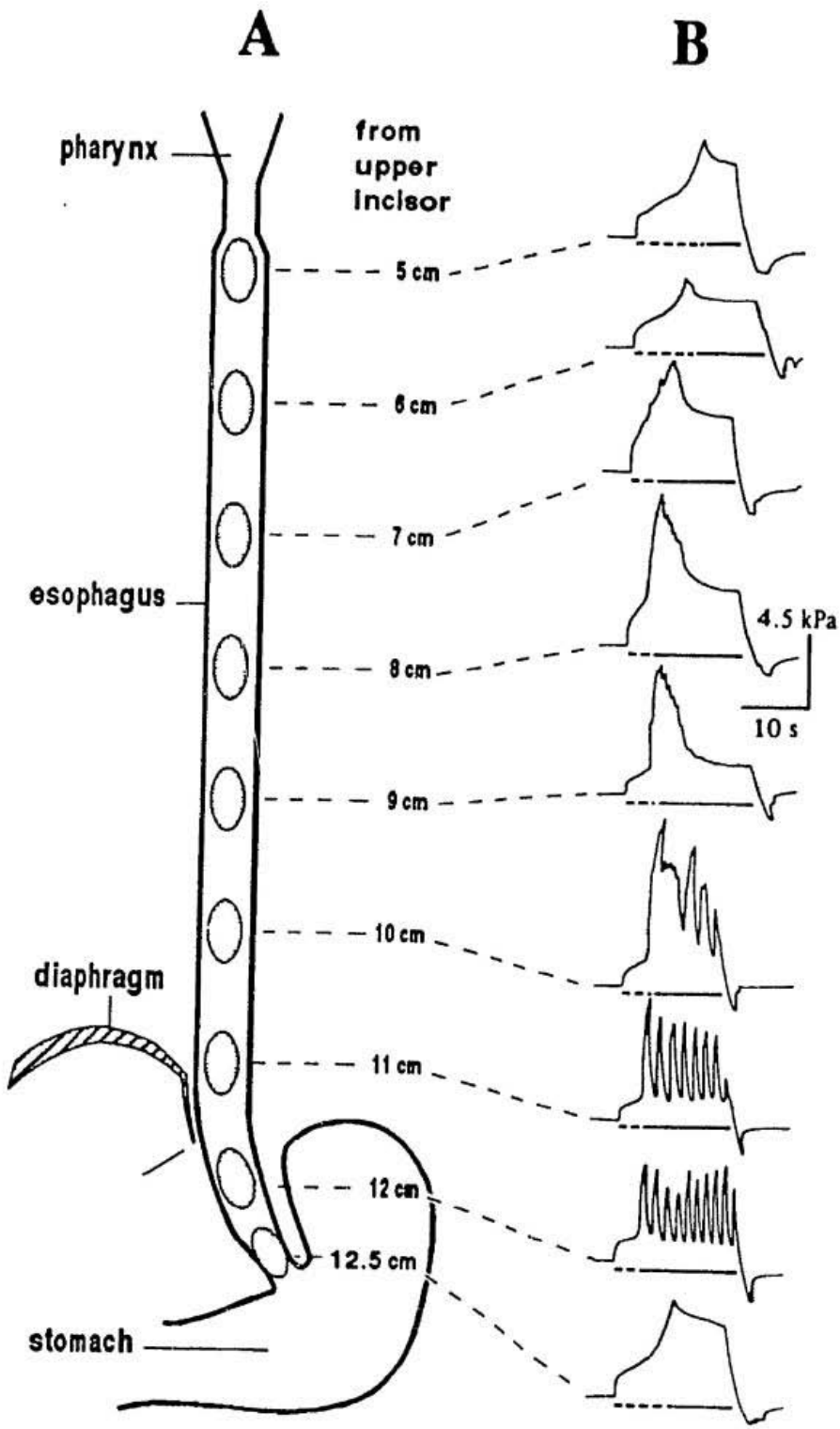
To ensure reproducibility of oesophageal reflex responses, the interval between distension trials in each protocol was kept between 2-3 min, and vagotomy and drug applications were performed after at least four consistent control responses were obtained in each oesophageal segment. Although reversible drug effects were repeated at least twice in each animal, only responses obtained in the first trial were used for quantitative analyses. The V_T and the mean amplitude of oesophageal pressure waves evoked before and after experimental manipulation were compared in each group of animals. The mean amplitude of rhythmic responses was calculated by averaging the amplitudes of pressure waves during the first 10 seconds of inflation. Graphs were constructed using a software package (SigmaPlot, Jandel Scientific). Data were expressed as means $\pm$ standard errors of the mean (S.E.M); the significance of differences was examined with Student's paired *t*-test at a $P < 0.05$.

2.2 Results

2.2.1 Characterization of Reflex Responses

Segmental patterns. Balloon distension applied at successive 1 cm intervals along the length of the oesophagus revealed consistent differences in responses between cervical, thoracic and intracrural portions, as evidenced by the pattern of the response elicited (n = 7). A representive example is depicted in Fig. 2.2. In the upper to mid-cervical portion, responses were variable or absent even at filling volumes of 100 to 150

Fig. 2.2 Segmental oesophageal responses to balloon inflation. **A.** Schematic diagram of rat oesophagus and balloon placements in oesophageal body. Positions are indicated with respect to distance from the upper incisors to the centre of the balloon. **B.** Intra-balloon pressure changes in different segments of oesophageal body during inflation at pump rate of 9 $\mu l.s^{-1}$ indicated by a broken line under each pressure trace. During the interval marked by the solid line, the pump is stopped until the balloon is manually deflated. Note the proximo-distal change in reflex responses from monophasic slow wave (type I) to repetitive fast wave (type II) activity. Superimposed small waves seen at levels 8-10 cm are synchronous with the respiratory cycle.


A
B
pharynx
from
upper
incisor
5 cm
6 cm
7 cm
esophagus
4.5 kPa
8 cm
10 s
9 cm
10 cm
diaphragm
11 cm
12 cm
12.5 cm
stomach

μl. In the lower cervical portion, a monophasic pressure wave was consistently seen at inflation volumes of 60 to 80 μl in 3 out of 7 animals tested. In the upper thoracic portion, a single monophasic pressure wave was reproducibly elicited in all cases. At low thoracic levels, either single monophasic or repetitive pressure waves were observed. The intracrural portion typically responded with robust repetitive activity. A local response to distension was usually absent when the inflation balloon was positioned at or near the gastroesophageal junction (12.5 or 13 cm level) (Fig. 2.2) although in one case a variable monophasic pressure wave was obtained. V_T values varied among animals (ranged from 40 to 70 μl; 62 $\pm$ 6.5 μl; n = 14); however, in a given preparation, V_T and amplitude of the evoked pressure wave(s) remained consistent for 2-3 hours, provided that inflation was applied at 2-3 min intervals.

The monophasic waves in the cervical and thoracic oesophagus, hereafter referred to as *type I* response, showed a relatively steep rise and a slow decay. Wave duration ranged from 4 to 9 s (5.3 $\pm$ 0.3 s; n = 21 trials in 7 animals). Repetitive pressure waves in the intracrural oesophagus, hereafter designated as *type II* response, had a highly regular rhythm in the range of 0.5 to 0.8 Hz (0.65 $\pm$ 0.1 Hz; n = 55). Individual waves had a mean duration of 0.89 $\pm$ 0.09 s (n = 50 waves from 10 operations on 10 animals) and a sawtooth-like configuration characterized by a steep rising phase followed by an abrupt relaxation. The mean amplitude of *type II* waves increased with the inflation volume (n = 14) from 3.0 $\pm$ 0.32 kPa at threshold to a maximum of 6.6 $\pm$ 0.5 Kpa at 75 to 80 μl.

When the inflation balloon was positioned in the thoracic oesophagus and left

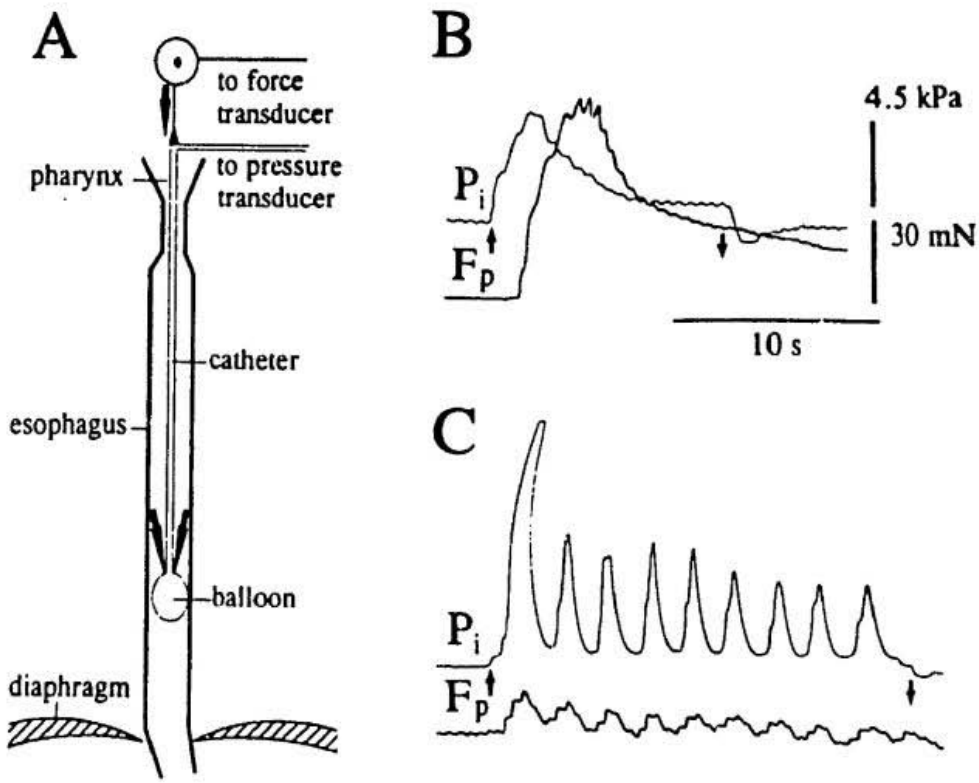


Fig. 2.3 Propulsive nature of the local oesophageal reflex elicited by inflation. **A.** Diagram showing experimental setup for simultaneous recording of intra-balloon pressure and aboral movement of catheter. **B.** When the tethered balloon is positioned in the thoracic portion of the oesophagus, rapid step inflation (↑) evokes a monophasic pressure wave followed by a monophasic force wave, indicating that the inflated balloon is propelled distally. The balloon does not return to the starting position as indicated by persistence of force after balloon deflation (↓). **C.** When the balloon is located in the intracrural portion, the rapid step inflation produces rhythmic force waves that follow rhythmic pressure waves in a phase-locked manner. Abbreviations: P_i, intra-balloon pressure; F_p, pulling force. Superimposed rapid wave activity is of respiratory origin.

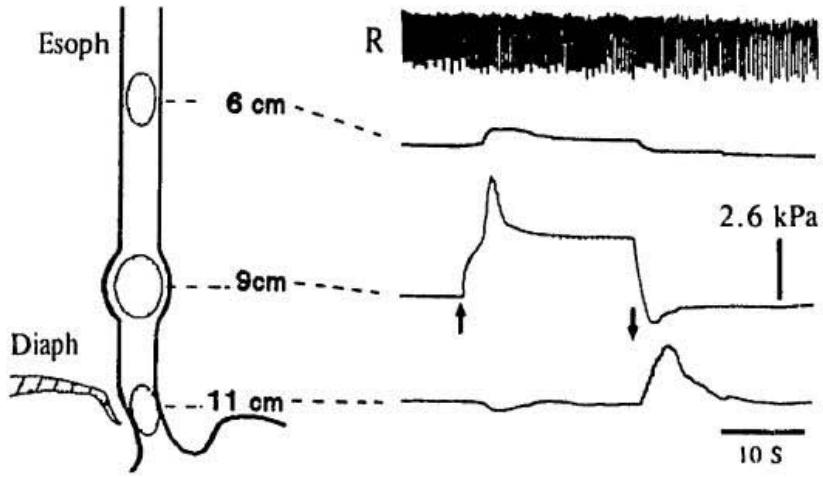


Fig. 2.4 Coordinated oesophageal reflex response. Three intraesophageal balloons are positioned at the depths indicated. One-step sustained inflation (↑) of the middle balloon evokes a high amplitude pressure wave in the distended segment coinciding with a low amplitude pressure rise in the proximal segment and a phasic pressure drop in the distal segment. Upon deflation (↓), a monophasic pressure wave is elicited in the distal segment. Rate and depth of respiration (R) remains unaltered during inflation of the oesophagus.

mobile, inflation resulted in a visible aboral movement. The latter could also be recorded as an aboral pulling force accompanying the reflex-evoked pressure activity (Fig. 2.3).

Coordinated responses. As recorded by a 3-balloon assembly (Fig. 2.4), the inflation-evoked monophasic (*type I*) pressure wave in the distended segment was accompanied by a low-amplitude sustained rise in pressure recorded in the adjacent oral segment (n = 10 / 10). In the segment aboral to the distension, intraluminal pressure showed a small transient drop (Fig. 2.4; n = 2 / 10), a small phasic rise (n = 5 / 10) or remained unchanged (n = 3 / 10). Except for one case where the monophasic pressure wave propagated from the inflated (thoracic) segment to the distal oesophagus (not shown), the *"inflation responses"* evoked above, at and below the stimulated segment occurred in a synchronous (non-propagated) manner. In most cases (n= 7 / 10), the pressure wave in the oral segment outlasted that in the inflated segment. Upon rapid, but not slow, deflation, a pressure wave invariably occurred in the aboral segment (Fig. 2.4). In the thoracic portion, the "*deflation-response*" was highly reproducible in all preparations tested (10 to 15 trials per animal, n = 10). In the cervical portion, however, a "*deflation-response*" could not be evoked in a reproducible manner. The "*deflation-response*" typically consisted of a monophasic pressure wave but occasionally showed a rhythmic pattern.

When inflation was applied via the distal-most balloon in the intracrural portion (11 or 12 cm level) of the oesophagus (Fig. 2.5), an attenuated *type II* response was recorded 2 cm proximal to the inflation balloon, while the cervical oesophagus remained quiescent. As shown at faster-speed records (Fig. 2.5B), the thoracic led distal pressure

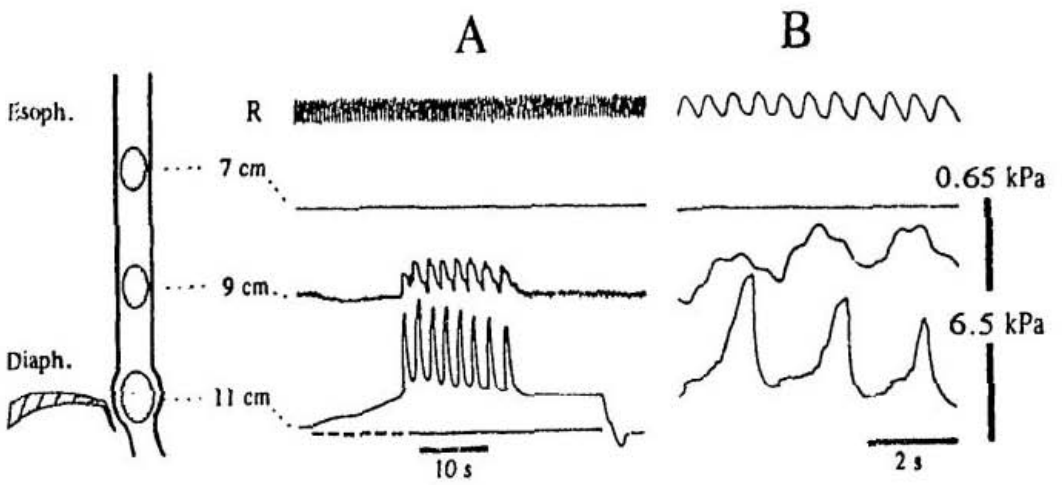


Fig. 2.5 Coordinated responses to distal oesophageal inflation. The distal balloon is filled at a pump rate of 4.5 $\mu l.s^{-1}$ indicated by the dashed line and kept inflated for a period indicated by the solid line. **A.** Evoked rhythmic pressure waves are present at the thoracic (9 cm) level and in the distended distal segment, but not at the upper thoracic (7 cm) level. **B.** Trace recorded at a faster speed shows that each pressure wave in the lower thoracic oesophagus precedes the pressure wave in the distal segment in a phase-locked manner. Note the different shape of the pressure waves recorded at the two levels.

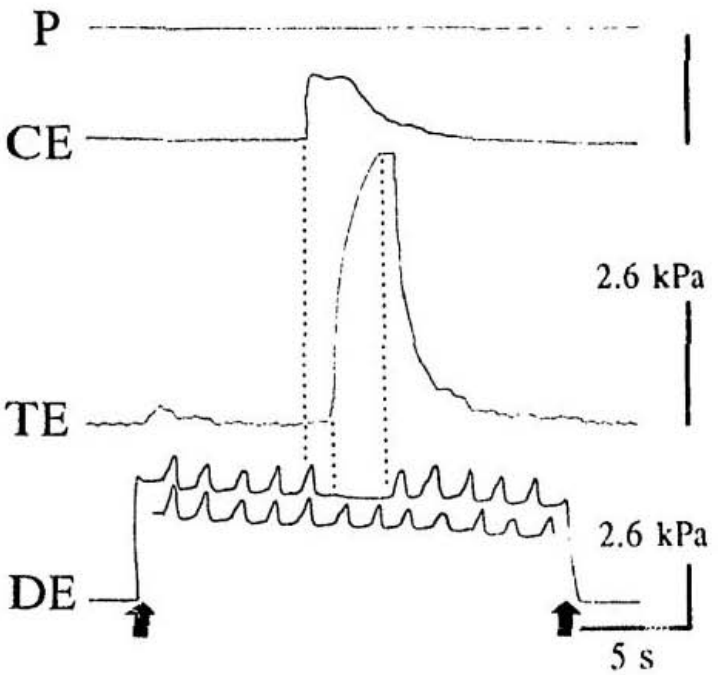


Fig. 2.6 Descending inhibition of rhythmic reflex response by proximal peristalsis. When a propulsive pressure wave in the cervical (CE) and thoracic oesophagus (TE) coincides with rhythmic reflex activity in the distal oesophagus (DE) evoked by distension (↑, inflation; ↓, deflation), the proximal pressure wave fails to propagate distally but depresses the rhythmic reflex response. A control rhythmic response is shown under the distal-pressure trace. Note a phase-shift of the rhythmic activity after a descending inhibition. The distal balloon is filled with room air, thus the pressure wave is attenuated. P, pharynx.

waves in a phase-locked manner although the pressure waves in the two portions showed distinct wave shapes. Depth and rate of respiration were unchanged during the type II response (Fig. 2.5).

The distension-evoked oesophageal pressure waves were occasionally associated with propulsive pressure waves in the proximal oesophagus. However, when a proximal peristaltic pressure wave coincided with *type II* rhythmic activity in the distal oesophagus, the proximal wave failed to propagate into the inflated segment, and instead was accompanied by an instantaneous inhibition of the coincident distal waves with resetting of the rhythm (Fig. 2.6).

2.2.2 Effects of Vagotomy and Curarization

Vagotomy. After unilateral vagotomy, the *type I* response in the thoracic oesophagus disappeared (Fig. 2.7A, n = 2). Unilateral vagotomy impaired the type II response in the distal oesophagus, as evidenced by an increase in the V_T, and a reduction in both the number and amplitude of the rhythmic pressure waves (n = 7, Fig. 2.7B). Bilateral vagotomy abolished the type II response (n = 7, data not shown).

Curarization. Intravenous D-tubocurarine abolished distension-evoked pressure waves, including the *type I* response in the proximal oesophagus (Fig. 2.8A-1, n = 4), the *type II* response in the distal oesophagus (Fig. 2.8A-2, n = 6) and the "off response" (Fig. 2.8B, n = 2). During paralysis, a change in pressure-volume relationship was evident in upper portions of the oesophagus (n = 4) indicative of an increased resistance of the oesophageal wall to inflation.

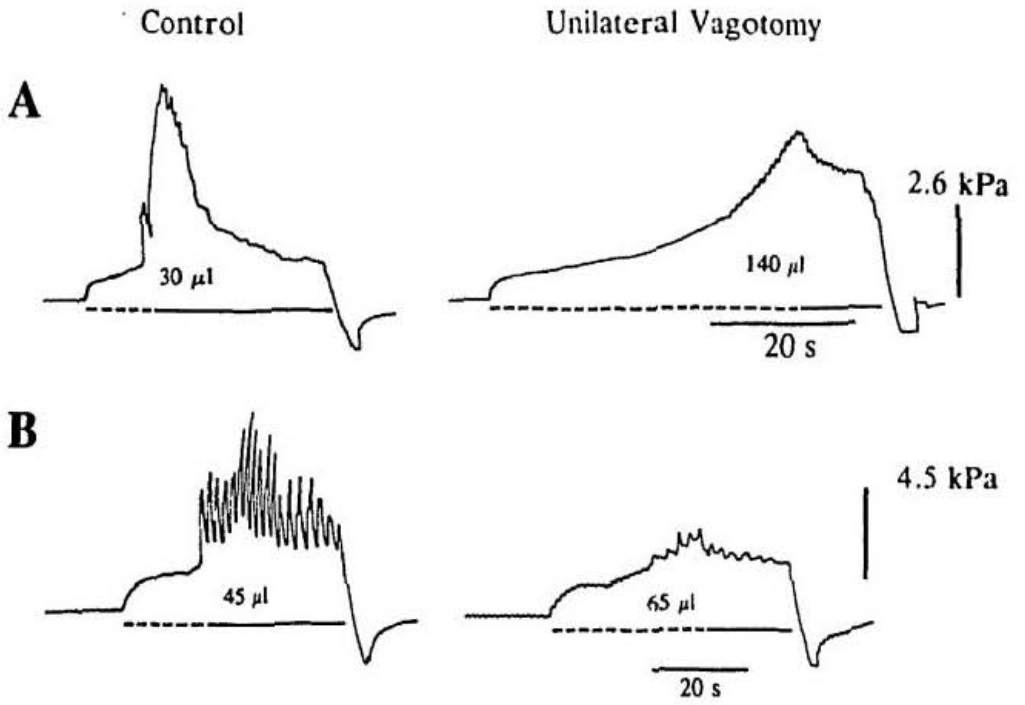
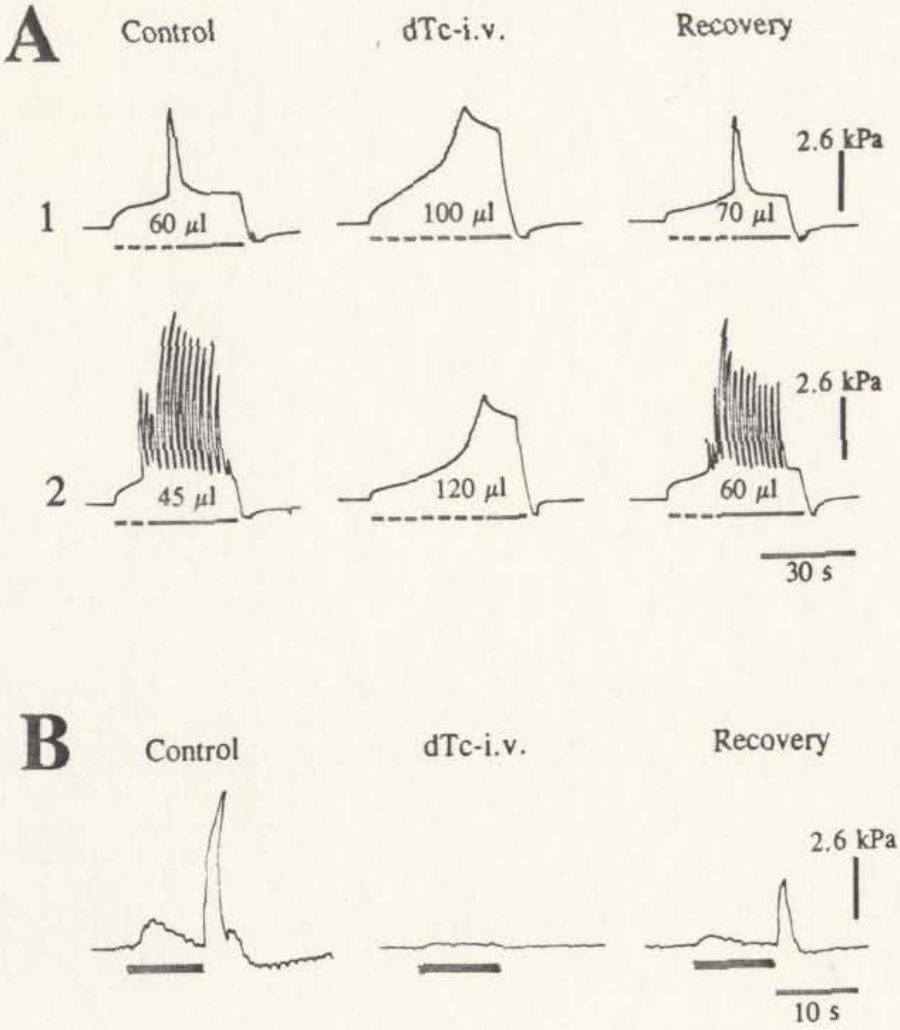


Fig. 2.7 Effect of acute unilateral vagotomy on the reflex oesophageal response. Reflex responses in the thoracic (**A**) and distal (**B**) segment before (left) and after (right) vagotomy. **A.** Unilateral vagotomy abolishes the monophasic response in the thoracic segment and increasing the inflation volume (indicated below each pressure trace) fails to restore the reflex. **B.** Rhythmic reflex activity in the distal segment is markedly attenuated. Broken portion of the line marks the period during which the balloon is being inflated, solid portion represents sustained inflation at the volume indicated.

Fig. 2.8 Inhibition of reflex oesophageal responses by curarization. A. Local reflex responses evoked by fixed-rate inflation at the upper thoracic (A-1) and the intracrural level (A-2) are reversibly abolished by D-tubocurarine (dTc, 0.15 μmol.kg^{-1} i.v.) and recover within 15 - 30 min. Increasing the inflation volume (indicated under each pressure trace) fails to overcome the blockade. Biphasic and steeper rise in intra-balloon pressure in the upper thoracic oesophagus during motor paralysis (with inflation volume less than 120 μl) probably indicates altered resistance of the oesophageal wall to distension. B. Rapid inflation (indicated by the bars under pressure trace) and deflation of the thoracic segment produce a complex reflex response in the distal segment aboral to the inflation balloon. Neuromuscular block with intravenous D-tubocurarine (0.15 μmol.kg^{-1}) eliminates all components of the complex reflex.


A
Control
dTc-i.v.
Recovery
2.6 kPa
1
60 µl
100 µl
70 µl
2.6 kPa
2
45 µl
120 µl
60 µl
30 s
B
Control
dTc-i.v.
Recovery
2.6 kPa
10 s

2.2.3 Cholinergic Effects

Type I and "deflation-response". Intravenous administration of 0.2 μmol.kg^{-1} methscopolamine, a CNS-impermeant mAChR antagonist (n = 4), did not affect the "*type I response*" or the "*deflation-response*" (Fig. 2.9). However, an equimolar i.v. dose of the CNS-permeant mAChR antagonist, scopolamine, produced a prolonged inhibition of both responses. The amplitude of the *type I* activity was reduced from 4.2 $\pm$ 0.9 kPa to 0.6 $\pm$ 0.3 kPa (n = 12 trials from 4 animals, $P<0.05$). The "off response" was abolished in all cases (n = 4).

Methscopolamine (50-100 pmol) applied bilaterally to the NTS surface abolished the "off-response" within 5-7 min (n = 3, not shown). During the following 60 min, neither the "*type I response*" nor the "*deflation-response*" recovered from the inhibition.

Type II Response. Muscarine 20-35 nmol.kg^{-1} i.v. evoked a transient, slow pressure rise (0.2 -0.4 kPa) in the cervical, thoracic and distal oesophagus (n = 3, not shown). Methscopolamine 0.2 μmol.kg^{-1} i.v. blocked the muscarine-induced response, however, at the same dose it did not affect the type II response in terms of either the V_T or the mean amplitude (Fig. 2.10A-2 and 2.10B, n = 6).

Scopolamine 0.2 μmol.kg^{-1} i.v. significantly depressed the type II response (Fig. 2.10A-3, n = 14) and in 5 animals caused a complete loss of response at inflation volumes as high as 160 to 180 μl. In the remaining 9 cases, the V_T value was increased by twofold and the mean amplitude was reduced (Fig. 2.10B).

Application of either methscopolamine or scopolamine (50 to 100 pmol in 0.01-0.02 μl) to the NTS surface strongly inhibited the *type II* activity. In 2 out of 12

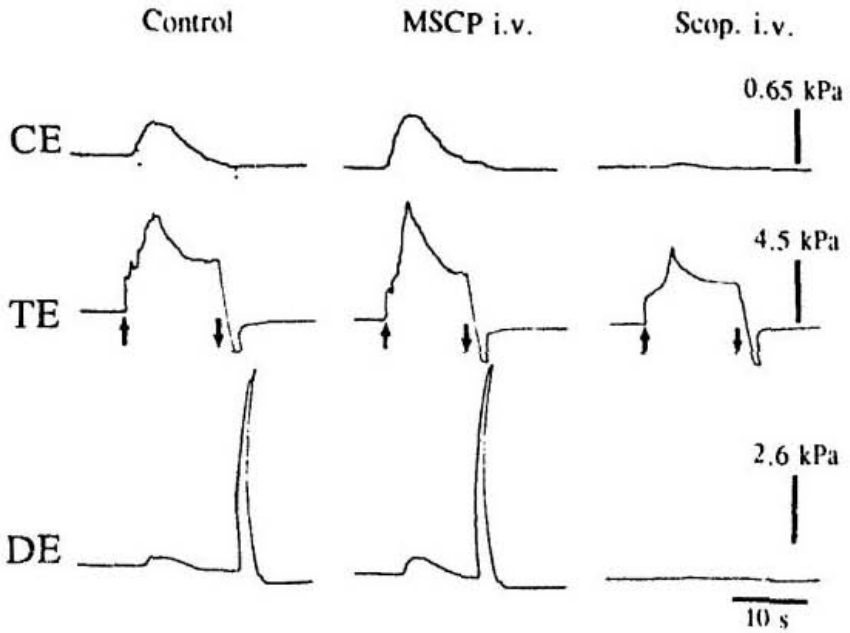
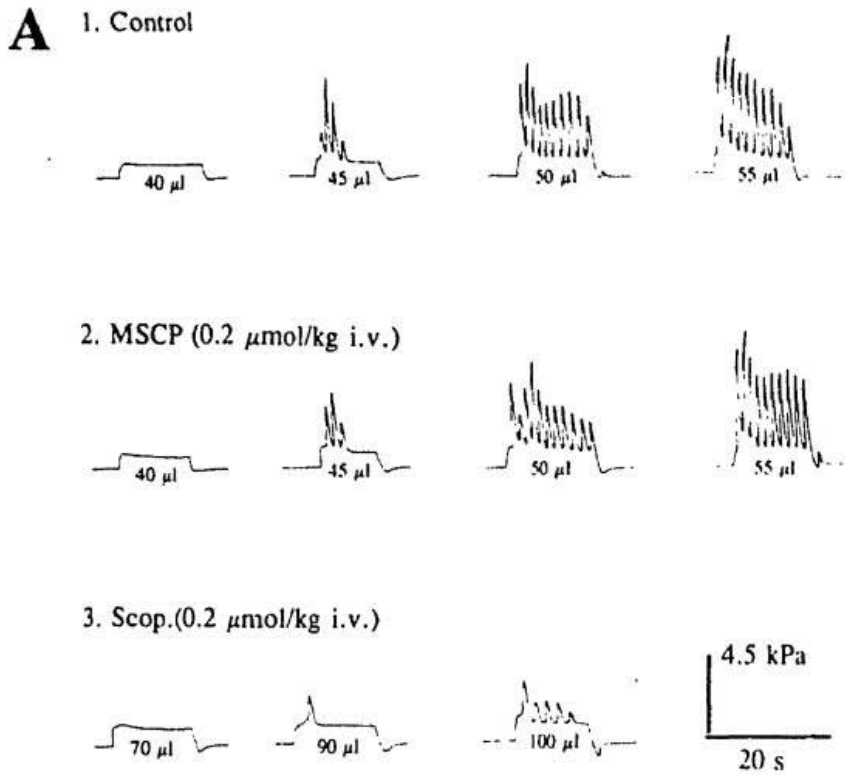
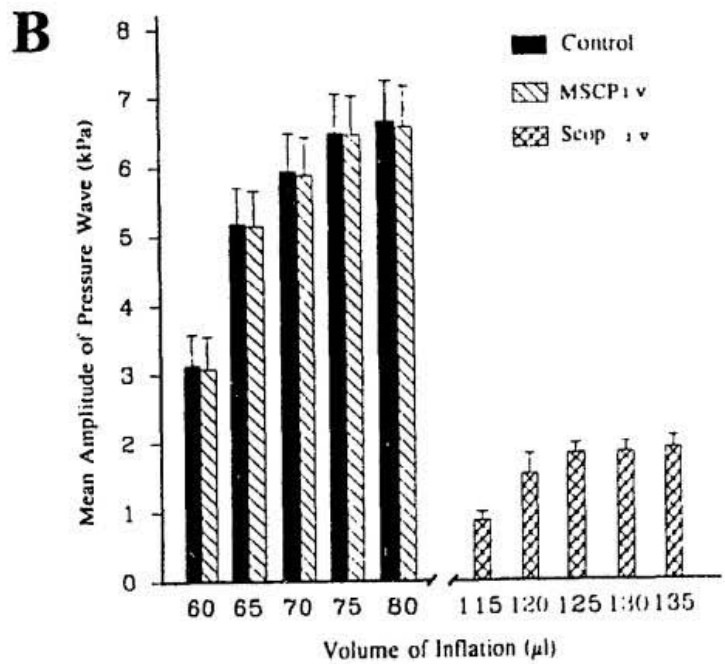


Fig. 2.9 Inhibition of the coordinated oesophageal reflex response by blockade of central muscarinic cholinoceptors. Three balloons are positioned in the cervical (CE), the thoracic (TE) and distal oesophagus (DE). During sustained inflation (↑) at the thoracic level, a high amplitude pressure wave (type I response) is seen in the inflated segment and low-amplitude pressure wave at CE and DE levels. Deflation (↓) triggers a pressure wave (off-response) in the distal but not the cervical oesophagus. Reflex responses are not affected by intravenous methscopolamine (MSCP, 0.2 μmol.kg^{-1}), but inhibited by an equimolar intravenous dose of scopolamine.

Fig. 2.10 Inhibition of reflex oesophageal responses by CNS-permeant, but not - impermeant mAChR antagonist. **A**. Rhythmic type II reflex pressure waves in the distal oesophagus (DE) at incremental inflation volumes (A-1) are not affected by CNS-impermeant antagonist methscopolamine (MSCP, 0.2 μmol.kg^{-1} i.v.) (A-2), but are strongly inhibited by same dose of the CNS-permeant scopolamine (Scop.) (A-3). **B**. Difference in effect of mAChR antagonists on the inflation-response relationship. Mean amplitudes of oesophageal contraction are averages of intraluminal pressure waves during first 10 seconds of each inflation trial, determined in 6 separate experiments. In contrast to MSCP, scopolamine inhibits the reflex by increasing V_T and reducing the mean amplitude of evoked pressure waves.

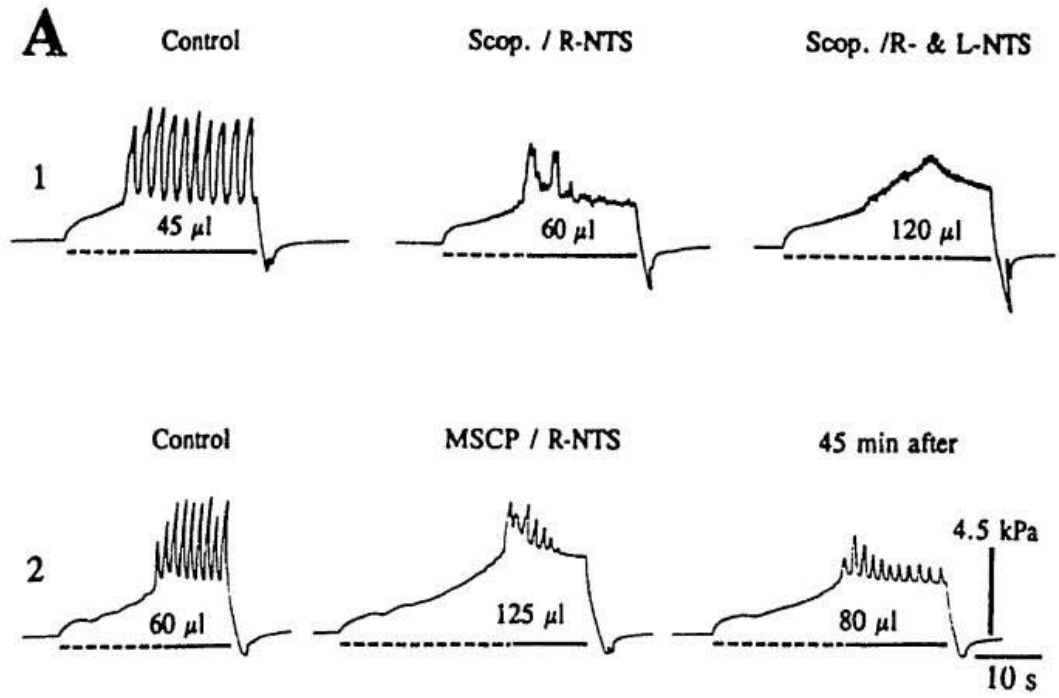

A
1. Control
40 μl
45 μl
50 μl
55 μl
2. MSCP (0.2 μmol/kg i.v.)
40 μl
45 μl
50 μl
55 μl
3. Scop.(0.2 μmol/kg i.v.)
70 μl
90 μl
100 μl
4.5 kPa
20 s


B
Control
MSCP i.v
Scop i.v
Mean Amplitude of Pressure Wave (kPa)
0
1
2
3
4
5
6
7
8
60 65 70 75 80
115 120 125 130 135
Volume of Inflation (μl)

methscopolamine-treated animals, the responses were absent even at elevated inflation volumes (160-180 μl). In the other 10 animals, an increase in V_T and reduction in mean amplitude were evident (Fig. 2.11A & B). A partial recovery was seen 2-3 h after topical application of methscopolamine. In control tests (n = 3 of each), methscopolamine (100 pmol in 0.02 μl) applied topically to the dorsal surface of the medulla oblongata surrounding the NTS (n = 4) or pressure-ejected into the AMB_c (n = 3) was without effect on the esophagomotor response to distension. Furthermore, 0.1 nmol dihydro-β-erythroidine, a central nicotinic cholinoceptor antagonist (Curtis & Ryall, 1966), applied to extraventricular surface of the NTS (n = 3) was ineffective.

After intravenous administration of 0.2 μmol.kg^{-1} BW284c51, a CNS-impermeant selective inhibitor of acetylcholine esterase, *type II* responses were unaffected (Fig. 2.12A-2 and Fig. 2.12B; n = 4), although all animals displayed overt signs of peripheral cholinoceptor overactivity including generalized muscle faciculations, sialorrhea, lachrymation, defecation and micturition. In contrast, after intravenous administration of 0.1-0.2 μmol.kg^{-1} physostigmine, a CNS-permeant anticholinesterase, the *type II* response was facilitated (Fig. 2.12A-3; n=7), as evidenced by a left- and upward shift of the volume-response relationship (Fig. 2.12B). Furthermore, slow pressure waves occurred also in the upper thoracic segment during inflation of the distal oesophagus (n=5/7;not shown) and exhibited a shape resembling that of a *type I* response. However, the proximal *type I*-like waves failed to propagate into the distended portion of the oesophagus, and instead were accompanied by inhibition of *type II* activity, as evidenced by a phase-shift in wave rhythm and a decrease in wave amplitude. When applied to the

Fig. 2.11 Inhibition of the type II response by mAChR antagonists applied to NTS surface. **A**. Both scopolamine (A-1) and methscopolamine (A-2) inhibit the reflex response. R- & L-NTS: right- & left-NTS. **B**. After bilateral methscopolamine (MSCP), V_T increases from 62 $\pm$ 5.5 to 118 $\pm$ 7.0 μl (B-2), whereas the mean amplitude decreases from 3.0 $\pm$ 0.25 to 1.3 $\pm$ 0.2 kPa (B-1). After bilateral scopolamine (Scop.), V_T increases from 62 $\pm$ 5.5 to 138 $\pm$ 12 μl (B-2) and the mean amplitude is decreased from 3.0 $\pm$ 0.25 to 1.2 $\pm$ 0.2 kPa (B-1). Asterisks denote significant difference vs. control ($P < 0.05$); ***n*** represents the number of trials with number of separate experiments given in parenthesis.


A
Control
Scop. / R-NTS
Scop. /R- & L-NTS
1
45 μl
60 μl
120 μl
Control
MSCP / R-NTS
45 min after
2
60 μl
125 μl
80 μl
4.5 kPa
10 s

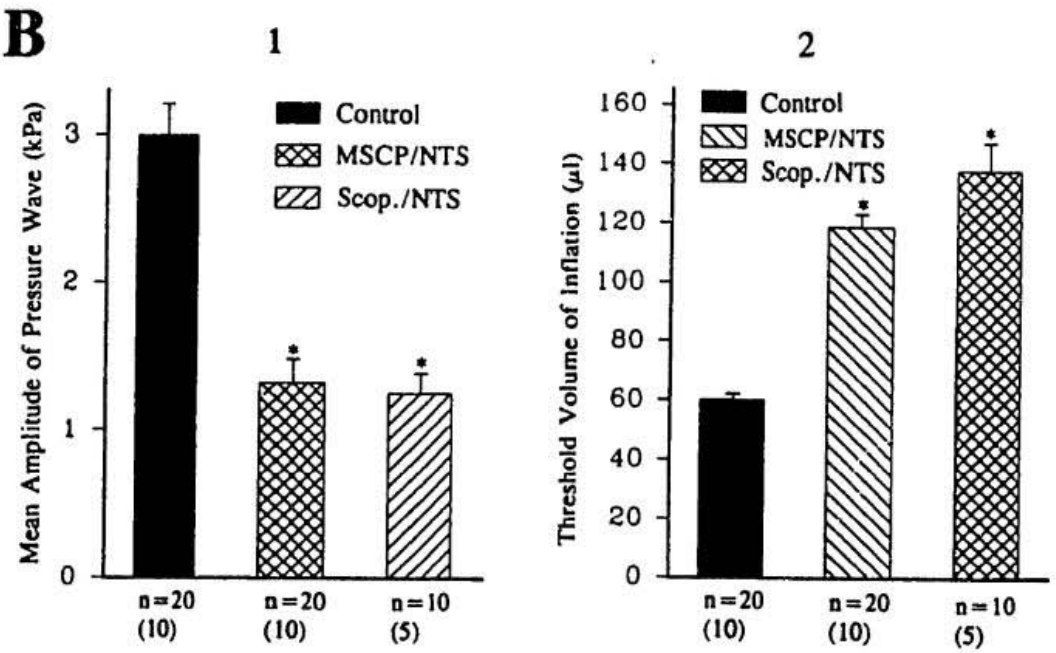
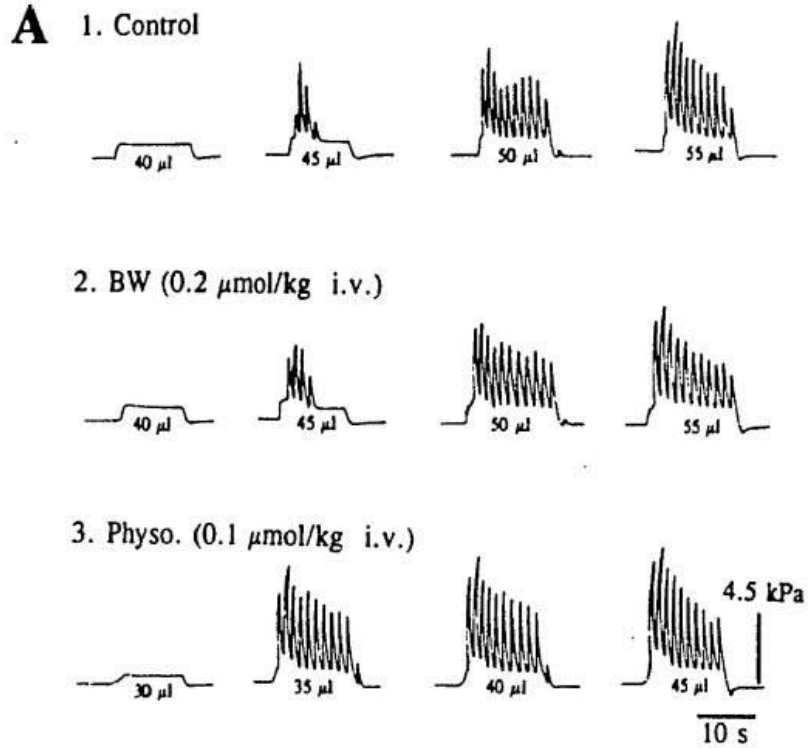
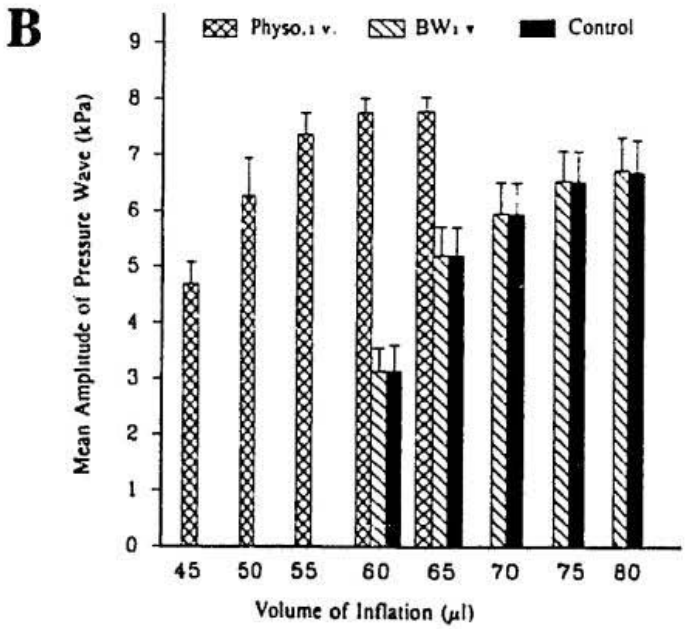

B
1
2
Mean Amplitude of Pressure Wave (kPa)
Threshold Volume of Inflation (μl)
Control
MSCP/NTS
Scop./NTS
n=20 (10)
n=20 (10)
n=10 (5)

Fig. 2.12 Effects on reflex oesophageal response of intravenous acetylcholinesterase (AChE)-inhibitors. **A.** A rapid step inflation of the distal oesophagus evokes rhythmic pressure waves whose mean amplitude increases with the inflation volume (indicated under each pressure trace, A-1). The reflex response is unaffected by BW284c51 (0.2 μmol.kg^{-1} i.v.)(A-2), but enhanced by physostigmine (A-3). **B.** Difference in effect of AChE-inhibitors on inflation-response relationship. Unlike BW284c51, physostigmine (0.1 to 0.2 μmol/kg i.v.) facilitates the reflex response by lowering the V_1 and enhancing the mean amplitude of oesophageal pressure waves.


A
1. Control
40 µl
45 µl
50 µl
55 µl
2. BW (0.2 µmol/kg i.v.)
40 µl
45 µl
50 µl
55 µl
3. Physo. (0.1 µmol/kg i.v.)
30 µl
35 µl
40 µl
45 µl
4.5 kPa
10 s


B
Physo.1 v.
BW1 v
Control
Mean Amplitude of Pressure Wave (kPa)
0
1
2
3
4
5
6
7
8
9
45
50
55
60
65
70
75
80
Volume of Inflation (µl)

NTS surface, both physostigmine (20-50 pmol) and BW284c51 (20-50 pmol) enhanced the *type II* response (Fig. 2.13).

2.2.4 Effect of NMDA Receptor Antagonists

Type I and "deflation-response". Topical application of AP-5 (10-50 nmol) to the NTS surface eliminated both the type I and the off-responses (n = 4 out of 4). Partial recovery occurred after 15-30 min; full recovery in 30 to 60 minutes in all animals tested (Fig. 2.14A, n = 4).

Type II response. The *type II* rhythmic activity in the intracrural oesophagus was highly sensitive to NMDAR blockade. Ketamine, a NMDA receptor channel blocker (Anis et al., 1983), given i.v. at a dose of 1-2 $mg.kg^{-1}$ invariably induced a complete inhibition (Fig. 2.14B-1, n = 7). The response partially recovered in 15-20 min and was fully restored in 50-60 min. After ketamine, spontaneous deglutition persisted, but its oesophageal component was eliminated. As shown in Fig. 2.14B-2, application of 100 nmol ketamine to the NTS surface eliminated the *type II* activity for 30 - 50 min (n = 4). The effect of topical application of AP-5 was tested in 9 animals. Two to five minutes following application of 10-50 nmol AP-5 to the NTS surface, rhythmic contractions could not be evoked by high volume (> 120 μl) inflation (n = 9 out of 9 tested animals; Fig. 14B-4). Full recovery of the response occurred between 30 - 40 min after application of AP-5. When 50-100 pmol of AP-5 was unilaterally injected into the region of the NTS_c, the V_T of the type II reflex response increased with a concomitant decrease in amplitude of the pressure waves (Fig. 2.14B-3).

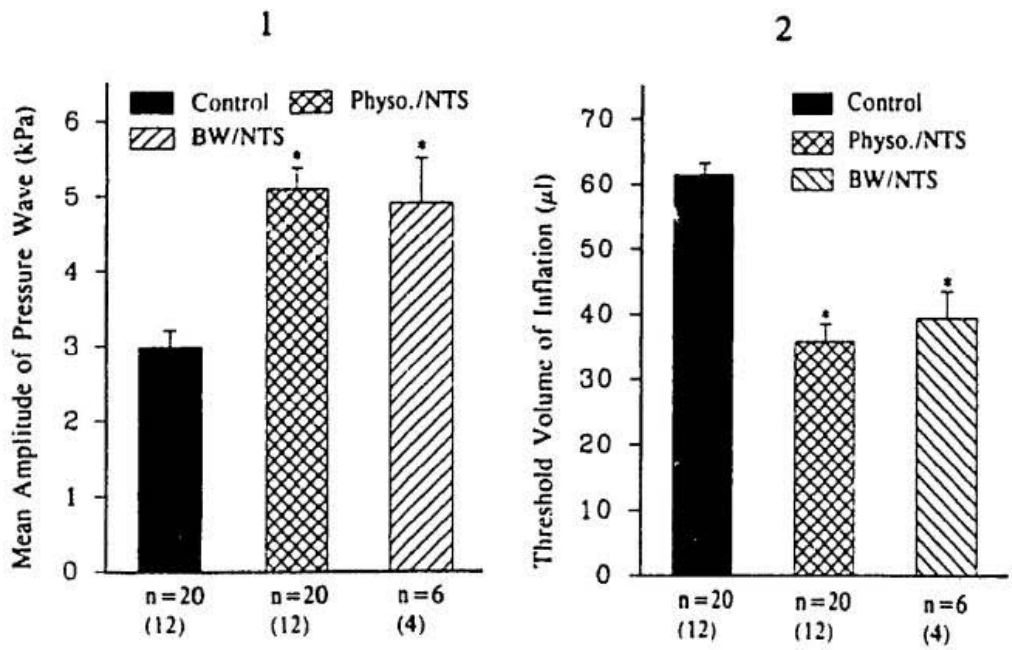
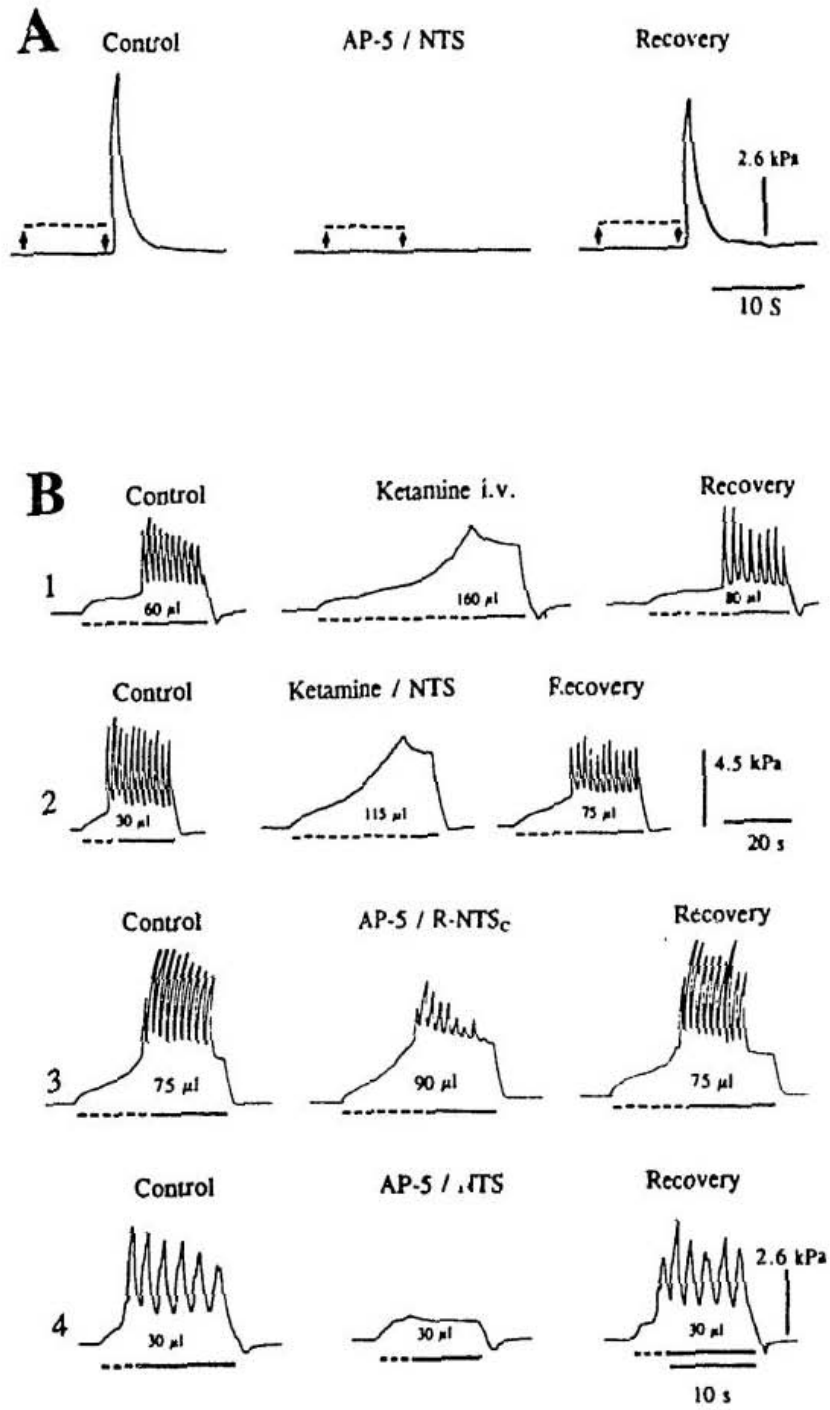


Fig. 2.13 Facilitation of the reflex response by AChE-inhibitors applied to the bilateral NTS surface. Both physostigmine and BW284c51 facilitate the type II reflex response by reducing the V_T and increasing the amplitude of evoked pressure waves. With physostigmine, the mean amplitude increases from 3.0 ± 0.25 to 5.2 ± 0.35 kPa, while the V_T decreases from 62 ± 5.5 to 36 ± 7.5 μl. BW284c51 increases the mean amplitude from 3.0 ± 0.25 to 4.9 ± 0.7 kPa; and lowers V_T from 62 ± 5.5 to 38.5 ± 8.5 μl. Asterisks denote significant difference vs. control ($P < 0.05$); ***n*** represents the number of trials with number of separate experiments given in parenthesis.

Fig. 2.14 Blockade of the oesophageal reflex response by N-methyl-D-aspartate receptor antagonists. **A.** Following a sustained inflation (indicated with a up-ward arrow and dashed line) of a balloon positioned in the thoracic oesophagus, deflation (down-ward arrow) of the balloon evokes a single contraction ("deflation response") at the distal portion of the oesophagus. The response is reversibly suppressed by application of (±)-2-amino-5-phosphonopentanoic acid (AP-5, 20 nmol) to the bilateral NTS surface and recovers within 10 min. **B.** Rhythmic (type II) response is reversibly blocked by ketamine, given i.v (1 $mg.kg^{-1}$)(B-1) or applied to the NTS surface (100 nmol)(B-2) and recovers within 15-25 min. When applied to the NTS surface (100 pmol, B-4) or pressure-ejected to the NTS_c region (20 pmol B-3), AP-5 causes an analogous inhibition.


A
Control
AP-5 / NTS
Recovery
2.6 kPa
10 S
B
Control
Ketamine i.v.
Recovery
1
60 µl
160 µl
80 µl
Control
Ketamine / NTS
Recovery
2
30 µl
115 µl
75 µl
4.5 kPa
20 s
Control
AP-5 / R-NTSc
Recovery
3
75 µl
90 µl
75 µl
Control
AP-5 / NTS
Recovery
4
30 µl
30 µl
30 µl
2.6 kPa
10 s

2.3 Discussion

The present study demonstrates that the rat striated muscle oesophagus possesses reflex capabilities analogous to those described in other mammals possessing a mixed striated-smooth muscle gullet. The diverse reflex responses are segmentally organized and dependent on cholinergic and EAAergic neurotransmission in the NTS region. As the oesophageal distensions were performed by controlled slow or one-step rapid inflation at a balloon volume just above the threshold, the pressure waves evoked in different segments are likely to represent the physiological reflex repertoire of the oesophageal body. Since all types of distension reflex responses were abolished by curare, but not affected by peripheral mAChR blockade, the smooth muscle component seems to be negligible.

2.3.1 Organization of Reflex Responses

Segmental patterns. An unexpected finding of the present investigation was the proximo-distal variation in distension-induced reflex oesophageal response, which belies the structural uniformity of the rat oesophagus (Gruber, 1978; Kauffmann et al.,1968; Marsh & Bieger, 1986). While both non-rhythmic and rhythmic reflex contractions have been described in various other laboratory animals (Blank et al.,1989; Christensen & Lund,1969; Christensen,1970; Falempin & Rousseau,1984; Paterson et al.,1991; Seller & Titchen,1959), and the human (Baylis et al.,1955; Creamer & Schlegel,1957; Ren et al.,1995), their segmental organization has not been clearly demonstrated to date.

In the rat, *type II* rhythmic reflex activity was more or less confined to the

intracrural (diaphragmatic) portion of the oesophagus. However, although its rhythm was in a narrow frequency band overlapping with that of breathing, it had no relationship to diaphragmatic activity. It should be noted that distension of the oesophagus in the cat (Jones et al.,1994) and dog (Holland et al.,1994; Oliven et al.,1989) has been reported to selectively inhibit phasic inspiratory activity in the crural portion of the diaphragm. If the same mechanism existed in the rat, it would rule out diaphragmatic movement as the cause of the rhythmic oesophageal pressure waves. More to the point, the *type II* rhythmic response was eliminated by vagotomy, or by blockade of NMDA receptors in the NTS with only minor changes in respiratory activity. The presence of a rhythmic reflex mechanism in the intracrural portion may relate to the requirement for efficient bolus propulsion through the distal oesophagus, as this region, surrounded by the crura of the diaphragm, probably imposes mechanical limitations on bolus size.

Both *type I* and *type II* local reflex responses were of a propulsive nature and in the latter case were observed to start above the distended portion of the oesophagus. Since the muscle fibers in the inflated segment were stretched to a greater degree, the response was stronger than that in the proximal segments. One may therefore consider these segmental reflex responses to be indistinguishable from true secondary peristalsis. In view of the vigorous *type I* and *type II* responses reproducibly evoked at the thoracic and distal segments in all animals, the apparent absence of responses in the cervical oesophagus in most cases is remarkable. A possible explanation would be surgical damage to oesophageal nerve fibers running in the ramus externus of SLN, which supply the rostral-most oesophagus.

The segmental variation in oesophageal reflex activity also manifested itself in terms of the different pressure wave forms observed in the thoracic and the intracrurual segments, suggesting that different oesophageal segments are individually controlled by subcircuits. Consistent with spinal cord "segmental neuronal circuits" subserving propulsive locomotion (Grillner et al., 1991), such an arrangement would confer flexibility on the esophagomotor pattern generator network. This concept is also supported by previous studies showing that (i) vagal afferents from the oesophagus viscerotopically project to the NTS_c (Altschuler et al., 1989); (ii) the oesophageal tunica muscularis propria receives a myotopically organized innervation from AMB_c motoneurons (Bieger & Hopkins, 1987; Barrett et al.,1994); (iii) microphoresis of iGluR or mAChR agonists along the rostro-caudal axis of the NTS_c leads to esophagomotor responses that involve discrete segments and show rhythmic or non-rhythmic patterns along the length of the oesophagus (Bieger, 1984; Hashim & Bieger, 1989). When present simultaneously, the two response types could interact in an inhibitory manner, such that the proximal *type I* response appeared to cause a transient phase delay and a weakening of distal *type II* rhythmic activity. A similar phenomenon has been observed in previous studies on sheep, in which inflation of a second balloon cranially in the oesophagus led to abolition of rhythmic afferent unit activity from the caudal segment where a balloon distension is maintained (Falempin & Rousseau, 1983). Taken together, these findings suggest the existence of a descending inhibitory mechanism. These segmental units could operate in a coordinated manner during primary peristalsis, but function independently when selectively activated by appropriate sensory inputs.

Coordinated reflex responses. The coordinated "*inflation*" and "*deflation*" responses of the rat oesophagus invite comparison with "*on*" and "*off*" responses of the smooth muscle oesophagus of the human (Creamer & Schlegel, 1957), the opossum (Christensen, 1970; Paterson et al.,1991) and the cat (Blank et al.,1989).

As defined in present study, the "*inflation*" response in the rat oesophagus was dependent on an intact vagal innervation and sensitive to blockade of central but not peripheral mAChRs (see below). The *in vivo* "*on*" response of the opossum smooth muscle oesophagus likewise appears to be vagally mediated (Paterson, 1991), however, is reportedly non-propulsive like that in the human (Paterson et al.,1991) and has an atropine-sensitivity that decreases in the aboral direction (Paterson et al. 1991). In apparent contradiction to these latter two species, the rat exhibited a propulsive "*inflation*" response that was evident only when the inflation balloon was left free to move. Arguably, this technique may produce a similar result in the other species.

The vagally-mediated "*deflation*" response in the rat resembled the "*off*"-response of other species, but would seem to be comparable only with that described in the feline striated muscle oesophagus (Blank et al.,1989), neither requiring transmission via peripheral mAChRs. The present study did not determine whether the "*deflation*" response in the rat was propulsive; however, "*off*"-responses in the smooth muscle oesophagus in all species examined to date are typically propulsive (Blank et al.,1989; Paterson et al.,1988; Paterson et al.,1991). Since the "*off*"-response of the opossum oesophagus can be elicited *in vitro* (Christensen & Lund,1969; Christensen,1970; Paterson & Indrakrishnan, 1995), it is thought to be coordinated by intramural neural

mechanisms, involving a rebound excitation of the muscle after inhibition by non-adrenergic non-cholinergic myenteric neurons (Paterson & Indrakrishnan, 1995). Nevertheless, the analogous *"deflation"* response in the rat was abolished by blockade of central mAChRs and NMDARs in the NTS, implicating its dependence on central links. While some workers equate the "*off*"-response with secondary peristalsis (Blank et al., 1989; Paterson et al., 1991), it may be reasonable to view this response as a component of a centrally coordinated reflex synergy, which operates at high velocities of bolus transport.

2.3.2 Central Cholinergic Modulation

The present study provides strong evidence that a cholinergic link in the NTS plays an integral part in reflex oesophageal peristalsis. Previous studies have demonstrated in the rat that intravenous administration of the mAChR antagonist, scopolamine, eliminates the oesophageal stage of fictive swallowing (Bieger, 1984; Wang & Bieger, 1991). Conversely, focal stimulation of mAChRs in the NTS_c produces rhythmic oesophageal peristaltic contractions (Bieger, 1984), implicating a cholinergic synapse in the NTS_c in the generation of oesophageal activity. As shown in the present study, all types of the reflex peristalsis in the rat oesophagus, including the "*inflation*"- and "*deflation*"-response, were susceptible to agents capable of gaining access from the circulation to brain cholinergic synapses. In contrast, agents restricted to extracerebral cholinergic sites, including those in oesophageal smooth muscle and intramural ganglia, failed to exert any effect on oesophageal reflexes. As expected, CNS-impermeant

compounds, BW284c51 and methscopolamine, proved highly effective when applied directly to the NTS. The central muscarinic receptors appear to operate at the level of NTS_c interneurons, rather than AMB_c motoneurons or ventral medullary interneurons, since methscopolamine produced its inhibitory effects only upon application to the NTS, but not the AMB_c. However, the cholinergic link in the NTS_c does not seem to mediate the esophagomotor reflex but instead plays a role in modulating the responsiveness of NTS_c premotor neurons to afferent inputs from the oesophagus.

In humans (Paterson et al., 1991) and cats (Blank et al., 1989), centrally-mediated smooth muscle responses evoked by oesophageal distension are atropine-sensitive. This effect generally has been attributed to a peripheral mechanism. However, the action of atropine could also involve central muscarinic cholinoceptors since atropine readily crosses the blood-brain barrier. While only sketchy evidence is available with regard to striated muscle oesophageal peristalsis in the cat (Blank et al., 1989), the contribution of central cholinergic mechanisms in oesophageal peristalsis needs to be confirmed in other mammals, including humans.

2.3.3 Excitatory Amino-Acidergic Transmission

EAAs are the major excitatory neurotransmitters in the CNS (Cotman & Iversen, 1987; Headley & Grillner, 1990) and the NTS of the medulla oblongata (Andresen & Yang, 1990; Dietrich et al., 1982; Drewe et al., 1990; Wang & Bradley, 1995). Previous studies from this laboratory (Bieger, 1984; Hashim & Bieger, 1989) also indicate that the EAA input is mediated through activation of different EAA receptor subtypes at different

NTS deglutitive loci. At oesophageal loci in the NTS_c, NMDA is more potent than other EAA agonists such as kainate and quisqualate (Hashim & Bieger 1989), suggesting the preferential association of the NMDA receptor subtype with oesophageal premotor neurons. Consistent with this observation, the intravenous administration of MK801, a non-competitive NMDA receptor antagonist, selectively suppresses the oesophageal component (primary peristalsis) of swallowing (Hashim, 1989). Furthermore, the competitive NMDA receptor antagonist, AP-5, reversibly blocks the oesophageal contraction evoked from the NTS_c by glutamate microphoresis (Hashim and Bieger, 1989). An EAA-ergic link in the NTS_c region is thus likely to contribute to esophagomotor control.

As expected, NMDAR antagonists were also effective in blocking oesophageal reflex peristalsis. Specifically, our data corroborate the NTS as a major site of action. Interestingly, the blocking effect of ketamine was seen at fairly low intravenous dosage. However, the apparent antimuscarinic action of this drug (Contreras et al., 1990; Durieux, 1995; Wilson et al., 1993) may be a contributing factor, as well as blockade of oesophageal motoneuronal NMDA receptors (Lu & Bieger 1996). It should be noted that ketamine has been employed as a general anaesthetic agent in many animal experiments, including studies of deglutitive function. Since NMDA receptors appear to be critically involved in esophagomotor control, results obtained from ketamine-anaesthetized preparations must be interpreted with caution.

In summary, the rat oesophagus generates segmentally organized reflex responses

to local distension with different segments showing different response patterns, suggesting the existence of segmental pattern generator subcircuits. The operation of these subcircuits depends on cholinergic and EAA-ergic neurotransmission at the brainstem NTS region, presumably in the oesophageal interneurons of the NTS_c. Based on these findings, the next step was to investigate the oesophageal premotor activity pattern with particular attention to the vagal afferent transmitter.

Chapter 3

OESOPHAGEAL REFLEXES: BRAINSTEM NEURAL CORRELATES AND VAGAL AFFERENT TRANSMISSION

According to Roman (1982) and Jean (1990), oesophageal interneurons form part of the swallowing pattern generator consisting of a dorsal group of generator elements, localized mainly in the NTS, and a ventral group of "switching" elements localized in the lateral reticular formation dorsal to the nucleus ambiguus. In this model, the deglutitive command pattern originating in the dorsal neurons is relayed to and distributed by the ventral neurons to the appropriate motoneuron pools, including those innervating the oesophageal muscle tunics. However, neuroanatomical studies in the rat have revealed that oesophageal second-order sensory neurons in the NTS_c send a massive monosynaptic projection to motoneurons in the AMB_c (Bieger, 1984; Cunningham & Sawchenko, 1989; Gai et al.,1995; Hashim, 1989). These neuroanatomical data have been interpreted to indicate the reflex nature of oesophagomotor control (Cunningham & Sawchenko, 1988, 1989, 1990); however, little if any electrophysiological information is currently available in this regard.

The synaptic transmitter released by oesophageal vagal afferents to the NTS_c interneurons is yet to be identified. The intriguing possibility that vagal afferents are cholinergic merits consideration because 1) ChAT-immunoreactivity has been demonstrated in nodose ganglionic perikarya of the rat (Palouzier et al., 1987) and rabbit

(Falempin et al., 1989; Ternaux et al., 1989); 2) the NTS_c contains a dense field of ChAT-immunoreactive terminals (Ruggiero et al.,1990); 3) identified propriobulbar inputs to the NTS_c appear to be sparse (Cunningham & Sawchenko, 1990); 4) activation of rat NTS_c mAChRs produces patterned oesophageal peristalsis (Bieger, 1984; Hashim, 1989); and 5) the reflex oesophageal response is eliminated or depressed by blockade of NTS mAChRs (Chapter 2). However, the pharmacological evidence available at present is equally consistent with a glutamatergic mechanism since 1) focal application of glutamate receptor agonists to the NTS_c produces an esophagomotor response (Bieger, 1984; Hashim & Bieger, 1989), and 2) reflex oesophageal peristalsis is completely blocked by NMDAR antagonists applied to the NTS surface (Chapter 2).

The purpose of the present study was to record extracellular unit activity of medulla oblongata neurons responsive to distension of the oesophagus, with a view to determine (i) the neural activity patterns underlying rhythmic and nonrhythmic reflex patterns (Chapter 2) and (ii) the contributions of ACh and EAA in mediating primary oesophageal afferent transmission. As an extension of the second objective, an attempt was made to determine the involvement of both transmitter substances in the generation of EPSPs evoked by electrical stimulation of the tractus solitarius afferents in brainstem slice preparations.

3.1 Methods and Materials

3.1.1 *In Vivo* experiments

Experiments were performed in 41 male Sprague-Dawley rats. General procedures and intraluminal pressure recordings were the same as described in Chapter 2.

i. *Oesophageal distension.* A rapid one-step air-injection was delivered by means of a manually operated 500 μl syringe connected to the inflation catheter. According to the experimental protocol, the inflation balloon was positioned either in the thoracic or the distal oesophagus. A supra-threshold volume for oesophageal distension was determined by increasing injections in 5-10 μl steps over the range of 100 - 200 μl. Once determined, the same inflation volume was used throughout the experiment. As a safeguard against possible fatigue of the oesophageal tension receptors, successive distensions were separated by at least 90 s.

ii. *Extracellular recording and drug application.* To establish the locations of neurons in the medulla oblongata responsive to oesophageal distension and to study the oesophagomotor reflex behaviour of these neurons, a microelectrode was used for extracellular recordings. The electrode consisted of a glass micro-pipette containing a fine carbon fibre (8 μm in diameter). The carbon fibre protruding from the pipette tip after pulling was cut, and then electrically etched to a length of 4-6 μm with chromic acid after the pipette was filled with 4 M NaCl. Under microscopic control, the micropipette was stereotaxically inserted into the medullary tissue with the rostral margin of the area postrema (AP) as a reference landmark. In light of previous work (Bieger 1984; Hashim and Bieger 1989), explorations of esophagomotor-related neurons were mainly performed within two medullary regions: namely the medial portion of the NTS and the rostral

portion of the AMB. Electrode penetrations were made 100-150 μm apart in both the mediolateral and rostrocaudal planes. The electrode was advanced in 50 μm dorsoventral steps with oesophageal distension applied between each step. The recording pipette was finally positioned at a site where unit discharges were reproducibly evoked by oesophageal distension (Fig. 3.1A). Unit discharges were monitored on a dual beam oscilloscope and discriminated by adjusting the window height of a spike-trigger (Neurolog). Discharge frequency was displayed on a Grass polygraph through a rate meter (Neurolog) along with intra-oesophageal pressure signals. Since the discharges represent multi-unit activity, peak discharge frequency was used as an index of the intensity of neuronal responsivity in the two regions. In 9 experiments, the recording pipette was filled with 4 M NaCl plus 4% lucifer yellow (Sigma). The fluorescent dye was electrophoretically ejected at the recording site with negative DC current pulses (500 ms, 2 Hz, 5-10 nA, 5-10 min) at the completion of recordings.

Drugs were either administered intravenously or applied to the NTS surface as described in Chapter 2. In 3 experiments, glutamate (0.2 M) was pressure-ejected near the recorded neurons through a separate barrel of the recording pipette.

iii. ***Histological examination.*** Fifteen minutes after the dye injection, the animals were perfused with 150 - 250 ml of saline i.v., followed by 250 ml of fixative (4% paraformaldehyde). The medulla oblongata was removed, stored overnight in the same fixative at room temperature, and sectioned in the transverse plane on a vibratome. Sections (75 or 100 μm thick) containing the recording site were mounted on slides in

0.1 M phosphate buffer and viewed under a fluorescence microscope. The recording sites were identified by their yellow fluorescence under dark field illumination and by the electrolytic lesion. Maps of recording sites were prepared based upon previous neuroanatomical studies (Altschuler et al. 1989; Bieger & Hopkins, 1987).

3.1.2 *In vitro* experiments

i. ***General procedures for slice preparation.*** Sprague-Dawley rats weighing 120-250 g were anaesthetized with urethane (0.8-1.0 g, i.p.). The brain was rapidly removed and placed in cooled (1-4°C), oxygenated (95% O_2 - 5% CO_2, modified artificial cerebrospinal fluid (ACSF). The brainstem was isolated and glued to a mounting block. From each brainstem, one horizontal slice containing NTS_c and solitary tract (400 μm thick) was cut on a vibratome and continuously bathed in oxygenated modified ACSF at room temperature. The procedure was completed within 10 min. Following 40 - 60 min recovery at room temperature in modified ACSF, slices were transferred to a submerged type recording chamber and perfused with normal ASCF at a flow rate of 2.0 ml/min and a temperature of 32-34°C. Normal ACSF consisted of (in mM): NaCl 126; KCl 3; $CaCl_2$ 2; $MgCl_2$ 2; KH_2PO_4 1.2; $NaHCO_3$ 26 and glucose 10, and was continuously bubbled with 95%O_2-CO_2 to maintain a pH of 7.3 - 7.4. In modified ACSF, NaCl was replaced by iso-osmolar sucrose (Aghajanian & Rasmussen 1989).

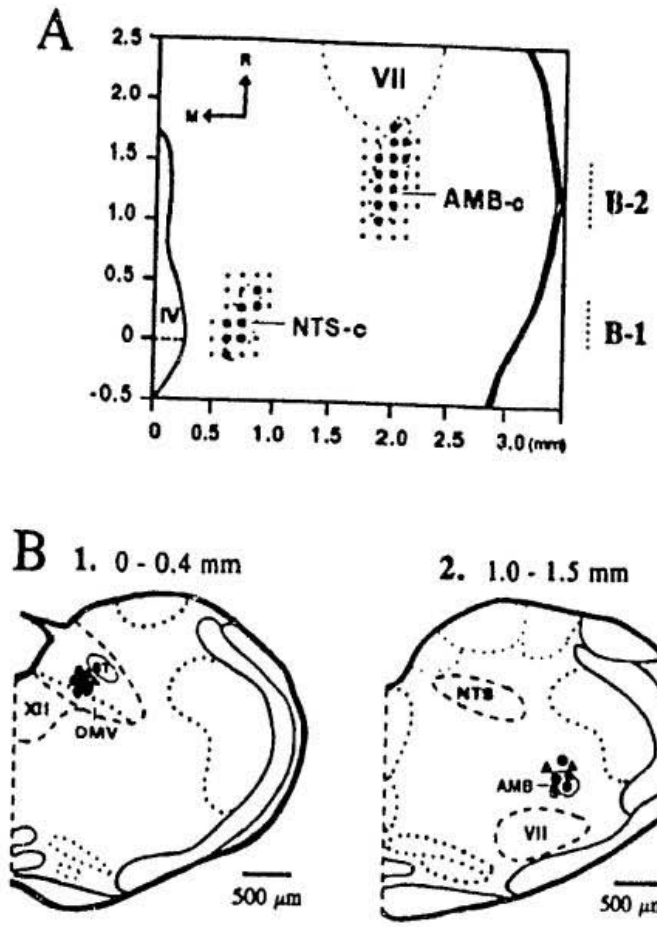
ii. ***Recording of EPSPs.*** The NTS_c region was identified in horizontal slice preparations with reference to anatomical studies (Altschuler et al. 1989; Barrett et al.

1994). Thirty-two horizontal brainstem slice preparations containing the NTS_t were used for the experiments. By using a dissecting microscope to visualize the NTS, whole cell recordings were made in the NTS_t region. Patch pipettes had resistances measured in ACSF ranging between 8-12 MΩ. Patch pipettes contained (in mM): K-gluconate 145; $MgCl_2$ 2; N-2-hydroxy-ethylpiperazine-N'-2-ethanesulfonic acid (Hepes) 5; 1,2-bis (2-aminophenoxy) ethane-N,N,N',N'-tetraacetic acid (BAPTA) 1.1; $CaCl_2$ 0.1; K_2ATP 5. A bipolar micro-electrode made of sharpened tungsten wire was placed in the solitary tract of the slice. Single monophasic square wave pulses (0.1 ms, 0.5-30 V) and/or pulse trains (1-5 V, 1-10 Hz, 1-5 s) were delivered to the solitary tract fibres to elicit postsynaptic potentials (PSPs) in NTS_t neurons. After stable NTS_t excitatory postsynaptic potentials (EPSPs) were obtained, effects of antagonists were examined. Drugs were either pressure-ejected in pulses of 50-200 pl from a multibarreled pipette positioned 100 μm from the recorded cell or applied by bath perfusion. All recordings were made with an Axoclamp II amplifier. The membrane potential of the neurons was displayed and captured on a Nicolet 310 digital oscilloscope and saved on a computer for off-line analysis. Data were averaged and analyzed using a suite of software routines written in Asyst (Asyst Laboratory. Technology, Rochester, N.Y.).

3.1.3 Drugs and statistics

Kynurenate, (±)-2-amino-7-phosphonoheptanoic acid (AP-7) and γ-D-glutamyl-glycine (γ-DGG) were purchased from Sigma; all other drugs were obtained from

Fig. 3.1 Distribution of medullary loci where unit-discharges are evoked by oesophageal distension. **A.** Dorsal view of electrode penetrations yielding responsive (large dots) and nonresponsive (small dots) loci. **B.** As projected onto the transverse planes spanning rostrocaudal levels B-1 and B-2, the responsive loci (n = 14 from 9 animal) are clustered in a dorsocaudal region coextensive with the subnucleus centralis of the NTS (NTS-c) and a rostroventral region comprising the compact formation of the nucleus ambiguus (AMB-c). Distances on the X- and Y-axis are marked in millimetres (mm) with reference to the midline and the cranial edge of the area postrema. R, rostral; M, medial; IV, fourth ventricle; VII, facial nucleus; ST, solitary tract; XII, hypoglossal nucleus; DMV, dorsal motor nucleus of the vagus.


A
2.5
2.0
1.5
1.0
0.5
0
-0.5
R
M
VII
AMB-c
B-2
IV
NTS-c
B-1
0
0.5
1.0
1.5
2.0
2.5
3.0 (mm)
B
1. 0 - 0.4 mm
XII
DMV
500 μm
2. 1.0 - 1.5 mm
NTS
AMB
VII
500 μm

commercial sources as described in Chapter 2.

Paired *t*-tests were done using SigmaStat (Jandel Scientific). All statistical values are presented as means ± SD. $P < 0.05$ was considered to be significant.

3.2 Results

3.2.1 Distension-Evoked Medullary Multi-Unit Discharges *In Vivo*

i. *Localization of medullary oesophageal neurons.* Extracellular recordings were obtained from oesophageal distension-responsive neurons in the dorsal and ventral medulla oblongata (Fig. 3.1A) The dorsal region extended between 100 μm caudal to and 400 μm rostral to the cranial edge of the area postrema (AP), 600 to 800 μm lateral to the midline, and 350 to 550 μm below the dorsal medullary surface. The ventral region was located between 1000 to 1800 μm rostral to the rostral edge of the AP, 1900 to 2200 μm lateral to the midline, and 2000 to 2300 μm below the dorsal medullary surface. The fluorescent marks and electrolytic lesions of the recording sites for 14 typical recordings were histologically verified in 9 animals (Fig. 3.1B). The medullary dorsal sites (n = 7) were located in the medial region of the NTS, coextensive with the NTS_c. In seven recordings in the ventral medulla, five recording sites were located within the boundary of the AMB_c and the other two recording tracks ended about 50-70 μm dorsal to the AMB_c.

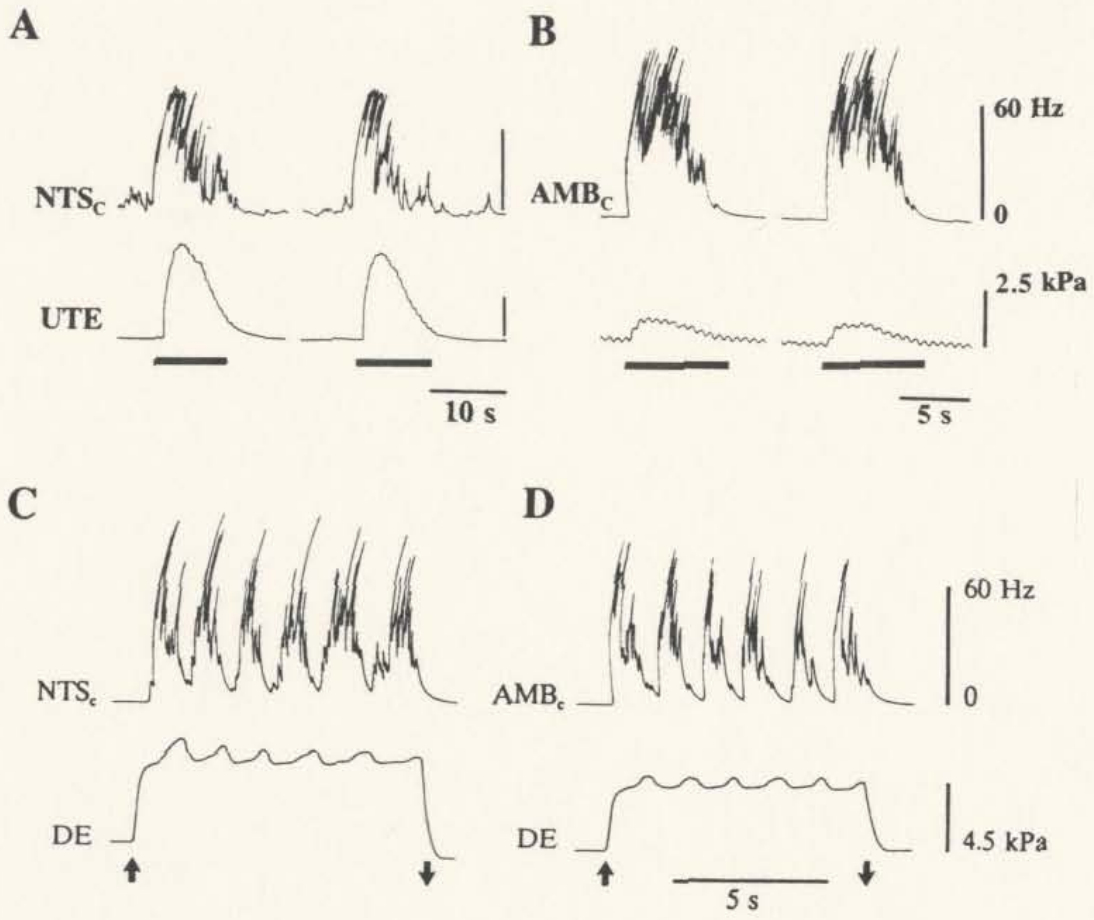


Fig. 3.2 Neural discharge patterns in the brainstem recorded during the distension-evoked reflex response of the oesophagus. Traces in A, B, C and D are obtained from four experimental cases. A non-rhythmic discharge occurs in the NTS_C (**A**) and AMB_C (**B**) upon inflation of the lower thoracic oesophagus (indicated by thick bar under pressure traces). The non-rhythmic discharges lead monophasic pressure waves in the upper thoracic oesophagus (UTE). Rhythmic discharges seen in the NTS_C (**C**) and AMB_C (**D**) during sustained distension of the distal oesophagus (DE), lead phase-locked pressure waves in distended segment. Pressure waves in **C** and **D** are greatly attenuated because they are recorded by an air-filled balloon. ↑, inflation; ↓, deflation.

ii. ***Segmental differences.*** At rest, tonic unit discharges (0.5 - 3 Hz) were observed in the NTS_c region (n = 19), while the majority of units in the AMB_c region (n = 16 out of 22 recordings) were silent in the absence of oesophageal stimulation. Oesophageal distension evoked burst unit discharges in the two regions. Burst discharges could be elicited in the NTS_c by small-volume inflations at which a detectable esophagomotor reflex response was not produced. In contrast, AMB_c bursts occurred only when reflex responses were observed.

Depending on the segment being inflated, two patterns of unit discharges were elicited. With inflation of the mid-thoracic oesophagus, single burst discharges were evoked in the NTS_c (n = 9, Fig. 3.2A) and AMB_c (n= 8, Fig. 3.2B). These discharges (n = 12 out 17 recordings) typically started with a high frequency burst and decayed gradually. The remaining 5 units (n = 5 / 17) fired for a 2-3 s period and then ceased abruptly. The single burst discharges in both the NTS_c and AMB_c region had a 1:1 phase relationship with type I reflex responses (Chapter 2). In contrast, distension of the distal oesophagus produced unit discharges in both the NTS_c (Fig. 3.2C, n = 10) and the AMB_c (Fig. 3.2D, n = 14) that were rhythmic and bore a fixed phase-relationship with type II reflex peristalsis (Chapter 2). Statistical analysis of typical recordings of type II responses (Fig. 3.3) demonstrated a highly regular burst-pause pattern of neuronal activity in the NTS_c and the AMB_c. In the NTS_c, peak frequency (F_{Peak}) of the burst discharge ranged from 80 to 165 Hz (mean 125 ± 17 Hz, n = 19). In the AMB_c, F_{Peak} values ranged from 50 to 130 Hz (mean 92 ± 16 Hz, n=22).

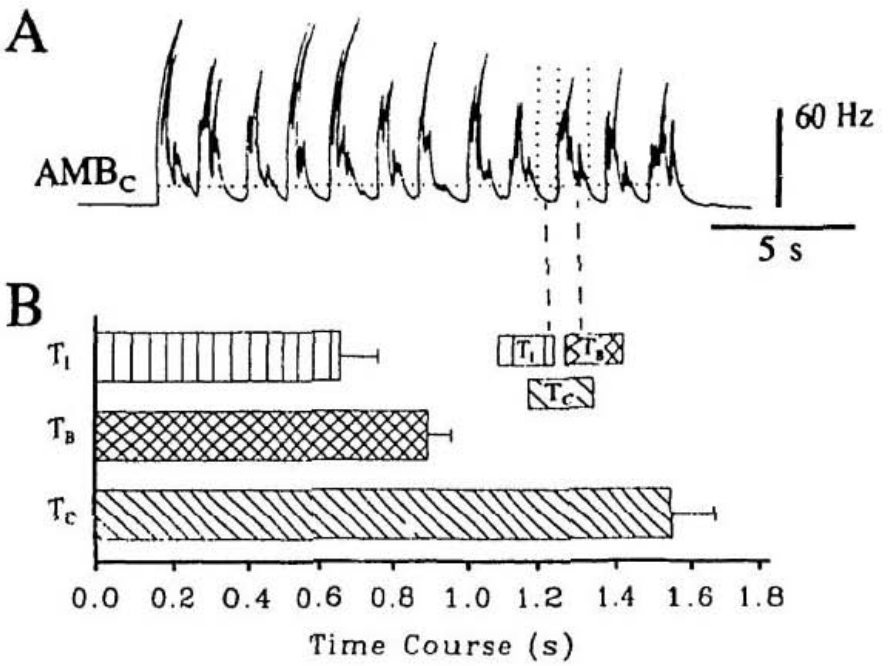
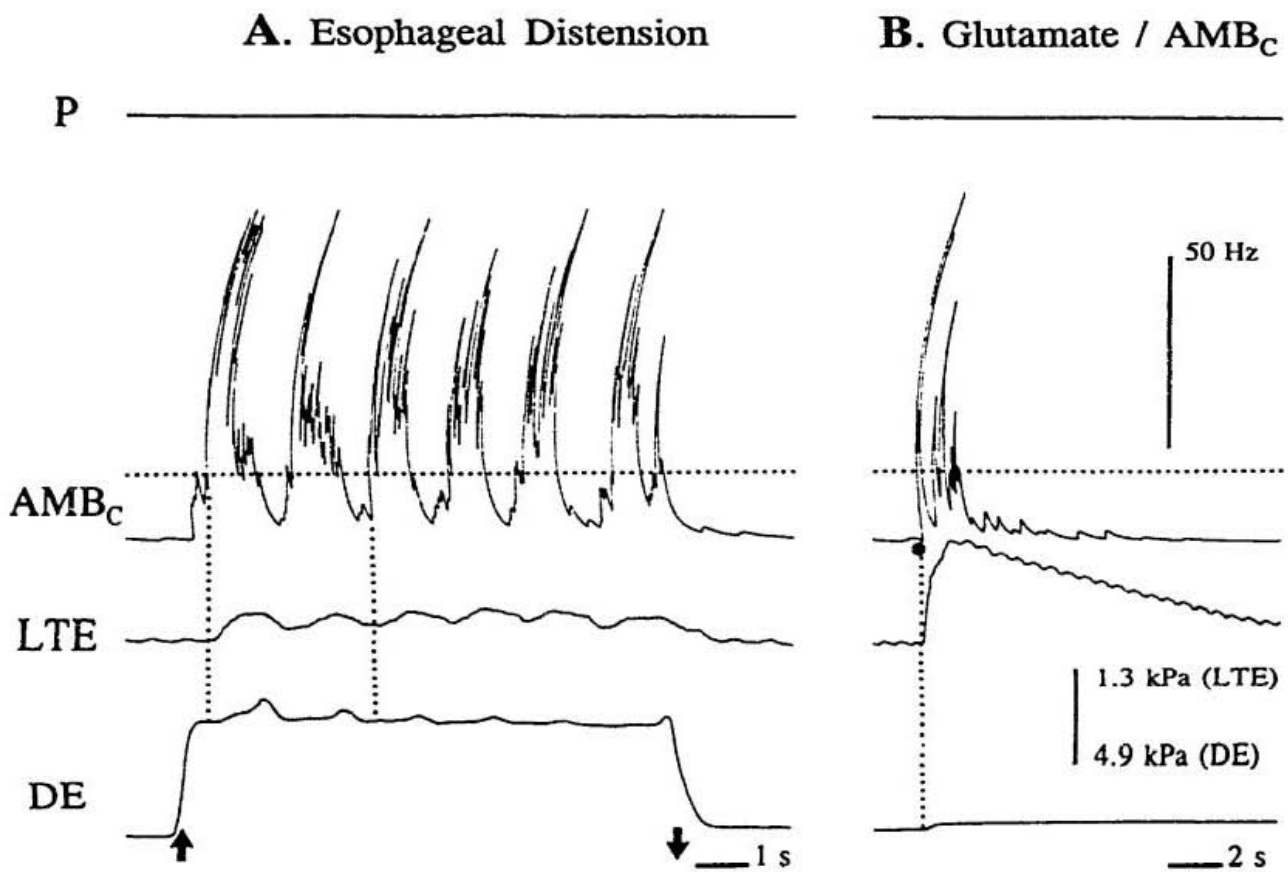


Fig. 3.3 Analysis of the reflex-evoked rhythmic esophagomotor discharge pattern. **A**. Representative example of burst activity in the AMB_C illustrates regularity of rhythm. The horizontal dotted line indicates level (15 to 20 Hz) at which the burst-pause phases are evident in all analyzed cases (n = 52 burst-pause cycles from 9 animals). **B**. The duration of each burst (T_B) is 0.90 ± 0.06 s. The mean interval between the bursts (T_I) is 0.65 ± 0.10 s. The period of each bursting cycle (T_C) is 1.55 ± 0.11 s. The frequency of the rhythmic bursts ($1/T_C$) is 0.64 ± 0.04 Hz.

Fig. 3.4 Phase-relationship between type II esophagomotor burst discharges and oesophageal pressure wave activity. **A.** Fast step distension (5 s) of the distal oesophagus (DE) evokes AMB_f rhythmic discharges that lead rhythmic propulsive pressure waves in the lower thoracic (LTE) and the distal oesophagus (DE) by ~0.2 s; note the lag between the thoracic and distal pressure wave, as well as the difference in wave shape. **B.** glutamate (0.2 M, ~20 pl) pulse-ejected at the same recording site in the AMB_f (indicated as a black dot) elicits a volley of unit discharges that leads a synchronous contraction in lower thoracic and distal segments of the oesophagus with a latency < 50 ms. Pressure signal recorded in the distal oesophagus is attenuated due to use of air as the inflation medium.


A. Esophageal Distension
B. Glutamate / AMBC
P
AMBC
LTE
DE
50 Hz
1.3 kPa (LTE)
4.9 kPa (DE)
1 s
2 s

Although the recording and stimulation technique employed in the present work did not permit precise measurement of the latency between the unit discharges and the oesophageal pressure wave, the records clearly showed that both the type I and type II unit discharges in the NTS_c and AMB_c preceded the reflex oesophageal pressure waves in a phase-locked manner. The latency between the start of the distension-evoked AMB_c type II burst discharges and the onset of the reflex oesophageal pressure wave in the thoracic segment immediately above the point of inflation was 0.15 to 0.18 s, while the corresponding latency of the pressure wave in the inflated distal segment itself was more than 0.3 s (Fig. 3.4A). However, glutamate (0.2 M, 20-50 pl) pulsed directly to the recording site in the AMB_c elicited unit discharges that were followed by a synchronized non-propulsive oesophageal pressure wave with a latency shorter than 50 ms (Fig.3.4B). None of the rhythmic unit discharges showed any phase-relationship with breathing.

iii. ***Effect of vagotomy.*** Contra- and ipsilateral vagotomies were performed in order to examine the laterality of afferent input to medullary oesophageal neurons. After contralateral vagotomy, the distension-evoked unit discharges in the NTS_c region persisted (Fig. 3.5A, n = 4). Ipsilateral vagotomy eliminated the evoked unit discharges in both the NTS_c (Fig. 3.5B, n = 6) and AMB_c region (Fig. 3.5C, n = 2).

iv. ***Effect of curarization.*** The effects of curarization on NTS_c (n = 5) or AMB_c (n = 6) unit discharges and oesophageal contractions were observed in 11 animals during artificial ventilation. Within 30 s after intravenous administration of D-tubocurarine (0.075 μmol.kg^{-1}), the amplitude of reflex oesophageal pressure waves

Fig. 3.5 Effects of contra- and ipsilateral vagotomy on oesophageal distension-evoked neural discharges in the medulla oblongata. Unit-discharges in the NTS_c region evoked by oesophageal distension (indicated by thick bar) persist after contralateral cervical vagotomy (**A**) but disappear following ipsilateral cervical vagotomy (**B**). Distension-evoked unit discharges in the AMB_c are also abolished by ipsilateral vagotomy (**C**).

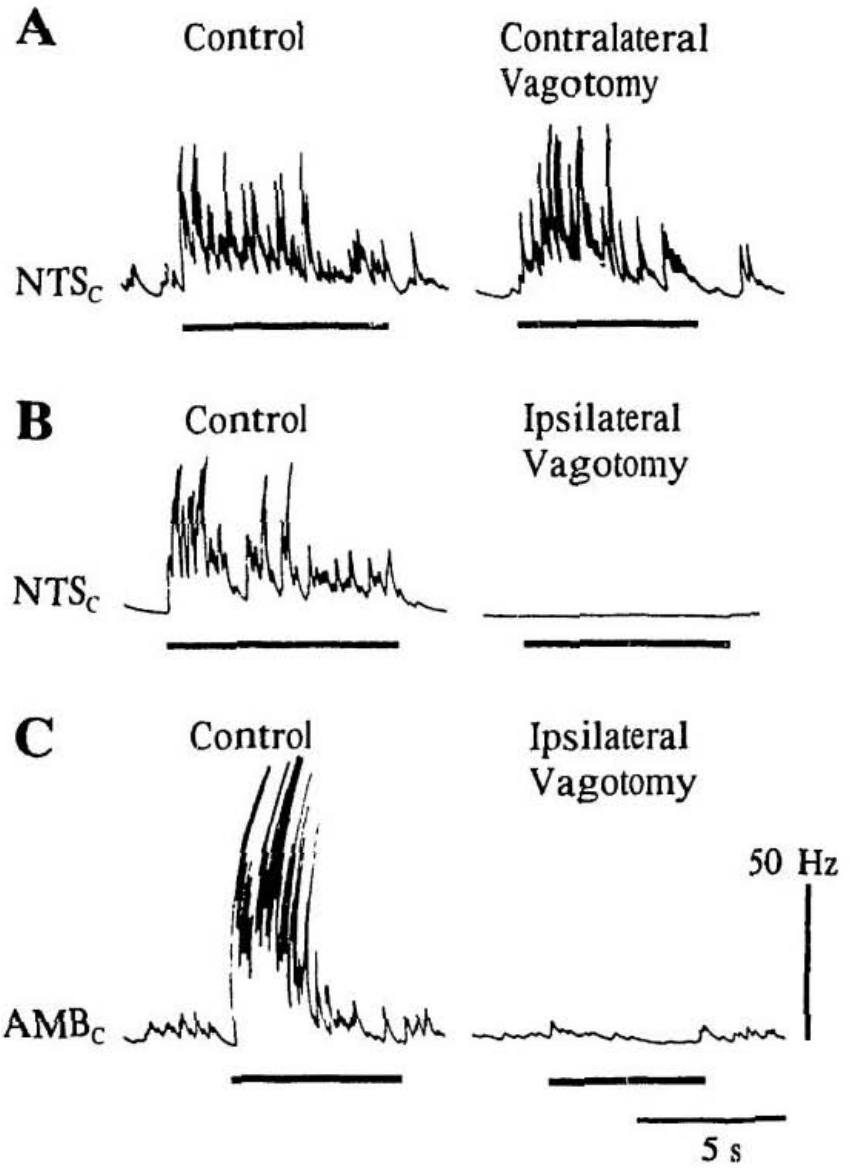
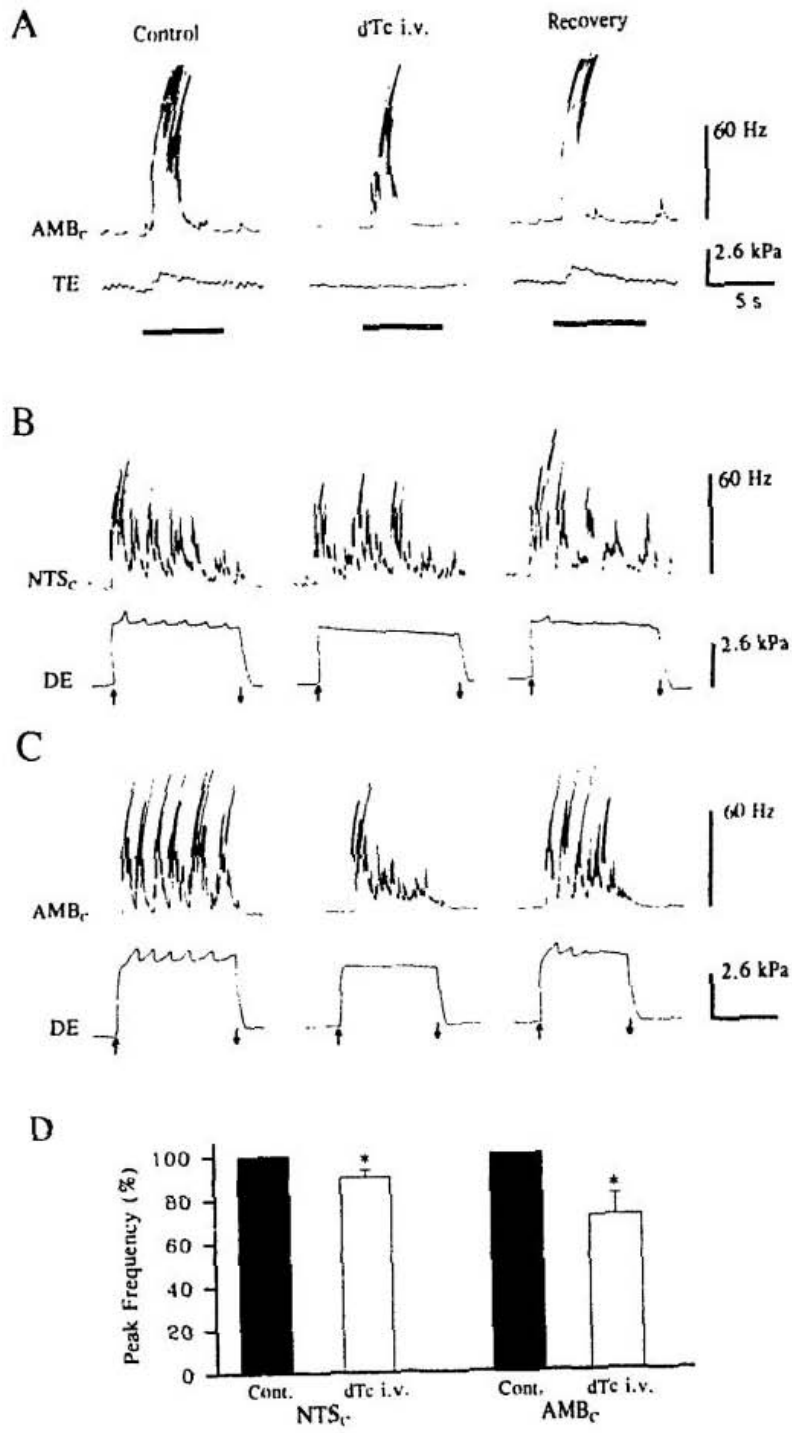

A
Control
Contralateral
Vagotomy
NTSc
B
Control
Ipsilateral
Vagotomy
NTSc
C
Control
Ipsilateral
Vagotomy
50 Hz
AMBc
5 s

Fig. 3.6 Effects of curarization on oesophageal distension-evoked activity at premotor and motoneuronal levels. After intravenous D-tubocurarine (dTc i.v.; 0.075 - 0.15 μmol.kg^{-1}), intensity of monophasic (type I) unit discharges in the AMB_c evoked by inflation of the thoracic oesophagus (TE) is reduced as evidenced by a delayed and decreased discharge (**A**); rhythmic (type II) burst activity in the NTS_c (**B**) and AMB_c (**C**) evoked by distension of the distal oesophagus (DE) shows altered periodicity and significant (*, $P < 0.05$) decrease in peak frequency (**D**).

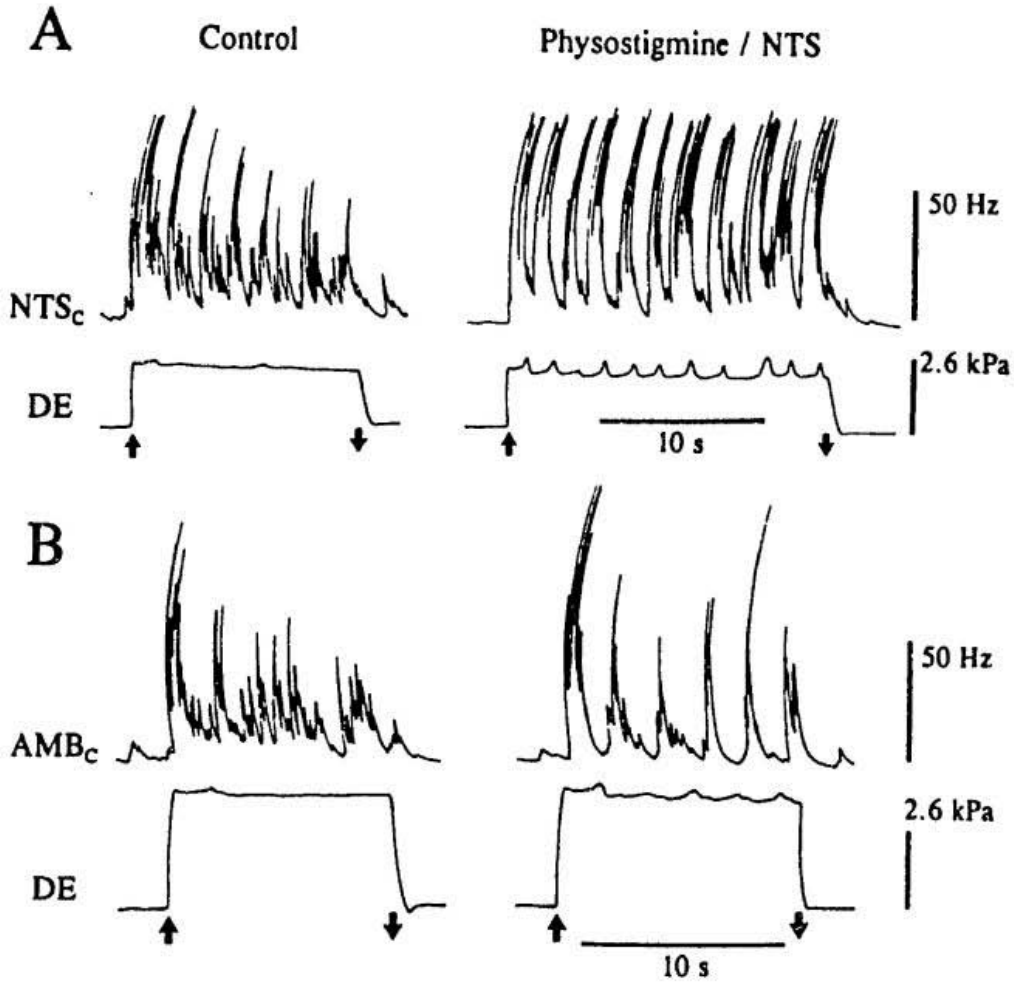

A
Control
dTc i.v.
Recovery
60 Hz
AMBc
2.6 kPa
TE
5 s
B
60 Hz
NTSc
2.6 kPa
DE
C
60 Hz
AMBc
2.6 kPa
DE
D
Peak Frequency (%)
100
80
60
40
20
0
Cont.
dTc i.v.
Cont.
dTc i.v.
NTSc
AMBc

declined to undetectable levels. At the same time, the F_{Peak} of type I unit discharges in the NTS_c (n = 3, not shown) and AMB_c (n = 3; Fig. 3.6A) was reduced. Likewise, type II unit discharges in the NTS_c (Fig. 3.6B, n = 3) and AMB_c (Fig. 3.6C, n = 5) were markedly altered. In the NTS_c region, the F_{Peak} was reduced to 90.5 ± 3.4 % of the pre-curare control (n = 6 trials from 3 animals, Fig. 3.6D-1). In the AMB_c region, the F_{Peak} was reduced to 70.8 ± 9.7 % of the pre-curare control (n = 6, Fig. 3.6D-2). Furthermore, the burst-pause pattern of the discharges became less distinct or was obliterated. During recovery of the rhythmic reflex peristaltic pressure waves, the burst-pause pattern reappeared and firing rates were restored.

v. ***Effects of activation and blockade of mAChRs in ipsilateral NTS*** . Following application of the AChE inhibitor physostigmine (20 pmol) to the ipsilateral NTS surface, the peak frequency of type II unit discharges evoked in both the NTS_c (Fig. 3.7A) and the AMB_c (Fig. 3.7B) was increased to 138.3 ± 19.2 % of the control (Fig. 3.7C-1) and 130.2 ± 13.4 % of the control (Fig. 3.7C-2), respectively. Intraesophageal pressure waves were also enhanced and the burst pause pattern of the rhythmic discharges became more distinct (Fig. 3.7A and 3.7B).

During blockade of reflex peristalsis following topical application of methscopolamine (0.1 - 1.0 nmol) to the ipsilateral NTS surface, the distension-evoked burst discharges in the NTS_c and the AMB_c were altered in a region-specific manner. In the NTS_c region, both type I (n = 4, Fig. 3.8A) and type II activity (n = 7, Fig. 3.8B) persisted, although the F_{Peak} of the neuronal responses was gradually reduced to

Fig. 3.7 Effects of ipsilateral activation of NTS mAChRs on premotor and motoneuronal activity evoked by distal oesophageal (DE) inflation. Evoked unit discharges in the NTS_c (**A**) and the AMB_c (**B**) are enhanced by application of physostigmine (20 pmol) to the ipsilateral NTS surface. The peak frequencies (F_{Peak}) of the discharges in the NTS_c (**C-1**) and the AMB_c (**C-2**) are significantly (*, $P < 0.05$) increased to 138.3 ± 19.2 % of the control value of 125 ± 17 Hz and 130.2 ± 13.4 % of the control value of 92 ± 12 Hz, respectively. Note the increase in the intra-oesophageal pressure waves (recorded by an air-filled balloon) and the change in the burst-pause pattern after physostigmine.


A
Control
Physostigmine / NTS
50 Hz
NTSc
DE
2.6 kPa
10 s
B
50 Hz
AMBc
2.6 kPa
DE
10 s

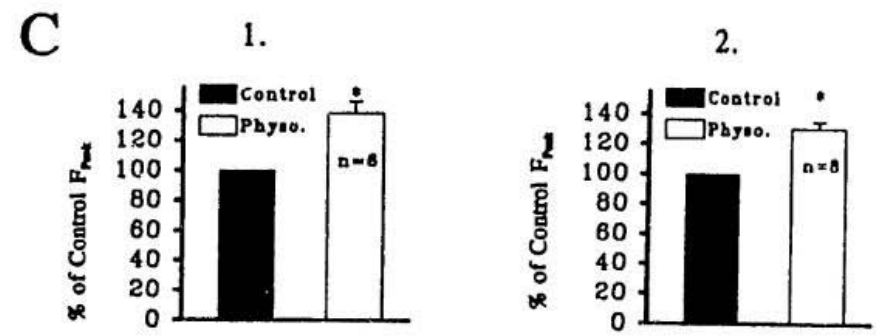

C
1.
2.
Control
Physo.
n=8
% of Control
140
120
100
80
60
40
20
0

Fig. 3.8 Effects of ipsilateral NTS mAChR blockade on premotor and motoneuronal activity evoked by oesophageal inflation. Five minutes after application of methscopolamine (MSCP 0.5 nmol) to the ipsilateral NTS surface, vigorous evoked discharges are still evident in the NTS_c (**A** and **B**), although evoked motoneuronal discharges in the AMB_c (**C**) along with reflex oesophageal pressure waves (**A**, **B** and **C**) are abolished. Note the altered pattern of type II burst discharges in the NTS_c after blockade of the esophagomotor output by methscopolamine. Five to thirty minutes after MSCP applied to the ipsilateral NTS, the F_{Peak} of the NTS_c bursts further declines from 77.3 ± 8.5 % to 58.4 ± 11.1 % of the control value of 125 ± 17 Hz (*, $P < 0.05$).

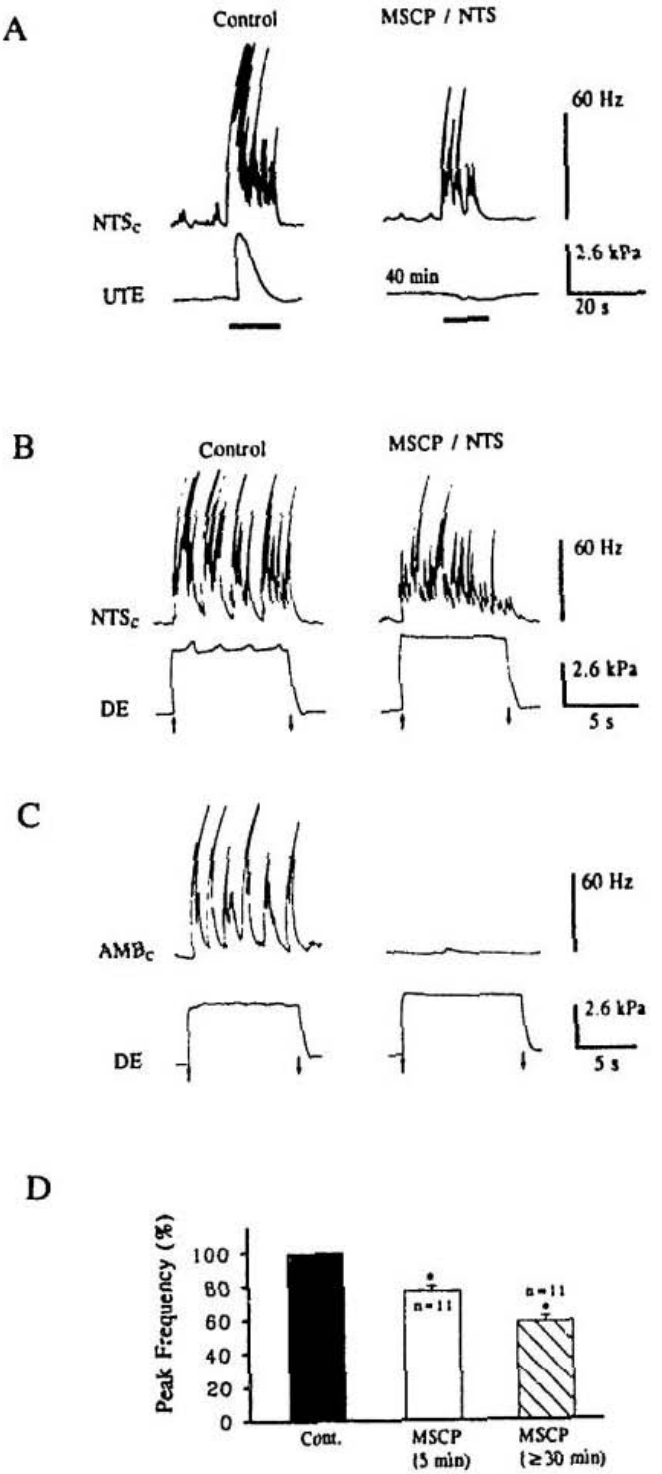
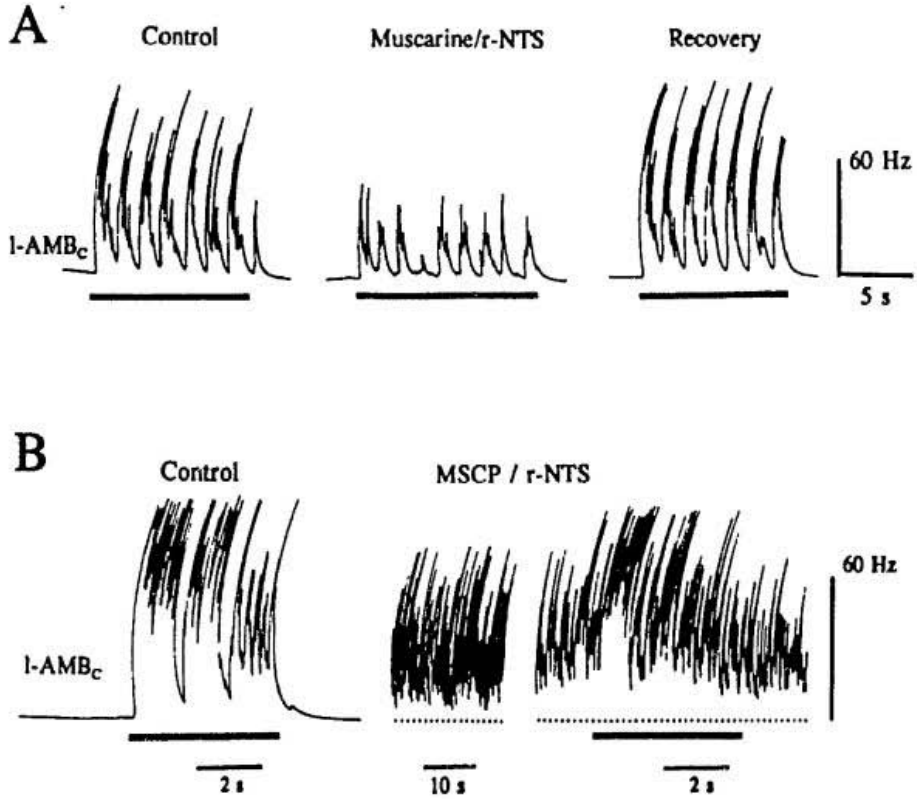

A
Control
MSCP / NTS
60 Hz
NTSc
UTE
40 min
2.6 kPa
20 s
B
Control
MSCP / NTS
60 Hz
NTSc
DE
2.6 kPa
5 s
C
60 Hz
AMBc
DE
2.6 kPa
5 s
D
Peak Frequency (%)
100
80
60
40
20
0
n=11
n=11
Cont.
MSCP
(5 min)
MSCP
(≥30 min)

Fig. 3.9 Effect of contralateral activation and blockade of NTS mAChRs on motoneuronal activity evoked by oesophageal inflation. **A**. Control shows an extracellular recording from the left AMB_c (l-AMB_c) region during distension of the distal oesophagus (indicated by heavy bar below the trace). Following application of a subthreshold-dose (12 pmol) of muscarine to the right (contralateral) NTS (r-NTS) surface, the evoked unit discharges in the left AMB_c are reversibly depressed and motoneuronal activity fully recovers in 15 min. **B**. Control (left panel) shows another extracellular recording in the left AMB_c region during distension of the distal oesophagus (thick bar below the trace). Methscopolamine (MSCP, 50 pmol) applied to the right (contralateral) NTS surface resulted in tonic discharges in the AMB_c in the absence of oesophageal distension (middle panel). In the presence of MSCP applied to the contralateral NTS, oesophageal distension causes an increased discharge (right panel). The dotted line indicates the base line of the trace. Note the different time scales. l-AMB_c: left AMB_c; rNTS: right NTS.

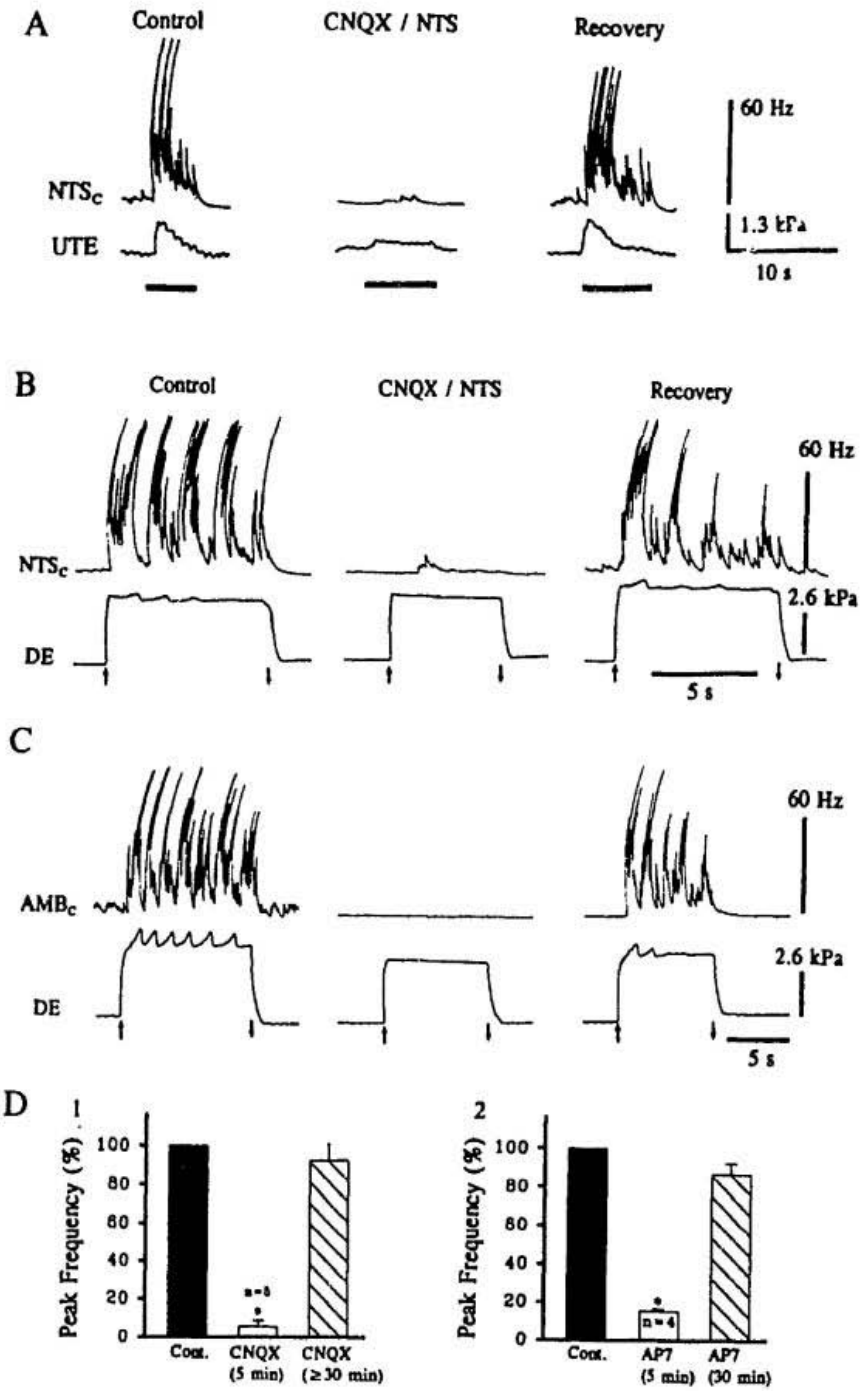

A
Control
Muscarine/r-NTS
Recovery
60 Hz
l-AMBc
5 s
B
Control
MSCP / r-NTS
60 Hz
l-AMBc
2 s
10 s
2 s

77.3 ± 8.5 % of the control (Fig. 3.8D); and the rhythmicity of type II discharges became indistinct (Fig. 3.8B). By contrast, in the AMB_c region, evoked unit discharges ceased completely when the esophagomotor output had disappeared (Fig. 3.8C, n = 4). Application to the ipsilateral NTS surface of D-β-E (10 to 20 nmol) did not affect the unit discharges in the NTS_c region (n = 3, not shown).

vi. ***Effects of activation and blockade of mAChRs in contralateral NTS.*** Activation of contralateral NTS mAChRs depressed AMB_c motoneuronal activity. As depicted in Fig. 3.9A, following muscarine (12 pmol) applied to the right NTS surface, the frequency of distension-evoked type II discharges in the left AMB_c was reversibly decreased for 7 to 15 min, but the burst-pause pattern of the rhythmic discharges remained unchanged (n = 3). By contrast, 2 to 3 min after application of methscopolamine (MSCP, 50 pmol) to the right NTS surface, the neurons in the left AMB_c started to discharge tonically (Fig. 3.9B). Within 5 min the tonic discharges reached peak-frequencies of 50 to 70 Hz then gradually slowed down and ceased in 30 to 40 min (n = 2). However, the peak frequency of evoked-discharges in the AMB_c was not changed.

vii. ***Effects of EAA antagonists.*** Both type I (Fig. 3.10A) and type II (Fig. 3.10B) discharges in the NTS_c were reversibly depressed by the application to the ipsilateral NTS surface of the competitive kainate/AMPA subtype glutamate receptor antagonist, CNQX (0.2 to 2.0 nmol). The effect reached a maximum within 5 min, NTS_c discharges being completely abolished in 3 out of 8 recordings, and in 5 other cases the

Fig. 3.10 Effect of glutamate receptor blockade in the NTS on oesophageal inflation-evoked neural activity in the subnucleus centralis (NTS_c) and nucleus ambiguus (AMB_c). Topical application of 6-cyano-7-nitroquinoxaline-2,3-dione (CNQX, 0.2-1.0 nmol) to the NTS surface reduces type I (**A**) and type II (**B**) burst-discharges in the NTS_c and eliminates type II response in the AMB_c (**C**) together with esophagomotor output. Application of AP-7 (5.0 - 10 nmol) to the NTS surface exerts similar effects (**D-2**). After CNQX (**D-1**) and AP-7 (**D-2**), the peak-frequency (F_{Peak}) of NTS_c discharges is reversibly reduced to 5.6 $\pm$ 6.6 % and 12.5 $\pm$ 2.5 % of the control value of 125 $\pm$ 17 Hz (*, $P < 0.05$), respectively.


A
Control
CNQX / NTS
Recovery
60 Hz
NTSc
UTE
1.3 kPa
10 s
B
Control
CNQX / NTS
Recovery
60 Hz
NTSc
2.6 kPa
DE
5 s
C
60 Hz
AMBc
2.6 kPa
DE
5 s
D
1
Peak Frequency (%)
100
80
60
40
20
0
n=6
Cont.
CNQX (5 min)
CNQX (≥30 min)
2
Peak Frequency (%)
100
80
60
40
20
0
n=4
Cont.
AP7 (5 min)
AP7 (30 min)

F_{Peak} of the discharges were reduced to 5.6 ± 6.6 % of the control level. Thirty to forty minutes after application of CNQX, the F_{Peak} of the unit discharges recovered to 93 ± 12 % of the control (Fig. 3.10D-1). Applied by the same route, γ-DGG (20 nmol, n = 2), a nonselective competitive glutamate receptor antagonist, qualitatively showed the same effect as CNQX (not shown), whereas the selective NMDA receptor antagonist, AP-7 (5.0 - 10 nmol), decreased F_{Peak} of the evoked NTS_c discharges to 15.5 ± 2.5 % of the control (n = 4). Recovery to 88 ± 5.5 % of the control occurred during the following 30 min (Fig. 3.10D-2). Furthermore, NTS surface application of either CNQX (Fig. 3.10C; n = 6) or AP-7 (n = 3, not shown) reversibly abolished the ipsilateral AMB_c unit discharges together with reflex esophagomotor output.

3.2.2 Evoked Synaptic Responses in the NTS_c *In Vitro*

i. ***EPSPs and miniature spikes.*** Successful recordings were obtained from 87 cells in the NTS_c region of the horizontal brainstem slice preparation (Fig. 3.11A). Cells were identified as neurons based on the presence of spikes (spontaneous or evoked by suprathreshold depolarizing current steps). The membrane potential of the neurons, after rupturing the membrane to achieve the whole-cell configuration, varied from -42 to -67 mV (-52 ± 8.0 mV). Most of the neurons with membrane potentials lower than -50 mV fired spontaneously with a prominent spike afterhyperpolarization. Thus, the membrane potential of the cells was held at -60 mV in the bridge mode. Fast EPSPs were evoked in 56 out of 87 recorded neurons by stimulation of the solitary tract (ST) with a

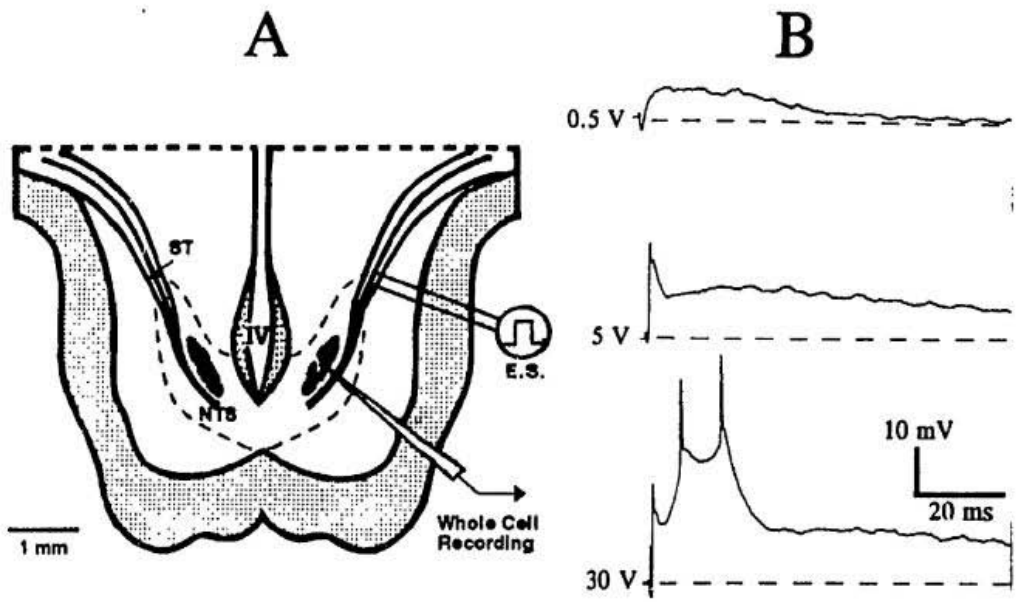


Fig. 3.11 Excitatory postsynaptic potentials (EPSPs) evoked by solitary tract stimulation in the subnucleus centralis region. **A**. Schematic sketch showing the horizontal brainstem slice preparation. A bipolar electrode is placed in the solitary tract (ST) for electrical stimulation (E.S.) and whole cell recordings are made in the NTS_c region (shaded area). IV, fourth ventricle. **B**. EPSPs in the same NTS_c neuron evoked by single pulse (0.1 ms) stimulation. Weak stimulation (top trace) evokes an EPSP only, whereas more intense stimulation elicits EPSPs with superimposed single spike (middle trace) or spikes (bottom trace). Dashed line indicates the held potential of -60 mV.

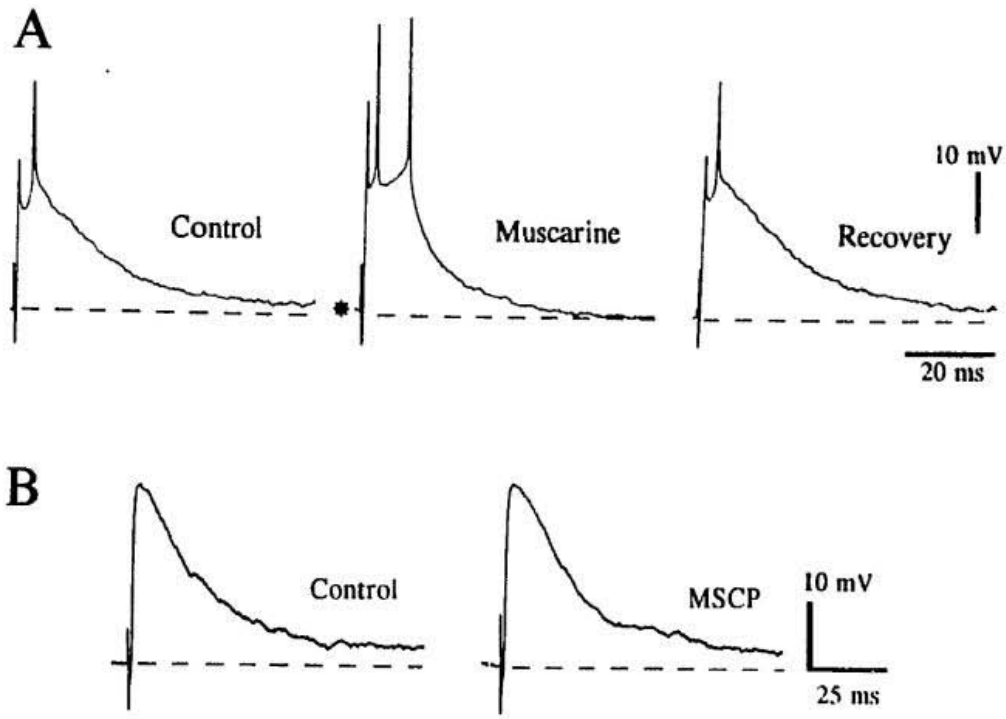


Fig. 3.12 Muscarinic effects on synaptic responses in the NTS_c. **A**. Left panel) shows a NTS_c EPSP with superimposed spikes. The number and amplitude of spikes superimposed on the EPSP are increased by a pulse of muscarine (asterisk, ~ 20 pmol) applied to NTS_c region (middle panel) and recover after 5 min washout. **B**. Bath perfusion of methscopolamine (MSCP, 10 μM) does not affect the EPSP of another cell in the NTS_c. The intrinsic membrane potential of these two cells is -52 mV (**A**) and -56 mV (**B**). The EPSPs of both neurons are elicited at a holding potential of -60 mV (dashed line).

single electrical pulse (0.1 ms). The peak amplitude and duration of the EPSPs varied with the intensity of the stimulation. At intensities of 6 to 8 V, the neurons produced EPSPs (12 to 25 mV, mean 17.2 ± 3.6 mV, n = 56), some of which were superimposed with spikes (Fig. 3.11B). Upon stimulation of the ST with pulse trains (2-5 V, 2-10 Hz, 1-5 s), no slow or late EPSPs were observed (n = 17, not shown). However, when held at potentials of -45 to -50 mV, 2 of 6 neurons produced a group of miniature spikes immediately following the stimulus train (see Fig. 3.14).

ii. ***Effects of mAChR stimulation or blockade.*** In 56 neurons that generated synaptic responses to stimulation (6-8 V) at a holding potential of -60 mV, pulses of muscarine (~ 100 pmol) produced a low-amplitude (3-5 mV), long-lasting (3-10 min) membrane depolarization (28/56) or hyperpolarization (4/56). Concomitantly, the peak amplitude of the EPSPs increased by 23 ± 11 % of the control (n = 32). Furthermore, the number of spikes riding on the EPSP was increased in 11 neurons (Fig. 3.12A). However, the peak amplitude of the EPSPs in all neurons tested (n = 56) was not affected by bath perfusion of the slices with 1-20 μM of methscopolamine (Fig. 3.12B).

iii. ***Effect of EAA antagonists.*** Bath application of the non-selective EAA receptor antagonist, kynurenate (1 mM), eliminated the fast component of the EPSP (Fig. 3.13A-2; n = 9), and the peak amplitude of the EPSP was reduced to 28 ± 12 % of the control (Fig. 3.13B). The effects on EPSPs of bath-applied CNQX (10 μM, n = 5) and γ-DGG (50 μM, n = 2, not shown) were qualitatively similar to that of kynurenate. When combined with kynurenate (1 mM), AP-7 (50 μM) further depressed the slow

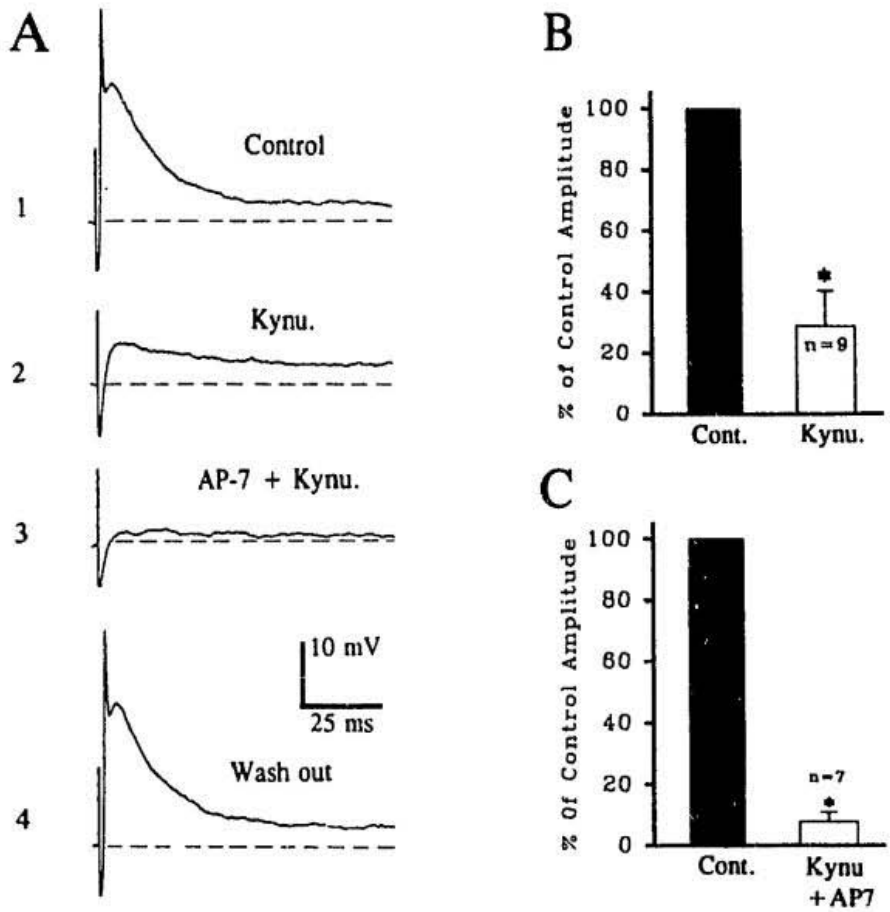


Fig. 3.13 Blocking effects of glutamate receptor antagonists on NTS_c synaptic response elicited by stimulation of the solitary tract. **A.** Fast single EPSP consisting of early and late components (**A-1**). After 12 min bath perfusion with kynurenate (1 mM), the early component of the EPSP and superimposed spike are eliminated, whereas the late component persists (**A-2**). The late component is abolished by bath-applied AP-7 (50 μM) plus the kynurenate (**A-3**); full recovery is seen after 27 min of wash. **B.** EPSP amplitude is significantly reduced to 28 $\pm$ 12 % and 7.5 $\pm$ 2.8 % of control by 1 mM kynurenate alone (**B**) and kynurenate / AP-7 (50 μM) combination (**C**), respectively.

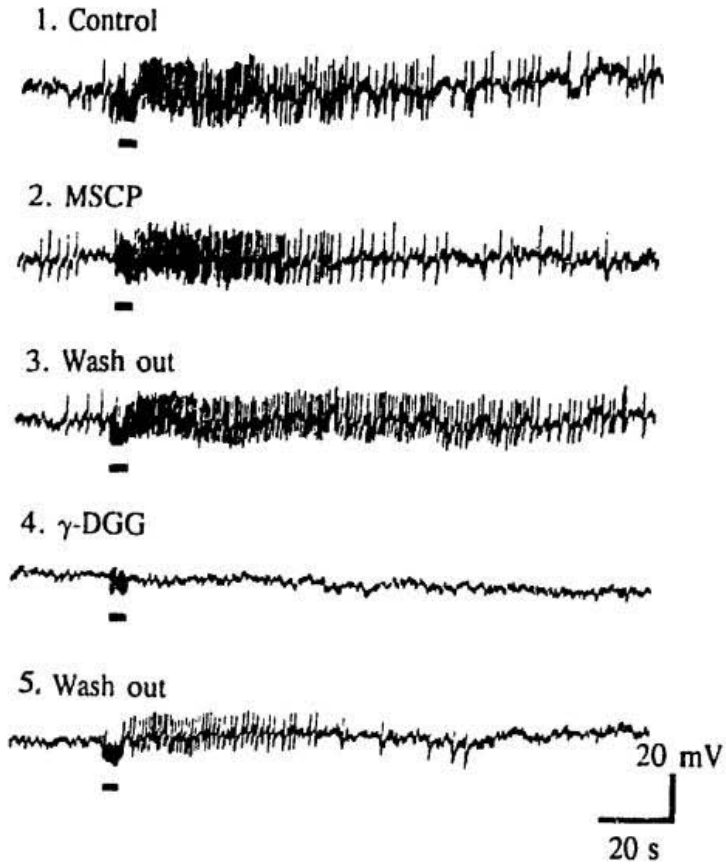


Fig. 3.14 Elimination of evoked miniature spikes by blockade of glutamate but not muscarinic receptors. Train of stimulus pulse (0.1 ms, 2 V, 3 Hz; indicated by the bar below the traces) evokes repetitive miniature spikes in an NTS_c neuron held at -50 mV (1). Following 10 min of bath perfusion with methscopolamine (MSCP, 10 μM), the evoked miniature spikes persist, although the duration of the response is slightly reduced (2). By contrast, the evoked response is eliminated following an 8 min perfusion with γ-DGG (50 μM) (4) and partially recovers after a 12 min wash (5).

component of the EPSP (Fig. 3.13A-3). The peak-amplitude of the EPSPs was reduced to 7.5 ± 2.8 % of the control (n = 7, Fig. 3.13C). The EPSPs recovered after a 15-30 min washout of the antagonist.

iv. ***Effects of mACh and EAAergic antagonists on evoked miniature spikes.*** As shown in Fig. 3.14, the miniature spikes evoked by a stimulus train were resistant to methscopolamine (5 - 10 μM, n = 2), but eliminated by perfusion of γ-DGG (50 μM, n = 2).

3.3 Discussion

3.3.1 Functional Anatomical Considerations

Previous electrophysiological work in the rat (Kessler & Jean 1985) has mapped the location in the medulla oblongata of deglutitive unit discharges occurring during reflex swallows elicited by stimulation of the superior laryngeal nerve (SLN). The dorsal and ventral groups of extracellularly recorded unit activity described in that report probably related mostly to the buccopharyngeal stage. Units active during the oesophageal stage of swallowing were not explicitly described, except for a few elements that discharged up to 140 ms after the onset of buccopharyngeal activity.

The present observations bear on the functional organization of medullary interneurons controlling reflex oesophageal peristalsis in the rat. Unit burst discharges induced by distension of different oesophageal segments were localized to two circumscribed medullary regions coextensive with the NTS_c and AMB_c. In light of the

neuroanatomical evidence (Altschuler et al.,1989; Barrett et al.,1994; Bieger & Hopkins, 1987; Cunningham & Sawchenko,1989; Gai et al.,1995), these two structures can be considered to form the medullary throughput of the oesophageal reflex arc. As expected, the neuronal discharges recorded in both regions and the esophagomotor output elicited showed a fixed phase-relationship. Due to technical limitations, the latency between the neuronal discharges and the oesophageal contractions could be determined only by approximation. Given the neuroanatomical evidence, however, it seems reasonable to regard NTS_{ℓ}- neuronal burst discharges as premotor output and AMB_{ℓ}- bursts as motoneuronal output. Oesophageal premotoneurons and motoneurons within the NTS_{ℓ}- and AMB_{ℓ}-, respectively, have a crude organotopic distribution with considerable rostrocaudal overlap (Altschuler et al.,1989; Barrett et al.,1994; Bieger & Hopkins, 1987). It is thus noteworthy that distension of different segments of the oesophagus produced distinct esophagomotor response patterns.

As described in Chapter 2, distension of the intracrural oesophagus evokes rhythmic (type II) contractions in the lower thoracic segment that propagate to the inflated segment itself. Indeed, evoked AMB_{ℓ}- rhythmic discharges were observed to lead the pressure wave activity in the inflated portion by about 0.3 s, however, in the segment just proximal to the level of inflation the lead-time between motoneuronal burst discharges and pressure waves was reduced by a factor of about 2. This phenomenon cannot be a recording artifact, because a pulse of glutamate delivered at the same recording site in the AMB_{ℓ}- motoneuronal pool produced volleys of unit discharges that

preceded an oesophageal contraction at a latency of $\leq$ 50 ms. It thus appears that segmental distension activates NTS_c subcircuits controlling motoneurons innervating oesophageal segments rostral to the level of inflation. This functional arrangement could assist aboral bolus propulsion towards the stomach. By contrast, chemostimulation of the AMB_c evoked an oesophageal contraction synchronized with motoneuronal discharges, suggesting that the peristaltic pattern is not programmed at the motoneuronal level.

It is evident that the oesophageal CPG network can be configured to perform different motor tasks. Intersegmental coordination of different motor patterns of single limbs or single body segments has been observed in walking and swimming animals. To explain the flexibility of CPG networks, Grillner and coworkers (Grillner et al., 1991, Grillner et al., 1988; Grillner & Wallén, 1985b) have proposed that spinal CPGs subserving locomotion can be divided into several smaller functional units, termed "segmental circuits", each of which can produce fictive locomotor activity with intersegmental coordination. Our findings are consistent with this hypothesis, in that different oesophageal segments appear to be controlled by their own "segmental circuit". The coupling between unit burst generators can be altered by signals from the periphery or central nervous system, thus allowing the same neuronal network to generate appropriate motor patterns under different physiological conditions.

3.3.2 Premotor Connectivity

Vagal sensory fibres innervating the oesophagus in the rat (Andrew 1956), cat

(Mei 1970; Mei et al. 1974) and sheep (Falempin et al. 1978) display spontaneous activity, but electromyographic activity is absent in the resting oesophagus (Christensen, 1987; Monges et al. 1968; Arimori et al. 1970; Hellemans et al. 1974). As shown here, the interneurons in the NTS_c are tonically active at rest, while the oesophageal motoneurons in the AMB_c are silent. One may therefore surmise that: 1) oesophageal interneurons receive tonic excitatory inputs originating from peripheral sensory receptors at rest; and 2) oesophageal motoneurons integrate premotor inputs and fire only when the discharge frequency of the interneurons reaches a threshold level. The latter assumption is consistent with the observation that following blockade of mAChRs in the NTS, the intensity of the evoked response in the NTS_c was reduced, whereas evoked motoneuronal activity in the AMB_c along with esophagomotor reflex activity was eliminated.

The oesophagus is controlled by bilateral inter- and moto-neuronal networks that are located in each half of the medulla oblongata (Altschuler et al., 1989; Barrett et al., 1994). In sheep, a small unilateral electrolytic lesion in the medial region of the NTS selectively eliminates the oesophageal stage of swallowing induced by ipsi-, but not contralateral stimulation of the SLN (Jean, 1972a). This result suggests two possibilities: 1) buccopharyngeal interneurons activated by SLN-afferents innervate mainly ipsilateral oesophageal interneurons; and/or 2) the oesophageal afferents in the SLN project to ipsilateral oesophageal interneurons.

In the present study, NTS_c interneuronal discharges induced by distension of the oesophagus were abolished by ipsi- but not contralateral vagotomy. This observation

supports the idea that afferents from the oesophagus in each vagal trunk project mainly to the ipsilateral NTS_c. This is in agreement with anterograde tracing experiments (Bieger, personal communication) showing that the central projection from the nodose ganglion to the NTS is uncrossed. Furthermore, consistent with neuroanatomical and functional data (Cunningham & Sawchenko, 1989; Hashim, 1989; Wang, 1992), the oesophageal motoneurons likewise would appear to receive excitatory input only from ipsilateral interneurons, since unilateral vagotomy completely eliminates distension-evoked unit discharges in the ipsilateral AMB_c.

Previous studies (Hashim, 1989) show that a subpopulation of NTS_c neurons projects to the contralateral NTS_c region. However, knowledge as to how the two premotor-motor neuronal networks (two "half-centers") in each side of the medulla are coordinated in esophagomotor control remains limited. Unpublished work from this laboratory reveals that the esophagomotor response evoked by unilateral chemostimulation of the NTS is enhanced by a midline-lesion of the medulla oblongata, suggesting "crossed-inhibition" between the "half-centres". This hypothesis is supported by the present results, in that the motoneuronal response is depressed by activation of contralateral premotoneurons and tonic motoneuronal activity is produced by inhibition of contralateral premotoneurons. Given the unilateral premotor-motor projection, this "crossed-inhibition" should occur at the premotor level.

3.3.3 Role of Reafferent Input

In the rat (Andrew, 1956), opossum (Sengupta et al.,1989), cat (Mei, 1970) and sheep (Falempin & Rousseau, 1984), bursts of spikes discharge in vagal afferent fibres during distension of the oesophagus or the oesophageal stage of swallowing. Rhythmic vagal afferent discharges associated with rhythmic oesophageal contractions in the sheep are elicited by sustained distension of the oesophagus (Falempin & Rousseau, 1984), suggesting that oesophageal mechanoreceptive impulses in response to stretch (feedforward) and contraction (feedback) are conveyed by two different sets of vagal afferent fibres. In the present study, sustained distension of the distal portion of the rat oesophagus could also produce rhythmic burst discharges in the NTS_c neurons. Since NTS_c neurons function dually as premotor neurons and second-order sensory neurons (Bieger, 1993), this rhythm of NTS_c neuronal activity may be generated by the neurons in response to tonic input conveyed by feedforward peripheral afferent fibers, or a response to phasic input from feedback afferent fibers.

Motor paralysis does not disrupt the sequential discharge of the cranial motor nerves during reflex-evoked swallowing (Jean, 1972b, Kessler and Jean,1985). Therefore it has been hypothesized that a medullary interneuronal network can program the entire motor sequence for oesophageal peristalsis without peripheral feedback (Jean,1990; Roman,1982). As regards rhythmic (type II) reflex oesophageal peristalsis in the rat, peripheral feedback appears to play a critical part as evidenced by the marked alteration of reflex activity of both NTS_c and AMB_c neurons during curarization. Since curarization

does not reduce the resistance of the oesophageal wall to stretch (Chapter 2), the observed attenuation of distension-evoked neuronal discharges cannot be attributed to slackening of the muscle tunic, but instead implies a role of re-afferent signals in the reinforcement of esophagomotor output. More strikingly, the disruption of the regular burst-pause pattern of type II discharges strongly suggests that reafferent feedback although not absolutely required for esophagomotor rhythmogenesis, is nonetheless essential for shaping the final motor patterns and for motoneuronal recruitment. The limitations inherent in extracellular multi-unit recording preclude a definitive answer to the question of whether the rhythmicity of the evoked type II burst activity was abolished altogether or shifted into a broader frequency range in different neurons. Single cell studies in NTS_{c} slice preparations (presented in Chapter 5) show that NTS_{c} neurons produce oscillations with a pattern similar to type II reflex activity during stimulation of EAA receptors, suggesting that NTS_{c} neurons can generate esophagomotor rhythm without phasic afferent input.

3.3.4 Oesophageal Reflex Afferent Neurotransmission

The oesophageal interneurons in the NTS_{c} and motoneurons in the AMB_{c} respond to fast step balloon inflation of the oesophagus with a short latency of onset and cease activity immediately upon deflation of the balloon, indicating that they are activated by a fast excitatory process. In the mammalian brain, most excitatory transmission occurs via the action of glutamate, acting on AMPA and NMDA receptors (Grillner et al.,

1991). Glutamate has been indicated as a neurotransmitter utilized by several visceral afferents to the NTS (Andresen & Yang, 1990; Dietrich et al., 1982; Drewe et al., 1990; Perrone, 1981; Wang & Bradley, 1995). Both the EAA and ACh are candidate neurotransmitters in the NTS_c oesophageal premotoneuronal pool (Bieger, 1984; Hashim & Bieger, 1989), however, their transmitter role in vagal afferents to the NTS_c is still unclear. As shown here, oesophageal distension-evoked NTS_c neuronal activity and the solitary tract-driven EPSPs were resistant to mAChR antagonists but abolished by EAA receptor blockade. These findings argue against the hypothesis that oesophageal afferents are cholinergic and instead support a role for EAAs.

If mAChRs in the NTS region (Wamsley et al., 1981) are innervated by vagal afferent fibres, slow long-lasting EPSPs might have occurred in NTS_c neurons upon solitary tract stimulation. However, in the *in vitro* studies, most of the recorded neurons showed fast synaptic responses to stimulation of the solitary tract and slow EPSPs were not observed in any of the neurons tested. The fast synaptic responses, including the EPSPs and miniature repetitive spikes, were methscopolamine-resistant but significantly reduced or blocked by EAA receptor antagonists. In this regard, our *in vitro* results support the idea that vagal afferent transmission in the NTS_c is mediated by an excitatory amino acid acting at both AMPA/kainate and NMDA receptor subtypes. At the same time, these data suggest that the cholinergic innervation of the NTS_c comes from propriobulbar sources.

The results of the present experiments shed further light on the role of the NTS_c

mAChRs in the control of oesophageal peristalsis. Although blockade of mAChRs *in vitro* did not disrupt synaptic transmission from vagal afferents to NTS_{ϵ} neurons, activation of mAChRs facilitated the production of spikes in these neurons. Furthermore, blockade of NTS cholinergic transmission *in vivo* resulted in an attenuation of evoked NTS_{ϵ} burst discharges and loss of AMB_{ϵ} motoneuronal output. Thus, muscarinic cholinergic input to the NTS_{ϵ} presumably from a *propriobulbar source* appears necessary for maintaining the excitability of these oesophageal premotoneurons at a level appropriate for activating their motoneuronal targets. Blockade of mAChRs also resulted in a loss of rhythmicity of unit discharges in the NTS_{ϵ} when the neuronal activity in the AMB_{ϵ} and the esophagomotor output in response to the oesophageal distension disappeared. A possible explanation for this phenomenon is that reduction in oesophageal premotor output due to blockade of mAChRs in the NTS results in the loss of motor output, hence a loss of reafferent regulation, as in the case of neuromuscular paralysis. As a modulatory mechanism, NTS_{ϵ} cholinergic transmission evidently plays a pivotal role in esophagomotor pattern generation.

In summary: (i) neurons in the NTS_{ϵ} and AMB_{ϵ} show correlated activity patterns in response to local oesophageal distension; (ii) vagal afferents from the oesophagus employ an EAA rather than ACh to convey excitatory input to the ipsilateral NTS_{ϵ}, suggesting a propriobulbar source of cholinergic innervation of the NTS_{ϵ}. These data raise the following questions: What is the role the cholinergic input to the NTS_{ϵ} in

esophagomotor initiation and pattern generation? Especially, does the cholinergic link enable rhythmic esophagomotor output to be generated without peripheral sensory input?

Chapter 4

CHOLINERGIC INPUT AND PATTERN GENERATION

Previous studies (Bieger, 1984; Wang and Bieger, 1991) have demonstrated in the rat that blockade of mAChRs in the NTS_c selectively eliminates the oesophageal stage of fictive swallowing, indicating a critical role of cholinergic neurons in oesophageal control. The findings described in Chapter 3 argue against the possibility that the cholinergic input comes from the periphery. Further study of central cholinergic input thus seemed warranted, particularly, since a potential source of cholinergic afferents to the intermediate solitarius complex has recently been identified in the zona intermedialis reticularis parvicellularis (ZIRP) by combined retrograde tracing and ChAT immunocytochemistry (Vyas et al., 1990; Wang, 1992).

While it is generally agreed that oesophageal peristalsis is subject to central control, the issue of how much sensory input from the oesophagus is required to program the motor sequence of the oesophageal phase of swallowing remains a matter of debate. Indeed, the viewpoint has recently been put forth that both primary and secondary peristalsis occur in response to oesophageal distension (Cunningham & Sawchenko, 1990). By implying a key role of sensory input in the initiation and maintenance of patterned esophagomotor output, this concept calls into question the existence of a oesophageal CPG.

With respect to the postulated cholinergic control of esophagomotor pattern

generation, this study sought to answer three basic questions: (i) What are the functional parameters involved? (ii) Is re-afferent input needed? (iii) Are neurons in the ZIRP involved?

The following strategies were used in this study.

1) To characterize the role of NTS cholinergic mechanisms in esophagomotor control, effects of muscarinic activation and blockade in the NTS were examined during evoked swallowing activity.

2) To demonstrate central links in pharyngo-oesophageal coupling, a unilateral section of the cervical vagus and SLN was combined with a contralateral section of the internal branch of the SLN.

3) To examine the role of re-afferent feedback in esophagomotor rhythmogenesis, rats were subjected to neuromuscular blockade during extracellular recording of rhythmic oesophagomotoneuronal activity in the AMB_c evoked by activation of mAChRs in the NTS. Further, in a brainstem slice preparation containing the medullary oesophagomotor network, synaptic activity in single oesophagomotoneurons was studied by activation of mAChRs in the NTS_c.

4) To explore the role of the ZIRP cholinergic neurons, two complementary approaches were taken to determine (*a*) whether stimulation of the ZIRP evoked esophagomotor activity and whether muscarinic blockade in the NTS would prevent this response; and (*b*) whether inhibition of the ZIRP neurons would affect oesophageal peristalsis resulting from facilitation of endogenous cholinergic transmission in the NTS.

4.1 Methods and Materials

4.1.1 Procedures for *In Vivo* Experiments

i. *Surgical preparation.* Experiments were done on male Sprague-Dawley rats weighing 250-450 g. Procedures for monitoring respiration, recording pressure changes in the upper alimentary tract, distension of the oesophagus and brain surgery were as described in Chapters 2 and 3. In some cases, the left or right femoral artery was cannulated for continuous measurement of arterial blood pressure and arterial pulse rate. Depending on the experimental protocol, the internal ramus of the left SLN, and right SLN and cervical vagal trunk were cut. During neuromuscular paralysis induced by intravenous D-tubocurarine (0.075-0.15 μmol.kg^{-1}), animals were ventilated with oxygen enriched air by the use of a positive pressure pump (90-100 strokes.min^{-1}, 2.5-3.0 ml stroke^{-1}).

ii. *Chemo- and electrostimulation of swallowing loci in the NTS and ZIRP.* Topical and pneumophoretic applications of drugs were used to activate or inhibit swallowing neurons in the NTS. The topical application of drugs was the same as described in Chapter 2 and 3.

In some experiments, the NTS oesophageal locus was electrically stimulated by means of a glass microelectrode which contained a carbon-fibre and was filled with 4 M NaCl. Stimulation consisted of positive square wave pulses of 0.1 ms duration, 1-5 V amplitude and 1-10 Hz frequency; the reference electrode was inserted in the nuchal musculature.

The ZIRP was defined as a region 1350-1600 μm rostral to the rostral edge of the AP, 1400-1600 μm lateral to the midline and 1200-1600 μm below the dorsal surface of the medulla. The chemostimulation sites were marked with a fluorescent dye which was ejected from the pipette before termination of the experiments.

iii. ***Extracellular recording.*** Extracellular recordings were made in the AMB_c as described in chapter 3. To stimulate neurons at the recording site, three-barrelled micropipettes were used. One barrel containing a carbon fiber and 4 M NaCl solution was used for recording. The other two barrels were filled with glutamate (0.2 M) and ACh (0.2 M), respectively. Both substances were pressure-ejected near the recorded neurons in pulses of low amplitude (10 psi) and short duration (5-10 ms).

4.1.2 *In Vitro* Experimental Procedures

i. ***Brainstem slice preparation.*** Anaesthesia, brain surgery, ACSF preparation, and slice perfusion procedure were as described in Chapter 3. Brainstem slices of 400 μm thick were cut in the transverse or oblique-sagittal plane (Fig. 4.1) on a vibratome.

ii. ***Intracellular and whole-cell recording.*** Following a 30 to 60 min equilibration period at room temperature in modified ACSF, intracellular or whole cell patch recordings were made in the AMB_c or NTS_c. Intracellular recording was performed by means of sharp glass pipettes filled with 3 M KCl (80-140 MΩ). Whole cell recording by means of patch pipettes with resistances measured in ACSF ranging between 8-12 MΩ. The intracellular solution was the same as described in Chapter 3.

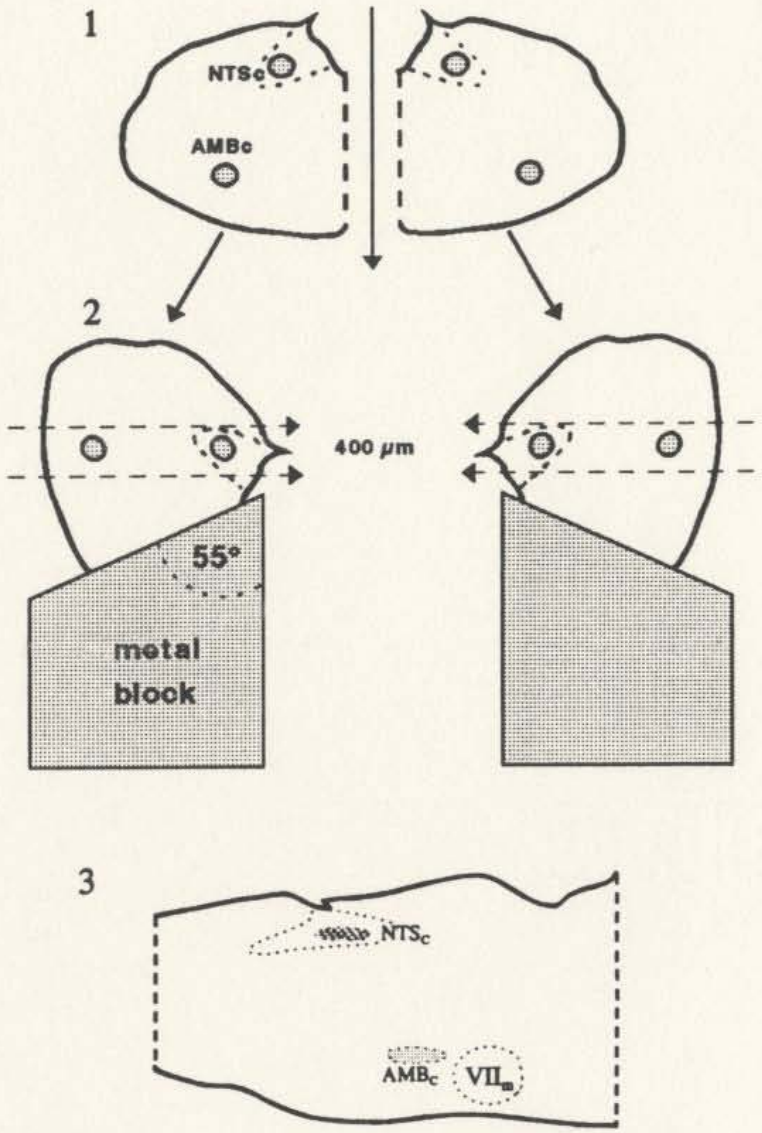


Fig. 4.1 Diagram illustrating procedure used to make oblique sagittal brainstem slice. Step 1: Lower brainstem (cross-section) is isolated and hemisected in the midline. Step 2: Each half of the brainstem is glued on its midline surface to a bevelled metal block and then sliced on a vibratome. Step 3: A 400 μm thick slice is cut from each hemimedulla so as to preserve the NTS_C, the AMB_C and the interconnecting pathway.

The boundary of the AMB_c was visually determined in the transilluminated oblique slice. The NTS_c region was identified as the mid-portion of a translucent triangular area at the dorsal edge of the slice, corresponding to the solitary complex. In keeping with previous work (Bieger 1984; Altschuler et al 1991), the NTS_c region in transverse brainstem slices was delimited as follows: 0-500 μm rostral to the obex, between 600-800 μm lateral to the midline and 400-600 μm ventral to the dorsal surface of the medulla. With reference to internal landmarks, clearly discernible in the transilluminated slice, the region under study extended 200 μm dorsally from the DMV and between 200-400 μm from the medial margin of the solitary tract.

AMB_c neurons were current-clamped at their resting potential. NTS_c neurons were current-clamped or voltage-clamped at -60 mV. Voltage-clamp was made in the single electrode mode at a sampling frequency of 3-4 kHz. The voltage at the head stage amplifier was monitored continuously on another oscilloscope to assure adequacy of the clamp. Only neurons capable of generating spikes in response to intracellular current injection or a glutamate pulse were included in the analysis. Changes in membrane potential or current were displayed on a Nicolet 310 digital oscilloscope and continuously recorded on a Gould 3000 pen writer.

iii. ***Drug applications.*** Agonists were applied to the NTS_c, AMB_c or ZIRP region of the slice preparation by pressure-ejection from a multibarrelled pipette. The tip of the pipette was placed within 50 μm of the surface of the slice and the volume of each pulse was kept within 0.1 nl. Drugs were applied by perfusion in some experiments.

Commercial sources of the drugs were the same as described in Chapter 3.

iv. ***NADPH-staining of the brainstem slice.*** To facilitate the anatomical identification of recording sites, the brainstem slices were fixed overnight in 4% paraformaldehyde and then reacted for NADPH diaphorase according to the method of Hope and Vincent (1989).

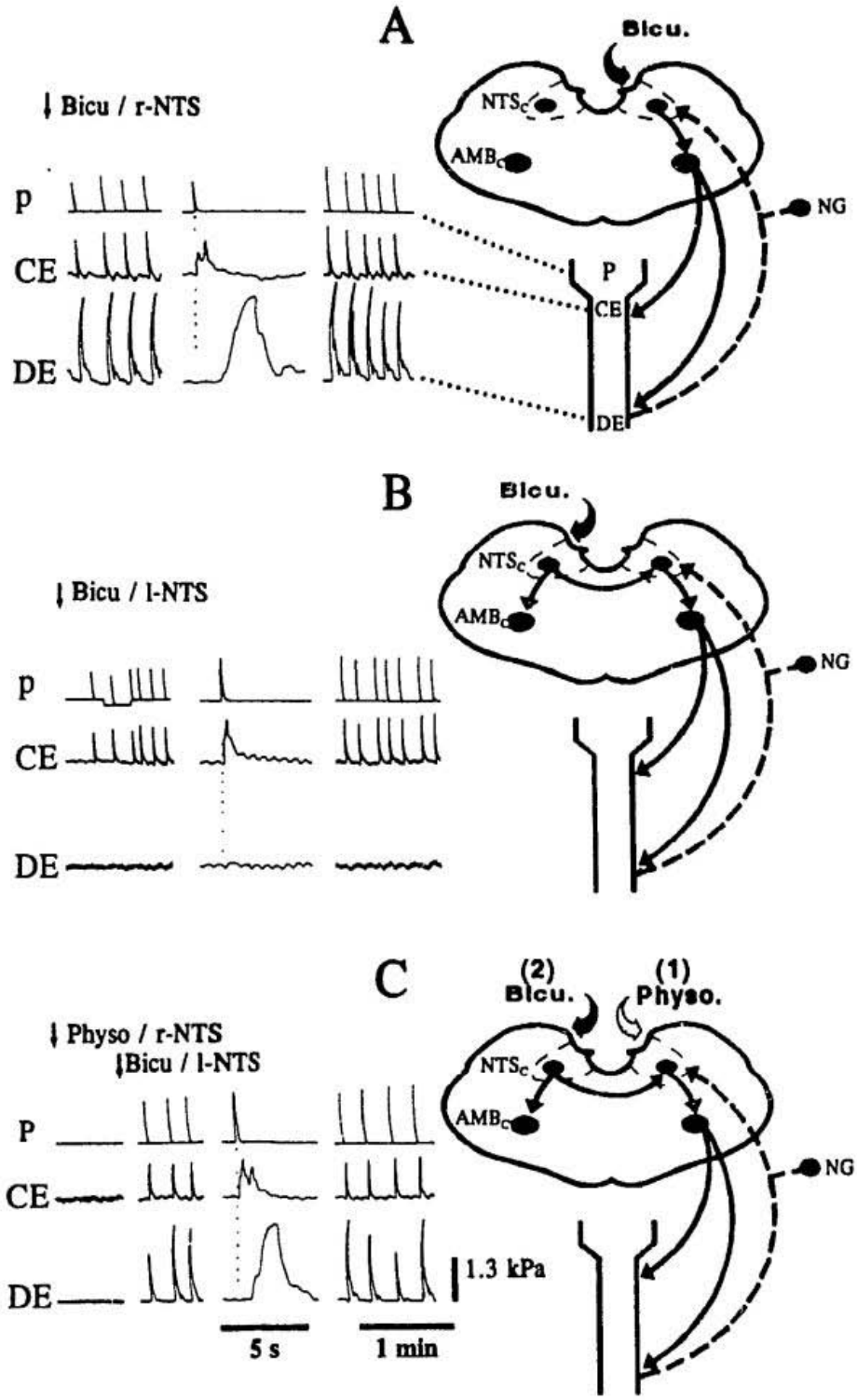
Statistical values are presented as mean ± SD (paired *t*-tests, SigmaStat, Jandel Scientific). $P < 0.05$ was considered to be significant.

4.2 Results

4.2.1 Facilitatory Effects on Oesophageal Peristalsis of Muscarinic Stimulation

To determine if the oesophageal stage of swallowing (primary peristalsis) required peripheral afferent input from the pharyngo-oesophageal junction, the latter region was deafferented by severing the internal (sensory) branch of the right SLN, and the entire left SLN. In addition, the left cervical vagal trunk was cut so as to restrict esophagomotor outflow to the right hemimedulla. In this preparation, application of bicuculline (0.1 nmol) to the right NTS surface produced repetitive complete swallows consisting of a fast pharyngeal pressure spike followed by a propagated slow pressure wave in the cervical and distal oesophagus (Fig. 4.2A). Application of bicuculline (0.1 nmol) to the left NTS surface evoked repetitive pharyngeal swallows with a coupled

Fig. 4.2 Demonstration of a central esophagomotor coupling mechanism in the rat. Intraluminal pressure traces are shown on the left panels. Postulated swallowing reflex pathway and experimental strategies are schematically illustrated on the right panel. Oesophageal afferents (broken line) project to the NTS_c and efferents (solid line) originate from the AMB_c. To restrict oesophageal vagal sensory/motor flow to/from one half of the medulla oblongata, acute transections are made of the cervical trunk plus the SLN on the left side. In addition, to eliminate vagal sensory flow from pharyngo-oesophageal junction and the upper cervical oesophagus, the internal (sensory) branch of the SLN is severed on the right side. Intraluminal pressure is recorded in the pharynx (P), the cervical (CE) and distal oesophagus (DE). **A.** Topical application of bicuculline (0.1 nmol) to the right NTS (r-NTS) results in repetitive pharyngeal swallows followed by phase-locked primary peristalsis progressing through the entire oesophagus. **B.** Application of bicuculline (0.1 nmol) to the left NTS (l-NTS) produces repetitive pharyngeal swallows with coupled primary peristalsis restricted to the cervical oesophagus. **C.** Physostigmine (40 pmol) applied to the right NTS surface is ineffective in producing a swallowing response but enables the primary peristalsis in the cervical oesophagus evoked by bicuculline applied to left (contralateral) NTS to propagate distally.


A
Bicu.
↓ Bicu / r-NTS
NTSc
AMBc
NG
p
CE
DE
P
CE
DE
B
Bicu.
↓ Bicu / l-NTS
NTSc
AMBc
NG
p
CE
DE
C
(2)
Bicu.
(1)
Physo.
↓ Physo / r-NTS
↓Bicu / l-NTS
NTSc
AMBc
NG
P
CE
DE
1.3 kPa
5 s
1 min

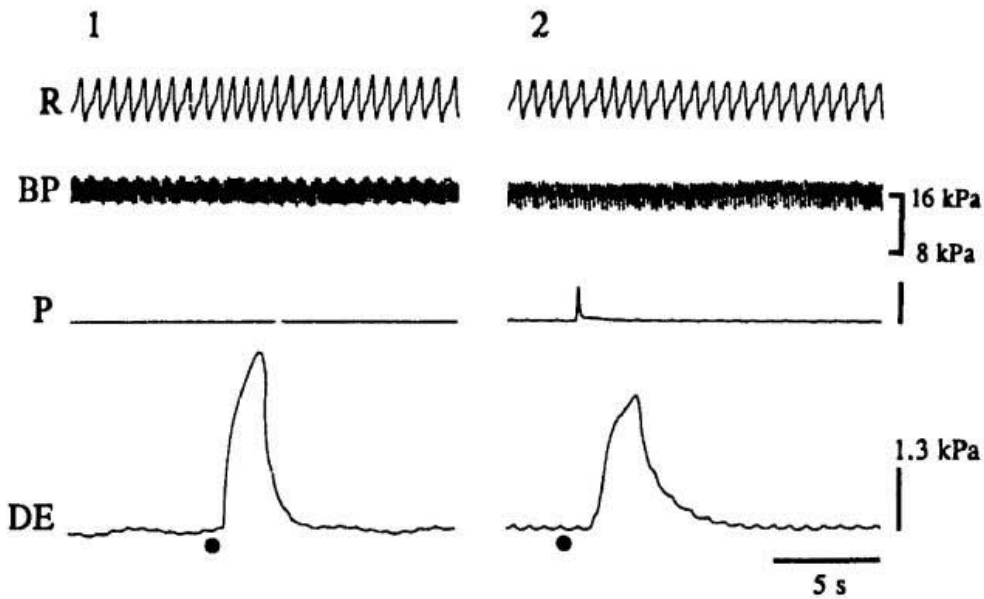


Fig. 4.3 Swallowing responses evoked by glutamate pulse-applied in swallowing loci of the caudal portion of the NTS. Glutamate (50 pmol) pressure-ejected in different swallowing loci of the NTS (indicated by black dot) evokes single pressure waves in the distal oesophagus (DE) (**1**) or a single swallow (**2**) with a short-latency. Note lack of change in respiration, other than swallow-associated, and blood pressure when glutamate is ejected at deglutitive sites.

pressure wave that was restricted to the cervical oesophagus (Fig. 4.2B). This nonpropagated pressure wave was converted into a propagated response upon concurrent application of physostigmine (40 pmol) to the right (Fig. 4.2C), but not the left NTS surface.

In intact animals, glutamate (50 -100 pmol) pressure-ejected into unilateral swallowing loci of the NTS evoked either a reproducible short-latency (< 1 s) single swallow consisting of a sharp pressure spike in the pharynx followed by a peristaltic oesophageal pressure wave; or a single pressure wave in the oesophagus (Fig. 4.3). Changes in blood pressure, heart rate and respiration were not observed when glutamate was ejected at oesophageal loci (Fig. 4.3; n = 4). Following physostigmine (30 to 50 pmol) was applied to the ipsilateral NTS surface, the pressure wave evoked in the cervical oesophagus propagated distally (Fig. 4.4; n = 4); and the amplitude of the pressure wave evoked in the distal oesophagus was enhanced as compared to control (n = 5). In contrast, when methscopolamine (0.2 nmol) was applied to the ipsilateral NTS surface, the oesophageal stage of glutamate-evoked swallowing was completely eliminated in 5 out of 7 animals; in the remaining two cases, however, a small pressure wave persisted in the cervical oesophagus (Fig. 4.5A).

Electrical stimulation of the caudal intermediate portion of the NTS with pulse trains reproducibly evoked a single swallow (n=3). Topical application of methscopolamine (0.2 nmol) to the ipsilateral NTS surface abolished the pressure wave in the distal oesophagus and reduced that in the cervical oesophagus (Fig. 4.5B).

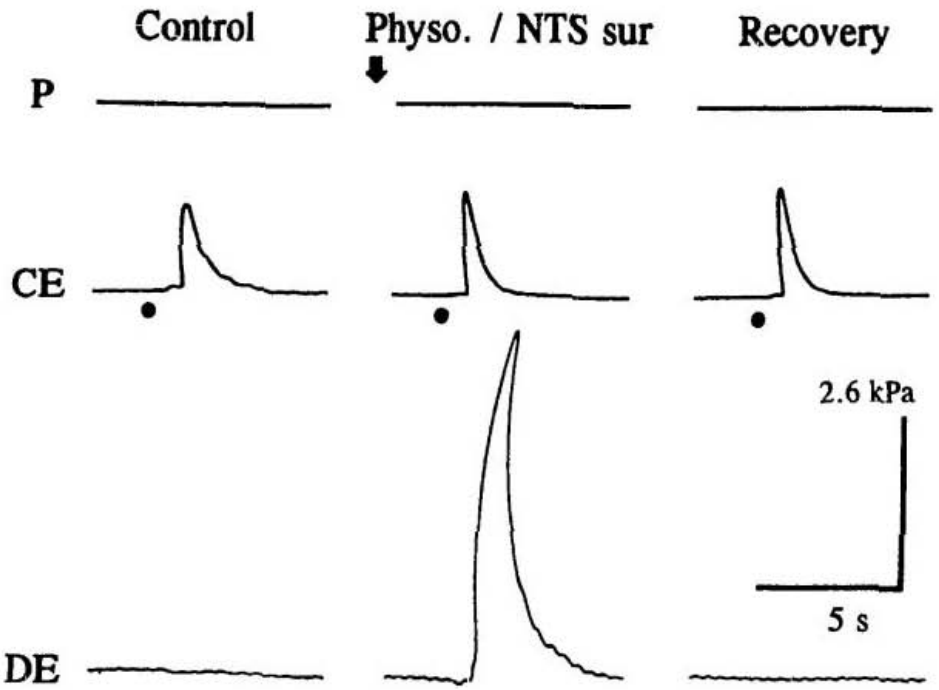
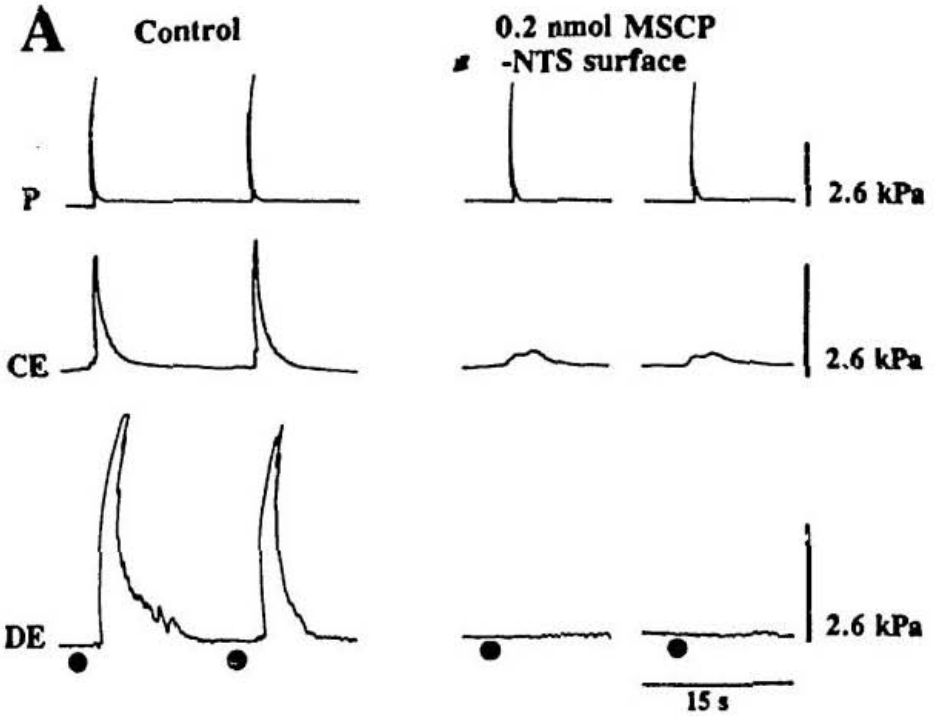
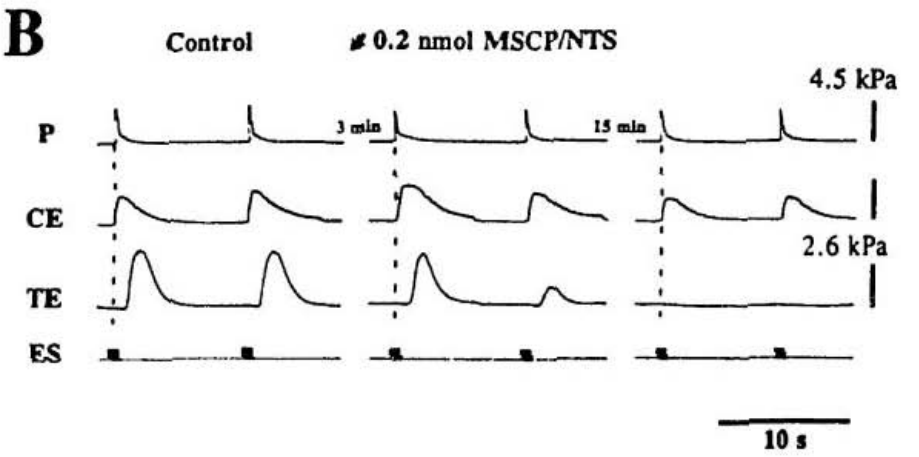


Fig. 4.4 Facilitation of peristaltic esophagomotor propagation by inhibition of cholinesterase in the NTS. Glutamate (40 pmol) ejected in the NTS_c (shown as the dot) evokes a single pressure wave in the cervical oesophagus (CE) (left panel). After topical application of physostigmine (40 pmol) to the ipsilateral NTS surface, the glutamate-evoked cervical oesophageal response propagates distally (middle panel). The responses return to baseline pattern 8 min later (right panel).

Fig. 4.5 Selective inhibition of the oesophageal stage of swallowing by muscarinic blockade in the NTS. **A.** Control deglutitive response evoked by pressure-ejection of glutamate (50 pmol, shown as the dot) in the intermediate NTS (left panel). Three minutes after application of methscopolamine (MSCP) to the ipsilateral NT, the amplitude of the primary peristaltic pressure wave in the cervical oesophagus is reduced and the response in the distal oesophagus eliminated (middle panel). Inhibition persists 18 min after methscopolamine (right panel). **B.** Electrical stimulation (ES) at the NTS swallowing locus with a stimulation pulse train (0.1 ms, 2 V, 10 Hz) evokes a swallow (left panel). Methscopolamine (0.2 nmol) induces progressive inhibition of the oesophageal component recorded 3 and 15 min (middle and right panels, respectively) after application to the ipsilateral NTS surface.


A
Control
0.2 nmol MSCP
-NTS surface
P
CE
DE
2.6 kPa
2.6 kPa
2.6 kPa
15 s


B
Control
0.2 nmol MSCP/NTS
4.5 kPa
P
3 min
15 min
CE
2.6 kPa
TE
ES
10 s

4.2.2 Effects of Activation and Blockade of NTS_c mAChRs on Rhythmic Oesophageal, Cardiovascular and Respiratory Activity

Pressure-ejection of muscarine (20 to 50 pmol) in the NTS_c region gave rise to rhythmic esophagomotor activity usually uncompanied by buccopharyngeal contractions (n = 18). The pattern and duration of esophagomotor activity induced by muscarine were relatively constant for a given NTS locus. The oesophageal body produced rhythmic peristaltic pressure waves (Fig. 4.6B), while the upper (UES) (Fig. 4.6A) and lower oesophageal sphincter (LES) generated rhythmic relaxations (Fig. 4.6C), indicative of a coordinated peristaltic pattern. When pressure-ejected in the NTS_c, bicuculline (20 to 50 pmol) also produced a similar peristaltic response (n = 2, not shown). The frequency of the evoked rhythmic peristaltic pressure waves ranged between 0.10 to 0.22 Hz (0.16 $\pm$ 0.04 Hz, n = 18).

Respiration, blood pressure and heart rate remained unchanged during rhythmic esophagomotor activity evoked by ejection of muscarine or bicuculline in the NTS_c region (Fig. 4.7A). However, application of muscarine (0.1 nmol) to the NTS surface caused an increase in respiratory rate and depth (see Fig. 4.7B) and a decrease in blood pressure (Fig. 4.7B). Methscopolamine (50 pmol to 0.1 nmol) applied to the NTS surface did not affect respiratory rate (n = 5) or pulse rate (n = 4), but abolished the rhythmic oesophageal responses to muscarine (n = 4) or bicuculline (n = 2) applied to the NTS_c (not shown).

In the AMB_c region, pressure-ejection of muscarine (50-100 pmol) failed to evoke

Fig. 4.6 Rhythmic activity patterns in the oesophagus evoked by muscarinic activation in the NTS_c. Traces shown in **A**, **B**, **C** are from 3 separate experiments. **A**. Pressure-ejection of muscarine (musc.; 50 pmol) to the NTS_c (marked by star) produces rhythmic relaxations in the upper oesophageal sphincter (UES) and phase-locked rhythmic pressure waves in the thoracic oesophagus (TE). Low-amplitude rhythmic relaxations are also detected by the pharyngeal balloon (P). **B**. A pulse of muscarine (40 pmol) applied to the NTS_c results in rhythmic peristalsis of the oesophageal body with cervical activity leading pressure waves in the distal portion. **C**. A relaxation followed by a slow pressure wave is evoked in the lower oesophageal sphincter (LES) by a pulse of glutamate (50 pmol, marked by a black dot) ejected to the NTS_c region (left panel). When ejected at the same locus, muscarine (5 pmol; marked by star) evokes rhythmic pressure waves in the cervical oesophagus coupled with relaxations in the LES (two middle panels). A larger pulse of muscarine (10 pmol) produces a stronger response in the cervical oesophagus (right panel). Calibration in **A** and **B** is the same. In **C**, the gain of the cervical trace is increased by 10 times in the two right panels.

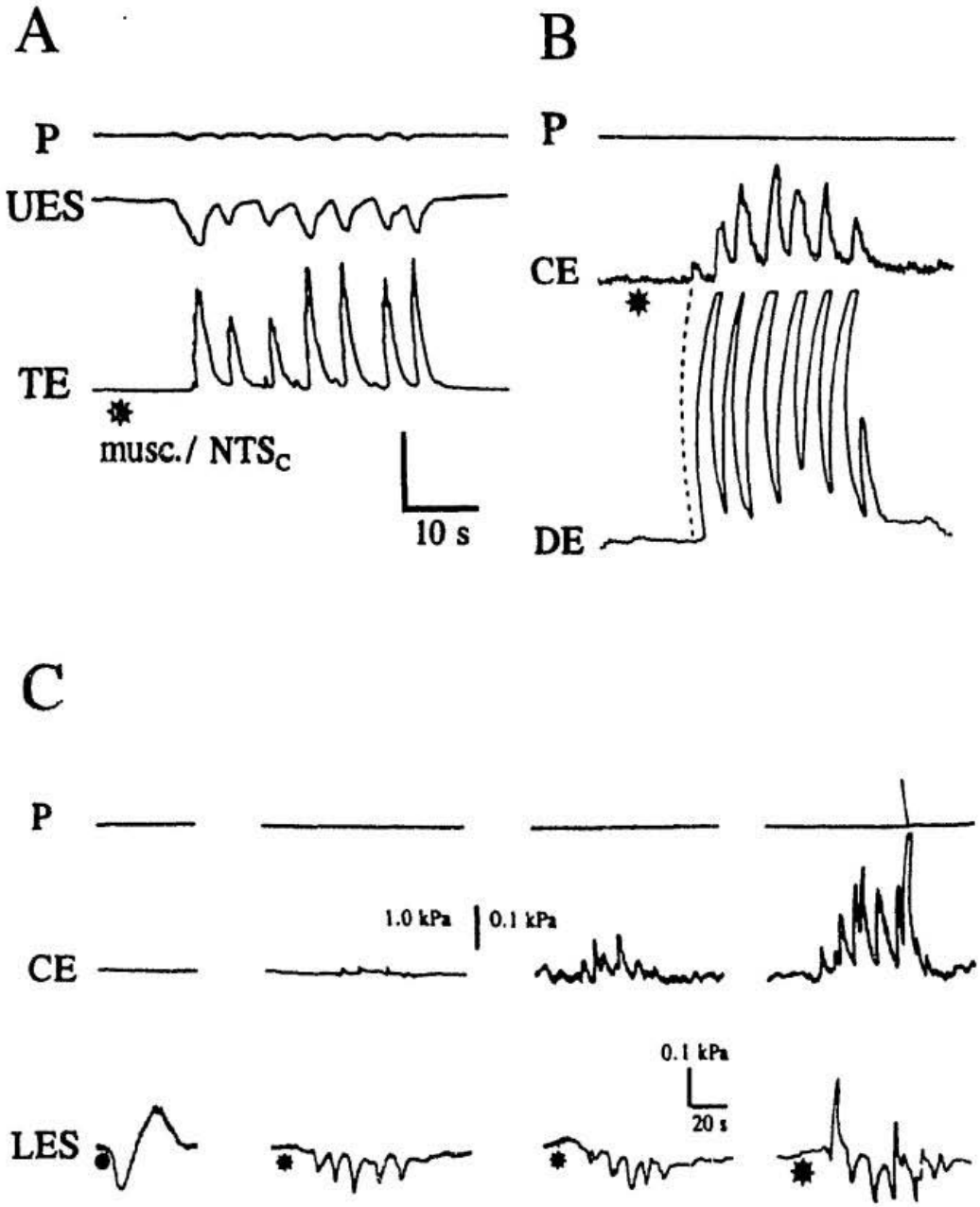
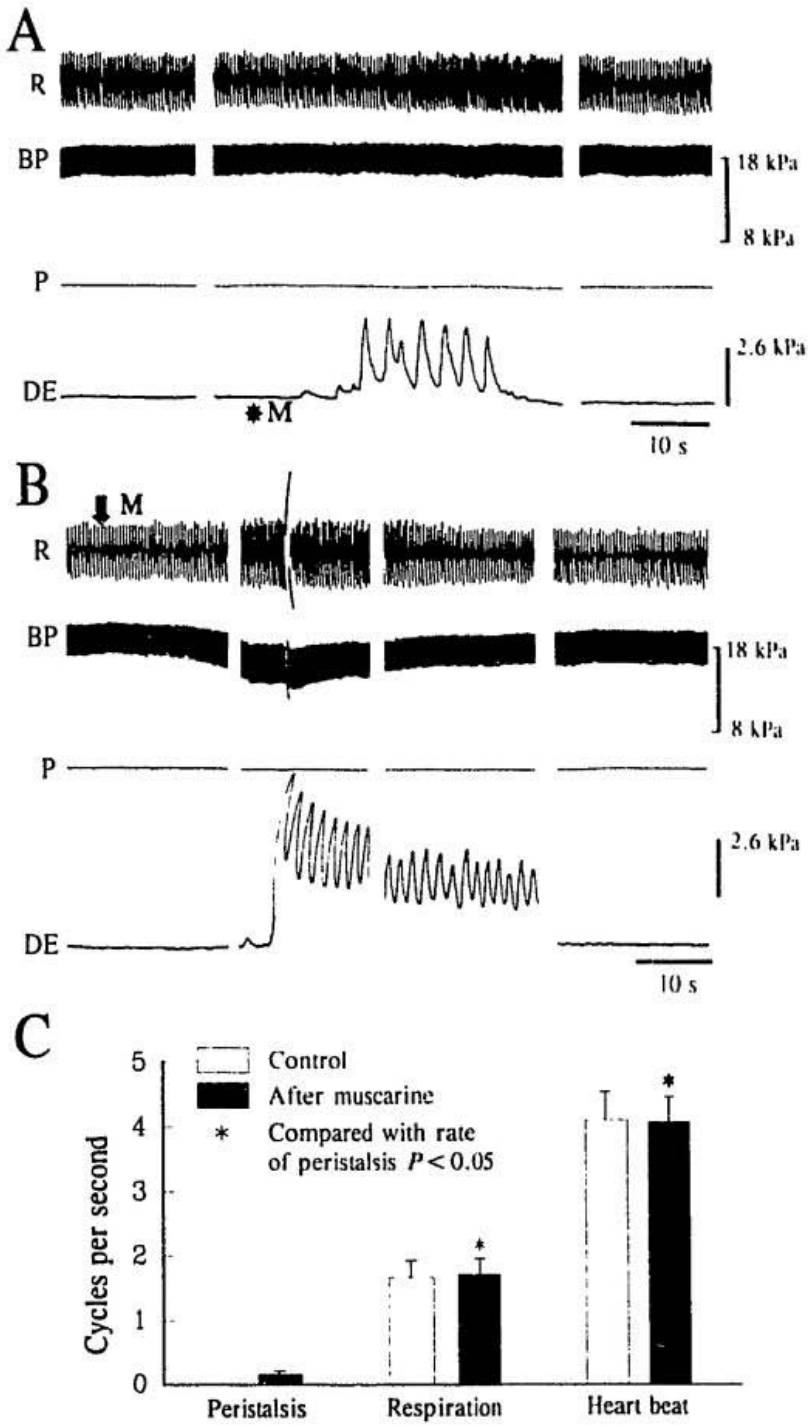

A
P
UES
TE
musc./ NTS$_c$
10 s
B
P
CE
DE
C
P
1.0 kPa
0.1 kPa
CE
0.1 kPa
20 s
LES

Fig. 4.7 Cardiovascular, respiratory and oesophageal responses to muscarinic cholinoceptor stimulation in the NTS. **A.** Muscarine (M; 10 pmol) ejected in the NTS_c (*) evokes rhythmic oesophageal peristalsis in the distal oesophagus (DE) without change in respiration (R) and arterial blood pressure (BP). **B.** Muscarine (0.1 nmol) applied to left NTS surface (↓) causes an immediate decrease in blood pressure and an increase in respiratory rate followed by oesophageal peristalsis. The gaps (10 to 15 s) in traces indicate portions omitted. **C.** Comparison of the muscarine effect on frequency of oesophageal peristalsis, respiration and heart rate. Pressure-ejection of the agonist in the NTS_c evokes rhythmic oesophageal peristalsis without change in respiratory frequency and arterial pulse rate. The frequency of muscarine-induced oesophageal peristalsis (0.16 $\pm$ 0.04 Hz, n = 18) differs significantly (*, $P < 0.05$) from that of respiration (1.66 $\pm$ 0.25 Hz, n = 8) and heart beat (4.1 $\pm$ 0.44 Hz, n = 8). P: pharynx; DE: distal esophagus.


A
R
BP
18 kPa
8 kPa
P
2.6 kPa
DE
M
10 s
B
M
R
BP
18 kPa
8 kPa
P
2.6 kPa
DE
10 s
C
Control
After muscarine
* Compared with rate of peristalsis $P < 0.05$
Cycles per second
0
1
2
3
4
5
Peristalsis
Respiration
Heart beat

detectable esophagomotor activity (n = 3), however, ejection of ACh (50-100 pmol) evoked a fast monophasic oesophageal pressure wave that was insensitive to methscopolamine ejected at the same locus (n = 4, not shown).

4.2.3 Responses of Oesophageal Motoneurons to Activation and Blockade of mAChRs in the NTS

Extracellular recordings were made in the AMB_c area (n = 22; Fig. 4.8A) where rhythmic multi-unit discharges were evoked by distension of the distal oesophagus (Fig. 4.8B-1). A small pulse of glutamate (20 pmol) applied at the recording site produced discharges that led a synchronous pressure wave in both the cervical and distal oesophagus (Fig. 4.8B-2). At the same site, ACh (20-50 pmol) also produced a short-latency nonrhythmic esophagomotor response (Fig. 4.8B-3).

Topical application of muscarine or physostigmine (0.1 - 0.2 nmol) to the ipsilateral NTS surface produced sustained bouts of rhythmic unit discharges (n = 16) with phase-locked oesophageal peristalsis lasting up to 4-15 min (Fig. 4.8C). The peak frequency within each burst ranged from 65 to 95 Hz.

Rhythmic unit discharges in the AMB_c were also observed during fictive swallowing induced by application of bicuculline (50 to 100 pmol) to the ipsilateral surface of the NTS (n = 5, not shown). Each burst discharge was preceded by a fast pharyngeal pressure wave and in turn was followed by a phase-locked peristaltic pressure wave in the oesophagus. Methscopolamine (50 to 100 pmol) applied to the ipsilateral

Fig. 4.8 *In vivo* oesophagomotoneuronal activity in the compact formation of the nucleus ambiguus (AMB_c). **A.** Drawing illustrating the oesophageal reflex pathway as projected on a transverse plane through the medulla oblongata and the method used for combined extracellular recording and chemostimulation of oesophageal motoneurons. X^{th}, vagal efferent to the oesophagus and afferents from the oesophagus; Glut., glutamate. **B.** Traces represent (from top to bottom) pharyngeal (P), cervical oesophageal (CE), thoracic oesophageal (TE) pressure and extracellular unit activity in the AMB_c as displayed by a rate-meter. Distension of the distal oesophagus (indicated by solid bar) evokes rhythmic firing in the AMB_c that leads rhythmic oesophageal pressure waves in the thoracic oesophagus (B-1). Glutamate (20 pmol, B-2) or ACh (20 pmol, B-3) pulsed into the AMB_c elicits a burst discharge leading a synchronous pressure wave in the cervical and thoracic oesophagus. **C.** In the same recording site, application of muscarine (0.1 nmol) to the ipsilateral NTS surface produces rhythmic discharges leading oesophageal peristalsis in a phase-locked manner.

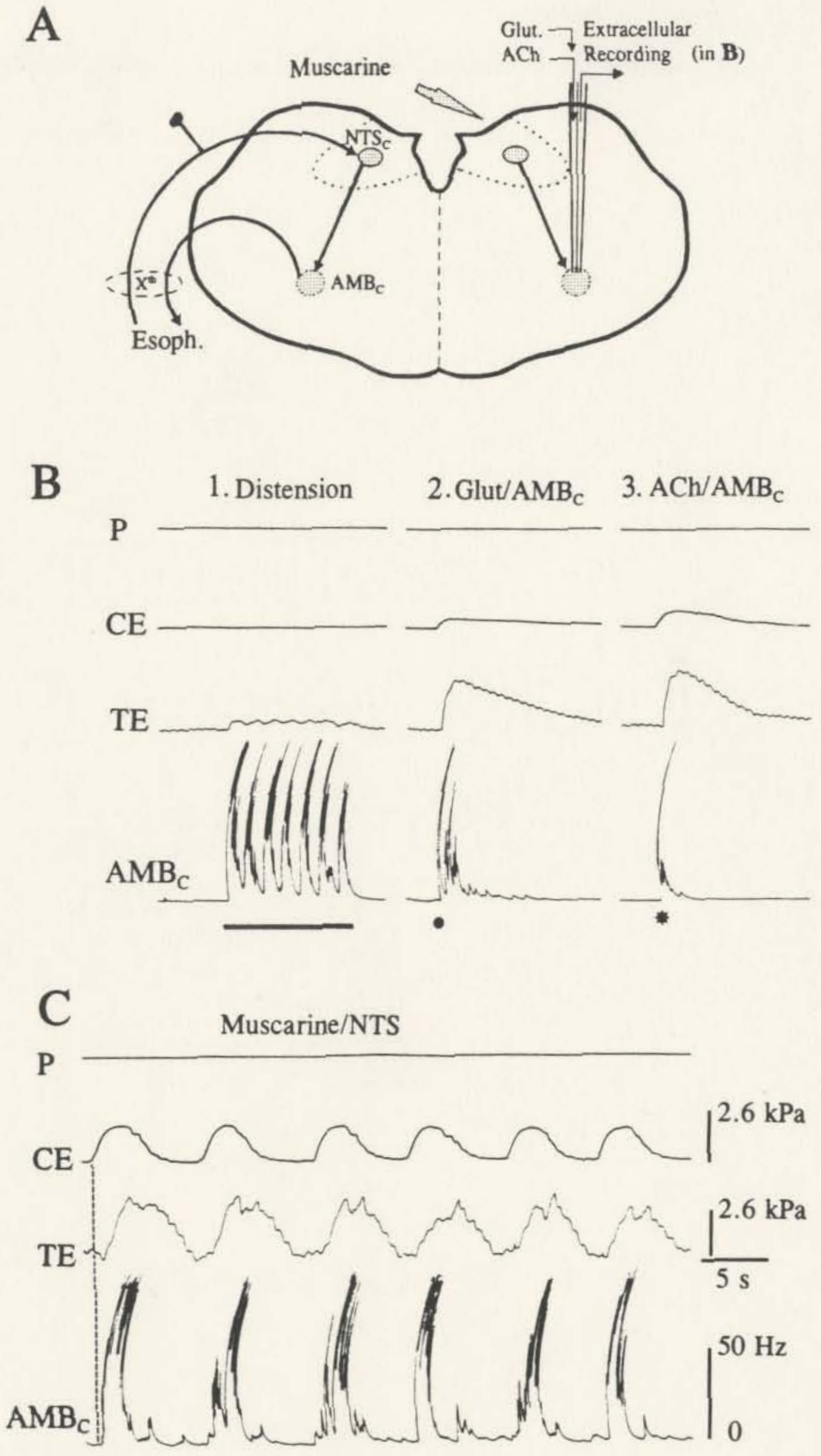
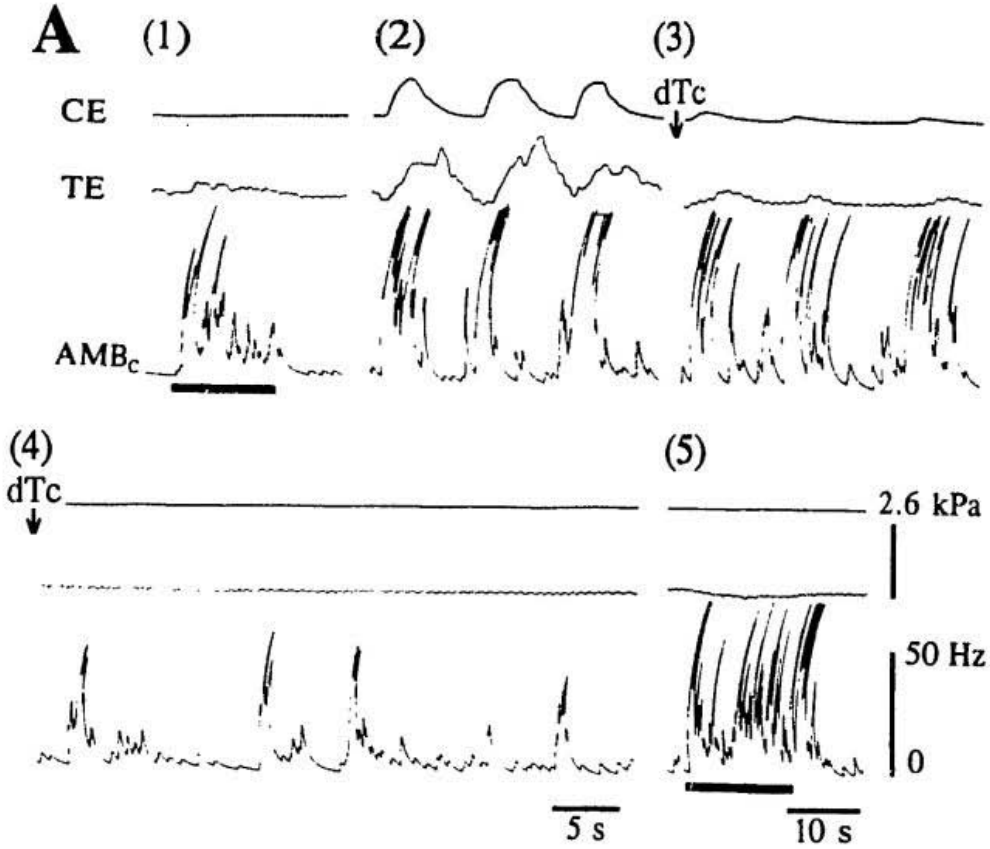
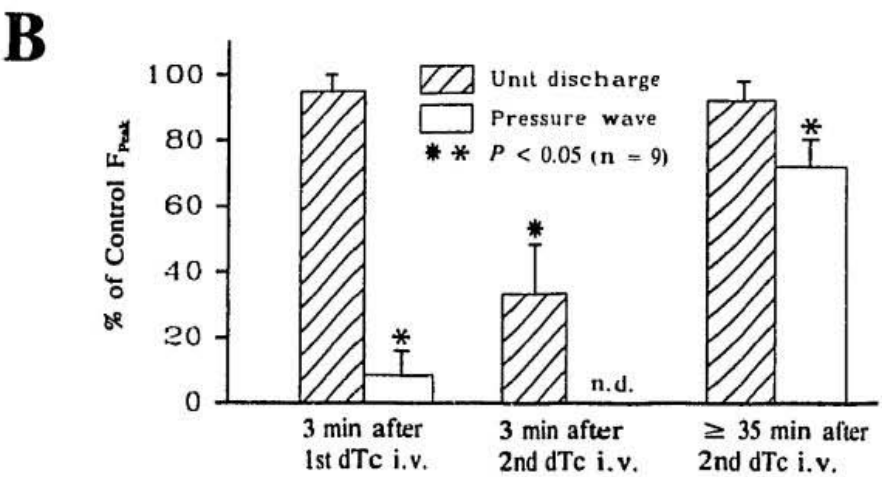

A
Glut.
ACh
Extracellular
Recording (in B)
Muscarine
NTSc
AMBc
X*
Esoph.
B
1. Distension
2. Glut/AMBc
3. ACh/AMBc
P
CE
TE
AMBc
C
Muscarine/NTS
P
CE
TE
AMBc
2.6 kPa
2.6 kPa
5 s
50 Hz
0

Fig. 4.9 Effect of curarization on rhythmic oesophagomotoneuronal activity. **A.** Recording site in AMB_c exhibits unit discharges evoked by distension of the distal oesophagus (indicated by heavy bars under the traces) (A-1). Topical application of muscarine (0.1 nmol) to the ipsilateral NTS surface (A-2) elicits low-frequency (0.12 Hz) rhythmic burst discharges in the AMB_c and phase-locked peristaltic pressure-waves in the oesophagus. After D-tubocurarine (dTc, 0.075 μmol.kg^{-1} i.v., given at downward arrow), the peak-frequency of each burst discharge in the AMB_c remains unchanged although the amplitude of oesophageal pressure waves is reduced by > 90% (A-3). When the oesophageal pressure waves are abolished by a second dose of D-tubocurarine (0.075 μmol.kg^{-1}), another challenge with muscarine results in an attenuated unit response and loss of regular rhythmic burst discharge (A-4). During complete motor paralysis, distension of the distal oesophagus still evokes robust discharges with peak frequency comparable to the control (A-5). Time calibrations in A-1 to 4 are the same. **B.** Pooled data from three experiments showing the effect of curarization on the peak-frequency (F_{Peak}) of burst discharge in the AMB_c and the amplitude of pressure waves in the cervical oesophagus evoked by muscarine (0.1-0.2 nmol) applied to the NTS. Each column represents the mean peak-frequency of three burst discharges recorded in each animal during the period indicated. Asterisks denote significant difference ($P < 0.05$) compared with pre-curare control; n.d., not detectable.


A
(1)
(2)
(3)
dTc
CE
TE
AMBc
(4)
dTc
(5)
2.6 kPa
50 Hz
0
5 s
10 s


B
% of Control F Peak
100
80
60
40
20
0
Unit discharge
Pressure wave
** P < 0.05 (n = 9)
n.d.
3 min after
1st dTc i.v.
3 min after
2nd dTc i.v.
≥ 35 min after
2nd dTc i.v.

NTS surface caused a progressive decline in motoneuronal discharges and a parallel decrease in oesophageal pressure waves but left the pharyngeal activity unaffected (n=2).

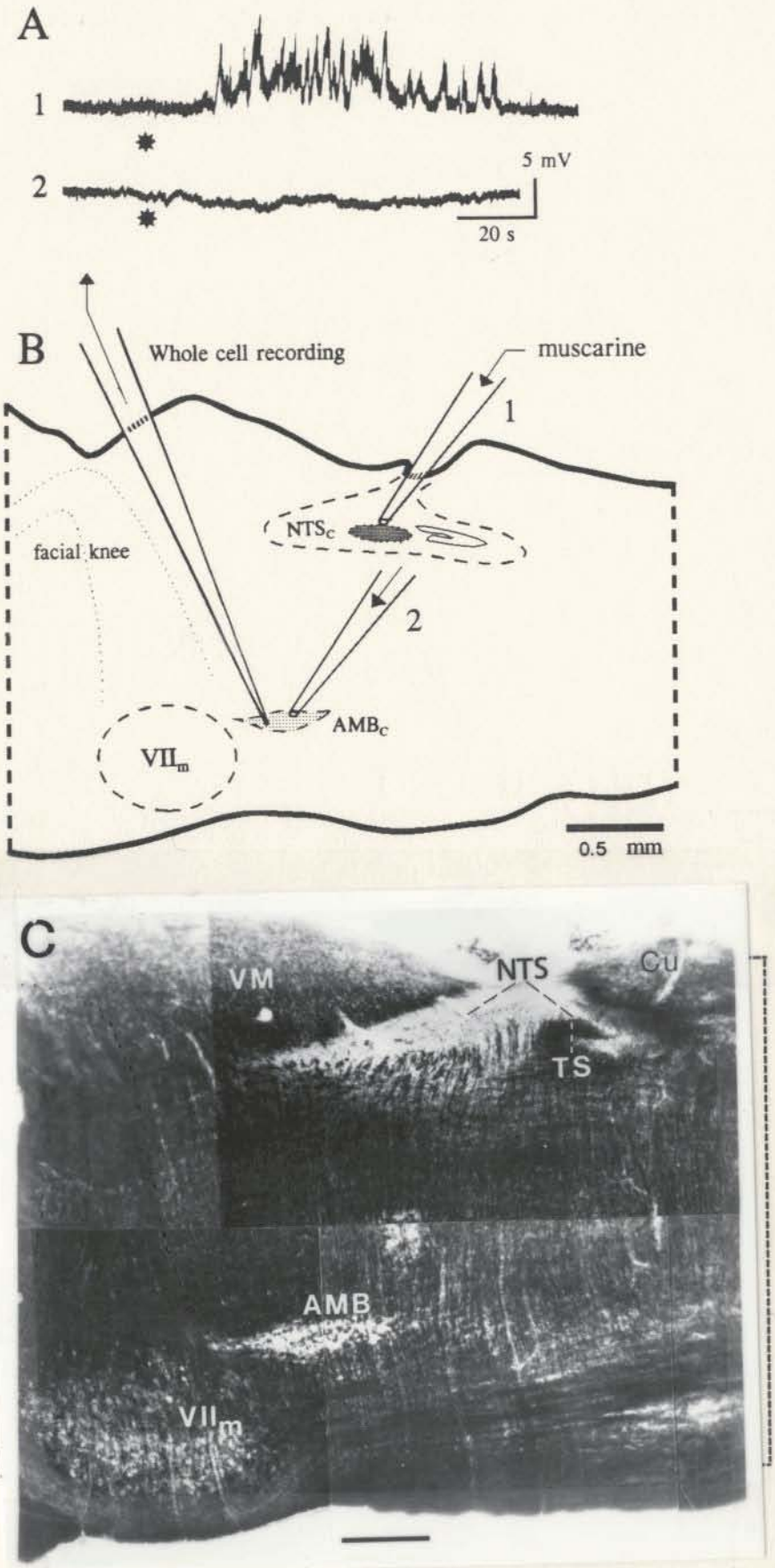
4.2.4 Effect of Curarization on Rhythmic Oesophagomotoneuronal Activity

Following intravenous administration of a single dose of D-tubocurarine (dTc, 0.075 μmol.kg^{-1}), the rhythmic burst discharges in the AMB_C evoked by muscarine in the NTS remained unchanged although the amplitude of rhythmic oesophageal pressure-waves decreased significantly (Fig. 4.9A-3). When the evoked oesophageal pressure waves declined to undetectable levels after additional doses of dTc (0.075 μmol.kg^{-1}), the burst discharge in the AMB_C was attenuated, as evidenced by a decrease in peak frequency and burst duration. In addition, the inter-burst interval became irregular (n = 16 trials on 9 animals tested, Fig. 4.9A-4). At the same time, however, oesophageal distension still evoked a vigorous unit discharge (n = 9; Fig. 4.9A-5). The peak frequency of the burst discharges was fully restored before oesophageal peristaltic pressure waves returned to the pre-curare level. Fig. 4.9B demonstrates the divergent time course of the effects of curarization on the peak frequency of motoneuronal discharges and the peak amplitude of oesophageal pressure waves.

4.2.5 Rhythmic AMB_C Neuronal Activity Induced by Activation of NTS_C mAChRs in a Brainstem Slice Preparation

Intracellular (n = 8) or whole-cell patch recordings (n = 15) from AMB_C cells

Fig. 4.10 Oesophagomotor rhythm generation in a medullary slice preparation. Cells in the AMB_c region are recorded intracellularly in an oblique sagittal brainstem slice as shown in a camera lucida drawing at middle (**B**). Rhythmic depolarizations are induced from a pulse of muscarine (about 0.1 nmol, marked by asterisk) pressure-ejected to the NTS_c region (**A-1**) but not by muscarine applied to the AMB_c region (**A-2**). VII_m, motor nucleus of VIIth cranial nerve. **C:** A brightfield photomontage showing the NTS and AMB_c region in an oblique sagittal unstained brainstem slice. Note the clarity of the anatomical structures. Cu, cuneate nucleus; VM, vestibular medial nucleus; TS, solitary tract.


A
1
2
5 mV
20 s
B
Whole cell recording
muscarine
1
2
facial knee
NTSc
AMBc
VIIm
0.5 mm
C
VM
NTS
Cu
TS
AMB
VIIm

were obtained in 21 oblique sagittal brainstem slices (Fig. 4.10). Patterns of the AMB_c neuronal activity observed in intracellular and whole cell recordings were indistinguishable. As described previously (Wang et al. 1991), AMB_c neurons had resting membrane potentials between -52 and -72 mV (-63.6 $\pm$ 4.5 mV, n = 15) and lacked spontaneous activity.

When muscarine (0.1-0.2 nmol, n = 8) or ACh (0.1-0.3 nmol, n = 15) was pulse-applied to the NTS_c region, the neurons in the AMB_c responded with rhythmic membrane activity (n = 23) as evidenced by repetitive depolarization (Fig. 4.10A-1). In some cases, these coincided with discrete bursts of EPSPs. The frequency of the rhythmic depolarization ranged between 0.1 to 0.2 Hz. Increasing the dosage of muscarinic agonist applied to the NTS_c region prolonged the duration of the evoked activity, but did not change its rhythm or the amplitude (n = 7). Rhythmic activity was absent when muscarine (0.1 - 0.2 nmol) was pulsed onto the AMB_c (Fig. 4.10A-2; n = 4), and sites with a distance $\geq$ 200 μm from the NTS_c (n = 3, not shown).

NADPH-diaphorase staining of slice preparations used in the experiments (n = 6) confirmed a dense group of positive neurons in the NTS, coextensive with the subnucleus centralis, and a weakly stained neuropil in the tegmentum of the medulla oblongata corresponding to the AMB_c (not shown).

The evoked rhythmic activity was eliminated by bath application of the mAChR antagonist methscopolamine (1 - 2μM, n=3) and partially recovered following a 35-50

Fig. 4.11 Effects on esophagomotor rhythm generation of mAChR activation or blockade in the medullary slice preparation. **A.** Rhythmic depolarization in the AMB_c (A 1) evoked by ACh (0.2 nmo) pulsed (at stars) to the NTS_c are eliminated by 6 min perfusion with 1 μM methscopolamine (MSCP, indicated by dashed line)(A-2) and partially recovered after 30 min washout (A-3). **B.** The same neuron responds to ACh (50 pmol, at star) applied to the AMB_c with a monophasic depolarization (B 1) that persists in the presence of methscopolamine (B-2). **C.** Rhythmic AMB_c activity in another slice preparation evoked by ACh pulsed to the NTS_c region remains unchanged after pulses of dihydro-β-erythroidine (D-β-E, about 50 pmol at filled squares) to the AMB_c.

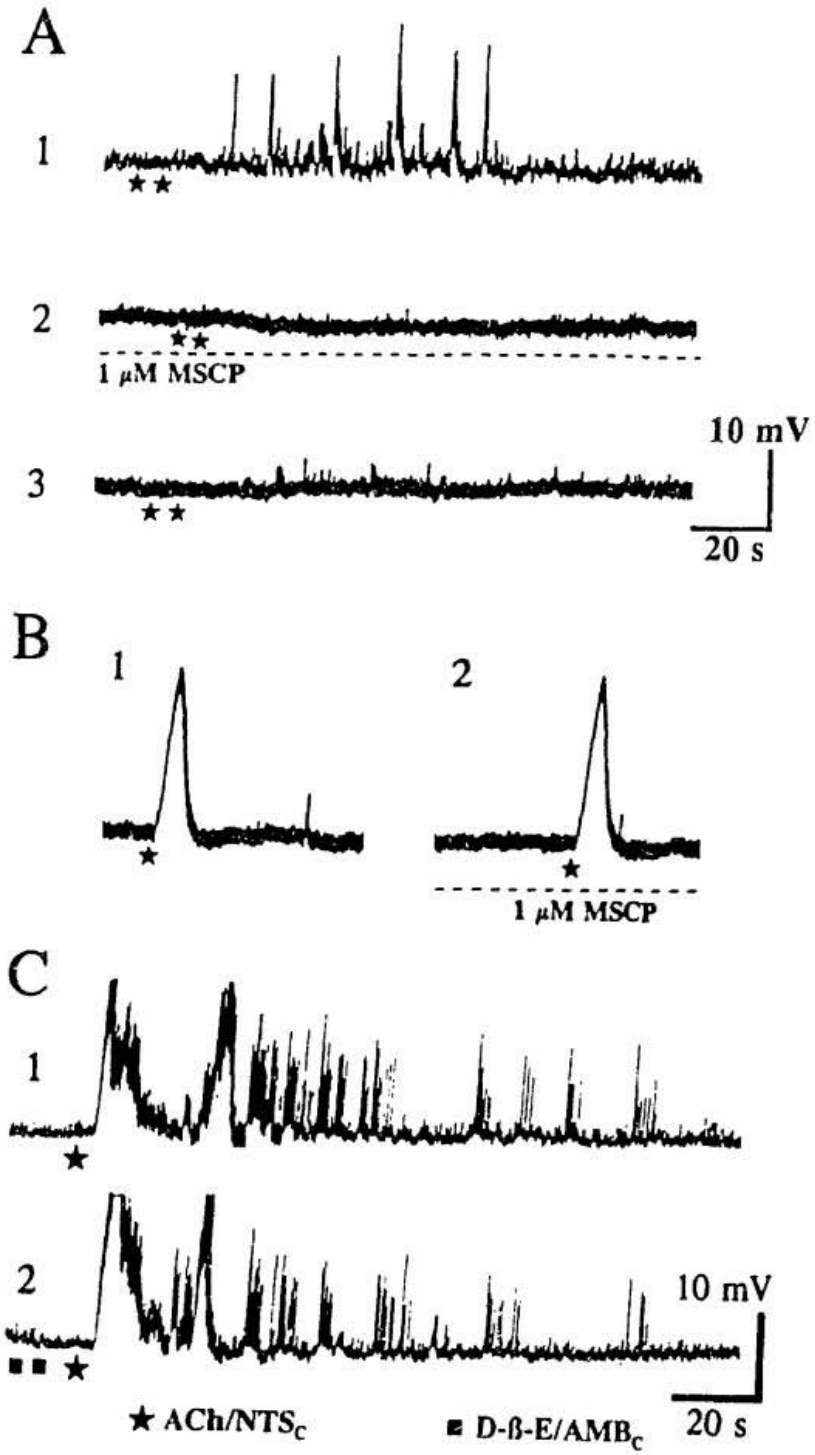
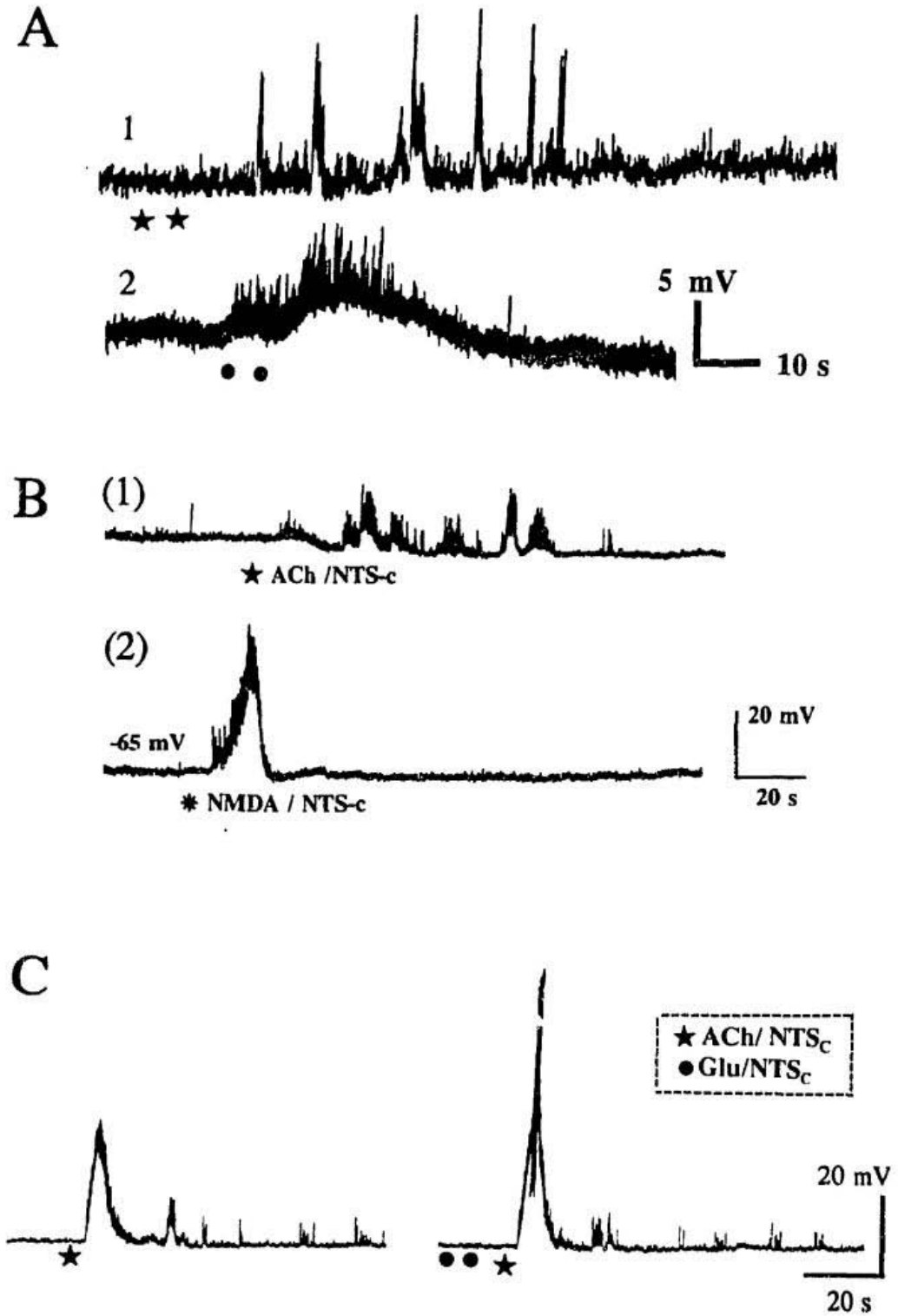

A
1
2
1 μM MSCP
10 mV
3
20 s
B
1
2
1 μM MSCP
C
1
2
10 mV
★ ACh/NTS$_c$
■ D-ß-E/AMB$_c$
20 s

Fig. 4.12 Difference in response patterns of oesophageal motoneurons evoked by stimulation of muscarinic and NMDA receptors in the NTS_c. Data in **A**, **B** and **C** are obtained from three AMB_c neurons. **A**. In the same AMB_c neuron, pulses of ACh (~ 0.2 nmol, applied at stars) to the NTS_c region elicits rhythmic depolarizations (A-1), whereas pulses of glutamate (~100 pmol, indicated by dots) results in long lasting depolarization with superimposed burst of EPSPs (A-2). **B**. A pulse of NMDA (~50 pmol, at asterisk) applied to the NTS_c evokes a monophasic depolarization (B-2) but a pulse of ACh (~50 pmol, at star) produces rhythmic activity (B-1). **C**. A pulse of ACh (~50 pmol, at star) applied to the NTS_c region produces repetitive depolarization and EPSP bursts (left). In the same AMB_c neurons, depolarization evoked by ACh ejected to the NTS_c region (with same dose as control) is enhanced by prepulses of glutamate (~20 pmol) ejected to the NTS_c region, evidenced as increase in amplitude and superimposed spikes (right).

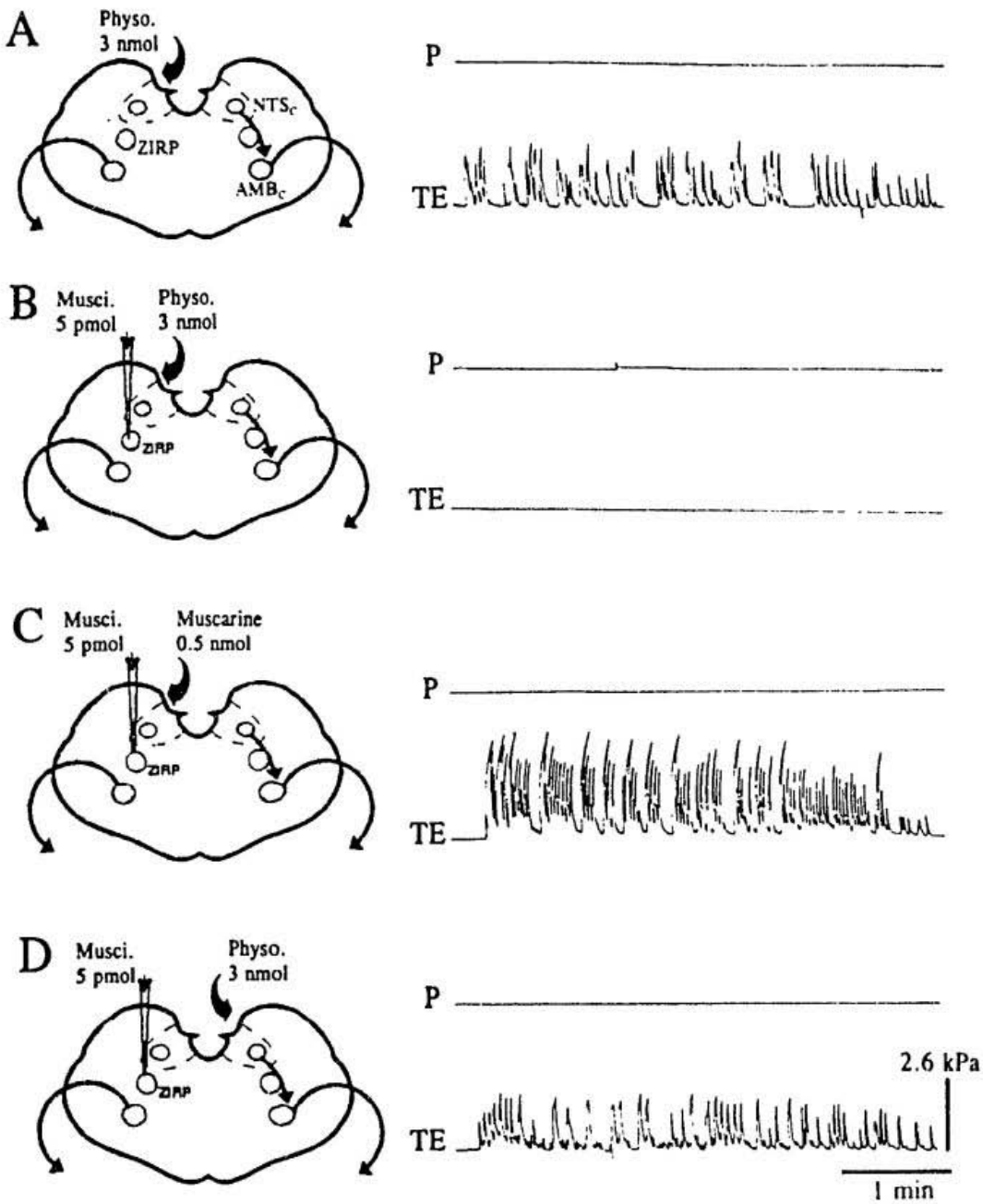

A
1
★ ★
2
5 mV
10 s
B
(1)
★ ACh /NTS-c
(2)
-65 mV
20 mV
20 s
✱ NMDA / NTS-c
C
★ ACh/ NTS$_C$
● Glu/NTS$_C$
20 mV
20 s

min washout period (Fig. 4.11A). ACh ejected near the AMB_c neurons produced a monophasic depolarization that persisted in the presence of methscopolamine 1-2 μM (Fig. 4.11B). Furthermore, when 0.1 to 0.2 nmol dihydro-β-erythroidine, a nicotinic cholinoceptor antagonis, was pulse-applied to the AMB_c, ACh ejected to the NTS_c region remained effective in eliciting rhythmic depolarization or repetitive bursts of EPSPs (Fig. 4.11C; n = 2).

In normal ACSF, the evoked rhythmic AMB_c activity was not accompanied by overt spiking (n = 23). Addition of Ba^{2+} (1 mM) to the bathing medium resulted in a slow depolarization (3 to 5 mV) but did not produce rhythmic activity (n = 3) in the absence of muscarinic stimulation of the NTS_c. However, Ba^{2+} enhanced the responsiveness of the AMB_c neurons as evidenced by the occurrence of spike discharges superimposed on the rhythmic depolarization waves in one out of three cases (not shown).

In contrast to muscarinic agonists, glutamate (50 to 100 pmol) or NMDA (50 pmol) pulse-applied to the NTS_c produced only a long lasting (3-10 s) monophasic depolarization or a prolonged burst of EPSPs at AMB_c neurons (Fig. 4.12, n = 8). However, a subthreshold dose of glutamate (10 to 20 pmol) pulsed to the NTS_c facilitated the ACh-evoked rhythmic motoneuronal activity, as evidenced by an enhanced amplitude of the first depolarization wave with concomitant spike production (n = 2 / 3; Fig. 4.12C).

Fig. 4.13 Effect of $GABA_A$ receptor stimulation in the ZIRP region on fictive peristalsis evoked by indirect and direct stimulation of mAChRs in the NTS. Experimental procedures are outlined in left hand diagrams with corresponding results presented in the right hand. Traces are parts of a continuous recording. Rhythmic oesophageal peristalsis evoked by physostigmine (Physo.) topically applied to left NTS (**A**) is inhibited by muscimol (Musci.) injected into ZIRP region (**B**). However, a rhythmic oesophageal response is evoked by application of muscarine to the ipsilateral NTS (**C**) or physostigmine to the controlateral NTS (**D**) in presence of muscimal in ZIRP region.


A
Physo.
3 nmol
NTS$_c$
ZIRP
AMB$_c$
P
TE
B
Musci.
5 pmol
Physo.
3 nmol
ZIRP
P
TE
C
Musci.
5 pmol
Muscarine
0.5 nmol
ZIRP
P
TE
D
Musci.
5 pmol
Physo.
3 nmol
ZIRP
P
2.6 kPa
TE
1 min

4.2.6 Effects of Stimulation and Inhibition of the ZIRP region *In Vivo*

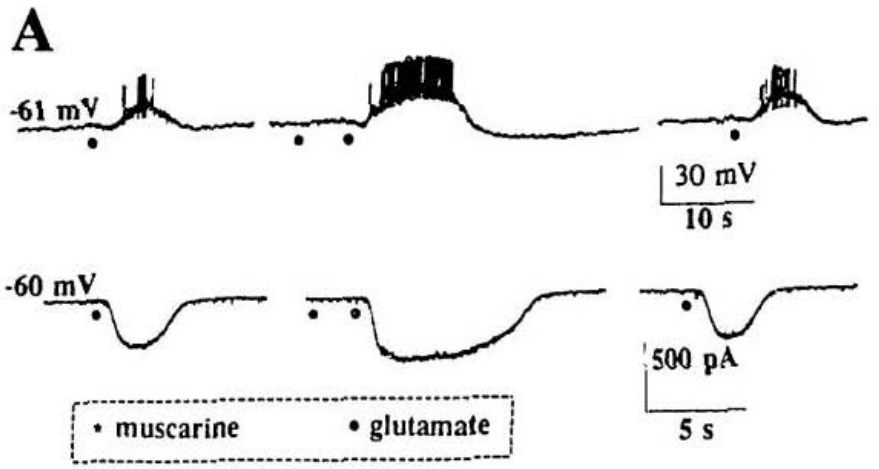
Pressure ejection of glutamate (50 to 100 pmol) into the ZIRP region did not evoke an oesophageal response (n = 5). However, repeated pulses of glutamate (300 to 500 pmol) caused repetitive swallowing (n = 3 / 3; not illustrated).

Physostigmine (0.1 - 0.3 nmol) applied unilaterally to the NTS surface produced rhythmic oesophageal peristalsis (n = 7, Fig. 4.13A). Five to ten minutes after pressure-ejection of the $GABA_A$ receptor agonist, muscimol (5 - 10 pmol), in the ZIRP region, physostigmine applied to the ipsilateral NTS was ineffective (Fig. 4.13B), but continued to elicit a response when applied to the contralateral NTS (Fig. 4.13D). However, muscarine (0.5 nmol) applied to the ipsilateral NTS surface remained effective in eliciting a rhythmic oesophageal response (Fig. 4.13C). As examined by fluorescence microscopy, injection sites (n = 3) were located in the rostral ZIRP comprising a region 300-500 μm medial and 300-500 μm dorsal to the rostral pole of the AMB_c.

4.2.7 Effects of Muscarinic Activation or ZIRP Stimulation on NTS_c Neuronal Response in the Brainstem Slice

In response to a glutamate pulse (50 to 100 pmol), neurons (n= 16) recorded in the NTS_c region in transverse slices produced a fast depolarization in the current-clamp mode or a fast inward current when voltage-clamped. In 9 out of 19 neurons, the glutamate response was enhanced by a prepulse of muscarine (5 - 15 pmol), as evidenced by an increase in its amplitude and duration (Fig. 4.14).

Fig. 4.14 Cholinergic facilitation of glutamate response in NTS_c cells. **A.** Left panel: a pulse of glutamate (about 50 pmol) produces a fast depolarization recorded in whole cell configuration in current-clamp mode (upper trace) or a fast inward current in another cell in voltage-clamp mode in the presence of tetrodotoxin (TTX 1 μM) (lower trace). Middle panel: a subthreshold prepulse of muscarine (5 pmol) facilitates the response to glutamate. Right panel: recovery of the glutamate response after 3 min washout. **B.** Average data from 8 NTS_c cells voltage-clamped at -60 mV demonstrate the facilitating effect of muscarine (5-10 pmol) on amplitude and duration of glutamate (30 - 50 pmol)-evoked inward current. Glu., glutamate; Mus., muscarine


A
-61 mV
30 mV
10 s
-60 mV
500 pA
5 s
• muscarine
• glutamate

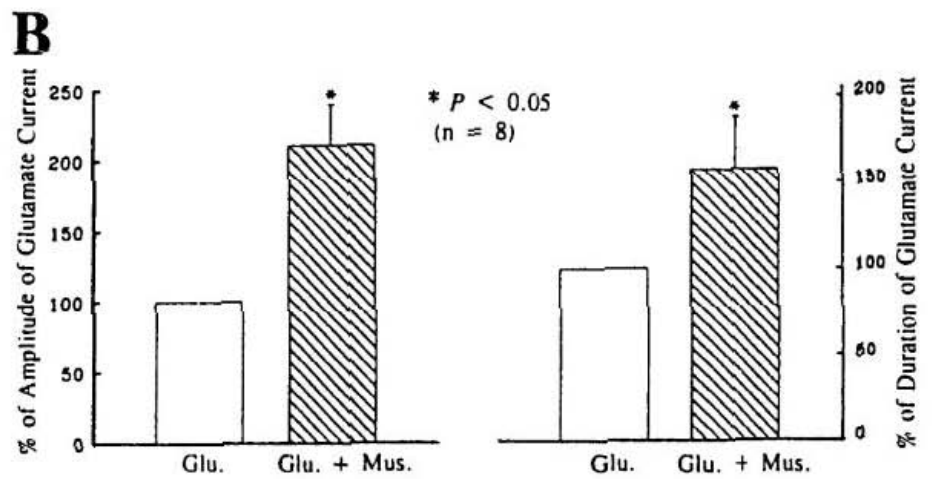
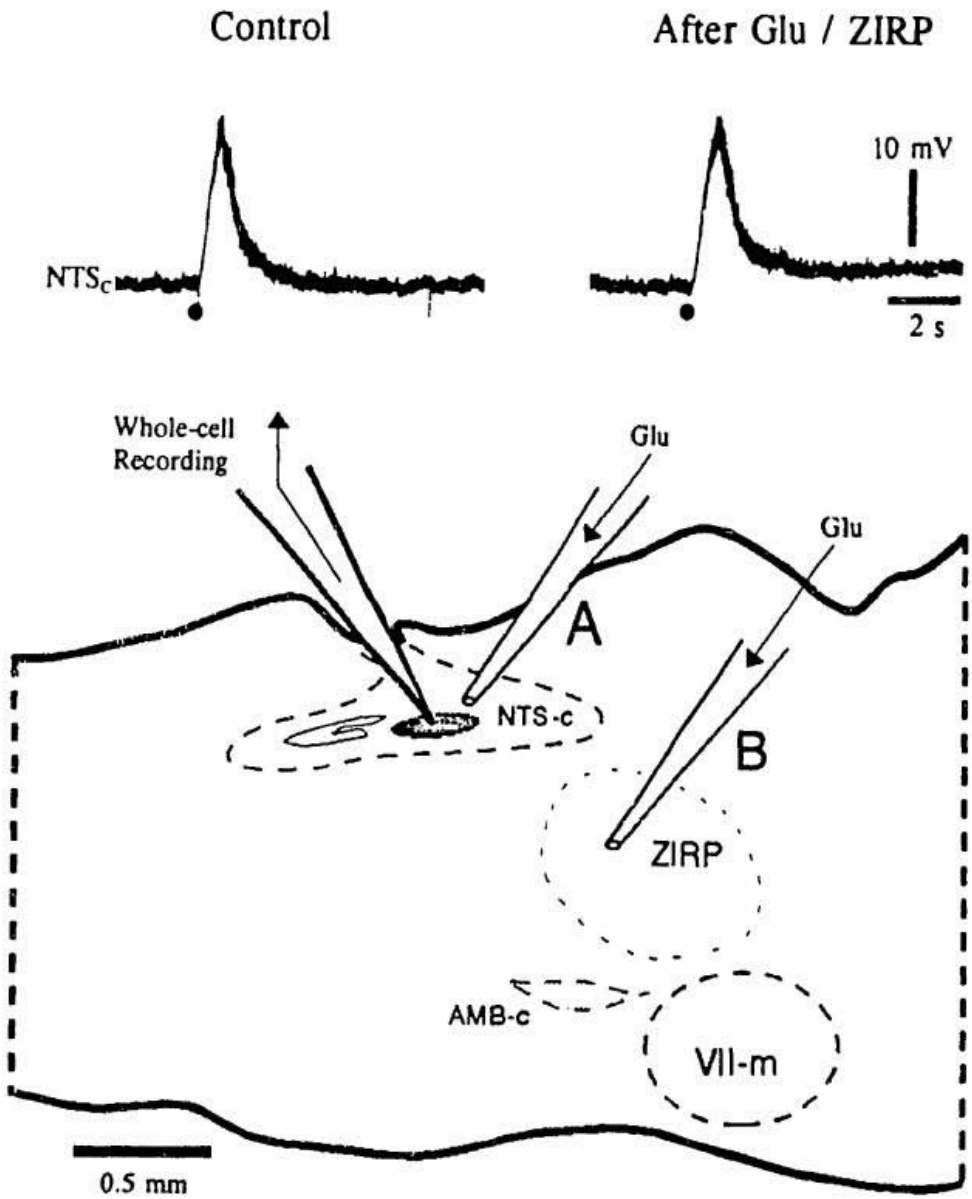

B
* P < 0.05
(n = 8)
% of Amplitude of Glutamate Current
250
200
150
100
50
0
Glu.
Glu. + Mus.
% of Duration of Glutamate Current
200
150
100
50
0
Glu.
Glu. + Mus.

Fig. 4.15 Failure of glutamatergic chemostimulation in the ZIRP region to facilitate NTS_t- excitability in oblique brainstem slice. Drug pipettes are pointed to the NTS_t- and the ZIRP region, respectively. A glutamate pulse (about 30 pmol) applied to an NTS_t- neuron produces a fast depolarization (control). Pulses of glutamate (about. 200 pmol) applied to the ZIRP region are ineffective in altering the NTS_t- neuronal response.


Control
After Glu / ZIRP
10 mV
2 s
NTS$_C$
Whole-cell
Recording
Glu
Glu
A
B
NTS-c
ZIRP
AMB-c
VII-m
0.5 mm

In oblique slices, neurons in the NTS_c region also produced a fast depolarization in response to glutamate pulse (50 - 100 pmol). However, the NTS_c neuronal response was not affected by chemostimulation of the ZIRP region with glutamate (0.2 to 0.4 nmol) (Fig. 4.15; n = 7 cells from 3 slices).

4.3 Discussion

The present investigations provide evidence supporting the hypothesis that propriobulbar cholinergic inputs to the NTS_c (i) are critically involved in esophagomotor pattern control; (ii) allow esophagomotor rhythm to be generated without afferent support; and (iii) originate, at least in part, from the ZIRP region of the rostral medulla oblongata.

4.3.1 Contributions of Cholinergic Mechanisms to Oesophagomotor Pattern Control

The data presented corroborate the idea that cholinergic transmission in the NTS_c participates in three aspects of esophagomotor control, namely (1) the coupling of the oesophageal stage of swallowing (primary peristalsis), (2) the aboral propagation of oesophageal peristalsis and (3) peristaltic rhythmogenesis.

Central coupling of swallowing stages. Regarding the initiation of the oesophageal stage of swallowing (primary peristalsis), Roman (1982) hypothesized that the two stages of swallowing are centrally coupled via a "central chain of neurons". On the contrary, Cunningham and Sawchenko (1990) propose that primary peristalsis, like

secondary peristalsis, is initiated by passive distension of the cervical oesophagus and hence operates in the manner of a chain reflex. The present findings argue against the latter notion, because deafferentation of the pharyngo-oesophageal junction did not eliminate the oesophageal stage of centrally triggered fictive swallowing, suggesting that primary peristalsis does not require afferent inputs from the periphery for its initiation but instead depends on central links between buccopharyngeal and oesophageal interneurons.

Jean (1972a) has hypothesized that buccopharyngeal stage interneurons in the dorsal medulla oblongata cannot activate contralateral oesophageal interneurons, because an electrolytic lesion of a small area in the sheep NTS, probably involving the NTS_c, selectively abolishes the thoracic oesophageal stage of swallowing induced by ipsi- but not contralateral SLN stimulation. In the present study, chemostimulation of swallowing interneurons in the "half center" on the de-efferented side produced pharyngeal deglutition with a coupled cervical oesophageal contraction. The former resulted probably from bilateral activation of pharyngeal stage premotor elements, the latter from excitation of oesophageal premotor elements in the contralateral NTS. In Jean's experiment (1972a), motor activity in the upper cervical oesophagus was also present upon stimulation of the SLN ipsilateral to the lesion but was not commented upon further. At variance with Jean's concept, in the present study the full oesophageal stage could be evoked by bicuculline application to the vagotomized side provided that cholinergic transmission was augmented in the contralateral NTS. Taken together, these results

suggest that the buccopharyngeal interneurons in each half-centre send bilateral excitatory projections to cervical oesophageal interneurons, although the crossed projection appears to exert a weak excitatory drive. It remains to be determined if the same holds for interneurons controlling more aboral portions of the gullet. Clearly, cholinergic input seems to regulate interneuron excitability in a critical manner.

In keeping with Roman's "central chain" model, one may hypothesize that each substage (including motility in different segments of the oesophagus) is controlled by its own neuronal "subcircuit" (as indicated in Fig. 4.16). These subcircuits can be activated separately by afferent inputs, but in a normal swallow they are coordinated by central links. Assuming that such a linkage mechanism needs to operate at considerable speed, one can speculate that the swallowing stages may not be linked by muscarinic cholinergic synapses, but instead by fast transmissive processes. The present data from single cell recordings *in vitro* supports the view that cholinergic input to the NTS_{c}, via postsynaptic mAChRs, up-regulate the excitability of oesophageal interneurons, thereby ensuring interstage-coupling. This hypothesis accords with data demonstrating that muscarinic blockade in the NTS partially depressed cervical oesophageal activity, but fully eliminated distal oesophageal responses during an evoked swallow (see Fig. 4.5).

Facilitation of peristaltic propagation. Cholinergic mechanisms in the NTS not only promote the central coupling between the buccopharyngeal and oesophageal stages, but also contribute to oesophageal peristaltic propagation, as evidenced by (1) the loss of distal oesophageal activity following selective muscarinic blockade in the NTS

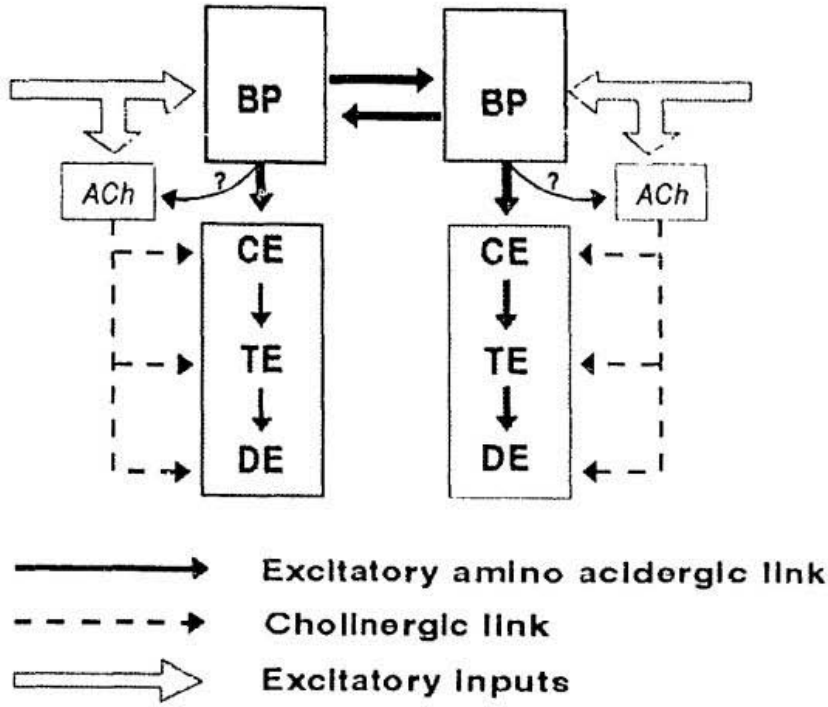


Fig. 4.16 Postulated premotor half center organization of swallowing. Each half center consists of the buccopharyngeal and oesophageal circuits. The oesophageal circuit may contain subcircuits controlling correlated oesophageal segments. The buccopharyngeal and oesophageal circuits are centrally coupled by excitatory amino acidergic links. By facilitating the excitability of cholinoceptive neurons in the oesophageal subcircuits, stage coupling and propagation of excitation through the oesophageal subcircuit chain is strengthened. The two buccopharyngeal half-centers are coupled by an excitatory link. Thus activation of each half center causes output from both centers. BP: buccopharyngeal premotor circuit; CE, TE and DE: cervical, thoracic and distal oesophageal premotor subcircuits; EAA: excitatory amino acid; ACh: acetylcholine.

and (ii) the distalward esophagomotor propagation during local "eserinization" in the NTS.

Generation of esophagomotor rhythm. In extending previous investigations in the rat (Bieger 1984; Hashim & Bieger 1989), the present work further demonstrates that focal activation of mAChRs in the rat NTS_c produces rhythmic esophagomotor synergies without pharyngeal activity. Thus, coordinated rhythmic relaxations in the upper and lower oesophageal sphincter were seen to accompany rhythmic peristaltic contractions in the oesophageal body. Releasing the NTS_c neurons from GABAergic inhibition (Wang & Bieger, 1991) also results in rhythmic oesophageal activity that is abolished by muscarinic blockade, further demonstrating the involvement of an endogenous cholinergic mechanisms in the NTS_c in esophagomotor rhythmogenesis. In contrast, focal activation of glutamate receptors in the NTS_c typically evokes a monophasic non-propulsive oesophageal contraction.

The solitary complex consists of subnuclei which subserve diverse visceral functions (Champagnat et al. 1986; Dekin, 1993; Dekin et al. 1987; Dekin & Getting, 1987; Tell & Jean 1993). The NTS_c is a circumscribed region in the medial portion of the NTS. Based on the observation that activation of mAChRs in the medial NTS causes changes in cardiovascular and respiratory activity, the cholinergic innervation of the NTS_c has been implicated in cardiovascular and respiratory regulation (Ruggiero et al. 1990). However, neuroanatomical studies have revealed that the NTS_c mainly, if not exclusively, receives peripheral afferent inputs from the oesophagus (Altschuler et al.

1989) and functional esophagomotor loci are confined to the NTS_c (Hashim and Bieger 1989). The present study further revealed that focal activation of muscarinic cholinergic mechanisms in the NTS_c evokes rhythmic oesophageal peristalsis without any detectable change in cardiovascular or respiratory activity. The evoked rhythmic esophagomotor activity cannot be a secondary response of oesophageal interneurons to excitatory afferents from cardiovascular or respiratory neurons, because its frequency is well outside the range of the rate of heart beat and respiration. Nevertheless, topical application of muscarine to the NTS surface caused complex cardiovascular and respiratory responses, as well as oesophageal peristalsis, suggesting that the cardiovascular and respiratory functions are regulated by cholinergic mechanisms in certain regions of the NTS, but not the NTS_c. From all these results, one may conclude that the muscarinic chemoceptive neurons in the NTS_c are not involved in cardiorespiratory regulation.

4.3.2 Generation of Oesophagomotor Rhythm by Muscarinic Stimulation of the NTS_c without Re-afferent Sensory Inputs

In vivo.

The oesophageal motoneurons in the AMB_c receive monosynaptic innervation from the ipsilateral NTS_c (Barrett et al. 1994; Cunningham & Sawchenko, 1989; Cai et al. 1995; Hashim 1989). In the present work, AMB_c motoneuronal responses to NTS_c input have been studied by means of extracellular recordings. The oesophagomotoneurons

were identified by their responses to two types of stimulation. First, the neurons in the AMB_c responded to distension of the distal oesophagus with rhythmic burst discharges which preceded phase-locked oesophageal peristalsis, confirming that the recorded neurons were involved in esophagomotor control. Second, chemostimulation of the recorded units with a glutamate pulse elicited a short-latency burst discharge followed by a synchronized oesophageal contraction. This confirms that the recording site was near motoneuronal somata rather than within bundles of passing fibers. As expected, activation of mAChRs in the NTS produced rhythmic discharges in the AMB_c neurons and rhythmic peristaltic oesophageal contractions. Given that the recording loci were located by distension of distal oesophagus, the evoked neuronal activity in the AMB_c led the peristaltic contractions only in the lower thoracic and distal oesophagus but followed those in the proximal segments.

Rat AMB_c neurons contain both nAChR (Wada et al. 1988, 1989) and mAChRs (Wamsley et al. 1981) and receive afferent input from ZIRP cholinergic neurons (Zhang et al. 1993). However, the mAChR-mediated rhythmic motoneuronal activity cannot be generated by the AMB_c neurons themselves, although some motoneurons have been reported as having the ability to generate rhythmic activity (Hochman et al., 1994b) Rather, rhythm generation requires input from interneurons in the NTS. Activation of the AMB_c cholinoceptors with an ACh pulse produced only a single burst discharge and a synchronous oesophageal contraction.

Neuromuscular paralysis caused a decrease in intensity of the evoked rhythmic

esophagomotor activity in the AMB_c. The decrease in burst frequency of the AMB_c discharges during motor paralysis is probably not an artifact, because (i) the animals were well ventilated with oxygenated air and quickly recovered from paralysis and (ii) neuronal discharges could still be evoked by distension during motor paralysis. Therefore, as discussed in Chapter 3, the results obtained here further strengthen the argument that afferent feedback reinforces esophagomotor activity. Since oesophageal afferent inputs project to the NTS_c, but not the AMB_c, the reinforcement should occur at the oesophageal premotor level.

The persistence of muscarine-evoked repetitive discharges during neuromuscular blockade suggests that rhythmic esophagomotor activity can be generated without sensory feedback. As to the alteration in rhythmicity of the evoked oesophagomotoneuronal activity, it could reflect a change in motor pattern generation in the NTS_c, but it could also result from a failure in spike generation in the AMB_c secondary to the decrease in premotor activity. The latter inference prompted us to pursue further studies with intracellular recordings in brainstem slices (see Chapter 5).

Fictive oesophageal peristalsis in vitro.

In light of previous anatomical work (Hashim, 1989), we developed an oblique sagittal brainstem slice containing the NTS_c and the AMB_c. In this brainstem preparation, mAChR activation in the NTS_c, but not cholinergic activation in the AMB_c region, caused rhythmic events in AMB_c neurons. On the premise that cholinergic afferents to the NTS originate from the bulbar reticular formation (Chapter 3), the

present data would suggest that patterned esophagomotor activity can be generated in a medullary network without peripheral afferent inputs. The esophagomotor pattern generator must include the NTS_c region, because the rhythmic motoneuronal activity could only be elicited by activation of mAChRs in the NTS_c. Since the rhythm of the evoked response *in vitro* mimics that of rhythmic peristaltic movements in the oesophagus, this type of oesophagomotoneuronal activity may be appropriately termed "fictive peristalsis".

One interesting aspect of the *in vitro* data is that evoked fictive peristalsis is evident only as a rhythmic depolarization or rhythmic EPSP discharge. That is, AMB_c neurons failed to generate spike bursts in response to muscarinic activation in the NTS_c. As summations of rhythmic synaptic events, the form and amplitude of the evoked rhythmic activity in the AMB_c motoneuron should depend either postsynaptically on the excitability of the AMB_c neuron, or presynaptically on the bursting frequency of the NTS_c neurons when evoked by mAChR activation. The failure of spike production is likely due to the high threshold of the AMB_c motoneurons (Wang et al. 1991b), although the neurons reproducibly generate spikes when sufficiently depolarized by glutamate or ACh. Conceivably, oesophageal premotoneurons in the NTS_c region are in a depressed functional state caused by deafferentation and lack of modulatory input. Evidence obtained in Chapter 3 suggests that oesophageal primary afferents to the NTS_c region are glutamatergic. Indeed, when the NTS_c neurons were stimulated with combined pulses of glutamate and ACh, the AMB_c motoneurons generated higher-amplitude

rhythmic depolarizations with superimposed spikes. Taken together, these data suggest that, under physiological conditions, peripheral afferents and inputs from other brain structures facilitate, via glutamate receptors, the NTS_c premotoneurons which, in turn, drive esophagomotor activity in the AMB_c. This concept also explains the observation that neuromuscular blockade altered the discharge-pattern in oesophagomotoneurons during muscarine-induced peristalsis.

Inactivation of M-current (I_M) by mAChR activation has been found to be one mechanism underlying mAChR-mediated responses in CNS neurons (Halliwell & Adams, 1982). Moreover, I_M has been identified in some neurons in the ventral and ventro lateral portion of the NTS (Champagnat et al 1986). However, inactivation of I_M per se does not appear to contribute to esophagomotor rhythmogenesis. Thus, in the presence of barium, a blocker of I_M (Constanti et al., 1981; Halliwell and Adams, 1982), fictive rhythmic peristalsis does not occur without activation of mAChRs in the NTS_c.

Consistent with *in vivo* results (Bieger 1984; Hashim and Bieger 1989), NMDA pulse-ejected in the NTS_c region only resulted in a monophasic depolarization or a volley of EPSPs in the AMB_c neurons in the oblique slice preparation, suggesting that activation of NTS_c neurons with exogenous NMDA alone cannot produce rhythmic esophagomotor activity. Therefore, mechanisms underlying oesophagomotor rhythmogenesis in the NTS_c remain to be studied.

4.3.3 Involvement of Propriobulbar Cholinergic Neurons

A group of propriobulbar cholinergic neurons in the ZIRP region were retrogradely labelled by depositing tracer at functionally defined oesophageal loci in the NTS_c (Wang 1992). Functional evidence obtained in the present study suggests that ZIRP cholinergic neurons may be a propriobulbar source of cholinergic innervation of the NTS_c.

Inhibition of ACh breakdown in the NTS produced rhythmic oesophagomotor activity, suggesting that under normal resting conditions endogenous ACh is tonically released at NTS oesophageal interneurons. Since evoked esophagomotor activity is abolished by activation of local GABA receptors in the ZIRP region, ACh release in the NTS may originate from ZIRP cholinergic neurons. The inhibition of esophagomotor activity could not have been due to GABAergic inhibition of oesophagomotoneurons in the AMB_c, because esophagomotor activity can be induced by direct activation of mAChRs in the NTS.

There may be at least two explanations of why glutamate chemostimulation of the ZIRP region does not evoke an oesophageal response *in vivo* and failed to facilitate the NTS_c neuronal responses in the oblique brainstem slice. First, cholinergic neurons in the ZIRP are scattered over a relatively large area (Ruggiero et al. 1990; Vyas et al., 1990). Thus, a pulse of glutamate in a restricted locus of the ZIRP may fail to evoke a detectable oesophageal response in intact animals. Second, the ZIRP cholinergic pathway to the NTS_c may have been damaged in the oblique sagittal brainstem slice preparation.

Anatomical studies show that the NTS_c contains a dense ChAT-positive terminal field, whereas the cholinergic neurons in the ZIRP are scattered (Ruggiero et al. 1990). The low density of retrogradely labelled scattered cholinergic neurons in the ZIRP (Wang 1992) is at odds with the dense ChAT-immunoreactive terminal field in the NTS_c (Ruggiero et al 1990). This suggests that the NTS_c may receive other propriobulbar cholinergic inputs. Indeed, scattered ChAT-immunoreactive neurons are located in the immediate vicinity of the NTS_c (Ruggiero et al. 1990), mainly representing the NTS_{im}. Given that NTS_{im} contains buccopharyngeal premotor neurons (Hashim 1989) it is plausible to propose that some cholinergic inputs to the NTS_c may derive from buccopharyngeal premotor neurons in the NTS_{im}.

In summary, propriobulbar cholinergic inputs to the NTS_c are critically involved in the oesophagomotor pattern generation, especially, rhythmogenesis.

Chapter 5

CHOLINERGIC AND GLUTAMATERGIC INTERACTION IN ESOPHAGOMOTOR RHYTHMOGENESIS

In anaesthetized rats, two types of slow oesophagomotor rhythms are evident. Distension of the distal portion of the oesophagus evokes localized 0.5 to 0.7 Hz rhythmic reflex peristalsis that is eliminated by blockade of NMDAR in the NTS (Chapter 2). Activation of muscarinic cholinoceptors in the solitary complex produces fictive peristalsis throughout the whole oesophageal body with a rhythm in the 0.05 - 0.2 Hz range (Bieger, 1984; Hashim and Bieger, 1989; Chapter 4). Taken together these data suggest that esophagomotor rhythm generation depends on both NMDA and muscarinic receptor activity in the NTS_c region.

The aim of this part of the work was to investigate the mechanisms underlying the genesis of rhythmic esophagomotor activity in the rat. Specifically, the following questions were addressed: (i) What activity patterns are generated in NTS_c neurons during fictive rhythmic peristalsis resulting from stimulation of muscarinic cholinoceptors and/or NMDA receptors in the solitarius complex? (ii) can activation of these receptors replicate a peristalsis-like rhythm in single NTS_c neurons deprived of phasic sensory input? (iii) what ionic conductances are involved?

5.1 Methods and Materials

5.1.1 Procedures for *In Vivo* Experiments

Neuronal responses to topical application of receptor agonists were extracellularly recorded in the NTS_c of male Sprague-Dawley rats. The procedures for animal anaesthesia, intraluminal pressure recording, brain surgery, extracellular recording and drug application were as described in the foregoing chapters.

5.1.2 Procedures for *In Vitro* Experiments

i. *Single neuron recordings in brainstem slices.*

The materials and basic procedures for transverse brainstem slice preparation and patch recordings were as described in Chapter Three. Transverse brainstem slices (400 μm thick) were cut and only the slice containing the NTS_c (from a plane 100 μm caudal to 400 μm rostral to the obex) was used for the experiments. Whole cell patch recordings were confined within the NTS_c region under microscopic control. In keeping with previous anatomical studies (Altschuler et al. 1989; Bieger 1984), this region was taken to lie between 800 to 1000 μm lateral to the midline and 500 to 700 μm ventral to the dorsal surface of the medulla. With reference to topographic landmarks, clearly discernible in the transilluminated slice, the region under study extended 200 μm dorsad from the adjacent DMV and between 200 to 400 μm from the medial margin of the solitary tract.

After formation of the whole-cell configuration, the cell was left to stabilize at its intrinsic membrane potential (E_m) for 5 to 10 min. The majority of recorded neurons exhibited spontaneous spiking activity. A baseline potential at which the cell was kept

quiescent by intracellularly injecting the smallest negative current was defined as intrinsic baseline E_m. Only cells with a baseline $E_m \geq$ -40 mV, input resistance $\geq$ 200 MΩ and Na^+-spikes, either spontaneous or evoked in response to intracellular current injection, were used for this study. Some neurons were voltage-clamped in the single electrode voltage clamp mode at a sample rate of 10 to 12 kHz. The switching voltage at the head stage amplifier was monitored continuously on another oscilloscope to assure adequacy of the clamp. Recordings from single neurons lasted from 30 min to 4 h.

Drugs were either pressure-ejected near recorded cells or applied by bath perfusion. The drugs were obtained from commercial sources as described in forgoing chapters except 3-((RS)-2-carboxypiperazin-4-yl)-propyl-1-phosphonic acid ((RS)-CPP) from Tocris Cookson Inc.

ii. *Cell labelling and histology*

In some recordings, the solution in the patch pipette was mixed with 2% neurobiotin (N-(2-aminoethyl)-biotinamide hydrochloride) for intracellular labelling. On termination of recording, the slice was immersed in 0.1 M phosphate-buffered 4 % paraformaldehyde for 16 to 18 h then cut on a vibratome in 80 μm sections for subsequent histochemical processing (using the Dimension Laboratories Inc. procedure). Briefly, after several rinses with PBS, sections were treated with Triton-X100 (0.4% in PBS) for 1 to 2 h and then incubated in the VECTASTAIN ABC Reagent in PBS for 2 h. After several rinses with PBS, slices were reacted with diaminobenzidine (DAB 0.05%) and H_2O_2 (0.003%) in PBS to visualize filled neuron(s). The sections were

mounted onto gelatin-coated slides, dried, defatted and cover-slipped. The stained neurons were examined in serial sections and drawn at 100 to 400 times magnification using a camera lucida microscope attachment.

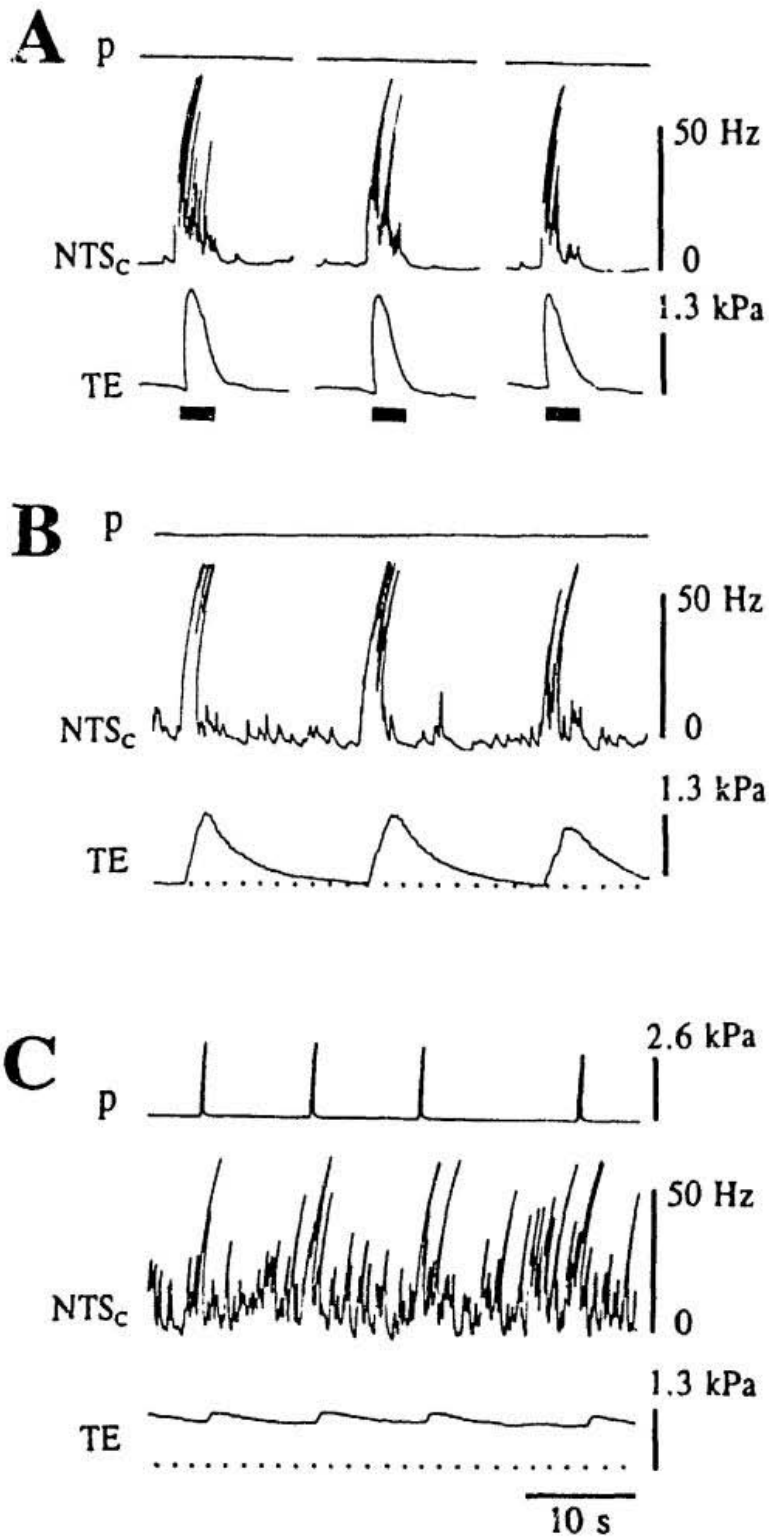
5.2 Results

5.2.1 *In Vivo* Multi-Unit Discharges

As described in Chapter 3, extracellular recordings were performed in different loci of the NTS_c where different burst discharge patterns were elicited by oesophageal distension. When recordings were made in loci in which a discharge burst was evoked by distension of the lower thoracic oesophagus, topical application of muscarine or physostigmine (0.1-0.2 nmol) applied to the NTS surface evoked slow rhythmic unit burst activity in a range of 0.05 to 0.12 Hz together with phase-locked oesophageal pressure waves (Fig. 5.1; n = 10). On application of NMDA (0.1 to 0.2 nmol) by the same route, neurons in the same loci responded with a rise in background firing and superimposed rhythmic burst discharges. The rate of bursting showed a 1:1 relationship with repetitive buccopharyngeal fast pressure waves and slow oesophageal pressure waves representing rhythmic swallowing. The burst discharges were synchronous in onset with the pharyngeal pressure waves but led phasic oesophageal pressure waves that were superimposed on a sustained but small intra-oesophageal pressure rise (Fig. 5.1, n = 3).

At loci where rhythmic (0.5 to 0.8 Hz) burst-discharges were elicited by inflation of the intracrural portion of the oesophagus, slow (0.1 to 0.25 Hz) rhythmic burst

Fig. 5.1 Unit discharge patterns in the NTS_c and motor responses of the upper alimentary tract evoked by application of muscarine and NMDA to the ipsilateral solitarius complex. Extracellular multi-unit activity recorded in the NTS_c region is displayed as rate meter signal (NTS_c) along with intrapharyngeal (P) and thoracic intraesophageal (TE) pressure. **A**: Burst discharge and monophasic pressure wave are reproducibly evoked by distension of lower thoracic oesophagus (indicated by bold bar). **B:** Muscarine (0.1 nmol, 4 min after application) produces rhythmic (0.05 Hz) bursts in the NTS_c that lead rhythmic oesophageal pressure waves in a phase-locked manner. **C**: NMDA (0.1 nmol, 5 min after application) induces a sustained rise in background firing with superimposed rhythmic burst discharges that are coupled to repetitive pressure waves propagating from the pharynx to the thoracic oesophagus. Note tonic pressure rise in oesophagus during activation of NMDA receptors.


A
p
50 Hz
NTSc
0
1.3 kPa
TE
B
p
50 Hz
NTSc
0
1.3 kPa
TE
C
2.6 kPa
p
50 Hz
NTSc
0
1.3 kPa
TE
10 s

discharges were also induced after application of muscarine (0.2 nmol) to the NTS surface (n = 2, not shown).

5.2.2 General Properties of Single NTS_c Neurons *In Vitro*

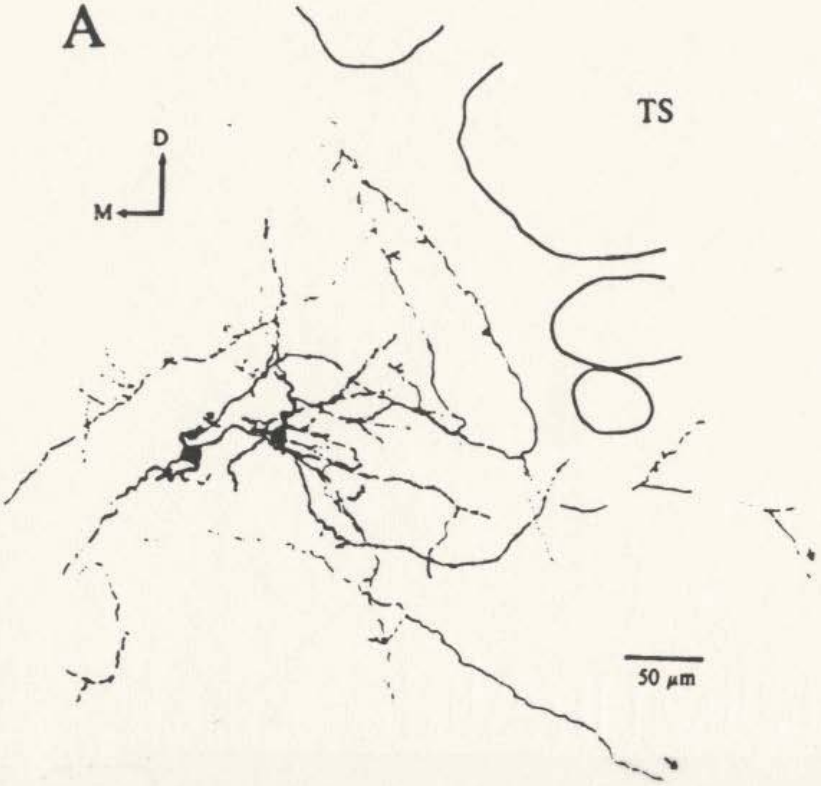
Successful whole-cell recordings were obtained in 212 neurons in the NTS_c region of 109 brainstem slices. Examination of the location of neurobiotin-labeled cells (n = 12) indicated that all recorded cells were within a 120 μm × 120 μm area coextensive with the NTS_c or its immediate surroundings (Fig. 5.2).

In the whole-cell configuration, baseline E_m of recorded neurons was determined in some neurons and ranged from -42 to -67 mV (-51 ± 6 mV; n = 62). At their intrinsic E_m, most neurons exhibited *tonic discharges* (155 / 212 cells); spontaneous *burst oscillations* were observed infrequently (5 / 212 cells). The remaining 52 cells were quiescent at their resting E_m (-54 to -67 mV) and exhibited spike discharges when the membrane was depolarized to around -50 mV by positive current injection. Application of hyperpolarizing current pulses to some recorded neurons revealed an input resistance between 330 and 1200 MΩ (663 ± 312 MΩ; n = 38).

i. *Spontaneous activity*

Tonic discharges. Fig. 5.3 depicts examples of neurons that exhibited tonic spiking activity. The spontaneous firing rates ranged between 1 and 5 Hz. Low-amplitude (15 to 35 mV) spikes were often observed (Fig. 5.3A) and a few neurons (3 / 155 cells) exhibited graded spikes (Fig. 5.3B). Each spike was followed by a prominent after-

Fig. 5.2 Neurobiotin-labeled neurons in the NTS_c region. **A.** Camera lucida drawing shows two neurobiotin-filled neurons, whose cell bodies are located in the NTS_c region within 250 μm medial to the solitary tract (TS). Note that the neurons have a small perikaryon, and long complex dendritic processes that spread into adjacent submuclei (**Insert** shows photograph of the two labeled cells. The dendritic processes are not all in focus). **B.** Responses of both filled cells to chemostimulation by single ACh pulses (50 to 100 pmol, indicated by asterisks). Note the hyperpolarization (cell I and II) and brief rebound burst discharge marked by arrow (cell II). D, dorsal; M, medial.


A
TS
D
M
50 μm

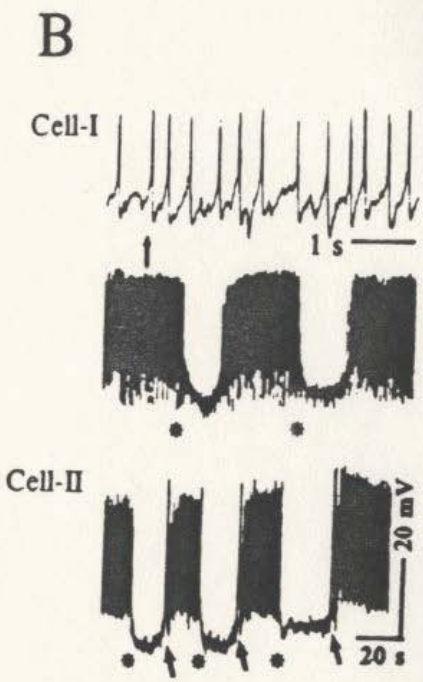
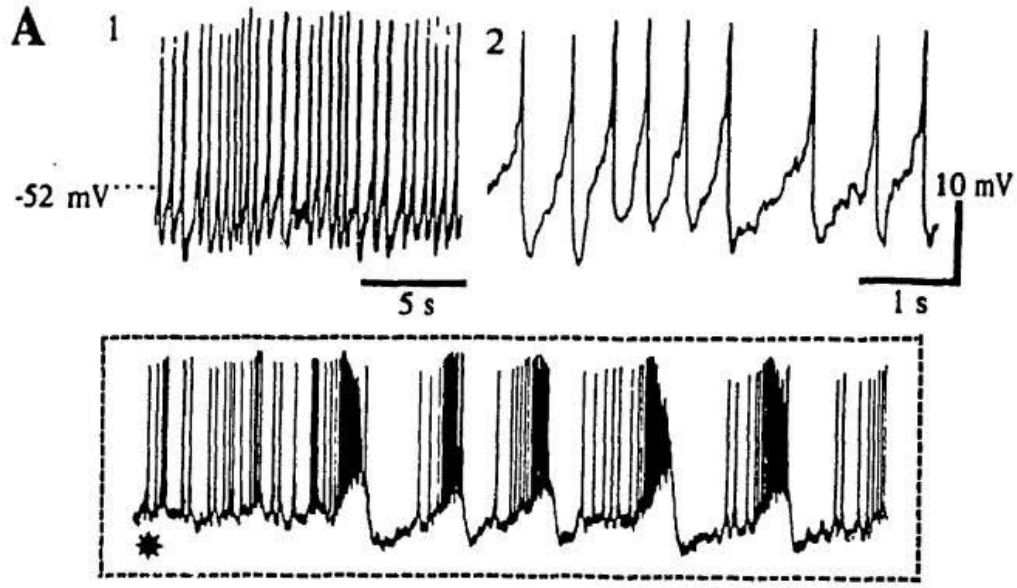
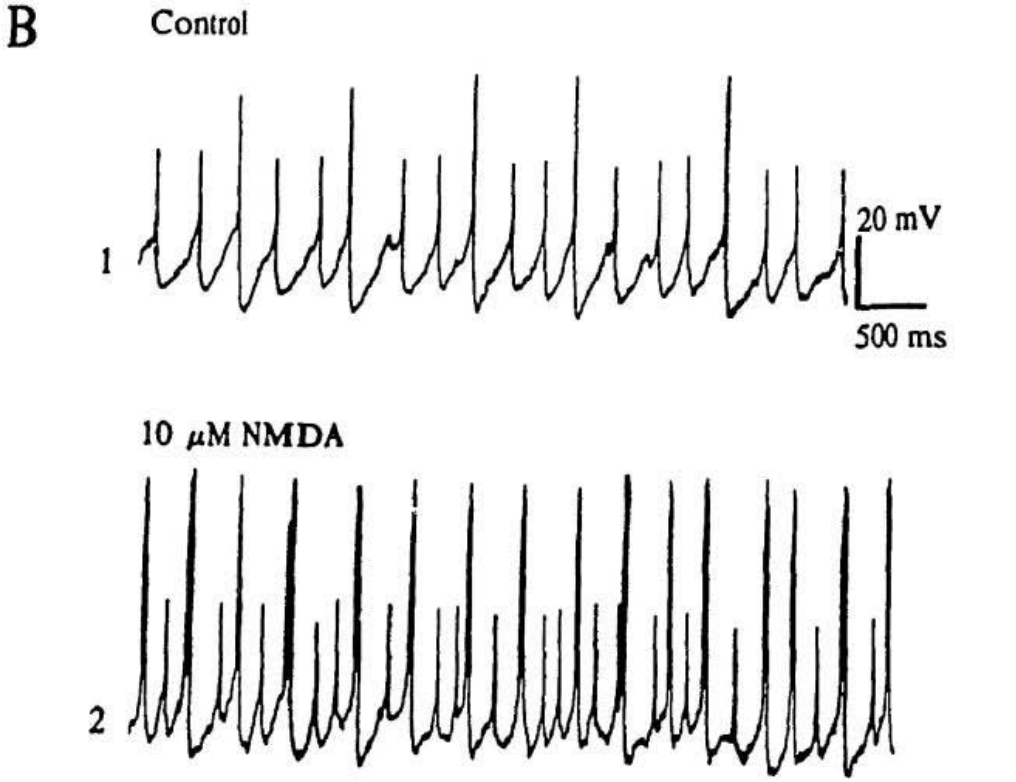

B
Cell-I
1 s
Cell-II
20 mV
20 s



Fig. 5.3 Different types of spontaneous spiking activity of neurons in the NTS_c region. **A.** Spontaneous tonic discharges recorded from a neuron that generated rhythmic burst oscillations (shown in the insert) in response to pulse-applied ACh (~ 0.1 nmol, asterisk). As illustrated at higher speed (A-2), the spike discharge is characterized by a slow pre-spike depolarization and abrupt long lasting afterhyperpolarization following the spike. **B.** Dual spike activity in another neuron (B-1) with development of rhythmic bursting during continuous perfusion with NMDA (10 μM, B-2).


A
1
2
-52 mV
10 mV
5 s
1 s


B
Control
1
20 mV
500 ms
10 μM NMDA
2

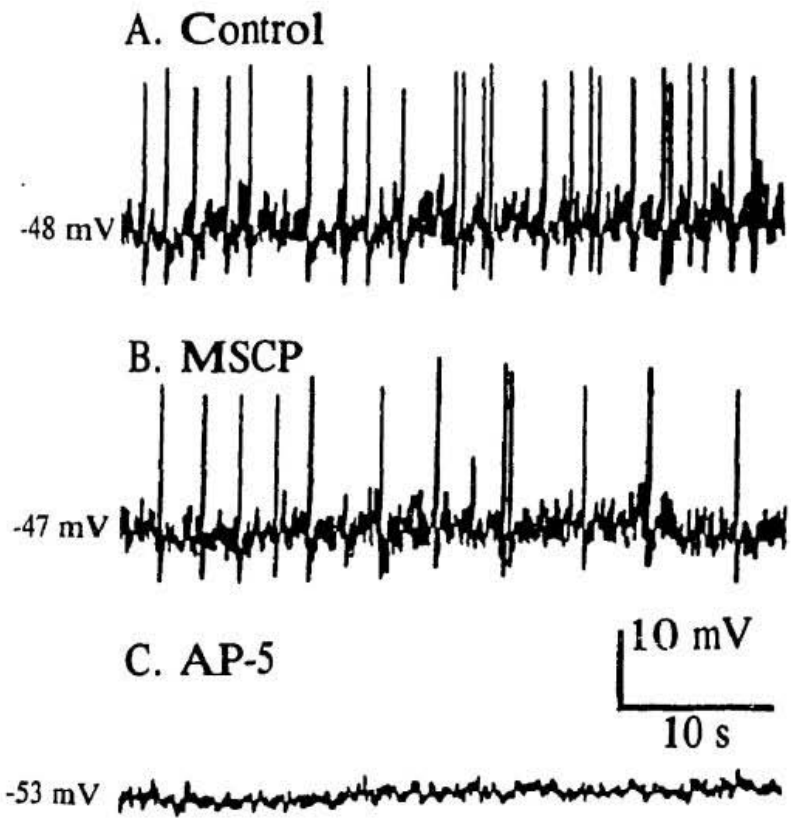


Fig. 5.4 Elimination of spontaneous firing of neurons in the NTS_c region by blockade of NMDARs. Spontaneous spiking is slightly reduced in frequency from control level (A) following 8 min perfusion with methscopolamine 5 μM (**B**). In contrast, firing is completely suppressed by 6 min perfusion with AP-5 (25 μM, **C**).

hyperpolarization (AHP, 8 - 18 mV) (Fig. 5.3A). When hyperpolarized below -60 mV, spontaneous spiking ceased, however, spontaneous potential fluctuations were still evident in some neurons. In all cells tested, the spontaneous spikes (n = 16) and membrane potential fluctuations (n = 5) were eliminated by bath application of tetrodotoxin (TTX, 0.5-1 μM). Within 5 to 20 min following perfusion with the NMDAR antagonists, AP-5 or AP-7 (10 to 25 μM), the E_m hyperpolarized by 4 to 8 mV and thus spontaneous spikes disappeared (Fig. 5.4; n = 7 / 8 cells tested). In contrast, spontaneous activity persisted during a 15 to 20 min perfusion with methscopolamine (1 to 2 μM, n = 5) albeit at a decreased frequency.

Burst oscillations. Burst oscillations were recorded immediately after achieving the whole cell configuration in 4 cells. Another cell exhibited oscillatory behaviour when depolarized. As depicted in Fig. 5.5, oscillations were characterized by recurring depolarizing plateau potentials with superimposed spike bursts. Each oscillatory cycle consisted of 4 phases: an initial slow depolarization, a fast depolarization, a plateau and a fast repolarization. The spontaneous burst oscillations varied in frequency (0.1 to 4.5 Hz) among different cells. Hyperpolarization of the membrane increased the amplitude of the plateau potential but decreased the frequency of the oscillation (Fig. 5.5A; 2 out of 2 neurons tested). After exposure to TTX (1 μM, n = 3), spontaneous oscillations together with spike bursting ceased in 2 cells tested. The remaining cell continued to oscillate at holding potentials between -40 and -50 mV, although the spikes were suppressed and the frequency of oscillation was reduced (Fig. 5.5B).

Fig. 5.5 Two examples of spontaneous burst-oscillations in the NTS_c region. **A.** low-frequency spontaneous burst oscillation is recorded at intrinsic membrane potential (left panel). The burst-oscillations decreased in frequency when membrane is hyperpolarized (right panel), suggesting that the oscillation is endogenous, i.e. not driven by phasic synaptic inputs. **B.** Another neuron exhibits high-frequency spontaneous oscillations when current-clamped at -45 mV (upper trace). The oscillations persist in the presence of 1 μM TTX (lower trace) albeit at a reduced frequency, but disappear when membrane is hyperpolarized below -50 mV. Break in the lower trace represents 40 s).

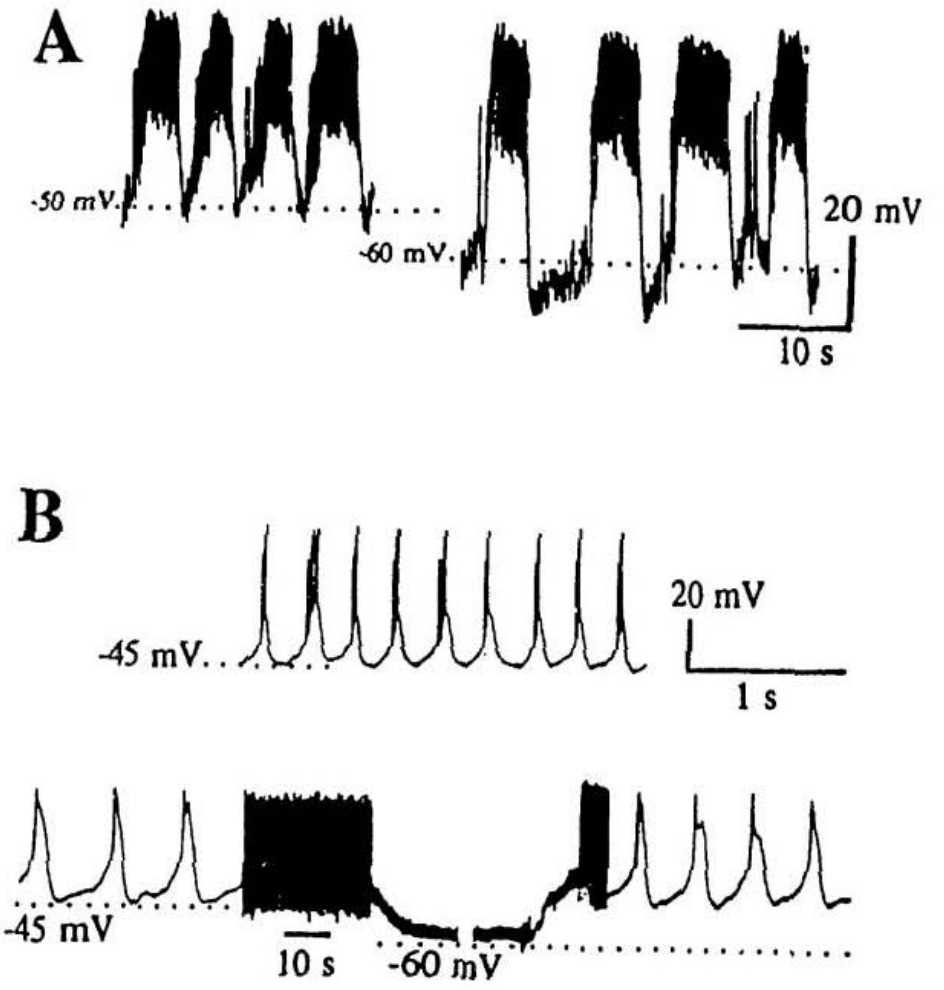
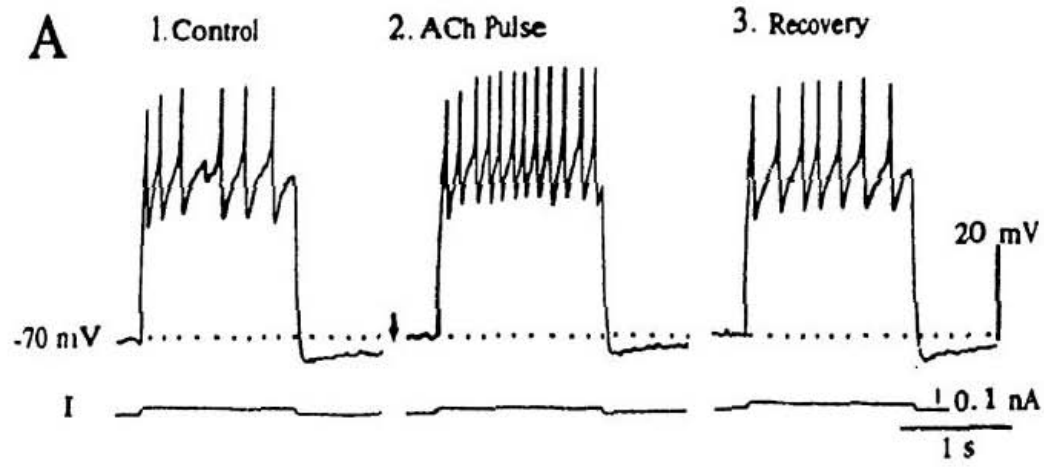
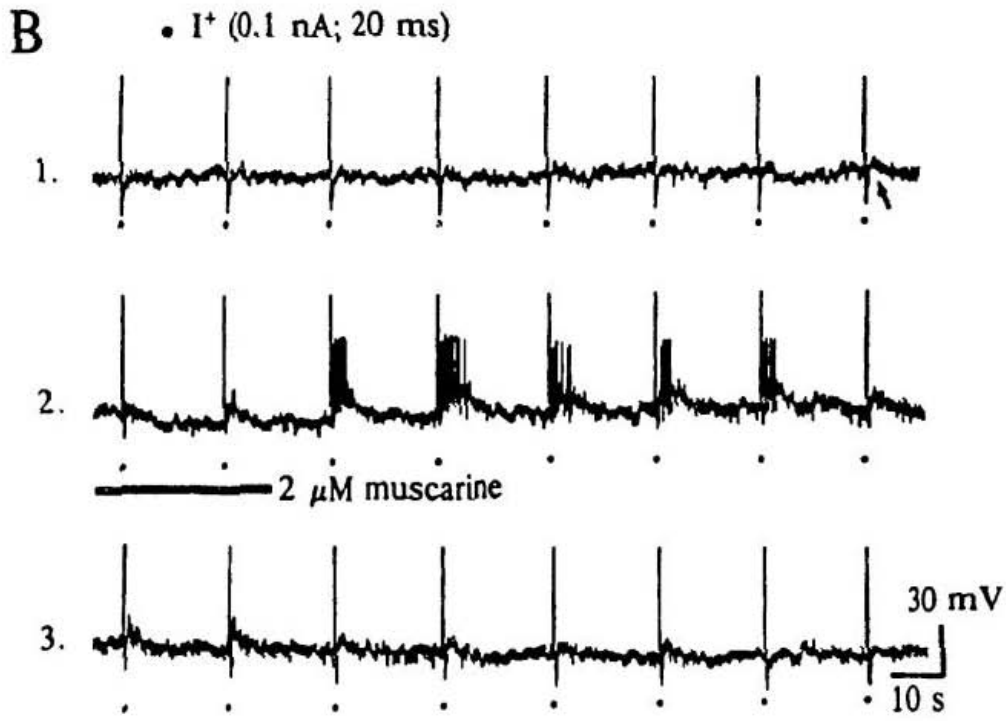

A
-50 mV
-60 mV
20 mV
10 s
B
-45 mV
20 mV
1 s
-45 mV
10 s
-60 mV

Fig. 5.6 Effects of mAChR activation on membrane excitability. **A.** A neuron current clamped at -70 mV produces repetitive spikes during a depolarizing current pulse (lower trace, 1.5 s, 0.1 nA) and a slow afterhyperpolarization (AHP) after the current pulse (A-1). The frequency of the evoked spikes is enhanced but amplitude of the evoked AHP is reduced 1 min after ACh (about 30 pmol, down-ward arrow) pressure-ejected in the vicinity of the neuron . Five minutes after the ACh pulse, the responses recover (A-3). **B.** Upon termination of short depolarizing pulses (0.1 nA, 20 ms, at black dots), another neuron held at -60 mV reproducibly produces slow AHPs that are occasionally followed by a small afterdepolarization (ADP, indicated by the arrow) (B-1). After 35 s perfusion with muscarine (2 μM, black bar), the AHP disappeared, but the ADP is reproducibly evoked (B-2). After 5 min washout, both the AHP and ADP recover to control level (B-3).


A
1. Control
2. ACh Pulse
3. Recovery
20 mV
-70 mV
I
0.1 nA
1 s


B
• I+ (0.1 nA; 20 ms)
1.
2.
2 μM muscarine
3.
30 mV
10 s

ii. *Responses to intracellular current- or voltage-pulse*

Depolarizing current pulses. Responses to long (0.5 to 1.5 s) and short duration (20 ms) depolarizing current pulses (0.1 to 0.2 nA) were tested in 48 neurons. When cells were held at their intrinsic E_m, a long depolarizing pulse (0.5 s, 0.1 nA) produced a sustained burst of spikes with a frequency of 15 to 50 Hz, followed by a slow AHP. The slow AHP lasted 2 to 5 s (3.1 $\pm$ 0.9 s; n = 22) and reached amplitudes of 8 to 18 mV (12 $\pm$ 3.2 mV; n = 22). All spontaneously firing neurons resumed repetitive spiking when repolarized from the AHP (n = 18). At holding potentials of -60 to -75 mV, spontaneous spiking ceased; however, a positive current injection (1 s, 0.1 to 0.2 nA) evoked a train of spikes with a frequency of 6 to 18 Hz (12 $\pm$ 3.2 Hz, n = 14; Fig. 5.6A-1). The onset of the spiking occurred with virtually no delay (n = 14 / 14). In the presence of TTX (0.5 μM), spikes failed to be evoked by a depolarizing step (n = 11 / 11), however, the slow AHP persisted although reduced. A short depolarizing pulse evoked a single spike in cells current-clamped at -60 to 65 mV (n = 6). Upon termination of the short depolarizing pulse, the cells generated an AHP that was occasionally followed by an afterdepolarization (ADP) (Fig. 5.6B-1).

Following 30 to 40 s perfusion with muscarine (0.5 to 2 μM) or pressure-ejection of muscarine (10 to 20 pmol) or ACh (20 to 40 pmol), the frequency of spikes evoked by a long depolarizing pulse (1 s, 0.1 to 0.2 nA) applied to neurons held at -60 to -75 mV was augmented from 12 $\pm$ 3.2 Hz to 19 $\pm$ 4.5 Hz (n = 9), whereas the slow AHP

was reduced (n = 5; Fig. 5.6A-2) or blocked (n = 4). The AHPs evoked by a short depolarizing current pulse were completely eliminated in all neurons tested (n= 6) and in some cases (2 / 6) replaced by a slow depolarization with a superimposed burst of action potentials (Fig. 5.6B-2).

Hyperpolarizing voltage- or current-pulses. When cells were voltage-clamped at -35 to -45 mV, a hyperpolarizing voltage-clamp step of 15 to 25 mV did not reveal the presence of I_M (n = 12, including 7 neurons that were demonstrated to be responsive to mAChR stimulation).

Membrane voltage responses to hyperpolarizing current-steps (0.5 s to 1.5 s, 0.1-0.5 nA) were tested in 48 neurons held at their intrinsic E_m, or at -60 mV. In 23 out of 48 neurons, an inward rectification was observed in the form of a sag in the voltage during the hyperpolarizing current injection (Fig. 5.7A). Upon termination of hyperpolarization, most neurons (n = 34 / 48) showed a postinhibitory rebound (PIR) activity (Fig. 5.7A). The PIR activity was manifest as a subthreshold depolarization, or a depolarization with superimposed action potentials (Fig. 5.7A) or slow voltage fluctuations (Fig. 5.7B-1), lasting between 1 to 6 s. Although varying from cell to cell, the amplitude of both the inward rectification and the PIR depended on the duration and intensity of the negative current pulse (Fig. 5.7A). Both the inward rectification and PIR (Fig. 5.8A) persisted in the presence of TTX (1 μM).

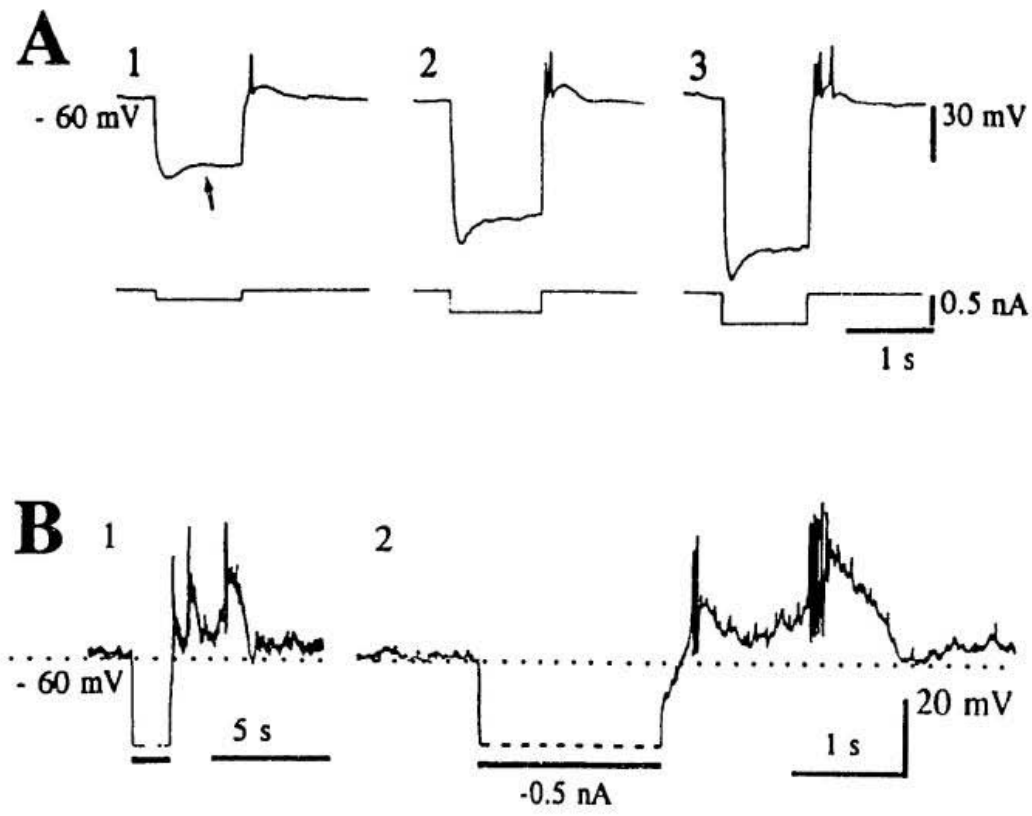
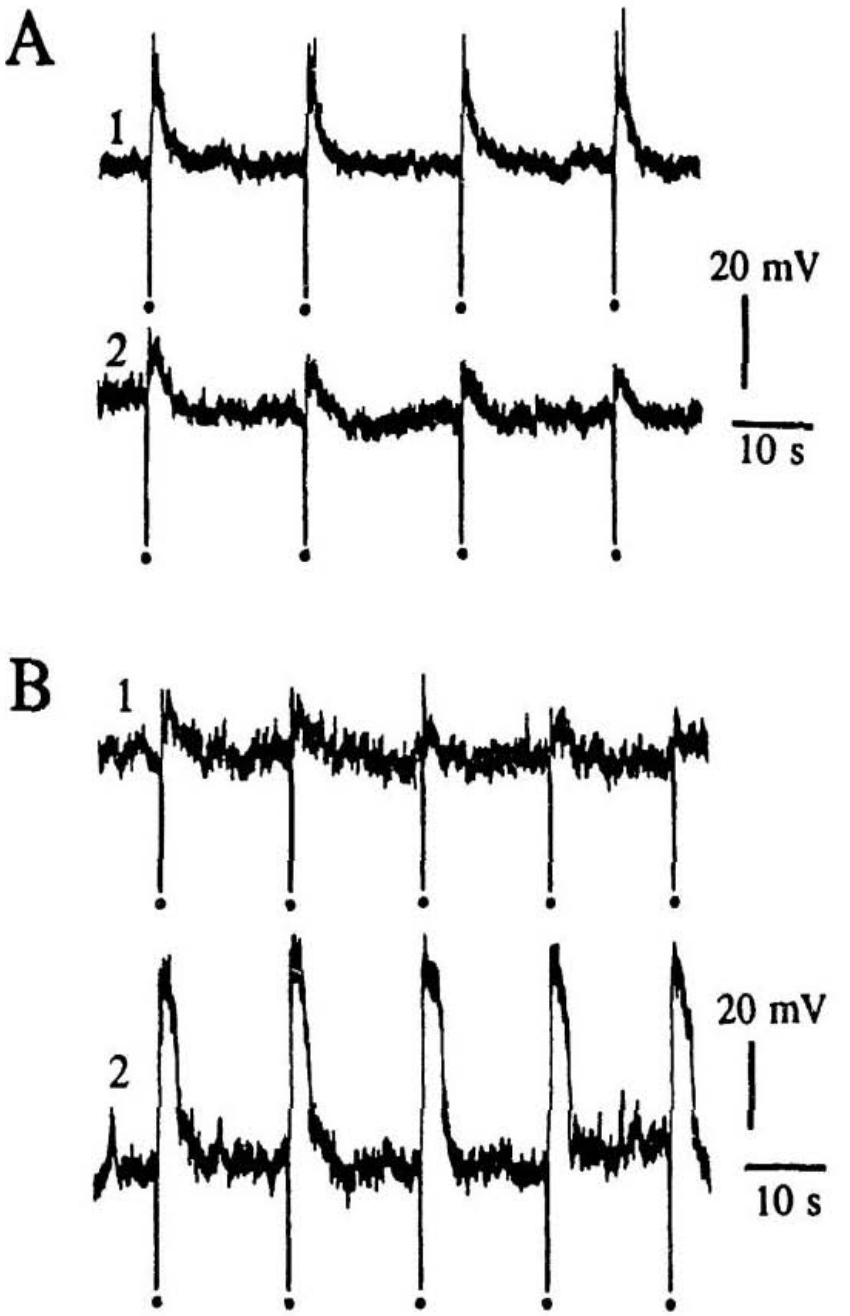


Fig. 5.7 Hyperpolarization-produced anomalous rectification followed by postinhibitory rebound (PIR). **A.** In a cell held at -60 mV by injecting a steady hyperpolarizing current, injection of a hyperpolarizing pulse produces an inward rectification (marked by arrow) and PIR with superimposed spikes. Increasing the amplitude of the current pulse results in greater anomalous rectification and PIR. **B.** In another neuron, termination of a hyperpolarizing current pulse (1.5 s, -0.5 nA) results in rhythmic membrane oscillations (B-1). As shown at higher speed (B-2), the rhythmic oscillations trigger burst discharges.

Fig. 5.8 Effect of muscarinic activation on PIR in the presence of tetrodotoxin. **A.** At termination of the hyperpolarizing current pulse (20 ms, -0.2 nA, small dot), a PIR with superimposed spikes is reproducibly evoked in a neuron held at -60 mV (A-1). After 10 min perfusion with tetrodotoxin (1 μM), the PIR persists with a loss of superimposed spikes (A-2). **B.** In another neuron held at -60 mV, a small PIR depolarization is evoked by intracellular negative current injection (20 ms, 0.1 nA) in the presence of tetrodotoxin (B-1). Amplitude of the PIR is enhanced by perfusion with muscarine (2 μM) for 30 s (B-2).


A
1
2
20 mV
10 s
B
1
2
20 mV
10 s

The effect of mAChR activation on the PIR was also investigated. After bath perfusion with muscarine (1 to 2 μM, 20 to 40 s), negative current pulses (20 ms, 0.1 nA) reproducibly evoked PIR (n = 6 / 6 neurons tested, Fig. 5.8B). The enhancing effect of muscarine on the PIR response persisted in the presence of TTX (1 μM, n = 4 / 4 tested). The PIR was resistant to the L-type Ca^{2+} channel blocker, nifedipine (1 μM, n = 2) and the NMDAR antagonist, AP-5 (20 μM, n = 2).

5.2.3 Agonist-Driven Oscillations in Single Neurons

Responses to NMDA (n = 117) or mAChR agonists (n = 184) were examined in NTS_c neurons (some of which were tested with both NMDA and mAChR agonists). In response to NMDA, all neurons tested showed depolarization from their intrinsic E_m and some exhibited membrane oscillations when hyperpolarized. About 70 % (132 / 184) neurons at the intrinsic E_m responded to ACh or muscarine. These responses included (i) a nonrhythmic depolarization (n=48); (ii) a simple hyperpolarization (n=31) or (iii) rhythmic (oscillatory) depolarizations with or without concomitant hyperpolarization (n=53). Only neurons exhibiting bursts or slow ($\leq$ 1.0 Hz) oscillatory behaviour were studied in more detail. In terms of their oscillatory responsiveness to agonist application, neurons were generally divided into *a*) *NMDAR-driven oscillators*, or *b*) *mAChR-driven oscillators*. In terms of their sensitivity to TTX, the latter, but not the former, could be further divided into TTX-sensitive and TTX-resistant subtypes (Table 5.1).

Table 5.1 Agonist-driven oscillator cells in the submucleus centralis of the nucleus tractus solitarii

	NMDAreceptor-driven (n=47)	mACh receptor-driven (n=53)	
	TTX-resistant	TTX-sensitive[1] (n=8/12)	TTX-resistant[1] (n=4/12)
Responsiveness to Agonist	NMDA [2] (0.1 nmol) NMDA 10-50 μM	ACh [2] (0.1-0.4 nmol) muscarine 2-5 μM	ACh [2] (0.1-0.4 nmol) muscarine 2-5 μM
Oscillatory Frequency	0.64±0.12 Hz	0.12±0.06 Hz	0.09±0.05 Hz
Requirement for Hyperpolarizing Current Injection	Yes	No	No
Sensitivity to NMDA Receptor Antagonist	Yes	Yes	No
Sensitivity to mACh Receptor Antagonist	No	Yes	Yes

[1] Only tested on 12 cells.
[2] Pulse-Applied

i. *NMDAR-driven oscillators*

At their intrinsic E_m, these neurons responded to NMDA with a slow depolarization and tonic firing. When hyperpolarized by 10 to 25 mV, 47 out of 117 neurons exhibited a regular rhythmic burst activity at an E_m of -60 to -85 mV. The frequency of the rhythmic activity ranged between 0.5 and 0.9 Hz (0.64 $\pm$ 0.12 Hz, n = 47). To distinguish these cells from others described below, they will hereafter be referred to as *NMDAR-driven oscillator neurons*.

Oscillations at hyperpolarized membrane potentials. Fig. 5.9A depicts responses of a NMDAR-driven oscillator neuron at different membrane potentials. At -50 mV (intrinsic E_m), the NMDA pulse ($\sim$ 50 pmol) produced a small depolarization (5 to 10 mV) and tonic spiking activity (Fig. 5.9A-1). A larger pulse of NMDA ($\sim$0.1 to 0.2 nmol) only slightly enhanced the amplitude of the slow membrane depolarization and prolonged the duration of the response (not shown). At -60 mV, however, burst oscillations were superimposed on the slow depolarization (Fig. 5.9A-2) and, at -70 mV (Fig. 5.9A-3), these increased in amplitude and duration. Bath application of NMDA (40 to 60 μM) produced a similar response. At the intrinsic E_m, neurons exhibited a slow depolarization (5 to 15 mV) with superimposed tonic spikes. At holding potentials between -65 and -80 mV, oscillatory activity was evident (Fig. 5.9D; n = 8 / 8). In the presence of TTX (1 μM), all neurons tested (n = 22) continued to generate repetitive plateau potentials without a change in frequency despite the absence of fast spikes. However, six to ten minutes after perfusion with AP-5 (10 μM), the depolarizing and

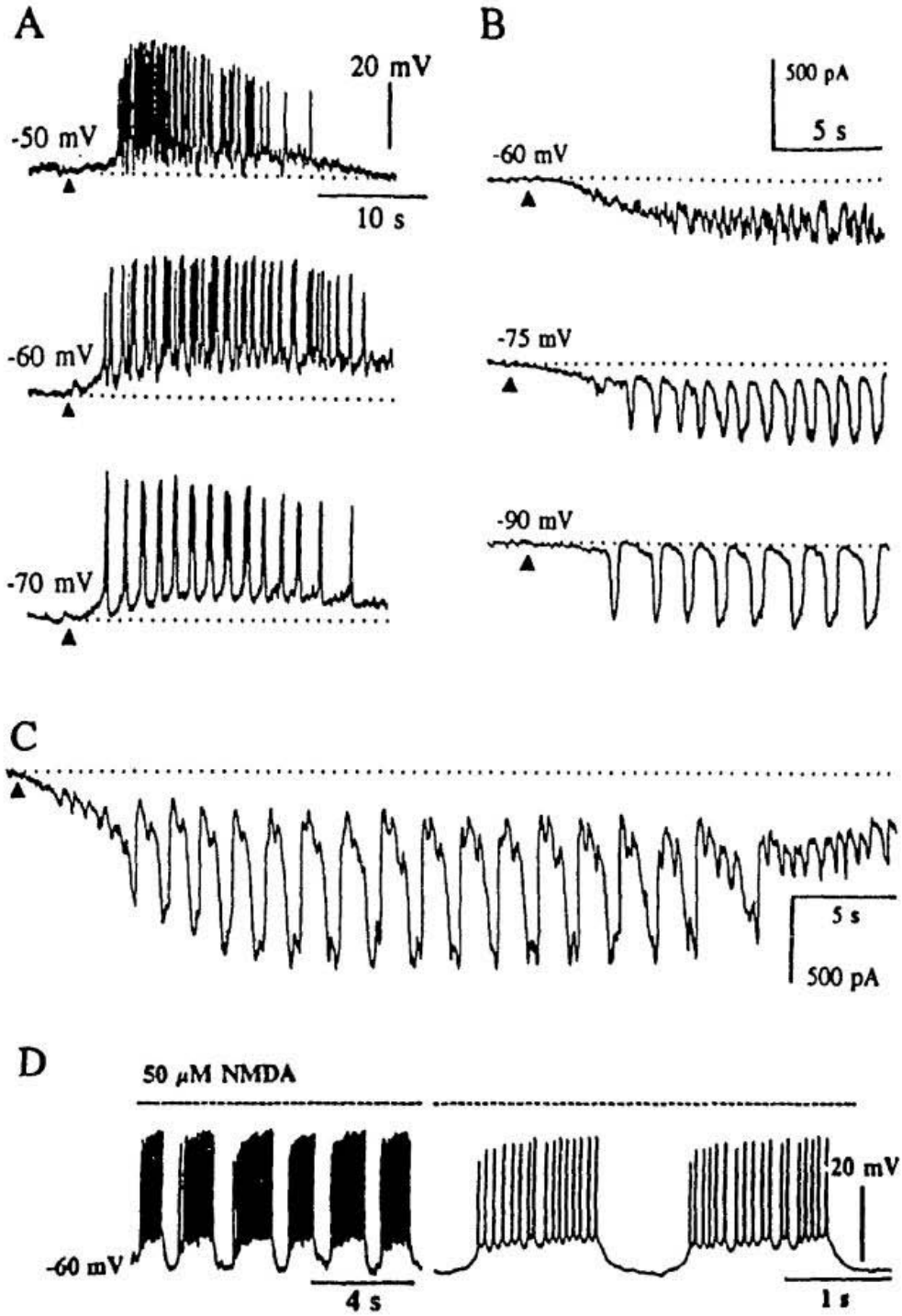
oscillatory response to NMDA was completely abolished (n = 3).

Oscillations under voltage clamp. In the presence of TTX (0.5-1.0 μM), NMDA-induced oscillations in membrane current were observed in all neurons that were under single electrode voltage clamp mode (n = 31). As shown in Fig. 5.9B, rhythmic current oscillations were superimposed on a slow inward current. Like the voltage oscillations, current oscillations were also dependent on the membrane potential. Hyperpolarization of the membrane enhanced the amplitude, but slowed the frequency of the current oscillations (n = 7, tested between -60 and -90 mV). In a given neuron, the frequency of NMDAR-driven oscillations were similar in voltage or current clamp. In response to NMDAR activation, a small subgroup of neurons (n = 4 / 47 NMDAR-driven oscillatory neurons) generated two types of oscillations: a fast (~ 1.5 to 2.0 Hz) low-amplitude oscillation interspersed with a slow (~0.5 Hz) high-amplitude current oscillation (Fig. 5.9C).

Effects of Mg^{2+} and Ca^{2+} on oscillation. Perfusion of the slice with Mg^{2+}-free medium for 8 to 10 min eliminated the current oscillation leaving a slow inward current. Re-perfusion of the slice with Mg^{2+}-containing ACSF for 15 to 20 min restored the oscillations (Fig. 5.10; n = 4 / 4 tested).

Perfusion of the slice with nominally Ca^{2+}-free medium completely eliminated NMDA-evoked membrane oscillations while enhancing the magnitude of the NMDA-evoked slow depolarization. (Fig. 5.11; n = 5 / 5 tested). On returning the slice to Ca^{2+}-containing ACSF, the oscillatory response was restored within 10 to 20 min.

Fig. 5.9 Examples of voltage-dependent NMDAR-driven membrane oscillations of neurons in NTS_c region. **A.** In response to pulse-applied NMDA (▲ 0.2 nmol), a neuron at intrinsic membrane potential (top) produces a slow depolarization with superimposed spiking, but exhibit rhythmic burst-oscillations at hyperpolarized membrane potentials (middle and bottom). **B.** In the presence of 1 μM TTX, a neuron voltage-clamped at hyperpolarized potentials produces current oscillations superimposed on a slow inward current in response to pulse-applied NMDA (▲, about 0.4 nmol). At holding potentials range between -60 and -90 mV, hyperpolarization slows the frequency and enhances the amplitude of the current oscillation. **C.** Following an NMDA pulse (▲, about 0.4 nmol), a neuron voltage-clamped at -75 mV, in the presence of TTX (1 μM), exhibit two types of membrane oscillations at the same time. Initial low-amplitude 2 Hz oscillations are interspersed with high-amplitude 0.7 Hz oscillations. **D.** Bath-applied NMDA (50 μM, indicated by broken line) produces rhythmic oscillations (about 0.5 Hz) in a neuron held at -60 mV. As shown at faster speed, oscillatory plateau potentials trigger spike trains.


A
20 mV
-50 mV
10 s
-60 mV
-70 mV
B
500 pA
5 s
-60 mV
-75 mV
-90 mV
C
5 s
500 pA
D
50 μM NMDA
-60 mV
4 s
20 mV
1 s

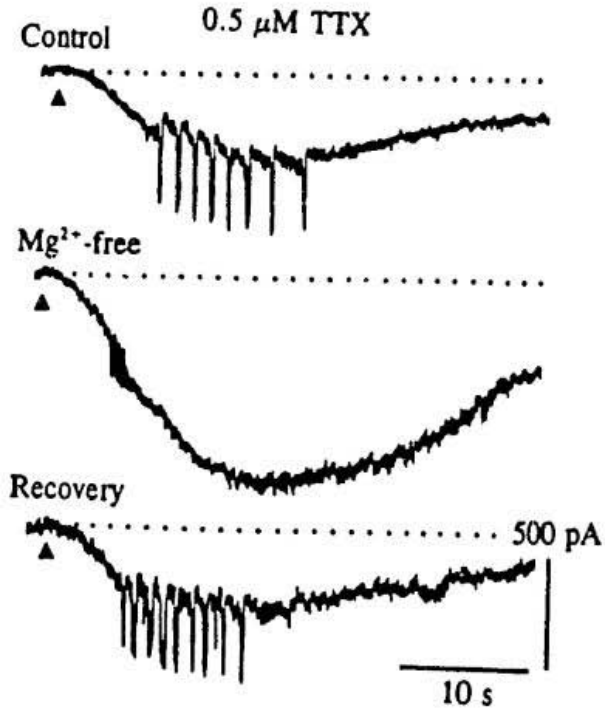


Fig. 5.10 Loss of NMDAR-driven current oscillations in Mg^{2+}-free ACSF. In the presence of TTX (0.5 μM), NMDA (▲ about 0.1 nmol) reproducibly evokes a slow inward current and superimposed current oscillations (**top**). After 5 min perfusion with Mg^{2+}-free ACSF, the NMDAR-driven current oscillations disappear, while the amplitude of the slow inward current increases (**middle**). The current oscillation recovers 10 min following reperfusion with control ACSF (**bottom**). The holding potential of the neuron is -70 mV (indicated by dotted line).

Dose-dependence of the NMDA response. Although no attempt was made to analyze the NMDA dose-response relationship in detail, the oscillatory pattern in NMDAR-driven oscillator neurons showed a complex relationship to NMDA dosage. As presented in Fig. 5.12, a 20 ms pulse of NMDA (~ 40 pmol) evoked a single plateau potential riding on a slow depolarization wave (Fig. 5.12A). A 35 ms pulse of NMDA (~ 70 pmol) produced repetitive oscillatory plateau potentials (Fig. 5.12B). A further increase in duration of the NMDA pulse to 50 ms (~ 100 pmol) resulted in a sustained plateau potential that terminated after 5 min (Fig. 5.12C). Despite the variation in response patterns, the amplitude of the slow depolarizing potential and the oscillatory plateau potentials attained the same level, indicative of a bi-stable membrane potential.

Enhancement by mAChR activation. At the intrinsic E_m, all NMDAR-driven slow oscillator neurons tested (n = 24) produced a slow depolarization under current-clamp or an inward current under voltage-clamp in response to an ACh pulse (0.1 nmol). At a holding potential of -70 to -85 mV, the ACh pulse itself failed to evoke an overt response (pulses of ACh produced a small outward current or hyperpolarization in some neurons), but prepulses of ACh increased the amplitude of the NMDAR-driven oscillations in the majority of neurons tested (Fig. 5.13; n = 17 / 24). During perfusion with methscopolamine (1 to 5 μM), however, the NMDA evoked oscillations remained unchanged in amplitude and frequency (n = 5 / 5).

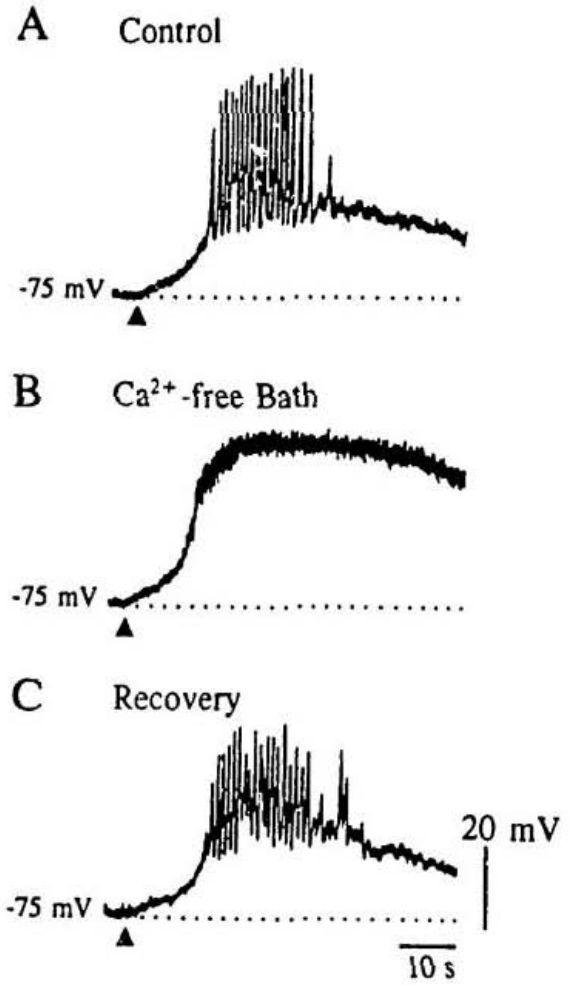


Fig. 5.11 Disappearance of NMDAR-driven oscillations in Ca^{2+}-free medium. In the presence of TTX (1 μM), a neuron held at -75 mV produces a slow depolarization with superimposed 0.8 Hz oscillations in response to NMDA (▲, about 0.1 nmol) (**A**). After 5 min perfusion with nominally Ca^{2+}-free ACSF, NMDA evokes a large depolarization without oscillations (**B**). The oscillatory response recovers following 15 min reperfusion with control ACSF (**C**).

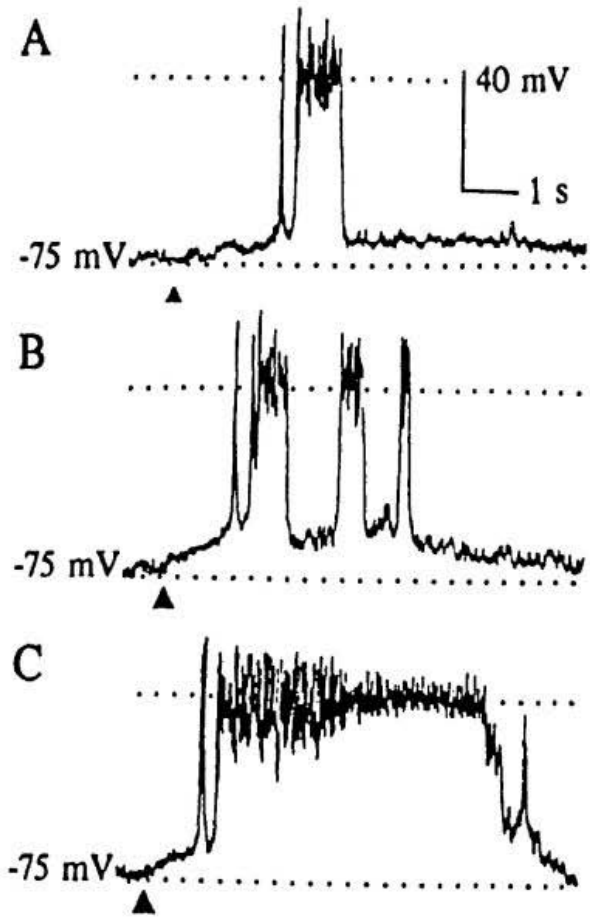


Fig. 5.12 Dose-dependence of NMDA oscillations. In the presence of TTX (0.5 μM), NMDA (▲) are ejected near a neuron held at -75 mV. The low dose (about 40 pmol) evokes a single short-duration plateau potential (**A**), the intermediate dose (about 70 pmol) a rhythmic oscillation (**B**) and the largest dose (about 100 pmol) a sustained plateau potential (**C**). Note that the amplitude of the plateau potential evoked by NMDA remains nearly constant.

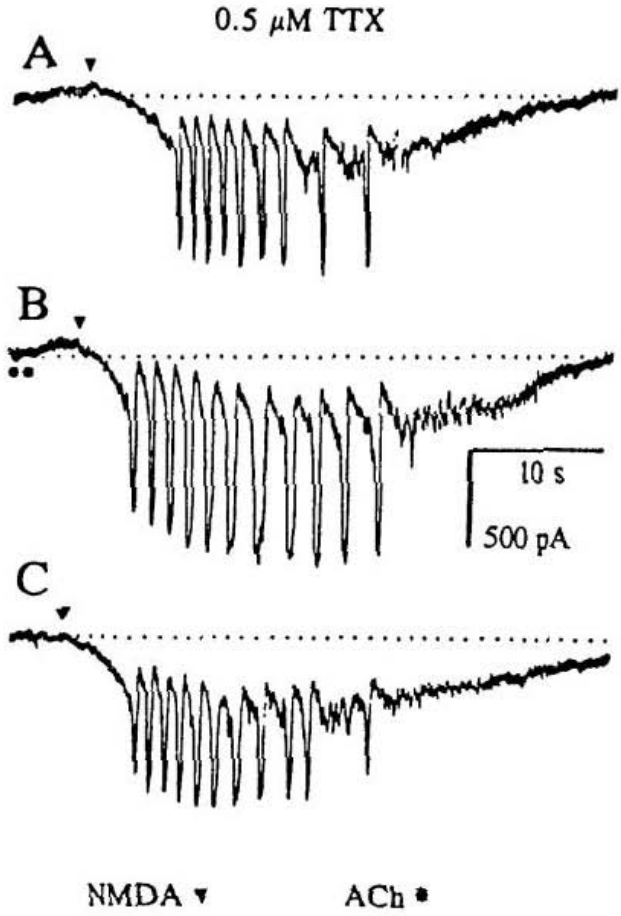


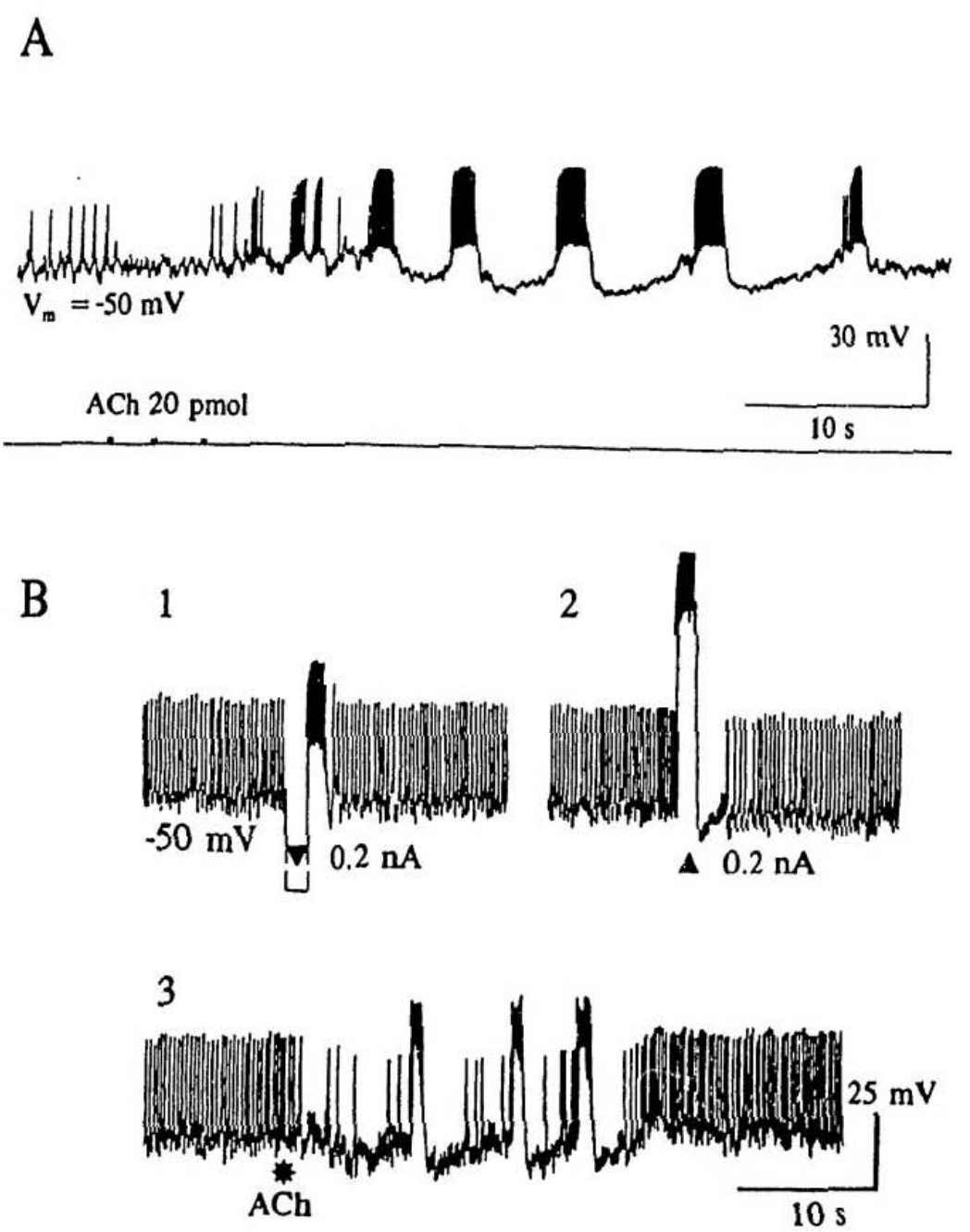
Fig. 5.13 Enhancement of NMDAR-driven oscillations by ACh. In response to NMDA (▼, about 0.1 nmol) a neuron voltage-clamped at -75 mV in the presence of 0.5 μM of TTX produces slow inward currents with superimposed oscillatory inward current (about 0.8 Hz) (**A**). Prepulses of ACh (at asterisks, 0.1 to 0.2 nmol) alone fail to produce overt response, but enhances the amplitude of the oscillatory currents (**B**). Without prepulses of ACh the oscillatory responses return to control level (**C**).

ii. *MAChR-driven oscillations*

In 53 out of 132 cholinoceptive neurons sampled in the NTS_c region, pulse-applied ACh (0.1 to 0.5 nmol) or bath-applied muscarine (2 to 5 μM) produced rhythmic oscillations of 0.05 to 0.25 Hz (n = 18, Fig. 5.14A). The oscillatory activity was evident at the intrinsic E_m and characterized by repetitive plateau potentials with superimposed high-frequency (80 to 120 Hz) bursts of spikes. This group of cells will hereafter be referred to as mAChR-driven oscillator neurons. In response to hyperpolarizing current injection, all mAChR-driven oscillator neurons tested (n = 23) exhibited PIR (Fig. 5.14B-1).

Oscillations accompanied by membrane hyperpolarization. The majority (n = 41 / 53) of the mAChR-driven oscillatory neurons started oscillating following (Fig. 5.14B-3) or during a membrane hyperpolarization (Fig. 5.14A). The hyperpolarizing response had an amplitude of 5 to 15 mV. Larger pulses of ACh prolonged the duration over which oscillations were observed, but did not alter the amplitude of the hyperpolarization or the frequency of the burst-oscillation. Hyperpolarizing current injection slowed the frequency of the oscillations. At hyperpolarizing potentials of -75 to -85 mV, the ACh-induced hyperpolarization and oscillations disappeared. The mAChR-driven slow oscillations could also be recorded (n = 4) when the neurons were held at -50 mV under voltage clamp (not shown).

Fig. 5.14 Examples of ACh-driven slow burst-oscillations in neurons of the NTS_c region. **A.** A single neuron current-clamped at its intrinsic membrane potential fires spontaneously. In response to pulse-applied ACh ($\sim$ 20 pmol / pulse) the neuron stops firing briefly and then develops rhythmic burst activity at a frequency of about 0.2 Hz. Top and bottom traces show transmembrane potential and event marker for drug ejection, respectively. **B.** In another spontaneously active neuron held at its intrinsic membrane potential, an intracellular hyperpolarizing current pulse (▼: 0.2 nA, record truncated) is followed by PIR burst (B-1), while an intracellular depolarizing pulse (▲: 0.2 nA) evokes a burst of spikes (truncated) that is followed by an AHP (B-2). In the same neuron, an ACh pulse (about 0.1 nmol, asterisk) produces a hyperpolarization and subsequent rhythmic slow burst-oscillations (B-3).


A
V_m = -50 mV
30 mV
ACh 20 pmol
10 s
B
1
2
-50 mV
0.2 nA
0.2 nA
3
25 mV
ACh
10 s

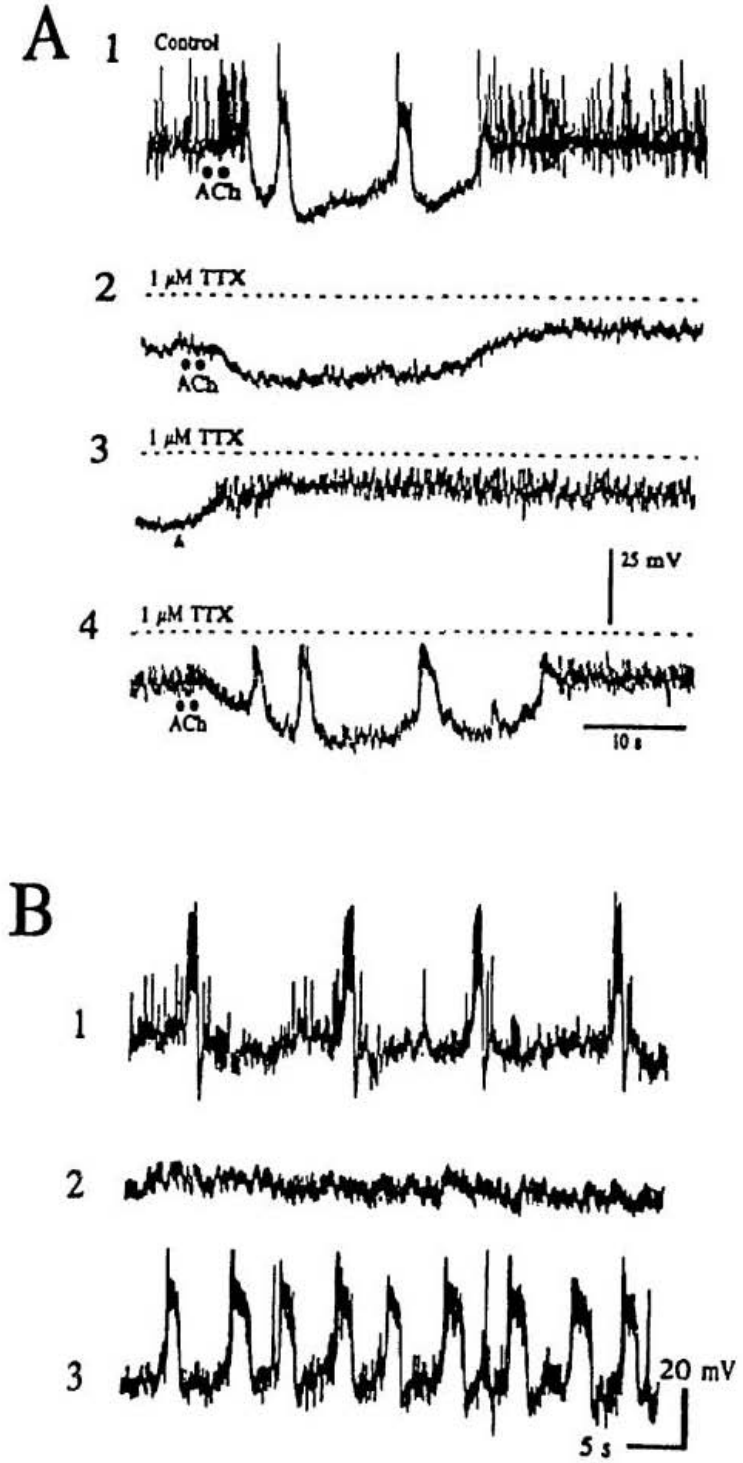
The membrane hyperpolarization and ensuing oscillations persisted in the presence of the $GABA_A$ receptor antagonist bicuculline (5 to 10 μM, n = 3, not shown), but were eliminated by bath application of 2 μM methscopolamine for 5-10 minutes (n = 6 / 6) and partially recovered in one cell after a 40 min washout (not shown).

Effects of Ca^{2+}, Cs^{2+} and Ba^{2+} on the oscillations. In a nominally Ca^{2+}-free medium, ACh pulses (0.2 to 0.3 nmol) did not produce slow oscillations (n = 3, not shown). In the presence of Cs^{2+} (1 mM), the oscillation disappeared (n = 2). In the presence of Ba^{2+} (1 mM), the neurons tested (n = 2) did not produce oscillatory behaviour until muscarine (2 μM) was added to the perfusate.

Effects of TTX. The effect of TTX on the oscillatory response was tested in 12 out of 53 mAChR-driven oscillator neurons. Exposure for 5 to 7 min to TTX (0.5 to 1.0 μM) caused a loss of the mAChR-mediated slow burst-oscillations in 8 out of 12 neurons, although the accompanying hyperpolarization persisted (see Fig. 5.15). In the 4 remaining cells, the slow oscillations continued although the superimposed spikes were all but eliminated (see Fig. 5.19).

Effect of NMDA and NMDAR-antagonists on TTX-sensitive oscillation. The mAChR agonist-evoked oscillations that were abolished by perfusion with TTX reappeared following a prepulse of NMDA or the addition of NMDA (5 to 10 μM) to

Fig. 5.15 Restoration of TTX-sensitive mAChR-driven oscillations in two representative neurons by concurrent stimulation of NMDARs. **A.** In a neuron current-clamped at its intrinsic membrane potential, ACh pulses (~0.12 nmol, asterisks) produce a hyperpolarization with superimposed rhythmic membrane voltage oscillations (A-1). After 4 min perfusion with TTX (1 μM, indicated by broken line), the ACh-evoked hyperpolarization persists while the membrane oscillations disappear (A-2). In the presence of TTX, pulse-applied NMDA (~0.2 nmol, filled triangle) alone produces a slow depolarization (A-3). Whereas, during activation of NMDA receptor, ACh pulses (~0.12 nmol, asterisks) produce a response comparable with the control (A-4). A-3 and A-4 are continued trace. **B.** In response to bath-applied muscarine (4 μM), a neuron current-clamped at its intrinsic potential of about -48 mV develops burst oscillations at a frequency of 0.08 Hz (B-1). After 5 min perfusion with muscarine (4 μM) and TTX (1 μM), the oscillations are absent (B-2). Combined perfusion with NMDA (10 μM), muscarine (4 μM) and TTX (1 μM) restores the oscillations. Note that the frequency of the oscillations is increased and the duration of each oscillatory plateau depolarization wave is prolonged (B-3).


A
1
Control
ACh
2
1 μM TTX
ACh
3
1 μM TTX
25 mV
4
1 μM TTX
ACh
10 s
B
1
2
3
20 mV
5 s

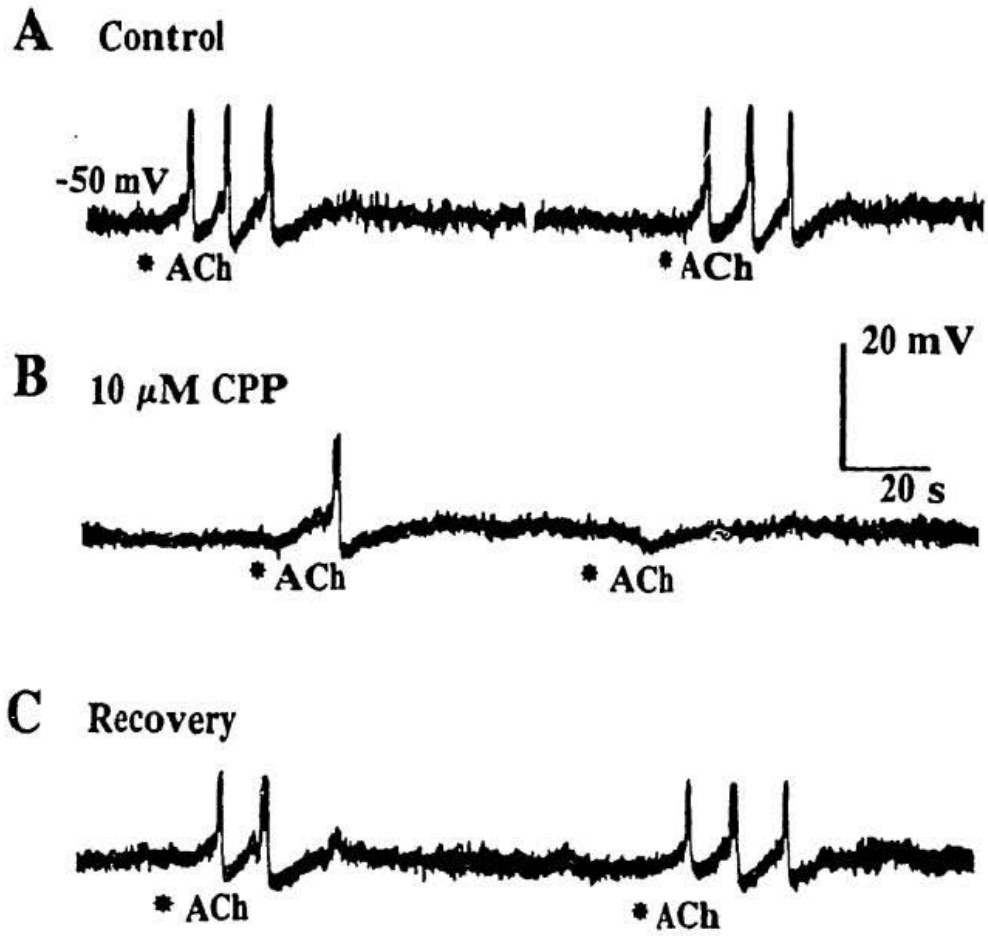


Fig. 5.16 Suppression of mAChR-driven oscillations in neurons of the NTS_c region by NMDAR blockade. Rhythmic bursting evoked by pulse-applied ACh (**A**) is inhibited during 5 to 7 min perfusion with the selective NMDAR antagonist, CPP (10 μM) (**B**). Response recovers after 10-15 min washout (**C**).

the medium although spike production remained suppressed (Fig. 5.15, n = 6). Conversely, when the NMDAR antagonists, CPP (10 to 20 μM, Fig. 5.16) or AP-5 (25 μM) were bath-applied for 5 to 10 min, the slow oscillations evoked by a pulse of ACh were eliminated in 4 cells tested and suppressed in a fifth cell. These results suggest that they are *NMDAR-dependent mAChR-driven oscillators*.

At membrane potentials of -70 to -85 mV, the TTX-sensitive mAChR-driven oscillator neurons continued to generate 2-4 Hz oscillation in response to pulse-applied NMDA (50 to 100 pmol) (n = 8 / 8; Fig. 5.17). At these hyperpolarized potentials, pulses of ACh alone did not produce detectable responses, but modulated NMDA-evoked oscillations, as evidenced by an increase in their amplitude and a decrease in their frequency (Fig. 5.18).

Effect of NMDAR-antagonist and NMDA on TTX-resistant oscillations. As shown in Fig. 5.19, muscarinic agonist-driven oscillations that were resistant to TTX (1 μM, Fig. 5.19A) were unaffected by bath-applied 25 μM AP-5 or 20 μM CPP (n = 3 / 3) in terms of both their amplitude and frequency (Fig. 5.19B), showing that these cells were *NMDAR-independent mAChR-driven oscillators*. In this group of neurons, bath-applied NMDA (20 μM) produced a slight (5 to 10 mV) depolarization and a concomitant nonrhythmic spike-discharge. When the membrane was hyperpolarized by 10 to 20 mV, the NMDA-evoked spike discharges ceased and oscillatory activity was not observed (n = 2 / 2). NMDA, however, prolonged the duration of the depolarizing plateau potential of mAChR-driven oscillations (Fig. 5.20).

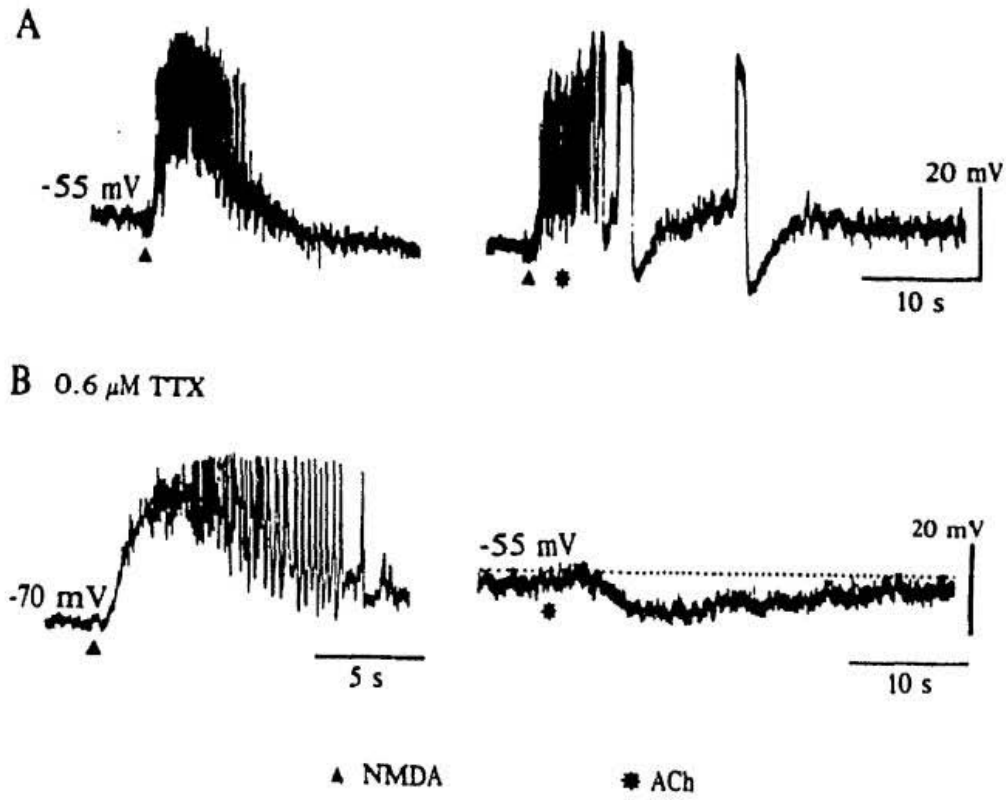


Fig. 5.17 NMDAR-mediated fast oscillations in TTX-sensitive mAChR-driven oscillator of the NTS_c region. **A.** At intrinsic resting membrane potential (-55 mV), pulse-applied NMDA (▲, about 80 pmol) evokes a membrane depolarization with superimposed spiking (left). During NMDA-evoked depolarization and tonic discharges, a pulse of ACh (applied at asterisk; about 50 pmol) produces slow oscillations. Note the high-amplitude plateau potentials and the large AHP (right). **B.** During perfusion with TTX (0.6 μM), NMDA pulse evokes a depolarization followed by membrane oscillations at 2 Hz when the cell was held at -70 mV (left). However, an ACh pulse failes to evoke slow oscillatory responses although hyperpolarization was still evident (right).

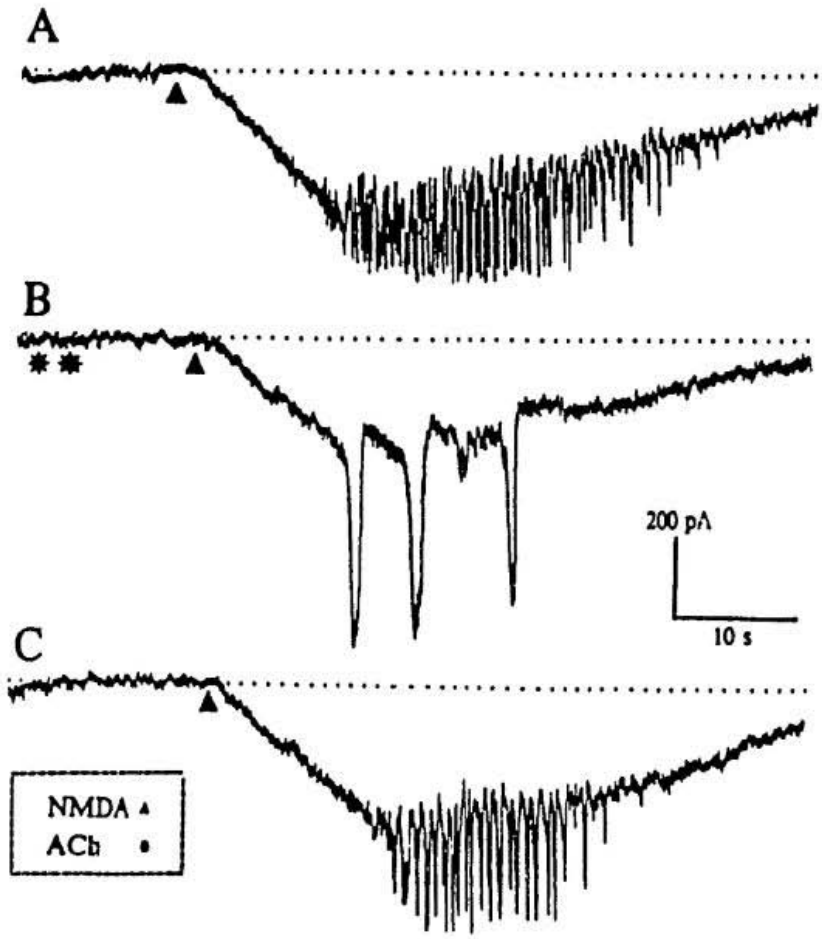


Fig. 5.18 Modulation of NMDAR-mediated fast oscillations by muscarinic cholinoceptor stimulation. In the presence of TTX (0.5 μM), a neuron voltage-clamped at -80 mV produces a slow inward current with superimposed inward current oscillations in response to NMDA pulse (▲, ~0.2 nmol) (**A**). Prepulses of ACh (applied at asterisks, about 0.1 nmol) don't produce overt response but modulate NMDAR-mediated oscillations, evidenced by increase in amplitude of oscillatory inward currents and decrease in frequency (**B**). NMDA-evoked response recovers 5 min after ACh pulses (**C**).

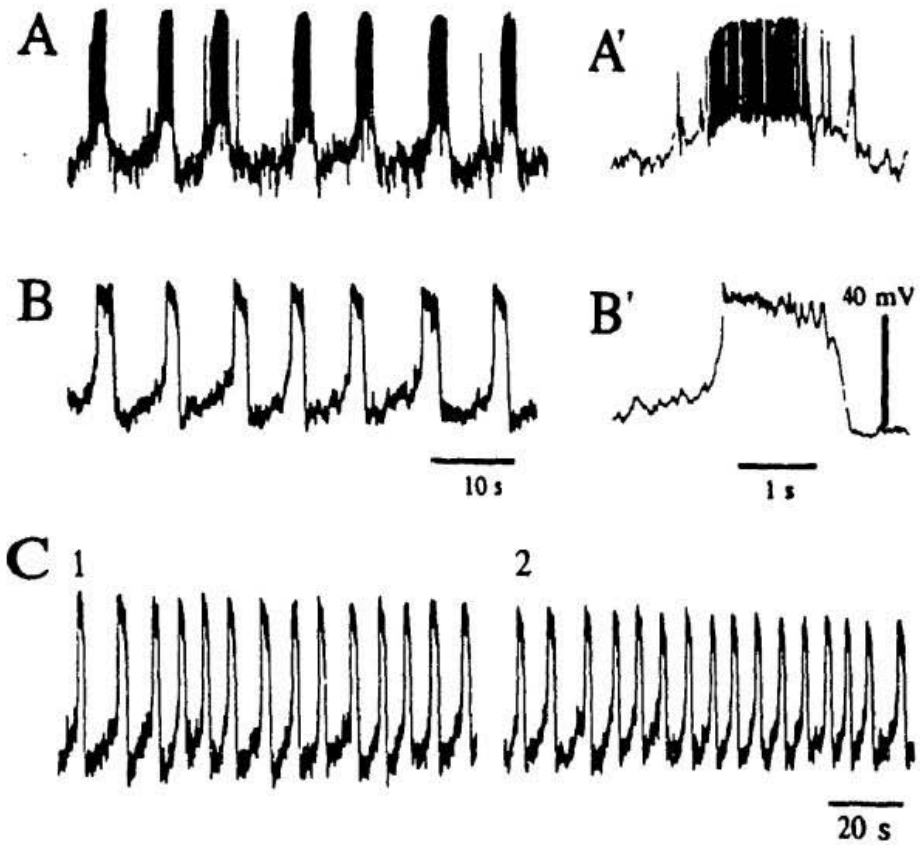
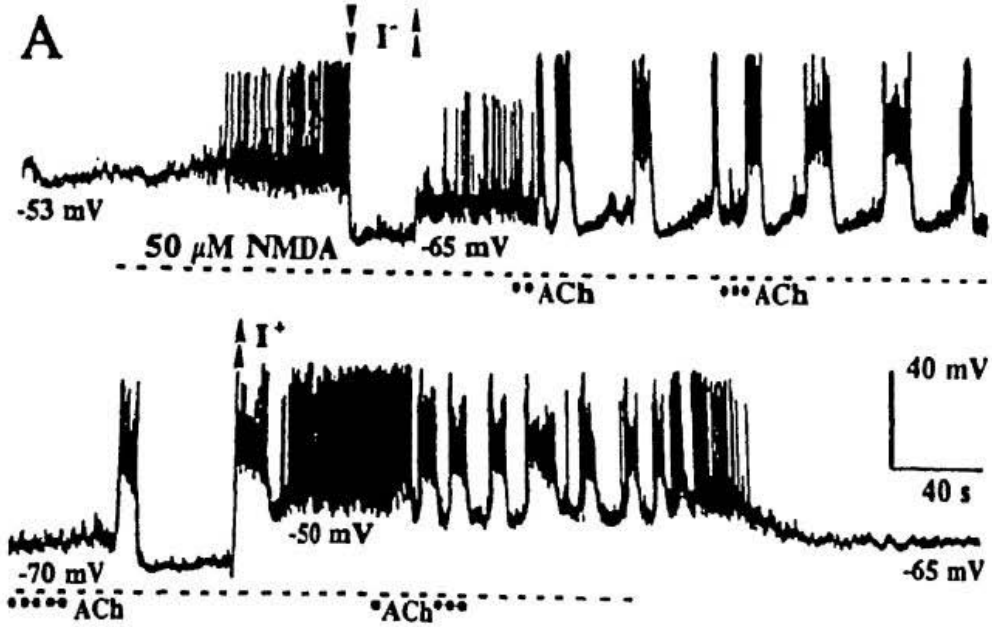
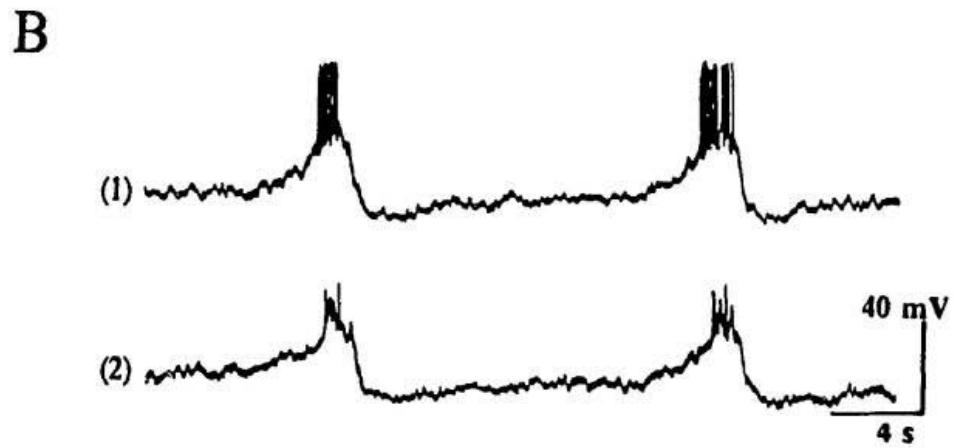


Fig. 5.19 Persistence of TTX-insensitive mAChR-driven oscillations in neurons in the NTS_C region during NMDAR blockade. Traces in A, B, C are obtained from the same neuron. **A.** Bath perfusion with muscarine (5 μM) produces burst-oscillations (0.08 Hz) at the intrinsic membrane potential of -50 mV. As shown in fast speed (**A'**), each burst is superimposed on a depolarizing wave. **B.** The mAChR-driven oscillations persists in the presence of TTX (1 μM) with suppression of spiking (**B'**). **C.** The mAChR-driven oscillations (C-1) persists after 10 min perfusion with 1 μM TTX and 25 μM CPP, an NMDA receptor antagonist (C-2).

Fig. 5.20 Absence of oscillations during NMDAR stimulation in TTX-insensitive mAChR-driven oscillator. **A.** In a neuron current-clamped at -53 mV, perfusion with NMDA (50 μM; indicated as dashed line) produces a small membrane depolarization and superimposed spiking. Holding the membrane hyperpolarized fails to produce an oscillatory response. However, pulses of ACh evoke rhythmic bursting response. I: injection of negative current; ▼: hyperpolarization; ▲: depolarization. **B.** The mAChR-driven oscillations (B-1) in the same neuron persist during perfusion with TTX (1 μM, B-2).


A
I⁻
-53 mV
50 μM NMDA
-65 mV
••ACh
•••ACh
I⁺
40 mV
40 s
-50 mV
-70 mV
-65 mV
••••• ACh
•ACh•••


B
(1)
(2)
40 mV
4 s

5.3 Discussion

The major conclusion to be drawn from the present investigations is that oesophageal premotor neurons of the NTS_c are capable of generating rhythmic activity both in the intact animal and in a slice preparation of the medulla oblongata. Accordingly, the basic cellular processes responsible for esophagomotor rhythmogenicity do not appear to depend on phasic afferent input from peripheral sensory organs and other brain structures. The data presented suggest that neurons in the region are not homogeneous with respect to conditional pacemaker properties. Moreover, these pacemaker properties are distinct from those recently reported for neurons in an adjacent NTS subregion (Tell & Jean, 1991b, 1993).

5.3.1 Oesophageal Premotor Rhythmic Activity

Rhythmic burst activity (0.05 to 0.25 Hz) was observed in the NTS_c region (where unit discharges were evoked by oesophageal distension) *in vivo* during fictive oesophageal peristalsis evoked by activation of mAChRs. The rhythmic burst activity in the NTS_c led esophagomotor output in a phase-locked manner. This suggests a premotor rather than a simple viscerosensory function. A premotor role of these neurons is furthermore borne out by the observation that NTS_c neurons that generated the fictive esophagomotor burst rhythm during cholinergic stimulation also generated a swallow-related phasic discharge leading primary peristalsis in fictive rhythmic swallowing evoked by NMDAR-stimulation (see Fig. 5.1).

As shown in Chapter 2 and 3, cells responding to the distension of the distal oesophagus fired rhythmic bursts of activity (in the range of 0.5 to 0.8 Hz). Since this reflex response is highly sensitive to NMDAR blockade, it may reflect primarily NMDAR-mediated activity. However, application of exogenous NMDA to the NTS region produced a complex response in NTS_c oesophageal premotor neurons and esophagomotor output. Since the rhythmic bursts in the NTS_c were phase-locked to repetitive buccopharyngeal swallows, they should be the oesophageal premotor responses to buccopharyngeal premotor input from adjacent NTS subnuclei, such as NTS_m and NTS_v, in which neurons generate rhythmic activity to NMDAR activation (Hashim, 1989; Tell and Jean, 1991b, 1993). The increased background discharges in the NTS_c and sustained pressure rise in the oesophagus may represent the direct response of oesophageal premotor neurons to the NMDA stimulation. Taken together with the *in vitro* data from single cells (see below), we conclude that at their intrinsic E_m, oesophageal premotor neurons in the NTS_c cannot generate slow esophagomotor rhythm in response to exogenous NMDA.

In view of the data obtained by extracellularly recording oesophageal motoneuronal activity (Chapter 4) and oesophageal premotor activity presented in this *in vivo* study, it seems safe to state that the fast ($\sim$0.6 Hz) rhythm induced by oesophageal distension and the slow ($\sim$0.12 Hz) rhythm evoked by cholinoceptor stimulation originate at the same recording site. However, an inherent limitation of the recorded multi-unit data is the lack of resolution regarding the cellular origin of the rhythmic

patterns observed in the NTS_c region, an area containing neurons of small size and very high packing density. Conceivably, each rhythm may therefore originate from a different cell type, an interpretation favoured by *in vitro* observations on single cells in the NTS_c region (discussed below).

5.3.2 Identification of NTS_C Neurons in Brainstem Slices

A shortcoming of the present *in vitro* approach is the lack of direct functional data permitting neurons under study to be identified unequivocally as oesophageal second order sensory or premotor elements. Thus, less reliable criteria had to be used such as the *topography* of the NTS_c region and *pharmacological characteristics* inferred from *in vivo* studies. Vagal afferents from the rat oesophagus mainly, if not exclusively, project to the NTS_c, one of the most cell-dense regions of the solitarial complex, that, however, is not sharply demarcated from the surrounding subnuclei (Altschuler et al. 1989; Bieger, 1993). In the present study, the recording electrode was aimed at a region lying within the boundaries of the NTS_c. The location of neurobiotin labeled neurons allowed histological confirmation of the NTS_c recording sites in some experiments. The majority of neurons described here possessed pharmacological properties consistent with *in vivo* data. More to the point, the timing of rhythmic oscillations in single NTS_c neurons observed in the present *in vitro* study closely resembled that of rhythmic oesophageal peristalsis. Therefore, it is reasonable to presume that the majority, if not all, of the neurons studied in the present work relate to esophagomotor control. Additional support

comes from *in vivo* data showing rhythmic premotor discharges to be evoked in the NTS_c by distension of the oesophagus or activation of NTS mAChRs.

Histochemically, neurons in the NTS_c seem to fall into at least two subpopulations. The larger of them expresses messenger RNA for enkephalin; the smaller subpopulation has been identified as somatostatinergic (Cunningham & Sawchenko, 1989; Cunningham et al. 1991). As shown here, although many neurons exhibited similar tonic discharges at intrinsic E_m, diverse types of burst-oscillations were evoked in NTS_c neurons in response to stimulation of both mACh and NMDA receptors, implying the existence of neuronal subtypes.

5.3.3 Spontaneous Activity

Consistent with data from *in vivo* extracellular recordings (Chapter 3), most of recorded neurons in the NTS_c region of the brainstem slice preparations fired spontaneously. Since the activity persisted throughout the recording, it did not appear to be an artifactual response to membrane rupture. The baseline E_m of the neurons slightly decreased and the spontaneous tonic discharges and associated membrane "noise" disappeared in the presence of TTX or NMDAR antagonists, as expected for synaptically-mediated events. The general consensus is that NMDAR activation is effective only when a prior depolarizing E_m is present. However, as Headley and Grillner (1990) emphasized, there is good evidence that NMDAR can mediate synaptic transmission without detectable prior non-NMDAR mediated depolarization (Davies et

al. 1986; Headley et al. 1987). More recently, functional NMDAR-, but not AMPAR-, mediated transmission at normal resting postsynaptic potential have been demonstrated in rat hippocampal CA1 pyramidal cells (Liao et al. 1995; Isaac et al. 1995). Rat NTS_c neurons exhibit a slightly depolarized intrinsic E_m (-51 $\pm$ 6 mV), and receive glutamatergic sensory afferent input (Chapter 3) and possess the NMDAR1 subtype of glutamate receptors (Broussard et al. 1994). Thus, it appears reasonable to assume that under "resting conditions", NTS_c cells are tonically activated by glutamatergic afferents, presumably mainly via dendritic NMDA receptors. This does not, however, negate the prediction that transmission in these neurons requires additional subtypes of glutamate receptors for afferent input, because the foregoing *in vivo* and *in vitro* studies (Chapter 3) have demonstrated that both NMDA and AMPA receptors in NTS_c neurons are involved in mediating vagal afferent-evoked transmission.

A large-amplitude and long-lasting slow AHP followed each spontaneous spike in NTS_c neurons. It is believed that slow AHP is mediated by distinct Ca^{2+}-activated K^+ conductance ($I_{K(Ca)}$) which is one of the key ionic conductances in the genesis of membrane oscillations (Hille, 1992). It has been hypothesized that membrane oscillation in some CNS neurons is due to the voltage-dependent NMDAR activation (MacDonald et al. 1982; Mayer and Westbrook, 1984) acting in concert with activation of endogenous $I_{K(Ca)}$ (Grillner and Wallén, 1985b). However, in causing the slow AHP, a large $I_{K(Ca)}$ would act to limit or oppose high-frequency bursting activity (Grillner et al. 1991). Thus the spontaneous tonic discharges may represent a type of NMDAR-mediated

dendritic membrane oscillation at a continuously slightly depolarized membrane potential. In contrast, a cholinergic input may play a modulatory but not prevalent role in the NTS_c neurons under "resting" conditions, because mAChR blockade only slightly reduced frequency but did not block spontaneous spiking.

Spontaneous burst-oscillations were also seen in a few cells in the NTS_c region. In most of these neurons, the burst-oscillations slowed in response to membrane hyperpolarization and disappeared in the presence of TTX, suggesting that they are driven by tonic but not phasic synaptic inputs. Although the frequency of these spontaneous burst-oscillations in most of cells (4 out of 5) was in the range of esophagomotor rhythmicity observed *in vivo*, based on the limited number of observation, one cannot say whether these spontaneous burst-oscillations related to esophagomotor rhythmogenesis. The burst frequency in the remaining spontaneous oscillator neuron was outside the range of *in vivo* esophagomotor rhythmicity. However, it is worth commenting on this neuron because it spontaneously oscillated in the presence of TTX, suggestive of true endogenous pacemaker activity.

5.3.4 NMDAR-Driven Burst Oscillations (0.5 - 0.9 Hz)

Ionic mechanisms. Like many mammalian CNS neurons, such as, neocortical (Flatman et al. 1986), hippocampal (Collingridge et al. 1983; Crunelli et al. 1984; Duchen et al. 1985; Ganong & Cotman, 1986; Peet et al. 1986), supraoptic (Hu & Bourque, 1992), dopaminergic mesencephalic (Johnson et al. 1992), neostriatal (Herriling

et al. 1983), rat NTS_{int} and NTS_V (Tell and Jean, 1991b, 1993), trigeminal motoneurons (Kim & Chandler, 1995), spinal cord (Durand, 1991; Engberg et al. 1984; Hochman et al. 1994a,b) and cultured spinal cord neurons (MacDonald et al. 1982), a subpopulation of NTS_c neurons generated membrane oscillation with a frequency of 0.5-1.0 Hz in response to NMDAR activation in the presence of TTX. This confirms that some NTS_c neurons possess conditional endogenous oscillatory properties, i.e. they can produce oscillations in response to tonic activation of NMDARs without phasic synaptic input as long as the membrane remains hyperpolarized by 5 to 20 mV. In response to NMDAR activation, all neurons tested produced a depolarization, but only a subpopulation generated oscillations. Thus, it is clear that not only NMDAR activation but also other intrinsic membrane ionic conductances are involved.

The voltage-dependence of NMDAR-driven oscillations reflects a voltage-gated channel blockade by physiological concentrations of extracellular Mg^{2+} (Nowak et al. 1984). If the NMDAR is activated and the channel is opened, the removal of Mg^{2+} from the NMDAR-coupled channel by certain slow membrane-depolarizing mechanisms results in an abrupt inward current which depolarizes the membrane and causes the entry of Ca^{2+}. In turn, the rise in intracellular Ca^{2+} activates the $I_{K(Ca)}$ which repolarizes the membrane and reinstates the Mg^{2+} blockade. According to this model, a negative slope conductance region in the steady-state I-V relationship endows the cell with the potential for bistable behaviour and membrane potential oscillation (Flatman et al. 1986; Hochman et al. 1994; Kim & Chandler, 1995; Wallén & Grillner, 1987). The negative slope

conductance revealed by NMDA receptor activation in neocortex (Flatman et al. 1986), spinal interneurons (Hochman et al. 1994a) and trigeminal motoneurons (Kim & Chandler, 1995) lies in a membrane potential region between -55 and -40 mV. As discussed above, most NTS_t neurons had intrinsic E_m around -51 mV. Further depolarization induced by exogenous NMDA would result in (i) membrane potential out side the negative slope conductance region; (ii) reduction in driving force for inward cation movement through NMDAR-coupled channels and (iii) increase in outward cation conductances, including $I_{K(Ca)}$. The combination of these factors would preclude the neurons from producing burst activity and instead result in tonic spike discharges. Conversely, hyperpolarization would return the membrane potential to more negative levels than the negative slope region so as to move Mg^{2+} back to the NMDA-channel and to reduce the driving force of $I_{K(Ca)}$. Furthermore, hyperpolarization can activate an inward rectification conductance, presumably I_h. This inward conductance slowly depolarizes the membrane and removes Mg^{2+} from the NMDA-channel so as to switch on the burst.

The NMDA-induced oscillatory plateau potential in rat NTS_{mt} neurons shows an initial ramp phase, a phenomenon attributed to "deinactivation" of the I_A conductance (Tell and Jean, 1993). However, the NMDA-induced oscillatory depolarization in NTS_t neurons were characterized by an abrupt depolarization followed by a plateau (see Fig. 5.12), suggesting an absence of I_A in these NTS_t neurons.

In the present study, agonists were applied by pressure injection and agonist

dosage could be controlled simply by varying the duration of the pressure pulse. Membrane oscillations in NTS_c neurons require NMDARs to be activated at a lower than maximal level, as already shown in rat spinal motoneurons (Hochman et al. 1994b). If NMDA activation is too extensive, presumably the outward conductances are insufficient to repolarize the membrane and start another cycle. The shape and time course of the plateau depolarization produced at supra-optimal dosage of NMDA (Fig. 5.12) suggests that these neurons have bistable property which has been seen in other neurons (Hochman et al. 1994b).

Dendritic source of oscillations. The oscillations in many neurons seemed to represent dendritic activity, because (i) most neurons had relatively small spikes in view of their high membrane input resistance; (ii) some neurons appeared to produce spikes of bimodal amplitude; and (iii) in low-Ca^{2+} ACSF, spontaneous spikes disappeared and NMDA pulses produced depolarization without spikes.

In rat supraoptic nucleus, voltage-clamping the cells eliminates NMDA-evoked membrane oscillation (Hu and Bourque, 1992). In the NTS_c, however, membrane oscillations could be recorded under voltage-clamp conditions. These oscillations only occur at hyperpolarized potentials and depend on extracellular Mg^{2+}, suggesting that the oscillation is still related to a voltage- and Mg^{2+}-dependent mechanism. Histological study with intracellular labelling has revealed that the NTS_c neurons have a relatively small cell body, but complex long dendrites. Therefore, it is unlikely that these dendrites were voltage-clamped at the same potential as that in cell body. Considering that high

concentrations of NMDA receptors are present on the dendritic spines of CNS neurons (Segal, 1995b), the current-oscillations recorded from the cell body may represent the NMDA receptor-channel mediated voltage oscillation occurring in the remote dendritic membrane of NTS_c neurons. This could also explain why NMDAR-driven voltage-oscillations were recorded in NTS_c neurons when the membrane was hyperpolarized and outside the negative slope conductance region.

Activation of NMDA receptors simultaneously produced faster (about 2.0 Hz) and slower (about 0.5 Hz) membrane oscillations in some NTS_c neurons, a phenomenon also observed in rat spinal motoneurons (Hochman et al. 1994b). Because the two types of oscillation persisted in the presence of TTX, they are unlikely due to interactions with other neurons, but reflect distinct oscillatory mechanisms associated with different dendritic branches.

5.3.5 MAChR-Driven Slow Burst Oscillations

Ionic mechanisms. The mAChR-driven slow oscillations in the majority of the neurons occurred after or during a concomitant hyperpolarization, implying an important role of the accompanying hyperpolarization in mAChR-mediated rhythmogenesis. The persistence of mAChR-mediated hyperpolarization in TTX is consistent with activation of mAChRs located directly on these cells. The subtype of mAChR involved is not yet known, but the M_2 subtype is positively coupled to a K^+ channel in CNS neurons (Egan & North, 1986; McCormick & Prince, 1986; Pan & Williams, 1994; Gerber et al. 1991;

Luebke et al. 1993). However, ionic mechanisms underlying mAChR-driven slow oscillations in NTS_c neurons remain unclear.

In several types of central neurons (Halliwell & Adams, 1982; Halliwell, 1989), mAChR-mediated slow depolarizing responses result from inhibition of a K^+ conductance, the I_M. I_M has been demonstrated in neurons of the ventral part of the NTS (NTS_V) (Champagnat et al., 1986). However, blockade of I_M does not evoke an oscillatory response in these neurons (Champagnat et al., 1986; Dekin, 1993). Blockade of I_M is unlikely to underlie mAChR-mediated oscillations in NTS_c neurons because (i) Ba^{2+}, an ion that blocks I_M (Brown & Adams, 1980; Constanti et al. 1981; Halliwell & Adams, 1982), failed to induce oscillations in NTS_c neurons; (ii) no I_M-like membrane conductance was observed in the NTS_c neurons and; (iii) most NTS_c neurons were hyperpolarized by ACh and not depolarized before, or during the generation of slow oscillations.

Like the neurons in the NTS_{int} (Tell & Jean, 1993) and the NTS_V (Dekin, 1993), the NTS_c neurons exhibited a hyperpolarization-activated inward current. This current is similar to the mixed Na^+-K^+ current referred to as I_H, I_Q or I_{AR} in various neurons (Halliwell and Adams, 1982; Mayer and Westbrook, 1983; Spain et al. 1987; Dekin, 1993) and I_h, I_F or I_{K2} in heart Purkinje cells (DiFrancesco et al. 1979; DiFrancesco, 1981; Yanagihara and Irisawa, 1980).

Unlike the neurons of the NTS_{int} (Tell and Jean, 1993) and NTS_V (Dekin, 1993), most neurons in the NTS_c appeared to lack the transient potassium current (I_A) and

therefore displayed a prominent PIR upon the termination of the hyperpolarization. Functioning to depolarize the membrane from hyperpolarized potentials, PIR is an important membrane mechanism for rhythmogenesis (Harris-Warrick, 1991). PIR results from activating I_h (Dekin, 1993; Johnson and Getting, 1991) or the low-threshold Ca^{2+}-current (Jahnsen and Llinas, 1984a,b). The PIR in NTS_c neurons is unlikely to result from the low-threshold Ca^{2+}-current because the time course of the low-threshold Ca^{2+}-current (20-25 ms) (Jahnsen and Llinás, 1984a) is much shorter than that of the PIR in NTS_c neurons. PIR in NTS_c neurons is abolished by cesium, an ion known to block I_h (Halliwell & Adams, 1982) and not $I_{T(Ca)}$. Therefore, the current responsible for PIR in NTS_c neurons appears to be I_h.

Two subpopulations of oscillatory neurons. Since PIR was observed in all mAChR-driven oscillatory neurons tested and PIR was greatly enhanced by mAChR activation, it seems warranted to ascribe a major role to PIR in rhythmogenesis in NTS_c neurons. Based on their differential sensitivity to TTX, mAChR-driven oscillator neurons in the NTS_c region appeared to be of two types that may use distinct ionic mechanisms for rhythmogenesis. However, since sensitivity to TTX was not tested in all mAChR-driven oscillators, a reliable estimate of the subpopulations of the two types of neurons is not yet available.

Membrane hyperpolarization results in oscillations in cat thalamocortical neurons *in vivo* (Steriade et al., 1993). The mAChR-mediated hyperpolarization and resultant enhancement of I_h may play a key role in the genesis of TTX-insensitive oscillatory

behaviour. Since mAChR activation in the NTS_c neurons also inhibits the slow AHP ($I_{K(Ca)}$), a prolonged burst discharge could result from the PIR. Once sufficient Ca^{2+} enters the cell during the burst phase, $I_{K(Ca)}$ would repolarize the membrane. The membrane oscillation would thus continue as long as the mAChR-mediated hyperpolarization persisted.

In TTX-sensitive mAChR-driven oscillator neurons, slow oscillations were eliminated by NMDAR antagonists. In the presence of TTX, slow oscillations could be restored by concurrent stimulation of NMDARs, suggesting a requirement for both cholinergic and glutamatergic synaptic input for rhythmogenesis. Furthermore, TTX-sensitive slow oscillator neurons responded to NMDAR activation at hyperpolarized potentials with fast oscillations (2.0 to 4.0 Hz) and mAChR activation slowed down the frequency of NMDA-oscillations. All these data suggest that TTX-sensitive slow oscillation may involve modulation of NMDAR-coupled channels. As demonstrated in the lamprey spinal cord, 5-HT reduces the frequency of NMDA-evoked rhythmic locomotion (Harris-Warrick & Cohen, 1985), an effect attributed to inhibition of $I_{K(Ca)}$ (Wallén et al., 1989). In NTS_c neurons, the mAChR-mediated increase in bursting duration and firing frequency could be due to a similar inhibition of $I_{K(Ca)}$. Alternatively, mAChRs could modulate the NMDA receptor-channel itself. Nevertheless, the mAChR-mediated hyperpolarization may also be a key step in triggering and maintaining the TTX-sensitive slow oscillation. Thus the mAChR-mediated hyperpolarization would not only increase the driving force and prolong the duration of the cation current through the

NMDA channel, but would also activate I_h. The latter would serve to depolarize the membrane thereby relieving the Mg^{2+} blockade of NMDA-channels and triggering the next plateau potential.

5.3.6 Physiological Implications

The two types of oesophageal peristaltic rhythms recorded *in vivo* from NTS_c neurons invite comparison with the two types of NTS_c neuronal rhythms observed *in vitro* during activation of NMDA and mACh receptors. Based on their temporal patterns it seems justified to postulate a causal relationship between these rhythmic activities.

i. ***NMDAR-driven oscillations***

Given that: i) the afferent input to the NTS_c from the oesophagus is mediated by glutamate (Chapter 3); ii) local reflex rhythmic esophagomotor activity *in vivo* is dependent on activation of NMDARs, but not mAChRs in the NTS (Chapter 2), and iii) the NMDA-driven oscillations mirror the pattern and rhythm of distal oesophageal peristalsis evoked by local distension, the NMDA-driven fast (0.5 to 1.0 Hz) oscillations in NTS_c neurons may represent the premotor correlate of reflex local rhythmic peristalsis ($\sim$0.6 Hz). This hypothesis is supported by the findings that activation of mAChRs augmented the amplitude of NMDAR-driven oscillations, but did not alter its pattern. This result is consistent with the *in vivo* observations demonstrating that facilitation of cholinergic transmission in the NTS enhances rhythmic reflex peristalsis (Chapter 2).

However, several caveats should be noted. Since NMDA-driven oscillations *in*

vitro can occur only when the cells (or their somata) are hyperpolarized, this hypothesis necessitates the further assumption that oesophageal distension-evoked afferent inputs not only activate NMDAR, but also hyperpolarize NTS_c neurons to an appropriate degree via other synaptic mechanisms. Our *in vivo* and *in vitro* data suggest that oesophageal vagal afferents are mainly glutamatergic and excite NTS_c neurons via AMPA and NMDA receptor subtypes (Chapter 3). In addition, some vagal afferent fibers also contain γ-amino butyric acid (Dietrich et al. 1982), serotonin, substance P and somatostatin (cited from Ternaux et al. 1989). Therefore, unlike the oscillations evoked by global activation of NMDA receptors in single neurons *in vitro*, the rhythmic reflex activity in NTS_c cells *in vivo* probably involves different subtypes of glutamate receptors and other as yet unknown transmitters, as well as the synchronization of NTS_c neurons by reafferent vagal feedback (Chapter 3).

ii. *mAChR-driven slow oscillations*

In the rat oesophagus, each peristaltic contraction takes about 3 s to propagate throughout the oesophagus (Wang and Bieger, 1991). In order to be translated into rhythmic full-length oesophageal peristalsis, NTS_c rhythmic burst activity obviously needs to have a frequency less than 0.3 Hz. The present work has revealed that NTS_c cholinoceptive oscillatory neurons can generate low-frequency bursts with a pattern and rhythm matching that of *in vivo* fictive rhythmic oesophageal peristalsis produced by activation of solitarius mAChRs (Bieger, 1984). These neurons are thus prime candidates

for premotor command elements responsible for the control of slow rhythmic peristalsis at all levels of the oesophagus.

The mAChR-mediated TTX-sensitive oscillations depend on a concomitant activation of NMDA receptors. In a previous *in vivo* study, however, mAChR-driven oesophageal peristalsis was shown to persist after focal blockade of NTS_c NMDARs (Hashim and Bieger, 1989). Nevertheless, with the experimental procedures used in that study, a complete blockade of more distant dendritic NMDARs may not have been achieved. Given that mAChR-driven TTX-resistant oscillations can be generated without NMDAR stimulation, coactivation of NMDAR does not seem to be an absolute prerequisite for slow esophagomotor rhythm generation, but probably plays a part in reinforcing rhythmic peristalsis through sensory feedback.

In vivo studies demonstrate that mAChR activation in the NTS_c contributes to the coordination of the esophagomotor sequence (Bieger, 1984; Chapter 4). The present *in vitro* study reveals that in many neurons in the NTS_c, mAChR-driven slow oscillations follow a hyperpolarization that varies in duration and amplitude. Since E_m in part determines response delay of the neurons to additional synaptic drive, the mAChR-mediated hyperpolarization may function to time NTS_c neuronal responses so as to control the progression of peristaltic activity.

Chapter 6

SUMMARY AND SYNTHESIS

The present investigations have provided new insights into the oesophageal premotor mechanisms subserved by the NTS_c in the rat. Four general issues were addressed, namely the functional organization of reflex (secondary) peristalsis with respect to the involvement of premotor cholinergic and glutamatergic links; (ii) reflex neural activity pattern and vagal afferent mediators; (iii) cholinergic innervation and esophagomotor pattern generation and (iv) cholinergic and EAAergic interaction in single premotor neurons for rhythmogenesis. The main results of the present study are summarized and synthesized as follows:

6.1 Summary

1. The rat striated muscle oesophagus generates segmentally organized reflex responses to local distension. As different segments have distinct response patterns, the esophagomotor pattern generator may consist of potentially independent premotor subcircuits. The oesophageal reflexes involve cholinergic and glutamatergic transmissions in the NTS.

2. The NTS_c-AMB_c pathway serves as the throughput (or central link) for reflex responses of the striated muscle oesophagus. Premotor neurons in the NTS_c provide the principal excitatory input to oesophageal motoneurons of the AMB_c, but do not

participate in a multifunctional capacity in cardiovascular and respiratory regulation.

3. Vagal afferents from the oesophagus do not utilize ACh, but instead employ an EAA as a major transmitter to carry excitatory information to ipsilateral NTS_c premotor neurons via NMDA and non-NMDA receptor subtypes.

4. Cholinergic neurons in the ZIRP region appear to be one of the propriobulbar sources of cholinergic input to the oesophageal premotor neurons. The cholinergic transmission in the NTS_c subserves at least three aspects of esophagomotor control, including facilitation of central coupling between buccopharyngeal and oesophageal stages of swallowing, aboral propagation of peristalsis and generation of a slow ($\sim$0.12 Hz) esophagomotor rhythm.

5. Cholinergic input to the NTS_c facilitates oesophageal premotor excitability. Unless premotor neurons of the NTS_c fire at a sufficiently high frequency, oesophageal motoneurons in the AMB_c cannot reach firing threshold or activity levels required for a functional response.

6. In a novel brainstem slice preparation containing oesophageal premotor- and motoneuronal components, chemostimulation of mAChRs in the premotor region evokes rhythmic synaptic activity ($\sim$0.12 Hz) in oesophageal motoneurons of the AMB_c, demonstrating that the interneuronal network in the NTS_c can generate patterned esophagomotor activity without support from peripheral afferent phasic inputs. However, afferent feedback critically contributes to oesophagomotor output by reinforcing ongoing

premotor activity.

7. The majority of neurons of the NTS_c recorded in slice preparations have intrinsic membrane potentials between -40 to -50 mV and exhibit spontaneous spikes that are eliminated by NMDAR blockade, suggesting background activation of NMDARs in these oesophageal premotor neurons.

8. Many neurons in the NTS_c exhibit $I_{K(Ca)}$, I_h and PIR. Activation of mAChR decreases $I_{K(Ca)}$ and increases PIR.

9. During activation of NMDA receptors, single neurons in the NTS_c generate membrane oscillations (~0.6 Hz) in the presence of TTX, indicating that oesophageal premotor neurons are endowed with conditional oscillatory properties. The oscillations are evident under single electrode voltage clamp mode, suggesting a dendritic source.

10. NMDAR-driven oscillations occur only at hyperpolarized membrane potentials and are dependent on extracellular Mg^{2+}, suggesting their dependence on a voltage-gated channel blockade by Mg^{2+}. Mirroring the pattern of distension-evoked rhythmic peristalsis, this type of NMDAR-driven oscillations may represent the premotor correlate of local rhythmic reflex peristalsis.

11. Replicating the pattern of fictive rhythmic peristalsis evoked by stimulation of mAChRs in the NTS_c, some oesophageal premotor neurons generate slower oscillations (~0.12 Hz) at their intrinsic membrane potential during mAChR activation. Thus these mAChR-driven oscillator cells are prime candidates for premotor command

elements responsible for rhythmic peristalsis at all levels of the oesophagus.

12. Two subpopulations of mAChR-driven oscillators exist in the oesophageal premotor network. In TTX-resistant mAChR-driven oscillators, activation of the hyperpolarization-induced inward rectification and PIR may underlie the generation of the slow oscillation. In TTX-sensitive mAChR-driven oscillators, rhythmogenesis may result from NMDA and mACh receptor interactions.

6.2 Synthesis

Based on data obtained from the present investigation, a general model of the rat brainstem esophagomotor network is proposed as follows:

As shown in Fig. 6.1, premotor drive of AMB_c oesophageal motoneurons (MNs) is programmed by an oesophagomotor pattern generator (EMPG) located in the NTS_c on each side of the medulla oblongata. Each EMPG receives afferent input from three sources comprising 1) the deglutitive central pattern generator (DCPG) representing an interneuronal bilateral network that resides in the NTS_{int} and NTS_v and coordinates the buccopharyngeal stage of swallowing; 2) vagal afferents from the oesophagus and 3) propriobulbar modulatory inputs. Triggered by input from the DCPG, the EMPG can program primary peristalsis without peripheral sensory support. When excited via peripheral afferents, the EMPG produces secondary peristalsis.

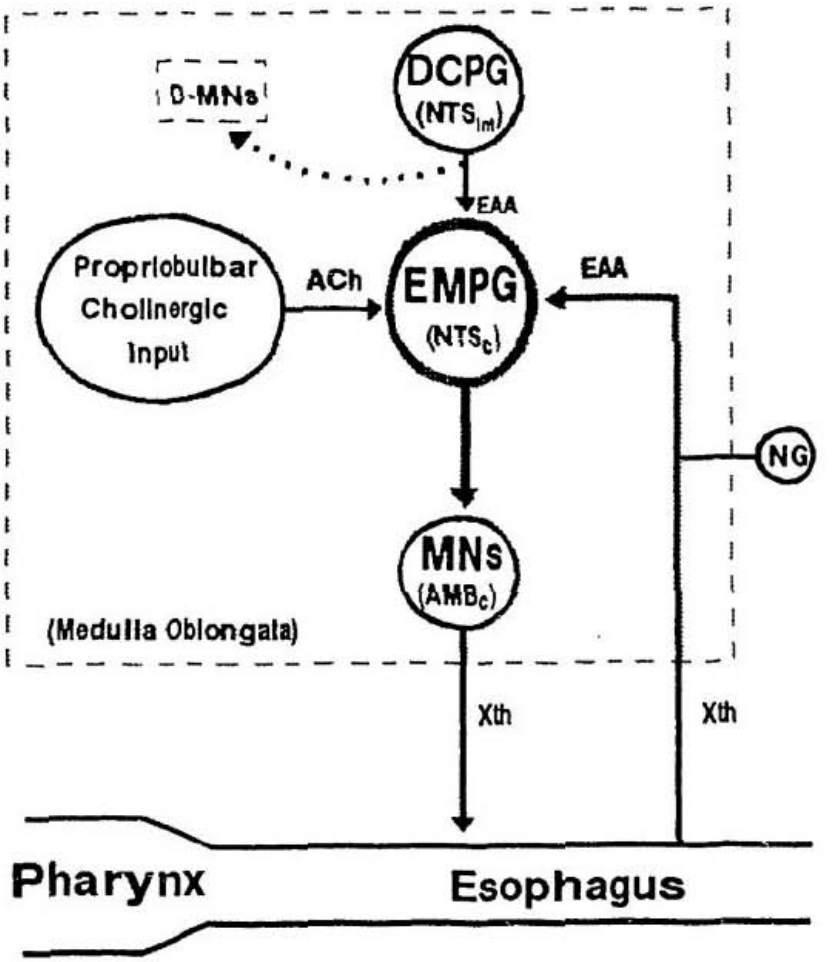


Fig. 6.1 Schematic diagram of postulated model of brainstem oesophagomotor network. Abbreviations: ACh, acetylcholine; EAA, excitatory amino acid; EMPG, oesophageal motor pattern generator; MNs, motoneurons; NG, nodose ganglion; DCPG, deglutitive central pattern generator; D-MNs, deglutitive motoneurons; Xth, vagus nerve.

The cholinergic links in the NTS_c represent propriobulbar inputs to the EMPG from the ZIRP region and probably also from cholinergic interneurons in the NTS. By activating the EMPG networks and/or modulating ionic conductances of single neurons in the EMPG network, the propriobulbar cholinergic inputs are critically involved in controlling primary and secondary oesophageal peristalsis.

Vagal afferent inputs from the oesophagus viscerotopically project to the EMPG in the NTS_c and utilize an excitatory amino acid for fast synaptic transmission via NMDA and non-NMDA receptor subtypes. The EMPG consists of multiple pattern generator subunits that generate distinct secondary peristalsis patterns when activated by appropriate segmental afferent inputs. The subunits function coordinatively during a swallow, i.e., primary peristalsis.

Commands from the DCPGs in the NTS_{int} and NTS_v trigger the EMPG through a central link to program primary peristalsis. By augmenting responsiveness of the oesophageal premotor neurons, the cholinergic inputs to the EMPG in the NTS_c strengthen the stage-coupling, facilitate the propagation of excitation through the "central chain" of premotor neurons, and also cause the EMPG to generate rhythmic oesophageal peristalsis.

Two types of esophagomotor rhythm are observed in the anaesthetized rat: distension of the intracrural oesophagus evokes a local reflex rhythmic peristalsis with a fast frequency of ~0.6 Hz. Activation of mAChRs in the NTS_c produces a slow

rhythmic peristalsis of ~0.12 Hz propagating through all levels of the oesophagus. The rhythmic esophagomotor pattern can be generated by the EMPG in the NTS_c without support from peripheral afferent inputs. However, peripheral feedback inputs to the EMPG exert important effects on the moment to moment output from the EMPG by reinforcing NTS_c neuronal activity.

In response to EAAergic and cholinergic excitation, single NTS_c neurons can generate distinct oscillatory activities in the presence of TTX and the patterns of these oscillatory responses in single neurons mirror that of oesophageal peristalsis, suggesting that single NTS_c neurons possess conditional oscillatory properties and can generate esophagomotor rhythm without phasic synaptic input.

Different types of esophagomotor rhythm are generated in different subpopulations of oesophageal premotor neurons, although some premotor neurons can generate two types of rhythm. Furthermore, the rhythm generation is subserved by different ionic mechanisms, such as NMDA receptor-gated current, I_h and $I_{K(Ca)}$. By modulating these ionic conductances, activation of mAChR plays a key role in oesophagomotor rhythmogenesis.

6.3 Future Directions

The present investigation has also raised several important issues which should be addressed in future studies.

1. NTS_c. Rhythmic (~0.6 Hz) activity evoked by distension of the distal oesophagus appears to be mediated by NMDA receptors. However, NMDAR-driven fast (~0.6 Hz) oscillations in single neurons of NTS_c region in slice preparations occur only at hyperpolarized potentials. The result suggests that in addition to NMDA receptor activation, other unknown transmitter-receptor mechanisms in the NTS_c are involved in the reflex rhythmic peristalsis. Given that oesophageal afferents to the NTS_c utilize a glutamate-like substance as mediator and metabotropic glutamate receptors (mGluR) appear to be involved in oesophageal premotor control (Lu and Bieger, 1994), the role of mGluRs in oesophageal premotor control needs to be examined further.

2. The role of oesophageal afferent feedback in esophagomotor control remains to be investigated in greater depth. For instance, *in vivo* extracellular multi-unit recordings in the present work have revealed that curarization not only reduces the firing frequency but also obscures the rhythmicity of premotor activity evoked by distension of the intracrural oesophagus, suggesting that apart from reinforcing the ongoing activity of premotor neurons, oesophageal afferent feedback may play a role in regulating esophagomotor pattern. Alternatively, the decay of premotor rhythmicity may reflect a change in premotor pattern or result from a desychronization of premotoneurons.

3. *In vivo* extracellular multi-unit recording in the NTS_c revealed that in the same site, neurons generating 0.6 Hz rhythmic discharges evoked by distension of the intracrural oesophagus produce slower (0.05 to 0.2 Hz) rhythmic discharges in response

to stimulation of mAChRs in the NTS_c. However, the two types of rhythm could be generated by the same, or by different neurons. Although single cells recorded in the brainstem slice preparation did not exhibit the two types of rhythms, with the relatively small number of cells studied, one cannot rule out the possibility that some neurons in the NTS_c can generate both types of esophagomotor rhythm. Intracellular recording of NTS_c neuronal activity *in vivo* will clarify these points.

4. Available immunohistochemical data suggest that neurons in the NTS_c are not homogeneous. Therefore, a full appreciation of the organization of oesophageal premotor neurons in controlling oesophageal peristalsis requires combined electrophysiological, anatomical and immunohistochemical studies to categorize subpopulations of NTS_c neurons with respect to their anatomical connectivity, neurotransmitter specificity, and responsivity to afferent stimulation.

5. As a corollary to issue 4, it remains unknown how oesophageal premotor neurons in different subpopulations structurally innervate and functionally control the motoneuron. A combination of whole cell recording and intracellular labelling of single NTS_c neurons in oblique sagittal brainstem slices with immunohistochemical studies would possibly reveal the anatomical and physiological relationship between oesophageal premotor and motoneurons.

REFERENCES

Adams, P.R., D.A. Brown and A. Constanti. (1982) Pharmacological inhibition of the M-current. *J. Physiol. (Lond.)* **332**:223-262.

Aghajanian, G.K. and K. Rasmussen. (1989) Intracellular studies in the facial nucleus illustrating a simple new method for obtaining viable motoneurons in adult rat brain slices. *Synapses* **3**: 331-338.

Allescher, H.-D., G. Tougas, P. Vergara, S. Lu and E.E. Daniel. (1992) Nitric oxide as putative nonadrenergic noncholinergic inhibitory transmitter in the canine pylorus *in vivo*. *Am. J. Physiol.* **262**: G695-G702.

Altschuler, S.M., X. M. Bao, D. Bieger, D. A. Hopkins and R. R. Miselis. (1989) Viscerotopic representation of the upper alimentary tract in the rat: sensory ganglia and nuclei of the solitary and spinal trigeminal tract. *J. Comp. Neurol.* **283**: 248-268.

Anand, N., and W.G. Paterson. (1994) Role of nitric oxide in esophageal peristalsis. *Am. J. Physiol.* **266**: G123-G131.

Andreollo, N.A., D.G. Thompson, G.P.N. Kendall and R.J. Earlam. (1987) Responses of the upper esophageal sphincter and esophageal body to graded intraluminal distension. *Brazilian J. Med. Biol. Res.* **20**: 165-173.

Andresen, M.C. and M.Y. Yang. (1990) Non-NMDA receptors mediate sensory afferent synaptic transmission in medial nucleus tractus solitarius. *Am. J. Physiol.* **259**: H1307-H1311.

Andrew, B.L. (1956) The nervous control of the cervical oesophagus of the rat during swallowing. *J. Physiol. (Lond.)* **134:** 729-740.

Anis, N.A., S.C. Berry, N.R. Burton and D. Lodge. (1983) The dissociative anaesthetics, ketamine and phencyclidine, selectively reduce excitation of central mammalian neurons by N-methyl-D-aspartate. *Br. J. Pharmacol.* **79**: 565-575.

Arimori, M., C.F. Code, J.F. Schlegel and R.E. Sturm. (1970) Electrical activity of the canine esophagus and gastroesophageal sphincter: its relation to intraluminal pressure and movement of material. *Am. J. Dig. Dis.* **15**: 191-208.

Arneric, S.P., R. Giuliano, P. Ernsberger, M.d. Underwood and D.J. Reis. (1990) Synthesis, release and receptor binding of acetylcholine in the C1 area of the rostral ventrolateral medulla: contributions in regulating arterial pressure. *Brain Res.* **511**:98-112.

Ascher, P. and L. Nowak. (1987) Electrophysiology studies of NMDA receptors. *TINS* **10**: 284-288.

Assad, K., S. Abd-El Rahman, N.N.Y. Nawar and Y. Mikhail. (1983) Intrinsic innervation of the oesophagus in dogs with special reference to the presence of muscle spindles. *Acta Anat.* **115**: 91-96.

Barrett, R.T., X. Bao, R.R. Miselis and S.M. Altschuler. (1994). Brain stem localization of rodent esophageal premotor neurons revealed by transneuronal passage of pseudorabies virus. *Gastroenterology* **107**: 728-737.

Bayguinov, O. and K.M. Sanders. (1993) Role of nitric oxide as an inhibitory neurotransmitter in the canine pyloric sphincter. *Am. J. Physiol.* **264**: G975-G983.

Baylis, J.H., Kauntze and J.R. Trounce. (1955) Observations on distension of the lower end of the oesophagus. *Qt. J. Med.* **24**: 143-153.

Benardo, L.S. and D.A. Prince. (1982a) Cholinergic excitation of mammalian hippocampal pyramidal cells. *Brain Res.* **249**: 315-331.

Benardo, L.S. and D.A. Prince. (1982b) Ionic mechanisms of cholinergic excitation in mammalian hippocampal pyramidal cells. *Brain Res.* **249**: 333-344.

Bieger, D. (1974) Influence of striatal dopamine receptor blockade on a bulbar motor reaction. *Neuropharmacology.* **13**: 1141-1152.

Bieger, D. (1981) Role of bulbar serotonergic neurotransmission in the initiation of swallowing in the rat. *Neuropharmacology.* **20**: 1073-1083.

Bieger, D. (1984) Muscarinic activation of rhombencephalic neurons controlling oesophageal peristalsis in the rat. *Neuropharmocology.* **23**: 1451-1464.

Bieger, D. (1991) Brain transmission system subserving deglutition: lessons from fictive swallowing. *Dysphagia* **6**: 147-164.

Bieger, D. (1993) The brainstem esophageal network pattern generator: A rodent model. *Dysphagia* **8**: 203-208.

Bieger, D. and R.S. Neuman. (1991) 5HT receptor subtypes mediating excitation and inhibition of fictive swallowing in the rat. Univ. of Birmingham Int. Conference on 5-HT receptor subtypes and brain function.

Bieger, D., S.A. Giles and C.H. Hockman. (1977) Dopaminergic influences on swallowing. *Neuropharmacology.* **16**: 245-252.

Bieger, D. and D.A. Hopkins. (1987) Viscerotopic representation of the upper alimentary tract in the medulla oblongata in the rat: the nucleus ambiguus. *J. Comp. Neurol.* **262**: 546-562.

Bieger, D., L. Larochelle and O. Hornykiewicz. (1972) A model for the quantitative study of central dopaminergic and serotoninergic activity. *Eur. J. Pharmacol.* **18**: 128-136.

Bieger, D. and C.R. Triggle. (1985) Pharmacological properties of mechanical response of the rat oesophageal muscularis mucosae to vagal and field stimulation. *Br. J. Pharmacol.* **84**: 93-106.

Bieger, D. and D.C. Marsh. (1990) Substance P modulates vagal cholinergic transmission in rat oesophageal striated and smooth muscle. *Eur. J. Pharmacol.* **183**: 2045.

Bieger, D, C.W. Loomis and I. Young. (1991) Rhythmic fictive swallowing as an index of naloxone-precipitated morphine withdrawal in the rat. *Abstract of Society for Neuroscience* (132.13), New Orleans, Louisiana.

Blank, E.L., B. Greenwood and W.J. Dodds. (1989) Cholinergic control of smooth muscle peristalsis in the cat esophagus. *Am. J. Physiol.* **257**: G517-G523.

Broussard, D.L., E.B. Wiedner, X. Li and S.M. Altschuler. (1994) NMDAR1 mRNA expression in the brainstem circuit controlling esophageal peristalsis. *Brain Res. Mol. Brain Res.* **27**: 329-332.

Brown, D.A. and P.R. Adams. (1980) Muscarinic suppression of a novel voltage sensitive K^+-current in a vertebrate neuron. *Nature* **283**: 673-676.

Camp, W.J.R. (1935) The reaction of the cervical portion of the dog's esophagus to drugs. *J. Pharm. Exp. Ther.* **54**: 306-308.

Cannon, W.B. (1907) Esophageal peristalsis after bilateral vagotomy. *Am. J. Physiol.* **19**: 436-444.

Carpenter, D.O. (1989) Central nervous system mechanisms in deglutition and emesis. In: The Gastrointestinal System I, *Handbook of Physiology*, edited by J.D. Wood, Bethesda: American Physiological Society, p.685-714.

Caulfield, M.P. (1993) Muscarinic receptors-characterization, coupling and function. *Pharmac. Ther.* **58**: 319-379.

Champagnat, J., T. Jacquin and D.W. Richter. (1986) Voltage-dependent currents in neurons of the nuclei of the solitary tract of rat brainstem slices. *Pflügers Arch* **406**: 372-379.

Chen, L. and L.Y.M. Huang. (1992) Protein kinase C reduces Mg^{2+} block of NMDA-receptor channels as a mechanism of modulation. *Nature* **356**: 521-523.

Christensen, J. and G.F. Lund. (1969) Esophageal responses to distension and electrical stimulation. *J. Clin. Invest.* **48**: 408-419.

Christensen, J. (1970) Patterns and origin of some esophageal responses to stretch and electrical stimulation. *Gastroenterology* **59**: 909-916.

Christensen, J. (1975) Pharmacology of esophageal motor function. *Annu. Rev. Pharmacol.* **15**: 243-258.

Christensen, J. (1978) The innervation and motility of the esophagus. *Front. Gastrointest. Res.* **3**:18-32.

Christensen, J. (1984) Origin of sensation in the esophagus. *Am. J. Physiol.* **246**: G221-G225.

Christensen, J. (1987) Motor functions of the pharynx and esophagus. In: *Physiology of the Gastrointestinal Tract*, Second Edition, edited by Leonard R. Johnson. Raven Press, New York, p.595-612.

Christinck, F., J. Jury, F. Cayabyab and E.E. Daniel. (1991) Nitric oxide may be the final mediator of non-adrenergic, non-cholinergic inhibitory junction potentials in the gut. *Can. J. Physiol. Pharmacol.* **69**: 1448-1458.

Clerc, N. and N. Mei. (1983a) Thoracic oesophageal mechanoreceptors connected with fibers following sympathetic pathways. *Brain Res. Bull.* **10**:1-7.

Clerc, N. and N. Mei. (1983b) Vagal mechanoreceptors located in the lower oesophageal sphincter of the cat. *J. Physiol. (Lond.)* **336**: 487-498.

Cole, A.E. and R.A. Nicoll. (1984) Characterization of a slow cholinergic post-synaptic potential recorded *in vitro* from rat hippocampal pyramidal cells. *J. Physiol. (Lond.)* **352**: 173-188.

Collingridge, G.L., S.J. Kehl and H. McLennan. (1983) The antagonism of amino acid-induced excitations of rat hippocampal CA1 neurons *in vitro*. *J. Physiol. (Lond.)* **334**: 19-31.

Collman, P.I., L. Tremblay and N.E. Diamant. (1993) The central vagal efferent supply to the esophagus and lower esophageal sphincter of the cat. *Gastroenterology* **104**: 1430-1438.

Constanti, A., P.R. Adams and D.A. Brown. (1981) Why do barium ions imitate acetylcholine? *Brain Res.* **206**: 244-250.

Contreras, C.M., M.L. Marvan, G. Mexicano, A. Puente and A. Morfin. (1990) Ketamine antagonizes toxic action of anticholinesterase agents. *Bol. Estud. Med. Biol.* **38**: 10-15.

Cotman, C. W. and L.L. Iversen. (1987) Excitatory amino acids in the brain-focus on NMDA receptors. *TINS* **10**: 263-265.

Creamer, B. and J. Schlegel. (1957) Motor responses of the esophagus to distension. *J. Appl. Physiol.* **10**: 494-504.

Crunelli, V., S. Fords and J.S. Kelly. (1984) The reversal potential of excitatory amino acid action on granule cells of the rat dentate gyrus. *J. Physiol. (Lond.)* **351**: 327-342.

Cunningham, E.T., Jr., R. Benoit and P.E. Sawchenko. (1988) Anatomical evidence for somatostatinergic interneurons subserving reflex control of esophageal motility in the rat. *Abstracts of the Society for Neuroscience*. 14.

Cunningham, E.T., Jr., and P.E. Sawchenko. (1989) A circumscribed projection from the nucleus of the solitary tract to the nucleus ambiguus in the rat: anatomical evidence for somatostatin-28-immunoreactive interneurons subserving reflex control of oesophageal motility. *J. Neurosci.* **9**: 1668-1682.

Cunningham, E.T., Jr., and P.E. Sawchenko. (1990) Central neural control of esophageal motility: a review. *Dysphagia* **5**: 35-51.

Cunningham, E.T., Jr, D.M. Simmons, L.W. Swanson and P.E. Sawchcko. (1991) Enkephalin immunoreactivity and messenger RNA in a discrete projection from the nucleus of the solitary tract to the nucleus ambiguus in the rat. *J. Comp. Neurol.* **307**: 1-16.

Curtis, D.R. and R. W. Ryall. (1966) The acetylcholine receptors of Renshaw cells. *Exp. Brain Res.* **2**: 66-80.

D'Angelo, E., P. Rossi and J. Garthwaite. (1990) Dual-component NMDA receptor currents at a single central synapse. *Nature* **346**: 467-470.

Davies, J., A.J. Miller and M.J. Sheardown. (1986) Amino acid receptor mediated excitatory synaptic transmission in the cat red nucleus. *J. Physiol. (Lond.)* **376**: 13-29.

Dean, J.B., M. Czyzyk-Krzeska and D.E. Millhorn. (1989) Experimentally induced postinhibitory rebound in rat nucleus ambiguus is dependent on hyperpolarization parameters and membrane potential. *Neurosci. Res.* **6**: 487-493.

Dekin, M.S., P.A. Getting and S.M. Johnson. (1987) *In vitro* characterization of neurons in the ventral part of the nucleus tractus solitarius. I. Identification of neuronal types and repetitive firing properties. *J. Neurophysiol.* **58**: 195-214.

Dekin, M.S., P.A. Getting. (1987) *In vitro* characterization of neurons in the ventral part of the nucleus tractus solitarius. II. Ionic basis for repetitive firing patterns. *J. Neurophysiol.* **58**: 215-229.

Dekin, M.S., G.B. Richerson and P.A. Getting. (1985) Thyrotropin-releasing hormone induces rhythmic bursting in neurons of the nucleus tractus solitarius. *Science* **229**:67-69.

Dekin, M.S. (1993) Inward rectification and its effects on the repetitive firing properties of bulbospinal neurons located in the ventral part of the nucleus tractus solitarius. *J. Neurophysiol.* **70**: 590-601.

Diamant, N.E. (1974) Electrical activity of the smooth muscle esophagus: a study of hyperpolarizing responses. In: *Proceedings of the Fourth International Symposium on Gastrointestinal Motility*. edited by E.E. Daniel. Vancouver: Mitchell, p593-605.

Diamant, N.E. (1989a) Physiology of esophageal motor function. *Gastroenterol. Clin. North. Am.* **18**: 179-194.

Diamant, N.E. (1989b) Physiology of the esophagus. In: *Gastrointestinal disease: Pathophysiology, Diagnosis, Management*. 4th edit, edited by M. Sleisenger and J.S. Fordtran, Philadelphia, WB Saunders Co. p.548-559.

Diamant, N.E. and T.Y. El-Sharkawy. (1977) Neural control of esophageal peristalsis: a conceptual analysis. *Gastroenterology* **72**: 546-556.

Dietrich, W.D., O.H. Lowry and A.D. Loewy. (1982) The distribution of glutamate, GABA and aspartate in the nucleus tractus solitarius of the cat. *Brain Res.* **237**: 254-260.

DiFrancesco, D. (1981) A new interpretation of the pace-maker current in calf Purkinje fibers. *J. Physiol. (Lond.)* **314**: 351-376.

DiFrancesco, D., M. Ohba and C. Ojeda. (1979) Measurement and significance of the reversal potential for the pace-maker current (i_{K2}) in sheep Purkinje fibers. *J. Physiol. (Lond.)* **297**: 135-162.

Dodds, W.J., J. Christensen, J. Dent, J. D. Wood and R.C. Arndorfer. (1978) Esophageal contractions induced by vagal stimulation in the opossum. *Am. J. Physiol.* **235**: E392-E401.

Dodds, W.J., J. Dent, W.J. Hogan and R.C. Arndorfer. (1981) Effect of atropine on esophageal motor function in humans. *Am. J. Physiol.* **240**: G290-G296.

Doty, R.W., W.H. Richmond and A.T. Storey. (1967) Effect of medullary lesion on coordination of deglutition. *Exp. Neurol.* **17**: 91-106.

Doty, R.W. (1968) Neural organization of deglutition. In: *Handbook of Physiology. Alimentary Canal.* edited by C.P. Code. Washington, DC: Am. Physiol. Soc., p1861-1902.

Doty, R.W. (1976) The concept of neural centers. In: *Simpler Networks and Behavior.* edited by J.C. Fentress. Sunderland, MA: Sinauer, p.251-265.

Drewe, J.A., R. Miles and D.L. Kunze. (1990) Excitatory amino acid receptors of guinea pig medial nucleus tractus solitarius neurons. *Am. J. Physiol.* **259**: H1389-H1395.

Duchen, M.R., N.R. Burton and T.J. Biscoe. (1985) An intracellular study of the interactions of N-methyl-D-aspartate with ketamine in the mouse hippocampal slice. *Brain Res.* **342**: 149-153.

Durand, J. (1991) NMDA actions on rat abducens motoneurons. *Eur. J. Neurosci.* **3**: 621-633.

Durieux, M.E. (1995) Inhibition by ketamine of muscarinic acetylcholine receptor function. *Anesth. Analg.* **81**: 57-62.

Egan, T.M. and R.A. North. (1986) Acetylcholine hyperpolarizes central neurons by acting on an M2 muscarinic receptor. *Nature* 319: 405-407.

Engberg, I., J.A. Flatman and J.D.C. Lanbert. (1984) Bistable behaviour of spinal cord motoneurons during amino-acid excitation. *Acta Physiol. Scand.* **121**: 6A.

Euchner-Wamser, I., J.N. Sengupta, G.F. Gebhart and S.T. Meller. (1993) Characterization of receptors of T_2-T_4 spinal cord neurons to esophageal distension in the rat. *J. Neurophysiol.* **69**: 868-883.

Falempin, M., N. Mei and J.P. Rousseau. (1978) Vagal mechanoreceptors of the inferior thoracic oesophagus, the lower oesophageal sphincter, and the stomach in sheep. *Pflügers Arch* **373**: 25-30.

Falempin, M. and J.P. Rousseau. (1984) Activity of lingual, laryngeal and oesophageal receptors in conscious sheep. *J. Physiol.* **347**: 47-58.

Falempin, M., J.P. Ternaux, B. Palouzier and M.C. Chamoin. (1989) Presence of cholinergic neurons in the vagal afferent system: involvement in a heterogeneous reinnervation. *J. Auton. Nerv. Syst.* **28**: 243-250.

Fazeli, M.S. (1992) Synaptic plasticity: on the trail of the retrograde messenger. *TINS* **15**: 115-121.

Flatman, J.A., P.C. Schwindt and W.E. Crill. (1986) The induction and modification of voltage-sensitive responses in cat neocortical neurons by N-methyl-D-aspartate. *Brain Res.* **363**: 62-77.

Fleshler, B., T.R. Hendrix, P. Kramer and F. J. Ingelfinger. (1959) The characteristics and similarity of primary and secondary peristalsis in the esophagus. *J. Clin. Invest.* **38**: 110-119.

Forsythe, I.D. and G.L. Westbrook. (1988) Slow excitatory postsynaptic currents mediated by N-methyl-D-aspartate receptors on cultured mouse central neurons. *J. Physiol. (Lond.)* **396**: 515-533.

Fox, K., H. Sato and N. Daw. (1990) The effect of varying stimulus intensity on NMDA-receptor activity in cat visual cortex. *J. Neurophysiol.* **64**: 1413-1427.

Gai, W.-P., J.P. Messenger, Y.-H. Yu, Z.J. Gieroba and W.W. Blessing. (1995) Nitric oxide-synthesising neurons in the central subnucleus of the nucleus tractus solitarius provide a major innervation of the rostral nucleus ambiguus in the rabbit. *J. Comp. Neurol.* **357**: 348-361.

Ganong, A.H. and C.W. Cotman. (1986) Kynurenic acid and quinolinic acid act at N-methyl-D-aspartate receptors in the rat hippocampus. *J. Pharmacol. Exp. Ther.* **236**: 293-299.

Garthwaite, J. (1991) Glutamate, nitric oxide and cell-cell signalling in the nervous system. *TINS* **14**: 60-67.

Gerber, U., D.R. Stevens, R.W. McCarley and R.W. Greene. (1991) Muscarinic agonists activate an inwardly rectifying potassium conductance in medial pontine reticular formation neurons of the rat *in vitro*. *J. Neurosci.* **11**: 3861-3867.

Getting, P.A. (1989) Emerging principles governing the operation of neural networks. *Annu. Rev. Neurosci.* **12:** 185-204.

Gidda, J.S. (1985) Control of oesophageal peristalsis. *Viewpoints Dig. Dis.* **17**: 13-16.

Gidda, J.S., B.W. Cobb and R.K. Goyal. (1981) Modulation of esophageal peristalsis by vagal efferent stimulation in opossum. *J. Clin. Invest.* **68**: 1411-1419.

Gidda, J.S. and J.P. Buyniski. (1986) Swallowing-evoked peristalsis in opossum esophagus: role of cholinergic mechanisms. *Am. J. Physiol.* **251**: G779-G785.

Gilbert, R.J. and W.J. Dodds. (1986) Effect of selective muscarinic antagonists on peristaltic contractions in opossum smooth muscle. *Am. J. Physiol.* **250**: G50-G59.

Goyal, R.K. and B.W. Cobb. (1981). Motility of the pharynx, oesophagus, and esophageal sphincter. In: *Physiology of the Gastrointestinal Tract*, Vol. 1, edited by L.R. Johnson, New York, Raven Press. p.359-393.

Goyal, R.K. and J.R. Crist. (1989) Neurology of the gut. In: *Gastrointestinal Disease: Pathophysiology, Diagnosis, Management*. 4th edit, edited by M. Sleisenger and J.S. Fordtran, Philadelphia, W.B. Saunders Co., p. 21-52.

Greengard, P., J. Jen, A.C. Nairn and C.F. Stevens. (1991) Enhancement of the glutamate response by cAMP-dependent protein kinase in hippocampal neurons. *Science* **253**: 1135-1138.

Greenwood, B., E. Blank and W.J. Dodds. (1992) Nicotine stimulates esophageal peristaltic contractions in cats by a central mechanism. *Am. J. Physiol.* **262**: G567-G571.

Grillner, S. and P. Wallén. (1985a) The ionic mechanisms underlying N-methyl-D-aspartate receptor-induced, tetrodotoxin-resistant membrane potential oscillations in lamprey neurons active during locomotion. *Neurosci. Lett.* **60**: 289-294.

Grillner, S. and P. Wallén. (1985b) Central pattern generators for locomotion, with special reference to vertebrates. *Ann. Rev. Neurosci.* **8**: 233-261.

Grillner, S., P. Wallén and L. Brodin. (1991) Neuronal network generating locomotor behavior in lamprey: circuitry, transmitters, membrane properties, and simulation. *Annu. Rev. Neurosci.* **14**: 169-199.

Grillner, S., J.T. Buchanan, P. Wallén and L. Brodin. (1988) Neural control of locomotion in lower vertebrates, from behavior to ionic mechanisms. In: *Neural Control of Rhythmic Movements in Vertebrates*. edited by A.H. Cohen, S. Rossignol & S. Grillner, John Wiley & Sons. p.1-40.

Gruber, H. (1978) Motor innervation of the striated esophagus muscle. Part I. Intramural distribution of the right and left vagus nerve in the rat esophagus as revealed by the glycogen depletion technique. *J. Neurol. Sci.* **36**: 41-53.

Halliwell, J.V. and P.R. Adams. (1982) Voltage-clamp analysis of muscarinic excitation in hippocampal neurons. *Brain Res.* **250**: 71-92.

Halliwell, J.V. (1989) Cholinergic responses in human neocortical neurons. *EXS* **57**: 138-49.

Harris, L.D., W.D. Ashworth and F.J. Ingelfinger. (1960) Esophageal aperistalsis and achalasia produced in dogs by prolonged cholinesterase inhibition. *J. Clin. Invest.* **39**: 1744-1751.

Harris-Warrick, R.M. and A.H. Cohen. (1985) Serotonin modulates the central pattern generator for locomotion in isolated lamprey spinal cord. *J. Exp. Biol.* **116**: 27-46.

Harris-Warrick, R.M. (1991) Modulation of neural network for behavior. *Ann. Rev. Neurosci.* **14**: 39-57.

Hashim, M.A. (1989) Premotoneuronal organization of swallowing in the rat (*Ph.D. thesis*). St. John's: Memorial University of Newfoundland.

Hashim, M.A. and D. Bieger. (1987) Excitatory action of 5-HT on deglutitive substrates in the rat solitary complex. *Brain Res. Bull.* **18**: 355-363.

Hashim. M.A. and Bieger. (1989) Excitatory amino acid receptor-mediated activation of solitarial deglutitive loci. *Neuropharmacology.* **28**: 913-921.

Hashim, M.A., G.T. Bolger and D. Bieger. (1989) Modulation of solitarial deglutitive N-methyl-D-aspartate receptors by dihydropyridines. *Neuropharmocology.* **28**: 923-929.

Hazarika, N.H., J. Coote and C.B.B. Downman. (1964) Gastrointestinal dorsal root viscerotomes in the cat. *J. Neurophysiol.* **27**: 107-116.

Headley, P.M. and S. Grillner. (1990) Excitatory amino acids and synaptic transmission: the evidence for a physiological function. *TIPS* **11**: 205-211.

Headley, P.M., C. G. Parsons and D.C. West. (1987) The role of N-methyl-D-aspartate receptors in mediating responses of rat and cat spinal neurons to defined sensory stimuli. *J. Physiol. (Lond.)* **385**: 169-188.

Headley, P.M., C.G. Parsons and D.C. West. (1987) The role of N-methyl-D-aspartate receptors in mediating responses of rat and cat spinal neurons to defined sensory stimuli. *J. Physiol. (Lond.)* **385**: 169-188.

Hellemans, J., G. Van Trappen and J. Janssens. (1974) Electromyography of the oesophagus. In: *Disease of the oesophagus, Handbuch der inneren Medizin*, edited by H. Schwiegk, Berlin: Spronger-Verlag, p.270-285.

Hendrix, T.R. (1980) The motility of the alimentary canal. In: *Medical Physiology*, 14th edit., edited by V.B. Mountcastle, St. Louis, C.V. Mosby Co., p. 1320-1347.

Herriling, P.L., R. Morris and T.E. Salt. (1983) Effects of excitatory amino acids and their antagonists on membrane and action potentials of cat caudate neurons. *J. Physiol. (Lond.)* **339**: 207-222.

Hille, B. (1992) *Ionic channels of excitable membranes*. Sunderland, MA: Sinauer.

Higgs, B. and F.H. Ellis Jr. (1965) The effect of bilateral supranodosal vagotomy on canine esophageal function. *Surgery* **58**: 828-834.

Hochman, S., L.M. Jordan and J.F. MacDonald. (1994a) N-methyl-D-aspartate receptor-mediated voltage oscillations in neurons surrounding the central canal in slices of rat spinal cord. *J. Neurophysiol.* **72**: 565-577.

Hochman, S., L.M. Jordan and B.J. Schmidt. (1994b) TTX-resistant NMDA receptor-mediated voltage-oscillations in mammalian lumbar motoneurons. *J. Neurophysiol.* **72**: 1559-2562.

Holland, C.T., P.M. Satchell and B.R. Farrow. (1994) Vagal afferent dysfunction in naturally occurring canine esophageal motility disorder. *Dig. Dis. Sci.* **39**: 2090-2098.

Hollis, J.B. and D.O. Castell. (1976) Effects of cholinergic stimulation on human esophageal peristalsis. *J. Appl. Physiol.* **40**: 40-43.

Hope, B.T. and S.R. Vincent. (1989) Histochemical characterization of neuronal NADPH-diaphorase. *J. Histochem. Cytochem.* **37**: 653-661.

Hu, B, and C.W. Bourque. (1992) NMDA receptor-mediated rhythmic bursting activity in rat supraoptic nucleus neurons *in vitro*. *J. Physiol.* **458**: 667-687.

Hudson, L.C. and J.F. Cummings. (1985) The origins of innervation of the esophagus of the dog. *Brain Res.* **326**: 125-136.

Hulme, E.C., N. J. M. Birdsall and N.J. Buckley. (1990) Muscarinic receptor subtypes. *Annu. Rev. Pharmacol. Toxicol.* **30**: 633-673.

Hwang, K., H.E. Essex and F.C. Mann. (1947) A study of certain problems resulting from vagotomy in dogs with special emphasis to emesis. *Am. J. Physiol.* **149**: 429-448.

Isaac, J.T., R.A. Nicoll and R.C. Malenka. (1995) Evidence for silent synapses: implications for the expression of LTP. *Neuron* **15**: 427-434.

Jahnsen, H. and R. Llinás. (1984a) Electrophysiological properties of guine-pig thalamic neurons: an *in vitro* study. *J. Physiol.* **349**: 205-226.

Jahnsen, H. and R. Llinás. (1984b) Ionic basis for the electroresponsiveness and oscillatory properties of guinea-pig thalamic neurons *in vitro*. *J. Physiol.* **349**: 227-247.

Jahr, C.E. and C.F. Stevens. (1990) A quantitative description of NMDA receptor channel kinetic behavior. *J. Neurosci.* **10**: 1830-1837.

Jahr, C.E. and C.F. Stevens. (1987) Glutamate activates multiple single channel conductances in hippocampal neurons. *Nature* **325**: 522-525.

Janssens, J. (1978) The peristaltic mechanism of the oesophagus. (*Ph. D. Dissertation*) Leuven, Belgium: University of Leuven.

Janssens, J., P. Valembois, J. Hellemans, G. Vantrappen and W. Pelemans. (1974) Studies on the necessity of a bolus for the progrssion of secondary peristalsis in the canine oesophagus. *Gastroenterology*. **67**: 245-251.

Janssens, J., I. Dewever, G. Vantrappen and J. Hellemans. (1976) Peristalsis in smooth muscle esophagus after transection and bolus deviation. *Gastroenterology* **71**:1004-1009.

Jean, A. (1972a) Effect de lésions localisées du bulbe rachidien sur le stade oesophagien de la déglutition. *J. Physiol. (Paris)* **64**: 507-516.

Jean, A. (1972b) Localisation et activité des neurons déglutiteurs bulbaires. *J. Physiol. (Paris)* **64**: 227-268.

Jean. A. (1984) Control of the central swallowing program by inputs from the peripheral receptors. A review. *J. Auton. Nerv. Syst.* **7**: 87-96.

Jean, A. (1990) Brainstem control of swallowing. In: *Neurophysiology of the Jaws and Teeth*, edited by Taylor, A. London, MacMillan, P. 294-321.

Johnson, J.W. and P. Ascher. (1987) Glycine potentiates the NMDA response in cultured mouse brain neurons. *Nature* **325**: 529-531.

Johnson, S.M. and P.A. Getting. (1991) Electrophysiological properties of neurons within the nucleus ambiguus of adult guinea pig. *J. Neurophysiol.* **66**: 744-761.

Johnson, S.W., V. Seutin and R.A. North (1992) Burst firing in dopamine neurons induced by N-methyl-D-aspartate: role of electrogenic sodium pump. *Science Wash. DC* **258**: 665-667.

Jones, J.F., D. McKeogh, P. Nolan and R.G. O'Regan. (1994) The effects of esophageal distension on diaphragm and laryngeal muscle activity in the anaesthetized cat. *Exp. Physiol.* **79**: 505-513.

Kauffmann, P., W. Lierse, W. Stark and F. Stelzner. (1968) Muskelanordung in der Speiseröhre (Mensch, Rhesusaffe, Kaninchen, Maus, Ratte, Seehung) *Erg Anat Entw-Gesch* **40**: 3-33.

Kessler, J.P. and A. Jean. (1985) Identification of the medullary swallowing region in the rat. *Exp. Brain. Res.* **57**:256-263.

Kessler, J.P. and A. Jean. (1986a) Effect of catecholamines on the swallowing reflex after pressure microinjections into the lateral solitary complex of the medulla oblongata. *Brain Res.* **386**: 69-77.

Kessler, J. P. and A. Jean. (1986b) Inhibitory influence of monoamines and brainstem monoaminergic regions on medullary swallowing reflex. *Neurosci. Lett.* **65**: 41-46.

Kessler, J.P., N. Cherkaoui, D. Catalin and A. Jean. (1990) Swallowing responses induced by microinjection of glutamate and glutamate agonists into the nucleus tractus solitarius of ketamine-anaesthetized rats. *Exp. Brain Res.* **83**: 151-158.

Kessler, M., T. Terramini, G. Lynch and M. Baudry. (1989) A glycine site associated with N-methyl-D-aspartic acid receptors: Characterization and idenfication of new class of antagonists. *J. Neurochem.* **52**: 1319-1328.

Khateb, A., P. Fort, M. Serafin, B.E. Jones, M. Muhlethaler. (1995) Rhythmical

bursts induced by NMDA in guinea-pig cholinergic nucleus basalis neurons *in vitro*. *J. Physiol. (Lond.)* **478**: 623-638.

Kim, Y.I. and S.H. Chandler. (1995) NMDA-induced burst discharge in guinea pig trigeminal motoneurons *in vitro*. *J. Neurophysiol.* **74**: 334-346.

Konnerth, A. B.U. Keller, K. Ballanyi and Y. Yaari. (1990) Voltage sensitivity of NMDA-receptor mediated postsynaptic currents. *Exp. Brain Res.* **81**: 209-212.

Larson-Prior, L.J., D.R. Mccrimmon and N.T. Slater. (1990) Slow excitatory amino acid receptor-mediated synaptic transmission in turtle cerebellar Purkinje cells. *J. Neurophysiol.* **63:** 637

Lerma, J., R. Suzannezukin and M.V.L. Bennett. (1990) Glycine decreases desensitization of N-methyl-D-aspartate (NMDA) receptors expressed in Xenopus oocytes and is required for NMDA responses. *Proc. Natl. Acad. Sci. USA* **87**:2354-2358.

Lerma, J. (1992) Spermine regulates N-methyl-D-aspartate receptor desensitization. *Neuron* **8**: 343-352.

Liao, D., N.A. Hessler and R. Malinow. (1995) Activation of postsynaptically silent synapses during paring-induced LTP in CA1 region of hippocampal slice. *Nature* **375**: 400-404.

Llinás, R. (1988) The intrinsic electrophysiological properties of mammalian neurons:insights into central nervous system function. *Science Wash. DC* **242:** 1654-1664.

Longhi, E.H., and P.H. Jordan, Jr. (1971) Necessity of a bolus for propagation of primary peristalsis in the canine esophagus. *Am. J. Physiol.* **220**: 609-612.

Lu, W.Y. and D. Bieger. (1996) Inhibition of nicotinic cholinoceptor-mediated current in vagal motor neurons by local anaesthetics. *Can. J. Physiol. Pharmacol.* Submitted.

Lu, W.Y. and D. Bieger. (1993) Dose nitric oxide contribute to the control of esophagomotor activity? *Abstract, Dysphagia Research Society*, Lake Geneva, Visconsin.

Luebke, J.I., R.W. McCarley and R.W. Greene. (1993) Inhibitory action of muscarinic agonists on neurons in the rat laterodorsal tegmental nucleus *in vitro*. *J. Neurophysiol.* **70**: 2128-2135.

Lund, G.F. and J. Christensen. (1969) Electrical stimulation of esophageal smooth muscle and effects of antagonists. *Am. J. Physiol.* **217**: 1369-1374.

Lü, Y., Y.-Q. Ding, B.-Z. Qin and J.-S. Li. (1994) The distribution and origin of axon terminals with NADPH diaphorase activity in the nucleus of the solitary tract of the rat. *Neurosci. Lett.* **171**: 70-72.

Lyrenäs, E. and H. Abrahamsson. (1986) Beta adrenergic influence on esophageal peristalsis in man. *Gut* **27**: 260-266.

MacDonald, J.F., A.V. Porietis and J.M. Wojtowicz. (1982) L-aspartic acid induces a region of negative slop conductance in the current-voltage relationship of cultured spinal cord neurons. *Brain Res.* **237**: 248-253.

MacDonald, J.F. and L. M. Nowak. (1990) Mechanisms of blockade of excitatory amino acid receptor channels. *TIPS* **11**: 167-171.

Madison, D.V., B. Lancaster and R.A. Nicoll. (1987) Voltage-clamp analysis of cholinergic action in the hippocampus. *J. Neurosci.* **3**: 733-741.

Markram, H. and M. Segal. (1990a) Long-lasting facilitation of excitatory postsynaptic potentials in the rat hippocampus by acetylcholine. *J. Physiol. (Lond.)* **427**: 381-393.

Markram, H. and M. Segal. (1990b) Acetylcholine potentiates responses to N-methyl-D-aspartate in the rat hippocampus. *Neurosci. Lett.* **113**: 62-65.

Marsh, D.C. and D. Bieger. (1986) Cholinoceptor-mediated mechanical and electrical responses of rat oesophageal striated musculature. A comparison of two *in vitro* methods. *Gen. Pharmac.* **18**: 657-663.

Mayer, M.L. and G.L. Westbrook. (1987) The physiology of excitatory amino acids in the vetebrate central nervous system. *Prog. Neurobiol.* **28**: 197-276.

Mayer, M.L. and G.L. Westbrook. (1983) A voltage-clamp analysis of inward (amomalous) rectification in mouse spinal sensory ganglion neurons. *J. Physiol. (Lond.)* **340**: 19-45.

Mayer, M.L. and G.L. Westbrook. (1984) Mixed-agonist action of excitatory amino acids on mouse spinal cord neurons in culture. *J. Physiol. (Lond.)* **354**: 29-53.

Mayer, M.L., G.L. Westbrook and P.B. Guthrie. (1984) Voltage-dependent block by Mg^{2+} of NMDA response in spinal cord neurons. *Nature* **309**: 261-263.

Mayrand, S., L. Tremblay and N. Diament. (1994) *In vivo* measurement of feline esophageal tone. *Am. J. Physiol.* **267**: G914-G921.

McCormick, D.A. and D.A. Prince. (1986) Acetylcholine induces burst firing in thalamic reticular neurons by activating a potassium conductance. *Nature* **319**: 402-405.

McLarnon, J.G. and K. Curry. (1990) Single channel properties of the N-methyl-D-aspartate receptor channel using NMDA and NMDA agonists: on-cell recordings. *Exp. Brain Res.* **82**: 82-88.

Mei, N. (1970) Macanorécepteurs digestifs chez le chat. *Exp. Brain Res.* **11**: 502-514.

Mei, N., M. Aubert, J. Crousillat and F. Ranieri. (1974) Sensory innervation of the lower esophagus of the cat. Comparison with the other parts of the digestive system. In: *Proceedings of the 4th International Symposium on Gastrointestinal Motility*. edited by E.E. Daniel. Vancouver: Mitchell Press, p.585-591.

Meltzer, S.J. (1899) On the causes of the orderly progress of the peristaltic movements in the esophagus. *Am. J. Physiol.* **2**: 266-272.

Meltzer, S.J. (1907) Secondary peristalsis of the esophagus. A demonstration on a dog with a permanent fistula. *Proc. Soc. Exp. Biol. Med.* **4**: 35-37.

Miller, A.J. (1972a) Characteristics of the swallowing reflex induced by peripheral nerve and brain stem stimulation. *Exp. Neurol.* **34**: 210-222.

Miller, A.J. (1972b) Significance of sensory inflow to the swallowing reflex. *Brain Res.* **43**: 147-159.

Miller, A.J. (1982) Deglutition. *Physiol. Rev.* **62**: 129-184.

Miller, A.J. (1986) Neurophysiology basis of swallowing. *Dysphagia* **1**: 91-100.

Miller, A.J. (1987) Swallowing: Neurophysiological control of the oesophageal phase. *Dysphagia* **2**: 72-82.

Miller, A., D. Bieger and J. Conkin. (1996) Functional controls of deglutition. In: *Deglutition and its Disorders: Anatomy, Physiology, Clinical Diagnosis, and Management*. edited by A. Perlman & K. Schultze-Delrieu, Singular Publishing Group, Inc., San Diego, CA.

Mittal, R.K., J. Ren and R.W. McCallum. (1990) Modulation of feline esophageal contractions by bolus volume and outflow obstruction. *Am. J. Physiol.* **258**: G208-G215.

Monges, H., J. Salducci and C. Roman. (1968) Etude E.M.G. de la contraction oesophagienne chez l'homme normal. *Archs Fr. Mal. Appar. Dig.* **57**: 545-560.

Mosso, A. (1876) Ueber die Bewegunguen der Speiserohre. *Untersuchungen zur Naturlehre des Menschen und der Thiere* **11**:327-349. (cited from Miller (1982))

Murray, J., C. Du, A. Ledlow, J.N. Bates and J. L. Conklin. (1991) Nitric oxide: mediator of nonadrenergic noncholinergic responses of opossum esophageal muscle. *Am. J. Physiol.* **261**: G401-G406.

Nakanishi, S. (1992) Molecular diversity of glutamate receptors and implications for brain function. *Science* **258**: 597-603.

Neil, J.P., J. Gonella and C. Roman. (1980) Localization parla technique de marquage a la peroxydase des corps cellulaires des neurons ortho et parasympathiques innervant le sphincter oesophagien inferieur du chat. *J. Physiol. (Paris)* **76**: 591-599.

Neuhuber, W.L., P.A. Sandoz and T. Fryscak. (1986) The central projections of primary afferent neurons of greater splanchnic and intercostal nerves in the rat. *Anat. Embryol.* **174**: 123-144.

Neuhuber, W.L. (1987) Sensory vagal innervation of the rat esophagus and cardia: a light and electron microscopic anterograde tracing study. *J. Auton. Nerv. Syst.* **20**: 243-255.

Neuhuber, W.L., J. Wörl, H.-R. Berthoud and B. Conte. (1994) NADPH disphorase-positive nerve fibers associated with motor endplates in the rat esophagus: new evidence for co-innervation of striated muscle by enteric neurons. *Cell & Tissue Res.* **276**: 23-30.

Nowak, L, P. Bregestovski, P. Ascher, A. Herbet and A. Prochiantz. (1984) Magnesium gates glutamate-activated channels in mouse central neurons. *Nature* **307**: 462-465.

Ohta, A., H. Takagi, T. Matsui, Y. Hamai, S. Iida and H. Esumi. (1993) Localization of nitric oxide synthase-immunoreactive neurons in the solitary nucleus and ventrolateral medulla oblongata of the rat: their relation to catecholaminergic neurons. *Neurosci. Lett.* **158**: 33-35.

Oliven, A., M. Haxhiu and S.G. Kelsen. (1989) Reflex effect of esophageal distension on respiratory muscle activity and pressure. *J. Appl. Physiol.* **66**: 536-541.

Palouzier, B., M.C. Barrit Chanmoin, P. Portalier, and J.P. Ternaux. (1987) Cholinergic neurons in the rat nodose ganglia. *Neurosci. Lett.* **80**: 147-152.

Pan, Z.Z. and J.T. Williams. (1994) Muscarine hyperpolarizes a subpopulation of neurons by activating an M2 muscarinic receptor in rat nucleus raphe magnus *in vitro*. *J. Neurosci.* **14**: 1332-1338.

Paterson, W.G. (1991) Neuromuscular mechanisms of esophageal responses at and proximal to a distending balloon. *Am. J. Physiol.* **260**: G148-G155.

Paterson, W.G., T.T. Hynna-Liepert and M. Selucky. (1991) Comparison of primary and secondary esophageal peristalsis in humans: Effect of atropine. *Am. J. Physiol.* **260**: G52-G57.

Paterson, W.G., S. Rattan and R.K. Goyal. (1988) Esophageal responses to transient and sustained esophageal distension. *Am. J. Physiol.* **255**: G587-G595.

Paterson, W.G. and B. Indrakrishnan. (1995) Descending peristaltic reflex in the opossum esophagus. *Am. J. Physiol.* **269**: G219-G224.

Pearson, K.G. (1993) Common principles of motor control in vertebrates and invertebrates. *Annu. Rev. Neurosci.* 16: 265-297.

Peet, M.J., H. Gregersen and H. Mclennan. (1986) 2-amino-5-phosphonovalerate and CO^{2+} selectively block depolarization and burst firing of rat hippocampal CA1 pyramidal neurons by N-methyl-D-aspartate. *Neurosci.* **17**: 635-641.

Perrone, M.H. (1981) Biochemical evidence that L-glutamate is a neurotransmitter of primary vagal afferent nerve fibers. *Brain res.* **230**: 283-293.

Rand, M.J. (1992) Nitrergic transmission: nitric oxide as a mediator of non-adrenergic, non-cholinergic neuro-effector transmission. *Clin. Exp. Pharmacol. Physiol.* **19**:147-169.

Ren, J., B.T. Massey, W.J. Dodds, M.K. Kern, J.G. Brasseur, R. Shaker, S.S. Harrington, W.J. Hogan and R.C. Arndorfer. (1993) Determinants of intrabolus pressure during esophageal peristaltic bolus transport. *Am. J. Physiol.* **264**: G407-G413.

Ren, J., R. Shaker, M.Kusano, B. Podvrsan, N. Metwally, K.S. Dua and Z. Sui. (1995) Effect of aging on the secondary esophageal peristalsis: presbyesophagus revisited. *Am. J. Physiol.* **268**: G772-G779.

Reynolds, R.P.E., T.Y. El-Sharkawy and N.E. Diamant. (1985) Esophageal peristalsis in the cat: the role of central innervation assessed by transient vagal blockade. *Can. J. Physiol. Pharmacol.* **63**: 122-130.

Roman, C. (1966) Contôle nerveux du péristaltisme oesophagien. *J. Physiol. (Paris)* **58**:79-108.

Roman, C. (1982) Nervous control of oesophageal and gastric motility. In: *Mediators and Drugs in Gastrointestinal Motility, I. Morphological Basis and Neurophysiological Control. Handbook of Experimental Pharmacology*, Vol. **59**(1), edited by G. Bertaccini Berlin: Springer, p.223-278.

Roman, C. (1986) Contôle nerveux de la déglutition et de la motricité oesophagienne chex les mammifères. *J. Physiol. (Paris)* **81**: 118-131.

Roman, C. and L. Tieffenbach. (1972) Enregitrement de l'activité unitaire des fibers motrices vagales destinées a l'oesophage du babouin. *J. Physiol. (Paris)* **64**: 479-506.

Roman, C. and J. Gonella. (1981) Extrinsic control of digestive tract motility. In: *Physiology of the Gastrointestinal Tract*, edited by L.R. Johnson, New York, Raven Press, p. 289-333.

Roman, C. and J. Gonella. (1987) Extrinsic control of digestive tract motility. In: *Physiology of the Gastrointestinal Tract*, 2nd edit. edited by L.R. Johnson, New York, Raven Press, p. 507-553.

Ruggiero, D.A., R. Giuliano, M. Anwar, R. Stornetta and D.J. Reis. (1990) Anatomical substrates of cholinergic-autonomic regulation in the rat. *J. Comp. Neurol.* **292**: 1-53.

Sah, P., S. Hestrin and R.A. Nicoll. (1989) Tonic activation of NMDA receptors by ambient glutamate enhances excitability of neurons. *Science* **246**:815

Sanchez, G.C., P. Kramer and F.J. Ingelfinger. (1953) Motor mechanisms of the esophagus particularly of its distal portion. *Gastroenterology* **25**: 321-332.

Sellers, A.F. and D.A. Titchen. (1959) Response to localized distension of the oesophagus in decerebrate sheep. *Nature* **184**: p. 645.

Segal, M. (1995a) Imaging of calcium variations in living dendritic spines of cultured rat hippocampal neurons. *J. Physiol. (Lond.)* **486**: 283-295.

Segal, M. (1995b) Morphological alterations in dendritic spines of rat hippocampal neurons exposed to N-methyl-D-aspartate. *Neurosci. Lett.* **193**: 73-76.

Sengupta, J.N., D. Kauvar and R.K. Goyal. (1989) Characteristics of vagal esophageal tension-sensitive afferent fibers in the opossum. *J. Neurophysiol.* **61**: 1001 1010.

Sengupta, J.N., J.K. Saha and R.K. Goyal. (1990) Stimulus-response function studies of esophageal mechanosensitive nociceptors in sympathetic afferents of opossum. *J. Neurophysiol.* **64**: 796-812.

Sessle, B.J. and J.L. Henry (1989) Neural mechanisms of swallowing: Neurophysiological and neurochemical studies on brain stem neurons in the solitary tract region. *Dysphagia* **4**: 61-75.

Sherrington, C.S. (1915) Some observations on the bucco-pharyngeal stage of reflex deglutition in the cat. *Qt. J. Exp. Physiol.* **9**: 147-186.

Sinclair M.E. and P.M. Suter. (1987) Lower oesophageal contractility as an indicator of brain daeth in paralysed and mechanically ventilated patients with head injury. *Br. Med. J.* **294**: 935-936.

Snyder, S.H. (1992) Nitric oxide: first in a new class of neurotransmitters. *Science* **257**:494-496.

Spain, W.J., P.C. Schwindt and W.E. Crill. (1987) Anomalous rectification in neurons from rat senorimotor cortex *in vitro*. *J. Neurophysiol.* **57**: 1555-1576.

Steriade, M., A. Nunez and F. Amzica. (1993). Intracellular analysis of relations between the slow (< 1 Hz) neocortical oscillation and other sleep rhythms of the electroencephalogram. *J. Neurosci.* **13**: 3266-3283.

Stone, T.W. and N.R. Burton. (1988) NMDA receptors and ligands in the vertebrate CNS. *Prog. Neurobiol.* **30**: 333-368.

Sumi, T. (1963) The activity of brain-stem respiratory neurons and spinal respiratory motoneurons during swallowing. *J. Neurophysiol.* **26**: 466-477.

Sumi, T. (1964) Neuronal mechanisms in swallowing. *Pflugers Arch. Ges. Physiol.* **278**: 467-477.

Swanson, L.W., D.M. Simmons, P.J. Whiting and J. Lindstrom. (1987) Immunohistochemical localization of neuronal nicotinic receptors in the rodent central nervous system. *J. Neurosci.* **7**: 3334-3342.

Tell, F. and A. Jean. (1990) Rhythmic bursting patterns induced in neurons of the rat nucleus tractus solitarii, in vitro, in response to N-methyl-D-aspartate. *Brain Res.* **533**: 152-156.

Tell, F., L. Fagni and A. Jean. (1990) Neurons of the nucleus tractus solitarius, in vitro, generate bursting activities by solitary tract stimulation. *Exp.Brain Res.***79**:436-440.

Tell, F. and A. Jean. (1991a) Bursting discharges evoked *in vitro*, by solitary tract stimulation or application of N-methyl-D-aspartate, in neurons of the rat nucleus tractus solitarii. *Neurosci. Lett.* 124:221-224.

Tell, F. and A. Jean. (1991b) Activation of N-methyl-D-aspartate receptors induces endogenous rhythmic bursting activities in nucleus tractus solitarii neurons: an intracellular study on adult rat brainstem slices. *Eur. J. Neurosci.* **3**: 1353-1365.

Tell, F. and A. Jean. (1993) Ionic basis for endogenous rhythmic patterns induced by activation of N-methyl-D-aspartate receptors in neurons of the rat nucleus tractus solitarii. *J. Neurophysiol.* **70**: 2379-2390.

Ternaux, J.P., M. Falempin, B. Palouzier, M.C. Chamoin and P. Portalier. (1989) Presence of cholinergic neurons in the vagal afferent system: biochemical and immunohistochemical approaches. *J. Auton. Nerv. Syst.* **28**: 233-242.

Thomson, A.M. (1990a) Glycine is a coagonist at the NMDA receptor/channel complex. *Prog. Neurobiol.* **35**: 53-74.

Thomson, A.M. (1990b) Augmentation by glycine and blockade by 6-cyano-7-nitroquinoxaline-2,3-dione (CNQX) of responses to excitatory amino acids in slices of rat neocortex. *Neurosci.* **39**: 69-79.

Thomson, A.M., V.E. Walker and D.M. Flynn. (1989) Glycine enhances NMDA-receptor mediated synaptic potential in neocortical slices. *Nature* **338**: 422-424.

Tieffenbach, L. and C. Roman. (1972) Role de l'innervation extrinsèque vagale dans la motricité de l'oesophage à musculeuse lisse: étude életromyographique chez le chat et le babouin. *J. Physiol. (Paris)* **64**: 193-226.

Tottrup, A., D. Svane and A. Forman. (1991) Nitric oxide mediating NANC inhibition in opossum lower esophageal sphincter. *Am. J. Physiol.* **260**: G385-G389.

Uddman, R., T. Grunditz, A. Luts, H. Dosai, G. Fernoström, and F. Sundler. (1995) Distribution and origin of the peripheral innervation of rat cervical esophagus. *Dysphagia* **10**: 203-212.

Ueda, M., J.F. Schlegel and C.F. Code. (1972) Electrical and motor activity of innervated and vagally denervated feline esophagus. *Am. J. Dig. Dis.* **17**: 1075-1088.

Valdez, D.T. and A. Salapatek. (1993) Swallowing and upper esophageal sphincter contraction with transcranial magnetic-induced electrical stimulation. *Am. J. Physiol.* **264**: G213-G219.

Vyas, D., Y.T. Wang and D. Bieger (1990) Nucleus reticularis intermedialis-possible cholinergic source subserving esophageal peristalsis in the rat. Society for Neuroscience, *Abstract* **16**, p.730.

Wada, E., K. Wada, J. Boulter, E. Deneris, S. Heinemann, J. Patrick and L.W. Swanson. (1989) Distribution of alpha2, alpha3, alpha4, and beta2 neuronal nicotinic receptor subunit mRNAs in the central nervous system: A hybridization histochemical study in the rat. *J. Comp. Neurol.* **284**: 314-335.

Wada, K., M. Ballivet, J. Boulter, J. Connolly, E. Wada, E.S. Deneris, L.W. Swanson, S. Heinemann and J. Patrick. (1988) Functional expression of a new pharmacological subtype of brain nicotinic acetylcholine receptor. *Science* **240**: 330-334.

Wallén, P. and S. Grillner. (1987) N-methyl-D-aspartate receptor-induced inherent oscillatory activity in neurones active during fictive locomotion in the lamprey. *J. Neurosci.* **7**: 2745-2755.

Wallén, P. J.J. Buchanan, S. Grillner, J. Christenson and T. Hökfelt. (1989) The effects of 5-hydroxytryptamine on the afterhyperpolarization, spike frequency regulation and oscillatory membrane properties in lamprey spinal cord neurons. *J. Neurophysiol.* **61**: 759-768.

Wamsley, J.K., W.S. Lewis, W.S. Young III and M.J. Kuhar. (1981) Autoradiographic localization of muscarinic cholinergic receptors in rat brainstem. *J. Neurosci.* **1**: 176-191.

Wang, L. and R.M. Bradley. (1995) *In vitro* study of afferent synaptic transmission in the rostral gustatory zone of the rat nucleus of the solitary tract. *Brain Res.* **702**:188-198.

Wang, Y.T. (1992) Brainstem mechanisms subserving oesophageal peristalsis in the rat. (*Ph. D. thesis*) St. John's: Memorial University of Newfoundland.

Wang, Y.T. and D. Bieger. (1991) The role of solitarial GABAergic mechanisms in the control of swallowing. *Am. J. Physiol.* **263**: R639-R646.

Wang, Y.T., R.S. Neuman and D. Bieger. (1991a) Nicotinic cholinoceptor-mediated excitation in ambigual motoneurons of the rat. *Neurosci.* **40**: 759-767.

Wang, Y.T., D. Bieger and R.S. Neuman. (1991b) Activation of NMDA receptors is necessary for fast information transfer at brainstem motoneurons. *Brain Res.* **567**:260-266.

Wang, Y.T., R.S. Neuman and D.Bieger. (1991c) Somatostatin inhibits nicotinic cholinoceptor mediated-excitation in rat ambigual motoneurons *in vitro*. *Neurosci. Lett.* **123**: 236-239.

Wang, Y.T., M. Zhang, R.S. Neuman and D. Bieger. (1993) Somatostatin regulates excitatory amino acid receptor-mediated fast excitatory postsynaptic potential components in vagal motoneurons. *Neuroscience.* **53**: 7-9.

Weerasuriya, A., D. Bieger and C.H. Hockman. (1980) Interaction between primary afferent nerves in the elicitation of reflex swallowing. *Am. J. Physiol.* **239**: R407-414.

Weisbrodt, N.W. (1976) Neuromuscular organization of esophageal and pharyngeal motility. *Arch Intern. Med.* **136**: 524-531.

Wiedner, E.B., X. Bao and S.M. Altschuler. (1995) Localization of nitric oxide synthase in the brain stem neural circuit controlling esophageal peristalsis in rats. *Gastroenterology* **108**: 367-375.

Wilson, L.E., D.J. Hatch and K. Rehder. (1993) Mechanisms of the relaxant action of ketamine on isolated porcine trachealis muscle. *Br. J. Anaesth.* **71**: 544-550.

Wörl, J., B. Mayer and W.L. Neuhuber. (1994) Nitrergic innervation of the rat esophagus: focus on motor endplates. *J. Auton. Nerv. Syst.* **49**: 227-233.

Wroblewski, J.T. and W. Danysz. (1989) Modulation of glutamate receptors: molecular mechanisms and functional implications. *Annu. Rev. Pharmacol. Toxicol.* **29**: 441-474.

Yamato, S., S. J. Spechler and R. K. Goyal. (1992) Role of nitric oxide in esophageal peristalsis in the opossum. *Gastroenterology* **103**: 197-204.

Yanagihara, K. and H. Irisawa. (1980) Inward current activated during hyperpolarization in the rabbit sinoatrial node cell. *Pfluegers Arch.* **385**: 11-19.

Zhang, M., Y.T. Wang, D. M. Vyas, R.S. Neuman and D. Bieger. (1993) Nicotinic cholinoceptor-mediated EPSPs in rat nucleus ambiguus. *Exp. Brain Res.* **96**: 83-88.